Acta Morphologica et Anthropologica 33 (1–2)

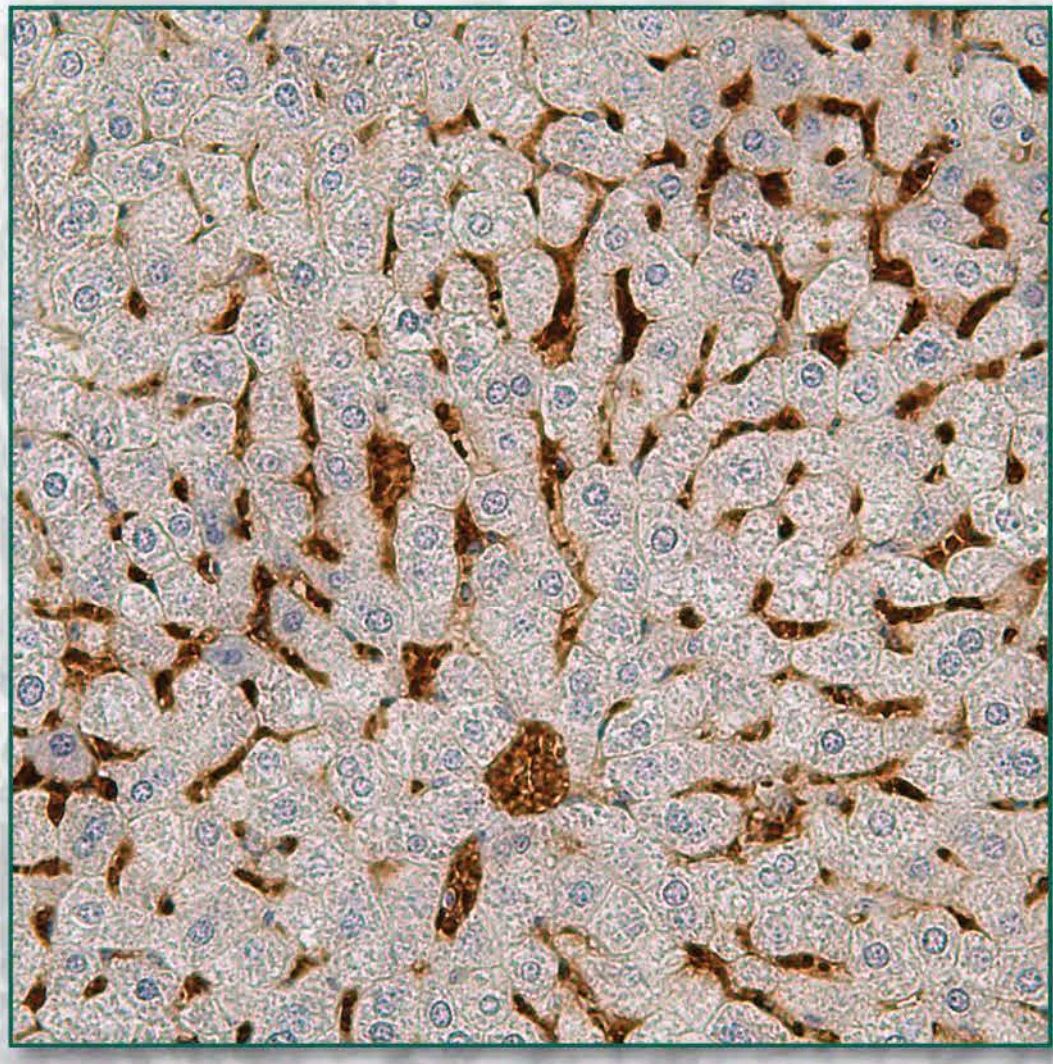

Acta Morphologica et Anthropologica
is the continuation of Acta cytobiologica et morphologica

Indexed in:

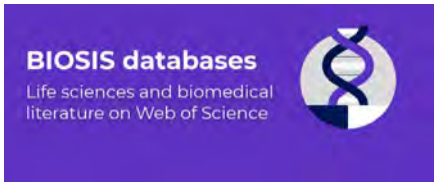

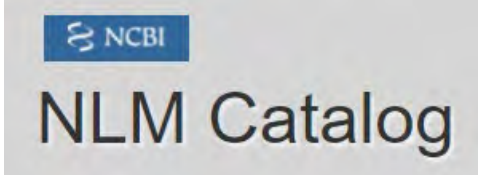

Editorial Correspondence
Institute of Experimental Morphology, Pathology and Anthropology with Museum
Bulgarian Academy of Sciences
Acta Morphologica et Anthropologica
Acad. Georgi Bonchev Str., Bl. 25
1113 Sofia, Bulgaria

E-mail: ama.journal@iempam.bas.bg; yordanka.gluhcheva@iempam.bas.bg; ygluhcheva@hotmail.com

Tel.: +359 2 979 2344

Издаването на настоящия том 33, книжки 1 и 2 е осъществено с финансовата подкрепа на Фонд „Научни изследвания“ по Договор КП-06-НП7/24 от 08.12.2025 г. Фонд „Научни изследвания“ не носи отговорност за съдържанието на материалите

Prof. Marin Drinov Publishing House of Bulgarian Academy of Sciences
Bulgaria, 1113 Sofia, Acad. Georgi Bonchev Str., Bl. 6

Graphic designer: Veronika Tomcheva.
Format 70×100/16 Printed sheets

Printing Office of Prof. Marin Drinov Publishing House of Bulgarian Academy of Sciences
Bulgaria, 1113 Sofia, Acad. Georgi Bonchev Str., Bl. 5

Acta Morphologica et Anthropologica

ISSN 1311-8773 (print)
ISSN 2535-0811 (online)

Acta Morphologica et Anthropologica 33 (1-2)

33 (1-2) ● Sofia ● 2026
Institute of Experimental Morphology, Pathology and Anthropology with Museum
Bulgarian Anatomical Society

Contents

MORPHOLOGY 33 (1)

Original Articles

Review Articles

Original Articles

Review Articles

Institute of Experimental Morphology, Pathology and Anthropology with Museum
Bulgarian Anatomical Society

Acta Morphologica et Anthropologica, 33 (1-2)
Sofia ● 2026

MORPHOLOGY 33 (1)

Original Articles

Altered Hemispheric Lateralization of Heschl's Gyrus in Schizophrenia with Auditory Verbal Hallucinations: A Resting-State fMRI Study

Vyara Zaykova[1], Ferihan Popova[1], Sevdalina Kandilarova[2], Drozdstoy Stoyanov[2]*

[1]Department of Anatomy, Histology and Embryology, Faculty of Medicine, Medical University of Plovdiv, Plovdiv, Bulgaria
[2]Department of Psychiatry and Medical Psychology, Research Institute and SRIPD-MUP, Translational and Computation Neuroscience Group, Faculty of Medicine, Medical University of Plovdiv, Plovdiv, Bulgaria

* Corresponding author e-mail: vyara.zaykova@mu-plovdiv.bg

Hemispheric lateralization plays a crucial role in language and auditory processing, typically showing left-hemispheric dominance. Alterations in this organization have been implicated in schizophrenia, particularly in relation to auditory verbal hallucinations. This study examined hemispheric lateralization of resting-state functional activity in Heschl's gyrus in schizophrenia patients with auditory verbal hallucinations. The sample included 105 participants (42 patients and 63 healthy controls). Resting-state fMRI data were acquired on a 3T scanner and analyzed using the CONN toolbox and SPM12. Seed-based connectivity analyses were conducted for bilateral Heschl's gyrus. Compared with controls, patients showed increased resting-state functional connectivity between the right Heschl's gyrus and the right postcentral gyrus, and between the left Heschl's gyrus and the right lateral occipital gyrus. These results suggest altered intrinsic connectivity of auditory cortical regions in schizophrenia, potentially reflecting disrupted functional lateralization associated with hallucinatory experiences.

Key words: schizophrenia, auditory verbal hallucinations, resting-state, functional magnetic resonance imaging, Heschl's gyrus

Introduction

Hemispheric lateralization is a fundamental organizational principle of the human brain that enables specialized cognitive and perceptual functions to be preferentially processed within one cerebral hemisphere. In healthy individuals, language and auditory processing typically show left-hemispheric dominance, reflecting the asymmetric organization of cortical networks involved in speech perception and production. Disruptions in hemispheric specialization have been proposed as a neurobiological feature of psychiatric disorders and may contribute to disturbances in language and auditory processing [1]. Early theoretical models suggested that abnormal cerebral lateralization may contribute to core cognitive and perceptual disturbances observed in schizophrenia, particularly those involving language and auditory processing [5]. Subsequent neuroimaging studies have supported this view, demonstrating altered structural and functional asymmetries in several cortical regions associated with language and auditory perception [14, 17].

Heschl's gyrus (HG), located on the superior temporal plane of the temporal lobe, contains the primary auditory cortex and represents the first cortical stage of auditory processing. It plays a key role in the analysis of fundamental acoustic properties such as frequency, intensity, and temporal structure that are necessary for the perception of complex sounds, including speech. In healthy populations, HG often shows structural asymmetry with a tendency toward leftward dominance. The region also demonstrates considerable anatomical variability, particularly in gyrification and duplication patterns, which may influence auditory cortical organization. Neuroimaging evidence suggests that atypical gyrification and duplication of HG may be associated with altered auditory processing and may occur more frequently in neuropsychiatric conditions such as schizophrenia [8].

Schizophrenia has been linked to structural and functional abnormalities within temporal lobe regions involved in auditory and language processing. These alterations may contribute to the frequently observed deficits in auditory perception and speech processing. Auditory verbal hallucinations (AVH) are among the most common symptoms of schizophrenia, affecting approximately 60–80% of patients during the course of the illness. AVH involve the perception of voices or speech in the absence of external auditory stimuli and are often experienced as intrusive and distressing. Neuroimaging studies have demonstrated increased activation in auditory cortical regions, including HG and the superior temporal cortex, during hallucinatory episodes [9], supporting the hypothesis that hallucinations may arise from abnormal activity within auditory processing networks.

Resting-state functional magnetic resonance imaging (rs-fMRI) provides an important method for examining intrinsic brain activity and functional connectivity by measuring spontaneous low-frequency fluctuations in the blood-oxygen-level-dependent (BOLD) signal. This approach is particularly useful in clinical populations because it minimizes confounding effects related to task performance. Studies using rs-fMRI have reported widespread connectivity disruptions in schizophrenia [20],

particularly within networks involving frontal and temporal regions [22]. Altered resting-state connectivity between auditory cortex and language-related regions has been associated with the presence and severity of AVH [13]. Additional work has reported disturbances in large-scale brain networks related to hallucinatory states [11] as well as abnormal connectivity involving thalamocortical and auditory cortical pathways in schizophrenia [19]. Structural and functional alterations in temporal cortical regions have also been linked to variations in hallucination severity and phenomenology [4, 7].

Despite increasing interest in the neural mechanisms of AVH, relatively few studies have specifically examined hemispheric lateralization of intrinsic functional activity within HG using resting-state fMRI. Investigating the functional organization of HG in schizophrenia patients experiencing AVH may therefore provide further insight into the neural mechanisms underlying hallucinatory experiences.

The present study aimed to examine hemispheric lateralization of resting-state functional activity in HG in schizophrenia patients experiencing AVH compared with healthy controls (HC) by analyzing intrinsic BOLD signal patterns within bilateral HG.

Material and Methods

Participants

The study included 105 participants (42 schizophrenia patients with auditory verbal hallucinations (AVH) and 63 age- and sex-matched HC), aged 18–61, after excluding five individuals due to poor-quality MRI data. Patients met DSM-5 criteria for schizophrenia and had severe AVH (Positive and negative syndrome scale (PANSS) P3 item > 3). Controls were recruited from the local community and screened to exclude neurological, psychiatric, or cognitive impairments. Additional exclusion criteria for all participants included metallic implants or MRI contraindications. All procedures were approved by the Ethics Committee of Medical University of Plovdiv (Protocol №1/11.01.2024), and written informed consent was obtained in accordance with the Helsinki Declaration.

MRI Acquisition

Imaging was performed on a 3T GE Discovery 750w scanner. High-resolution structural images were acquired using a sagittal 3D T1-weighted sequence (1 mm isotropic voxels, TR = 7.2 ms, TE = 2.3 ms, flip angle = 12°). Resting-state functional images were collected using a 2D EPI sequence (TR = 2s, TE = 30ms, 36 slices, voxel size = 3.44 × 3.44 × 3.5mm^3, 160 volumes). Participants were instructed to keep their eyes closed, remain still, and avoid focused thoughts.

Image Processing and Statistical Analysis

Functional data were preprocessed and analyzed using CONN toolbox 21.a with SPM12 in MATLAB R2024a. Standard preprocessing included motion correction, slice-timing correction, normalization to MNI space, outlier detection, and 8-mm FWHM smoothing. Denoising included regression of white matter and cerebrospinal fluid signals. Seed-based connectivity analyses were conducted for the right and left

HG. Group-level analyses were thresholded at $p<0.05$, FWE-corrected. Demographic and clinical variables were analyzed using IBM SPSS Version 28.0 (NY: IBM Corp). Student's t-test and chi-square test were used for the statistical analysis. The level of statistical significance was set at $p<0.05$ for all tests.

Results

Socio-demographic and clinical characteristics

The study revealed that there were no statistically significant differences between the patients with schizophrenia and the healthy controls with regard to age or sex. Expectedly, due to the early clinical onset of the condition, statistically significant disparities were identified between the two groups with respect to education. As anticipated, the PANSS scores were found to be significantly higher for the patient group than for the control group (**Table 1**).

Table 1. Socio-demographic and clinical characteristics.

	P (n=42)	**HC (n=63)**	**p**
Age (mean, SD)	35.3 ± 12.4	36.0 ± 12.5	**0.770**[a]
Sex (M/F)	26/16	31/32	**0.234**[b]
****Education (primary/ secondary/higher)**	8/26/6	1/33/29	***0.000**[b]
*****PANSSP3 score (mean, SD)**	5.1 ± 0.6	1.0 ± 0.0	***0.000**[a]

P – patients, HC – Healthy controls, SD – Standard Deviation, [a]Student's t-test, [b]$\chi 2$ – test, *p<0.05, **Two of the patients were excluded from the analysis due to missing data on education, ***PANSSP3 score – AVH (Auditory Verbal Hallucinations)

Functional connectivity of the Heschl's gyrus

The comparison between the patients with schizophrenia and the HC revealed increased FC between the right HG and a cluster encompassing the right postcentral gyrus in the patient group as compared to the control group (**Table 2, Figure 1**).

Table 2. Between group differences of functional connectivity of the Right Heschl's Gyrus seed.

Between-group contrast	**MNI coordinates x, y, z**	**Cluster-size**	**Cluster-threshold (*p<0.05*, FWE)**	**Regions within the cluster**
P>HC	+34 -32 +48	211	0.001	Right Postcentral Gyrus

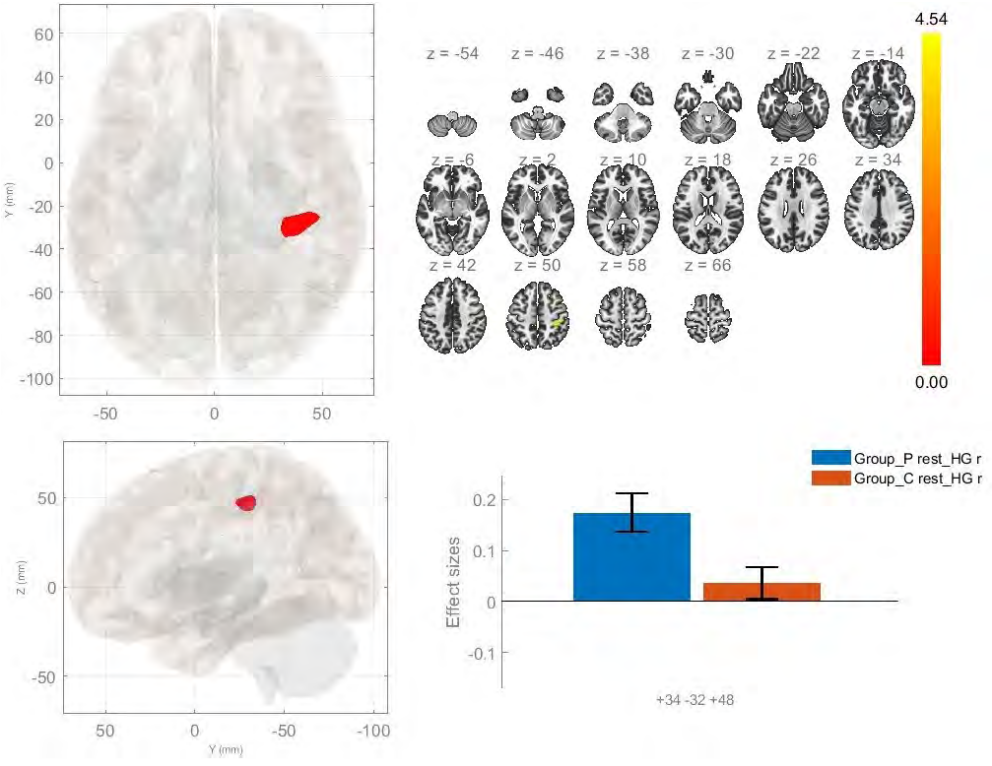

Fig. 1. Functional connectivity of the right Heschl's gyrus seed in schizophrenia compared to the HC group and effect sizes for each significant cluster with a cluster threshold p<0.05 cluster-level FWE correction. Increased rsFC between the right Heschl's gyrus and the right postcentral gyrus (cluster coordinates +34 -32 +48) in the patient group in comparison with HC was observed.

Hyperconnectivity was detected also between the left HG and the right lateral occipital gyrus, superior division in schizophrenia in contrast to the HC (**Table 3, Figure 2**).

Table 3. Between group differences of functional connectivity of the Left Heschl's Gyrus seed.

Between-group contrast	**MNI coordinates x, y, z**	**Cluster-size**	**Cluster-threshold (*p<0.05*, FWE)**	**Regions within the cluster**
P>HC	+36 -62 +38	177	0.002	Right Lateral Occipital Cortex, Superior Division

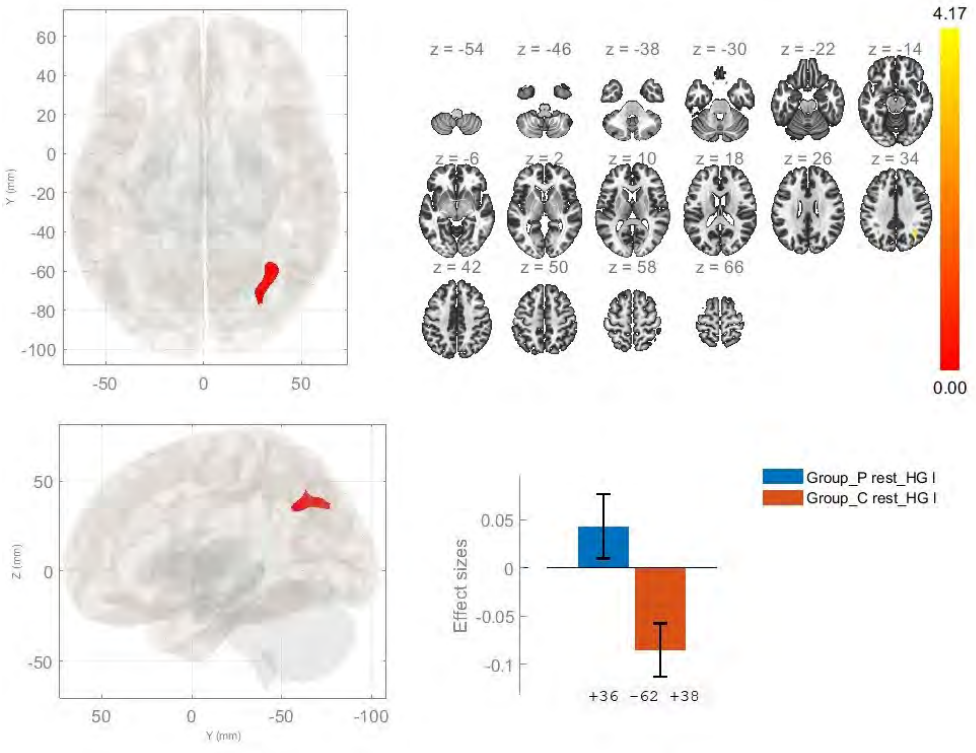

Fig. 2. Functional connectivity of the left Heschl's gyrus seed in schizophrenia compared to the HC group and effect sizes for each significant cluster with a cluster threshold $p<0.05$ cluster-level FWE correction. Increased rsFC between the left Heschl's gyrus and the right lateral occipital cortex, superior division (cluster coordinates +36 -62 +38) in the patient group in comparison with HC was observed.

Furthermore, we repeated the analyses, incorporating the level of education as a covariate of no interest. The results remained consistent in terms of the number of significant clusters, the regions within them, and the peak coordinates. A non-significant change in the size of the clusters was observed, with a reduction amounting to a couple of voxels.

Discussion

The current study identified several significant differences in the rsFC of the HG in patients with AVH as compared to HC. First, an enhanced rsFC was identified between the right HG and the right postcentral gyrus in the patient group in comparison to the control group. Next, we identified hyperconnectivity between the left HG and the superior division of the right lateral occipital cortex in schizophrenia, as opposed to the control group.

The present findings are consistent with the mounting evidence from neuroimaging studies that suggests altered FC in the temporal region. The current analysis revealed increased rsFC between the right HG and the postcentral gyrus in the AVH group. The primary somatosensory cortex is known to be located in the postcentral gyrus. This region has been implicated in the pivotal role of integrating information regarding mouth movements into the process of speech perception [15]. Multiple studies have reported abnormal rsFC between this region and the temporal cortex in schizophrenia [10, 16]. Defective monitoring of inner speech has been identified as a contributing factor to the onset of AVH, and has been linked to the disruption of integration of sensorimotor processing and the processing of auditory information. The elevated risk of experiencing AVH has been demonstrated to be positively correlated with such language-related disturbances [2, 6].

Our findings also identified increased rsFC between the left HG and the right lateral occipital cortex in the patient group. The occipital lobe is known to be involved in phonological and semantic modulation. It has been hypothesized that disturbances in such functions may be indicative of the pathophysiology of schizophrenia. In consideration of the potential relationship between abnormal semantic processing and the development of AVH, the existence of any anomalies in the FC between the occipital lobe and the primary auditory cortex might also serve as a contributing factor to the observed impairments in auditory perception [18]. As postulated by Xue et al., the underlying mechanisms of AVH occurrence in schizophrenia may be associated with aberrant dynamic FC between occipital and temporal regions [21]. The findings of the present study are consistent with those reported in the extant literature, suggesting that aberrant occipito-temporal connectivity may potentially contribute to the development of AVH.

One notable finding of the current study was that the pattern of dysconnectivity in HG was limited to regions of the right hemisphere, thereby indicating a predominant right-hemisphere involvement in AVH. As indicated by previous studies, diminished functional lateralization has been found to demonstrate a negative correlation with the severity of positive symptoms, as measured by the PANSS. Furthermore, reduced left>right language asymmetry has been shown to correlate negatively with the onset of AVH, thus indicating that the reduced lateralization is implicated in the development of AVH [3, 12].

Conclusion

The present study elucidated lateralized impairment in the FC of the right and left HG. Aberrant connections were identified between the explored temporal regions and right postcentral gyrus and right lateral occipital cortex. The observed dysconnectivity lends support to the hypothesis of reduced functional L > R asymmetry in AVH, indicating the reduced functional lateralization as an underlying pathophysiological mechanism in schizophrenia.

Acknowledgments: S.K. and D.S. have been funded by the European Union-NextGenerationEU, through the National Recovery and Resilience Plan of the Republic of Bulgaria, project № BG-RRP-2.004-0007-C03.

References

1. Beshkov, A., M. Topolov, F. Ahmed-Popova, S. Sivkov. A Review of Neuroimaging Studies on Working Memory Paradigms in Patients with Bipolar Disorder. – *Curr. Top. Med. Chem.*, **18**(21), 2018, 1883-1892.

2. Chang, X., G. Collin, Y. Xi, L. Cui, L. H. Scholtens, I. E. Sommer, H. Wang, H. Yin, R. S. Kahn, M. P. van den Heuvel. Resting-state functional connectivity in medication-naïve schizophrenia patients with and without auditory verbal hallucinations: A preliminary report. – *Schizophr. Res.*, **188**, 2017, 75-81.

3. Chen, C., H. Huang, X. Qin, L. Zhang, B. Rong, G. Wang, H. Wang. Reduced inter-hemispheric auditory and memory-related network interactions in patients with schizophrenia experiencing auditory verbal hallucinations. – *Front. Psychiatry.*, **13**, 2022, 956895.

4. Conring, F., N. Gangl, M. Derome, R. Wiest, A. Federspiel, S. Walther, K. Stegmayer. Associations of resting-state perfusion and auditory verbal hallucinations with and without emotional content in schizophrenia. – *Neuroimage Clin*., **40**, 2023, 103527.

5. Crow, T. J. Schizophrenia as failure of hemispheric dominance for language. – *Trends Neurosci*., **20**(8), 1997, 339-343.

6. DeLisi, L. E. Speech Disorder in Schizophrenia: Review of the Literature and Exploration of Its Relation to the Uniquely Human Capacity for Language. – *Schizophr. Bull*., **27** (3), 2001, 481-496.

7. Guo, Z., Z. Zhou, S. Wang, L. Yang, X. Gao, Y. Xia, Y. Yang, Z. Shan, H. Huang, L. Tian. Alterations in sulcal depth and associated functional connectivity in schizophrenia with auditory verbal hallucinations. – *Front. Psychiatry*, **16**, 2025, 1641190.

8. Hubl, D., T. Koenig, W. Strik, L. M. Garcia, T. Dierks, T. Koenig. Structural analysis of Heschl's gyrus in schizophrenia patients with auditory hallucinations. – *Neuropsychobiology*, **61**(1), 2010, 1-9.

9. Jardri, R., A. Pouchet, D. Pins, P. Thomas. Cortical activations during auditory verbal hallucinations in schizophrenia: A coordinate-based meta-analysis. – *Am. J. Psychiatry*., **168**(1), 2011, 73-81.

10. Li, H., W. Zhang, H. Song, L. Zhuo, H. Yao, H. Sun, R. Liu, R. Feng, C. Tang, S. Lui. Altered temporal lobe connectivity is associated with psychotic symptoms in drug-naïve adolescent patients with first-episode schizophrenia. – *Eur. Child Adolesc. Psychiatry*, **34**(1), 2025, 237-247.

11. Mo, F., H. Zhao, Y. Li, H. Cai, Y. Song, R. Wang, Y. Yu, J. Zhu. Network localization of state and trait of auditory verbal hallucinations in schizophrenia. – *Schizophr Bull*., **50**(6), 2024, 1326-1336.

12. **Oertel, V., C. Knöchel, A. Rotarska-Jagiela, R. Schönmeyer, M. Lindner, V. van de Ven, C. Haenschel, P. Uhlhaas, K. Maurer, D. E. J. Linden.** Reduced laterality as a trait marker of schizophrenia--evidence from structural and functional neuroimaging. – *J. Neurosci.* **30**(6), 2010, 2289-2299.
13. **Okuneye, V. T., S. Meda, G. D. Pearlson, B. A. Clementz, M. S. Keshavan, C. A. Tamminga, E. Ivleva, J. A. Sweeney, E. S. Gershon, S. K. Keedy.** Resting state auditory-language cortex connectivity is associated with hallucinations in clinical and biological subtypes of psychotic disorders. - *Neuroimage Clin*., **27**, 2020, 102358.
14. **Petty, R. G.** Structural asymmetries of the human brain and their disturbance in schizophrenia. - *Schizophr Bull*., **25**(1), 1999, 121-139.
15. **Skipper, J. I., H. C. Nusbaum, S. L. Small.** Listening to talking faces: motor cortical activation during speech perception. – *NeuroImage,* **25**, 2005, 76-89.
16. **Skudlarski, P., K. Jagannathan, K. Anderson, M. C. Stevens, V. D. Calhoun, B. A. Skudlarska, G. Pearlson**. Brain connectivity is not only lower but different in schizophrenia: A combined anatomical and functional approach. - *Biol. Psychiatry*, **68**, 2010, 61-69.
17. **Sommer, I. E., A. Aleman, N. F. Ramsey, R. S. Kahn, K. Hugdahl.** Handedness, language lateralisation and anatomical asymmetry in schizophrenia: Meta-analysis. – *Br. J. Psychiatry*., **178**(4), 2001, 344-351.
18. **Tohid, H., M. Faizan, U. Faizan.** Alterations of the occipital lobe in schizophrenia. – *Neuroscience*, **20**, 2015, 213-224.
19. **Williams, J. C., P. N. Tubiolo, R. B. Gil, Z. J. Zheng, E. B. Silver-Frankel, N. K. Haubold, S. K. Abeykoon, D. T. Pham, N. Ojeil, K. Bobchin, M. Slifstein, J. J. Weinstein, G. Perlman, G. Horga, A. Abi-Dargham, J. X. Van Snellenberg.** Auditory and visual thalamocortical connectivity alterations in unmedicated people with schizophrenia: An individualized sensory thalamic localization and resting-state functional connectivity study. – *Biol. Psychiatry Cogn. Neurosci. Neuroimaging*, **10**(12), 2025, 1239-1248.
20. **Xie, Y., M. Guan, Z. Wang, Z. Ma, H. Wang, P. Fang.** Alterations in brain connectivity patterns in schizophrenia patients with auditory verbal hallucinations during low-frequency repetitive transcranial magnetic stimulation. – *Psychiatry Res*.: *Neuroimaging,* **328**, 2023, 115457.
21. **Xue, K., J. Chen, Y. Wei, Y. Chen, S. Han, C. Wang, Y. Zhang, X. Song, J. Cheng.** Altered dynamic functional connectivity of auditory cortex and medial geniculate nucleus in first-episode, drug-naïve schizophrenia patients with and without auditory verbal hallucinations. – *Front. Psychiatry.*, **13**, 2022, 963634.
22. **Zaykova, V., S. Kandilarova, R. Paunova, F. Popova, D. Stoyanov.** Lateralized brain connectivity in auditory verbal hallucinations: fMRI insights into the superior and middle temporal gyri. - *Front. Hum. Neurosci.*, **19**, 2025, 1650178.

Institute of Experimental Morphology, Pathology and Anthropology with Museum
Bulgarian Anatomical Society

Acta Morphologica et Anthropologica, 33 (1-2)
Sofia ● 2026

Malignant Paraganglioma in the Left Parotid Region

Alexander Ivanov [1,2,3], Iliya Bivolarski[1], Mariya Popivanova[1,2,3]*

[1]Department of General and Clinical Pathology, Medical University, Plovdiv, Bulgaria
[2]Department of Clinical Pathology, UMHAT "St. George", Plovdiv, Bulgaria
[3]Regular PhD students in Medical University, Plovdiv, Bulgaria

*Corresponding author e-mail: aleksandar.ivanov@mu-plovdiv.bg

Paragangliomas are rare tumors arising from paraganglionic tissue derived from neural crest cells. In the head and neck region, these tumors most commonly originate from the carotid body, vagal paraganglia or the jugulotympanic area, whereas involvement of the parotid gland is extremely uncommon. We report a case of a 54-year-old male patient presenting with a large infiltrative tumor involving the left parotid region. Computed tomography revealed a heterogenous soft tissue mass extending from the skull base to the level of the fifth cervical vertebra, with invasion of surrounding structures and regional lymphadenopathy. Histopathological examination demonstrated tumor cell nests arranged in a characteristic pattern. Immunohistochemical analysis was also performed for confirmation. The findings determined the diagnosis of malignant paraganglioma. Following surgical treatment, the patient was referred to for postoperative radiotherapy. This case highlights the rarity, aggressive behavior and diagnostic challenges associated with parotid paragangliomas, with only isolated cases described in the literature.

Key words: malignant paraganglioma, parotid, head and neck tumor

Introduction

Paragangliomas (also called extra-adrenal or sympathetic paragangliomas) are rare neuroendocrine tumors originating from paraganglionic cells derived from the neural crest [6, 10]. They are closely related to pheochromocytomas, with a histological similarity as well [5]. Paragangliomas can develop in various anatomical locations along the autonomic nervous system.

Within the head and neck region, paragangliomas most commonly arise from the carotid body, jugulotympanic region, and vagal paraganglia [2, 7]. Involvement of

the parotid gland is exceptionally rare and only a limited number of cases have been described in the literature [2, 8]. Although categorization into benign and malignant is discouraged because all paragangliomas have a metastatic potential [4, 9], depending on the tumor presentation, we can predict its behavior to help determine the treatment and prognosis.

Because of their rarity and nonspecific clinical presentation, malignant paragangliomas may pose a significant diagnostic challenge. Imaging tests combined with histopathological and immunohistochemical examination are essential for establishing the correct diagnosis [5, 9]. Our report describes a rare case of malignant paraganglioma involving the left parotid region.

Case Report

We present a case of a case of a 54-year-old male patient with a massive soft tissue tumor formation detected during computed tomography (CT) examination. The lesion had an irregular shape and was located predominantly in the left parotid region. Radiological evaluation demonstrated that the tumor originated from the skull base on the left side and extended caudally to the level of the fifth cervical vertebra (C5). The lesion showed invasive growth with involvement of the surrounding structures, including the pharynx and larynx, which were displaced to the right. The tumor caused lysis of the skull base and infiltration of the left sternocleidomastoid muscle and the left parotid gland. Extension toward the left cerebellar hemisphere was also observed. The mass had an axial dimension of 5.6 x 8.9 cm and a coronal dimensional of 7.9 cm. The lesion demonstrated a native density of approximately 48 HU (Hounsfield units), increasing to 65-130 HU in the arterial phase and 68-104 HU in the venous phase following contrast administration. Additionally, diffuse packages of cervical and submandibular lymph nodes of varying size were detected bilaterally, with maximal diameters up to 1.5 cm. The patient had previously undergone long-term treatment for benign paraganglioma. Following the recurrence of the tumor and subsequent surgical intervention, the histopathological examination revealed a malignant transformation of the lesion.

Tissue specimens were fixed in 10% neutral buffered formalin and embedded in paraffin. Sections of 4 μm thickness were obtained for histological analysis. Further immunohistochemical testing was performed to confirm the diagnosis using the following antibodies – Synaptophysin, Chromogranin, S-100 protein. All the antibodies are supplied by Dako and are ready-to-use (pre-diluted). The staining protocols are validated by Dako.

Hematoxylin and eosin (H&E) staining revealed: Tumor tissue composed of nests and trabeculae of atypical cells arranged within a richly vascularized stroma, consistent with the characteristics of paraganglioma. The tumor cells are invading the capsule and surrounding tissues (**Figs. 1 and 2**).

Immunohistochemical analysis supported this diagnosis: Synaptophysin: diffuse positive staining (++) in tumor cells, Chromogranin: weak diffuse positivity (+) in tumor cells, S-100 protein: positive staining in sustentacular cells surrounding tumor nests (**Fig. 3**).

The extensive imaging tests combined with the information of the tumor behavior, histological and immunohistochemical panel confirmed the final diagnosis of malignant paraganglioma as supported by the images below:

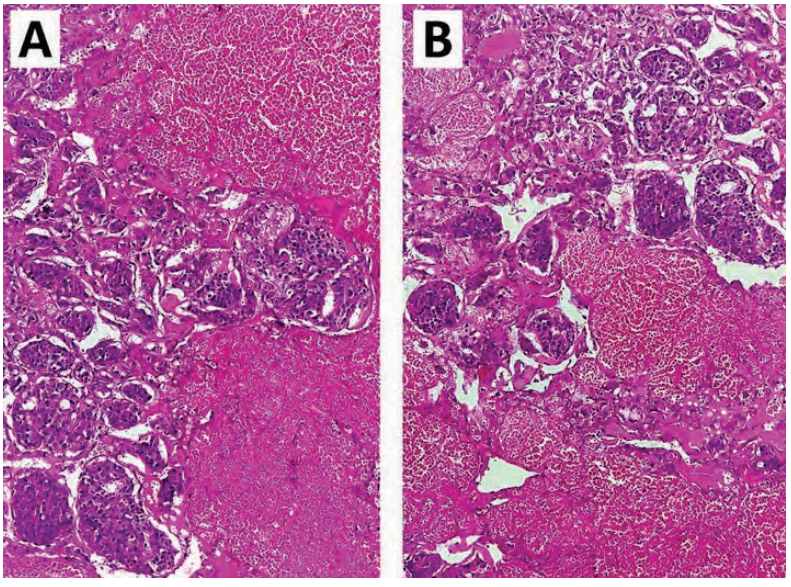

Fig. 1. Both pictures show nests of tumor cells arranged in typical zellballen pattern separated by delicate fibrovascular septa. The cells are polygonal, with eosinophilic cytoplasm and round to oval nuclei. **A.** Vast necrotic areas. (H-E x100). **B.** Lots of hemorrhages (H-E x200).

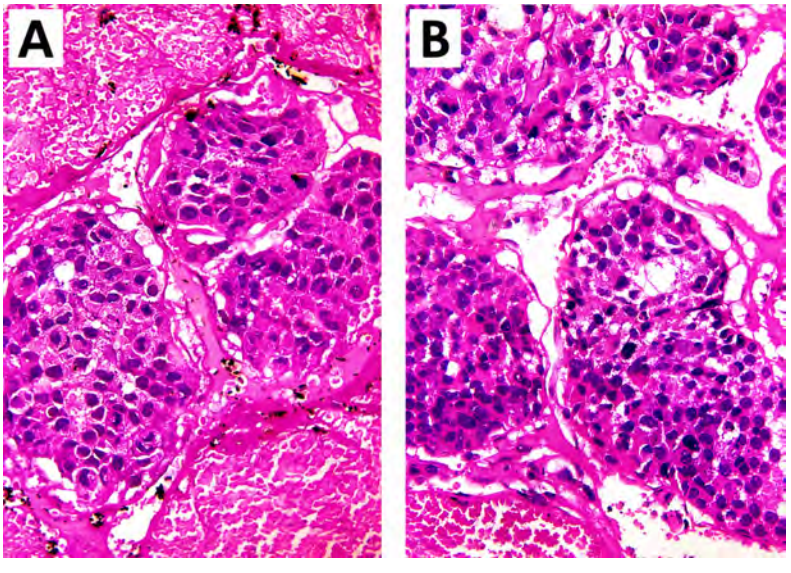

Fig. 2. A. Higher magnification of the same area demonstrates the classic tumor cell pattern, as well as the expressed atypia and mitoses. Necrosis is also seen. (H-E x200). **B.** Emphasis on the vascularized stroma of the tumor. (H-E x400)

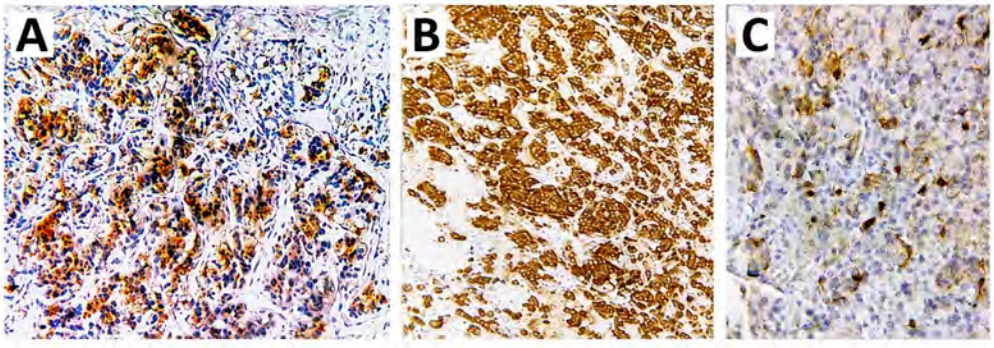

Fig. 3. A. Chromogranin showing diffuse cytoplasmic positivity in tumor cells. **B.** Diffuse cytoplasmic expression of Synaptophysin in tumor cells. **C.** S-100 highlighting sustentacular cells surrounding tumor nests.

Discussion

Paragangliomas of the head and neck represent approximately 0.5% of all tumors in this area [2, 7]. They arise most frequently from the carotid body, jugulotympanic region, and vagal paraganglia [2, 7, 10]. To our knowledge, this is the first reported case of malignant paraganglioma in the parotid region.

Although the majority of paragangliomas exhibit benign biological behavior, malignant transformation can occur in a small percentage of cases [3, 4]. The diagnosis is usually based on imaging, the presence of regional or distant metastases, local invasion, recurrence and histological features.

Radiological imaging plays a crucial role in evaluating tumor extension and its relationship to surrounding structures. Computed tomography and magnetic resonance imaging are particularly useful in assessing the vascularity and extent of the lesions [3, 4].

Histopathological examination is vital for a definitive diagnosis. The typical "zellballen" pattern, consisting of nests of tumor cells separated by fibrovascular septa, is characteristic of paragangliomas [5, 9]. Immunohistochemical markers such as Synaptophysin and Chromogranin confirm neuroendocrine differentiation, while S-100 protein highlights sustentacular cells surrounding tumor nests [5, 9].

Treatment of malignant paraganglioma usually involves surgical resection followed by radiotherapy [4, 8], particularly in cases with incomplete resection or aggressive tumor behavior. Despite treatment, these tumors may demonstrate a tendency for recurrence and metastasis [3, 4].

The differential diagnosis of malignant paraganglioma in the parotid region includes several tumors and tumor-like lesions:

- Vagal schwannoma
- Carotid body paraganglioma
- Metastatic lymphadenopathy

- Medullary thyroid carcinoma
- Hemangioblastoma

Because of the overlapping clinical and radiological features, histopathological examination together with immunohistochemical analysis is essential for establishing the correct diagnosis [7, 8, 10].

The reported 5-year survival of malignant paraganglioma varies depending on the presence of regional or distant metastases, with poorer prognosis in cases with the latter [3, 8].

Conclusion

Malignant paraganglioma of the parotid gland is an extremely rare neoplasm that may present diagnostic and therapeutic challenges. Imaging studies combined with histopathological and immunohistochemical evaluation are essential for establishing the diagnosis. Early detection and appropriate management are crucial due to the potential aggressive behavior, local invasion and recurrence. Reporting rare cases such as this contributes to a better understanding of the biological behavior and clinical management of these tumors, especially in unusual areas like the parotid region.

Patient consent

The authors certify obtaining the patient's consent for using of the information, age and gender, as well as pictures of the microscopic slides.

References

1. **Barnes, L., J. W. Eveson, P. Reichart, D. Sidransky.** *World Health Organization classification of tumours: Pathology and genetics of head and neck tumours*. IARC Press, Lyon, 2017.
2. **Boedeker, C. C., G. J. Ridder, J. Schipper.** Paragangliomas of the head and neck: diagnosis and treatment. – *Fam. Cancer,* **4(1)**, 2005, 55-59.
3. **Erickson, D., Y. C. Kudva, M. J. Ebersold, G. B. Thompson, C. S. Grant, J. van Heerden, W. F. Young Jr**. Benign Paragangliomas: Clinical Presentation and Treatment Outcomes in 236 Patients. – *Clin. Endocrinol. Metab.,* **86 (11)**, 2001, 5210-5216.
4. **Fishbein, L.** Pheochromocytoma and paraganglioma: genetics, diagnosis, and treatment. – *Hematol Oncol Clin North Am.,* **30(1)**, 2016, 135-150.
5. **Krijger, R., A. Tischler, S. Asa, E. Lack, M. Volante**. *Tumors of the adrenal glands and extra-adrenal paraganglia. Atlases of tumor and non-tumor pathology*, 2024 .
6. **Lloyd, R. V., R.Y. Osamura, G. Klöppel, K. Rosai.** *WHO Classification of tumours of endocrine organs.* IARC Press, Lyon, 2017.

7. Offergeld, C., C. Brase, S. Yaremchuk, I. Mader, H. C. Rischke, S. Gläsker, K.W. Schmid, T. Wiech, S. F. Preuss, C. Suárez, T. Kopeć, A. Patocs, N. Wohllk, M. Malekpour, C. C. Boedeker, H. P. Neumann. Head and neck paragangliomas: clinical and molecular genetic classification. – *Clinics (Sao Paulo)*, **67**, 2012, 19-28.

8. Palade, D. O, R. Hainarosie, A. Zamfir, D. Vrinceanu, M. Pertea, M. Tusaliu, F. Mocanu, C. Voiosu. Paragangliomas of the head and neck: A Review of the latest diagnostic and treatment methods. – *Medicina (Kaunas),* **60,** 2024, 914.

9. Pathology Outlines.com website. Paraganglioma.

10. Tischler, A. S. Pheochromocytoma and extra-adrenal paraganglioma: updates. – *Arch. Pathol. Lab. Med.,* **132(8)**, 2008 1272-1284.

Institute of Experimental Morphology, Pathology and Anthropology with Museum
Bulgarian Anatomical Society

Acta Morphologica et Anthropologica, 33 (1-2)
Sofia ● 2026

Morphological Assessment for Application of Biopuncture and Myofascial Release in Lumbar Hernia Rehabilitation-Case report

Daniela Kovacheva-Predovska[1], Shengyun Halil[2]

[1]Department of Physical Medicine and Rehabilitation, Medical University-Sofia, Bulgaria
[2]Department of Neurosurgery, University Hospital "Saint Anna"Sofia, Bulgaria

*Corresponding author e-mail: didi.kovacheva@gmail.com

Lumbar disc herniation is a prevalent spinal disorder associated with low back pain, radiculopathy, and functional impairment. This report describes a 36-year-old patient presenting with low back pain and tibial paresis who underwent a 4-month, protocol-based rehabilitation program. Morphological assessment of degenerative changes in lumbar spine by MRI was applied for development of novel therapeutic approach integrated biopuncture (Traumeel SR, Lyphomiosot, Discus Compositum), myofascial release therapy, analytical gymnastics and electrotherapeutic modalities including magnetotherapy and transcutaneous electrical nerve stimulation (TENS). Clinical outcomes were evaluated using the Visual Analog Scale (VAS), manual muscle testing(MMT), the Timed Up and Go test, and the Roland–Morris Disability Questionnaire. The patient demonstrated substantial reductions in pain and muscle hypertonicity, improved gait control, and enhanced overall functional status. This case underscores the potential value of multimodal rehabilitation strategies based on patho-morphological assessment using MRI in the management of lumbar disc–related low back pain.

Key words: biopuncture, MRI scan, lumbar disc herniation, myofascial release therapy

Introduction

Approximately 80% of individuals experience low back pain over their lifetime, generating more than $100 billion in annual healthcare expenditures in the United States. The condition affects 1–3% of the population each year, with peak prevalence among adults aged 30–50 [8]. Lumbar disc herniation constitutes a major contributor to this burden, leading to substantial reductions in functional capacity and quality of life. Low

back pain is further associated with psychological comorbidities such as depression and anxiety**,** both of which may adversely influence clinical outcomes [2]. We performed morphological assessment of degenerative changes in lumbar spine by MRI for development of novel strategy for treatment and rehabilitation of lumbar hernia.

Case report

A 36-year-old woman with obesity presented with severe low back pain, right ankle pain, numbness along the right lower limb, and progressive gait impairment. She had completed a 6-day course of NSAIDs (nonsteroidal anti-inflammatory drugs), mannitol, dexamethasone, and B-complex vitamins in a Neurology department prior to admission.

On examination, she was alert, cooperative, and fully oriented, with intact cranial nerve function. Gait was cautious with a mild right-sided limp, and pain intensified with exertion and transitions from sitting to standing. The straight-leg-raise test was positive on the right at 30–40°, eliciting radiating pain along the sciatic nerve to the lateral foot.

Sensory assessment demonstrated pain, paresthesias, and hypoesthesia in the right S1 dermatome, with a Visual Analog Scale (VAS) score of 9. Motor testing revealed mild weakness of right plantar flexion (m. triceps surae), graded 3/5 on manual muscle testing, and reduced performance on toe-walking, while dorsiflexion remained preserved. The deficit pattern was consistent with tibial nerve involvement secondary to S1 root compression. The right Achilles reflex was diminished; patellar reflexes were symmetric. No pathological reflexes were present, and sphincter control was intact. The clinical findings were indicative of right-sided S1 radiculopathy with mild tibial paresis.

Morphological observations by MRI of the lumbosacral spine demonstrated degenerative changes of the L5–S1 intervertebral disc, characterized by reduced T2 signal intensity and decreased disc height. A right-sided paramedian disc herniation with a broad base was identified, extending into the right lateral recess and compressing the right S1 nerve root, accompanied by deformation of the adjacent dural sac (**Figs. 1, 2**).

The patient completed two rehabilitation courses, the first lasting 7 days and the second 10 days, separated by an interval of approximately 15 days. The rehabilitation program consisted of transcutaneous electrical nerve stimulation (TENS)**,** magnetotherapy**,** biopuncture (Lymphomiosot, Discus Compositum, Traumeel SR), and kinesitherapy with emphasis on myofascial release techniques. During the initial course, the patient additionally received dexamethasone according to a structured regimen. Following completion of the first rehabilitation phase, pregabalin 75 mg was prescribed for one month, alongside ibuprofen as needed and a proton pump inhibitor.

Clinical evaluation demonstrated a significant reduction in pain intensity, accompanied by improved lower-limb muscle strength, mobility, and gait performance**.**

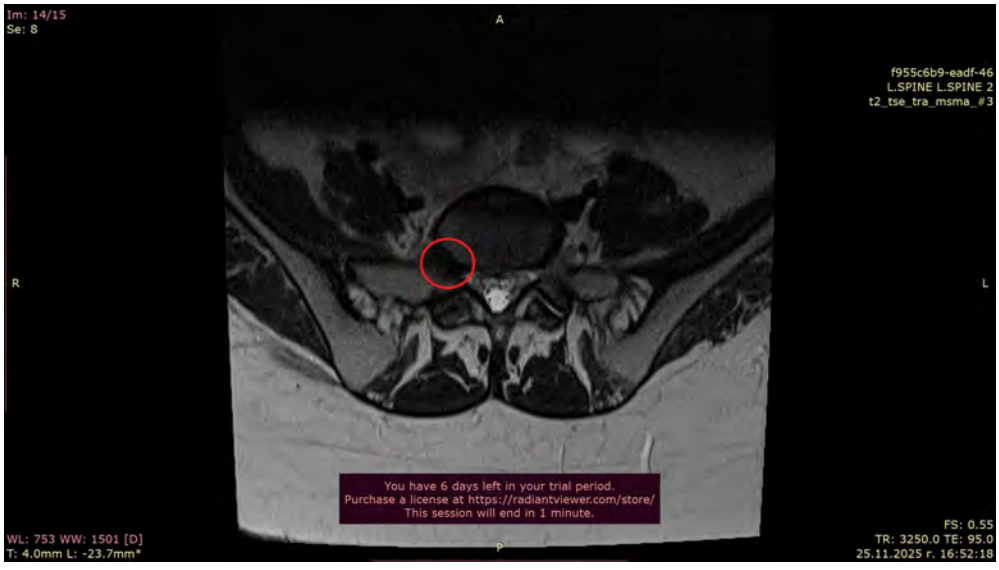

Fig. 1. Axial MRI at L5–S1 showing a right paramedian disc herniation with mass effect on the S1 nerve root.

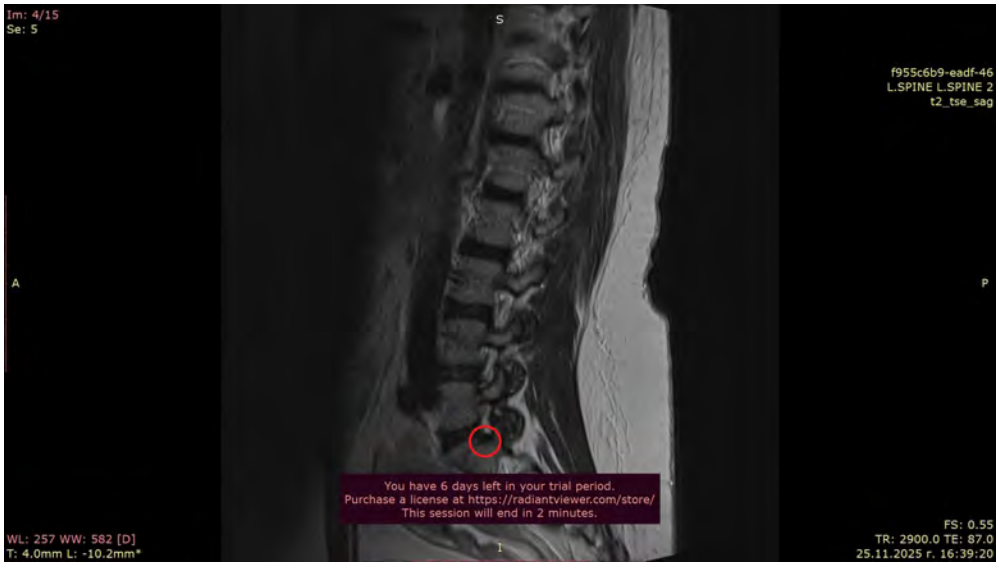

Fig. 2. Sagittal T2weighted MRI of the lumbar spine showing degenerative changes and a rightsided paramedian L5–S1 disc herniation with mass effect on the S1 nerve root.

These functional gains were associated with a measurable enhancement in overall quality of life. The outcomes are summarized in **Table 1**.

Table1. Clinical Measures at Beginning and End of treatment

Measure	Beginning of the treatment	End of the treatment
VAS	9	3
MMT	3	5
TUG	40 sec.	15 sec.
Roland–Morris Disability Questionnaire	19	4

Discussion

The presented clinical case is particularly valuable, as it demonstrates a situation in which the severity of clinical symptoms and patho-morphological imaging findings would suggest surgical treatment, yet significant improvement is achieved through a multimodal conservative approach. The patient presents with pronounced pain syndrome, radicular symptoms along the course of S1, and the presence of a motor deficit – a combination that in clinical practice is often interpreted as a relative indication for surgical decompression.

A key aspect of the case is the discrepancy between the patho-morphological imaging findings and the clinical outcome. The presence of nerve root compression and dural sac deformation on MRI does not lead to progression; on the contrary, it leads to clinical improvement following conservative therapy. This corresponds to contemporary data showing that morphological changes do not always correlate with symptoms and prognosis, which limit their value as an independent predictor for therapeutic decisions [1, 3].

Modern pathophysiological concepts consider lumbar disc herniation as a multifactorial condition. In addition to mechanical compression, inflammatory and biochemical mechanisms play a key role. The herniated disc material induces the release of pro-inflammatory cytokines, such as TNF-α, IL-1β, and IL-6, which lead to sensitization of neural structures and sustain the pain syndrome [6]. This explains the clinically observed discrepancy between the degree of compression and the severity of symptoms. Additionally, there is evidence that the inflammatory process is also involved in the spontaneous resorption of disc material, observed in a significant percentage of patients (up to 60–90%), which accounts for the potential for a favorable outcome with conservative treatment [9]. This emphasizes the need for careful individualization of the therapeutic approach.

In this context, the choice of therapy targeting the inflammatory component can be pathophysiologically justified. Biopuncture, although with a limited high-quality

evidence base, can be considered as a method for local modulation of inflammation and pain. Some experimental and clinical data indicate that the used preparations have the potential to influence pro-inflammatory mediators and support regulatory processes [4]. The myofascial component is also of essential importance. Secondary musculoskeletal-fascial disorders, including increased muscle tone and the formation of trigger points, can maintain the pain syndrome independent of the primary disc pathology. Contemporary systematic reviews show that myofascial release can lead to a statistically significant reduction in pain and improvement in function in patients with lumbar pain [7].

From the perspective of clinical behavior, the presented case supports the recommendation that indications for surgical treatment should be based primarily on clinical dynamics. Contemporary guidelines emphasize that surgery is indicated in the presence of progressive neurological deficit or persistent, therapy-resistant pain [3, 5]. In this case, the absence of deterioration and the reported improvement indicate that the mechanical compressive factor is not dominant and does not necessitate surgical intervention.

Conclusion

In conclusion, the case illustrates how morphological assessment by MRI can help for contemporary understanding of lumbar disc herniation as a multifactorial condition in which mechanical, inflammatory, and myofascial factors interact. It emphasizes the importance of an integrated therapeutic approach and demonstrates that conservative treatment can be effective even in the presence of a neurological deficit.

References

1. **Brinjikji, W., F. E. Diehn, J. G. Jarvik, C. M. Carr, D. F. Kallmes, M. H. Murad, et al.** MRI findings of disc degeneration are more prevalent in adults with low back pain than in asymptomatic controls: A systematic review and meta-analysis. – *Am. J. Neuroradiol*., **36**, 2015, 2394-2399.
2. **Cao, L., B. Deng, X. Wang, T. Fang, K. A. N. Umoh, L. Liu, et al.** The potential relationship between low back pain and depression: A comprehensive review. – *Brain Behav.,* **15**, 2025, e71026.
3. **Foster, N. E., J. R. Anema, D. Cherkin, R. Chou, S. P. Cohen, D. P. Gross, et al.** Prevention and treatment of low back pain: evidence, challenges, and promising directions. – *Lancet,* **391**, 2018, 2368-2383.
4. **Grech, D., J. Velagala, D. J. Dembek, B. Tabaac.** Critical literature review of the homeopathic compound traumeel for treatment of inflammation. – *Pharmacol. Pharm.,* **9**, 2018, 67-83.
5. **National Institute for Health and Care Excellence (NICE)**. Low back pain and sciatica in over 16s: assessment and management. 2020. Available at https://www.nice.org.uk/guidance/ng59

6. Takahashi, H., T. Suguro, Y. Okazima, M. Motegi, Y. Okada, T. Kakiuchi. Inflammatory cytokines in the herniated disc of the lumbar spine. – *Spine (Phila Pa 1976)*, **21**, 1996, 218-24

7. Wu, Z., Y. Wang, X. Ye, Z. Chen, R. Zhou, Z. Ye, et al. Myofascial release for chronic low back pain: A systematic review and meta-analysis. – *Front. Med. (Lausanne),* **8**, 2021.

8. Zhang, A. S., A. Xu, K. Ansari, K. Hardacker, G. Anderson, D. Alsoof, et al. Lumbar Disc Herniation: Diagnosis and Management. – *Am. J. Med.,* **136**, 2023, 645–651.

9. Zhong, M., J. T. Liu, H. Jiang, W. Mo, P.-F. Yu, et al. Incidence of spontaneous resorption of lumbar disc herniation: a meta-analysis - systematic review. – *Pain Physician*, **20**, 2017, E45-E52.

Institute of Experimental Morphology, Pathology and Anthropology with Museum
Bulgarian Anatomical Society

Acta Morphologica et Anthropologica, 33 (1-2)
Sofia ● 2026

Review Articles

Immunohistochemical and Molecular Biomarkers Bridging Pathogenesis and Precision Medicine in Endometrial Carcinoma: A Systematic Review

Gergana Trenova[1], Neli Doneva[2], Angelina Mollova-Kyosebekirova[1], Ekaterina Uchikova[2], Anna Mihaylova[3], Mariya Koleva-Ivanova[1], Mariana Parahuleva[4], Nikoleta Parahuleva[2]*

[1] Department of General and Clinical Pathology, Medical University of Plovdiv, Plovdiv, Bulgaria

[2] Department of Obstetrics and Gynecology, Faculty of Medicine, Medical University of Plovdiv, Plovdiv, Bulgaria

[3] Department of Healthcare Management, Faculty of Public Health, Medical University of Plovdiv, Plovdiv, Bulgaria

[4] Universitätsklinikum Gießen und Marburg Standort Marburg, Marburg, Germany

*Corresponding author e-mail: gergana.trenova@mu-plovdiv.bg

Endometrial carcinoma is a heterogeneous malignancy driven by diverse molecular alterations. Immunohistochemical and molecular biomarkers have increasingly been incorporated into diagnostic algorithms, linking histopathology with genomic profiling and facilitating precision oncology. This systematic searching approach followed PRISMA 2020 guidelines and was registered in PROSPERO (CRD420251184261). A comprehensive search of PubMed, Scopus, Web of Science, ScienceDirect, and Google Scholar (January 2000–March 2025) identified studies evaluating immunohistochemical and/or molecular biomarkers in atypical endometrial hyperplasia/endometrioid intraepithelial neoplasia or endometrial carcinoma. Fifty-nine studies met the inclusion criteria. Investigated biomarkers included PTEN, PAX2, β-catenin, p53, mismatch repair proteins, HER2, ER, PR, Ki67, and PD-L1. These markers delineate the molecular continuum from precursor lesions to invasive carcinoma and correspond closely to The Cancer Genome Atlas molecular subtypes. MMR deficiency and PD-L1 expression predict response to immune checkpoint inhibitors, whereas HER2 amplification characterizes aggressive serous carcinoma. PTEN and PAX2 loss characterized AEH/EIN, while p53 abnormalities identify copy-number-high tumors associated with adverse prognosis.

Key words: Endometrial carcinoma; atypical endometrial hyperplasia; immunohistochemistry; molecular biomarkers; TCGA classification.

Introduction

Endometrial carcinoma (EC) is the most common malignancy of the uterine corpus and remains a major global health burden, with incidence continuing to rise due to increasing life expectancy, obesity, metabolic syndrome, and hormonal factors [36,41]. Although many cases are diagnosed at an early stage and associated with favorable outcomes, a substantial proportion exhibit biologically aggressive behavior characterized by high-grade histology, deep myometrial invasion, lymphovascular space involvement, and metastatic potential. Improving diagnostic accuracy and refining risk stratification are therefore essential for optimizing management and outcomes.

Historically, EC has been categorized according to the dualistic Bokhman model, dividing tumors into estrogen-dependent endometrioid (Type I) and estrogen-independent non-endometrioid (Type II) groups [5]. While this framework provided important clinical distinctions, accumulating evidence demonstrates that EC represents a heterogeneous disease continuum rather than two discrete entities. The advent of molecular profiling—particularly the landmark genomic classification proposed by The Cancer Genome Atlas (TCGA)—has fundamentally reshaped our understanding of EC biology. TCGA delineates four molecular subtypes: POLE-ultramutated, mismatch repair-deficient/microsatellite instability-high (dMMR/MSI-H), p53-abnormal (copy-number high), and no specific molecular profile (NSMP), each associated with distinct clinical behavior, treatment response, and prognosis [12, 23, 39, 44].

Immunohistochemistry (IHC) has emerged as a practical surrogate for genomic testing, offering a cost-effective and clinically accessible means of implementing molecular classification. Markers such as PTEN, PAX2, β-catenin, p53, MMR proteins, ER, PR, HER2, Ki67, and PD-L1 provide insights into the pathways driving carcinogenesis and enable clearer distinction between precursor lesions and invasive carcinoma. Atypical endometrial hyperplasia/endometrioid intraepithelial neoplasia (AEH/EIN), the precursor of most endometrioid carcinomas, is frequently associated with PTEN and PAX2 loss, as well as activation of PI3K/AKT and Wnt/β-catenin signaling pathways [30,40,46]. In contrast, endometrial glandular dysplasia (EmGD), a precursor of serous carcinoma, is characterized by aberrant p53 overexpression and HER2 amplification [1, 21].

Given the molecular diversity of EC and the increasing emphasis on precision oncology, integrating immunohistochemical and molecular biomarkers into diagnostic and therapeutic decision-making has become essential. This systematic review synthesizes current evidence on key biomarkers involved in endometrial carcinogenesis, evaluates their diagnostic, prognostic, and predictive roles, and contextualizes them within the modern molecular classification framework.

This systematic searching approach was conducted in accordance with PRISMA 2020 guidelines and was prospectively registered in PROSPERO (CRD420251184261).

1. PRISMA-Based Systematic Review Approach

1.1. Study design

This study was conducted as a systematic review following the Preferred Reporting Items for Systematic Reviews and Meta-Analyses (PRISMA 2020) guidelines. The review protocol was prospectively registered in the International Prospective Register of Systematic Reviews (PROSPERO; Registration ID: CRD420251184261).

1.2. Eligibility criteria

Studies were included if they met the following criteria:

1. **Population:** Human subjects with atypical endometrial hyperplasia/ endometrioid intraepithelial neoplasia (AEH/EIN) or endometrial carcinoma.
2. **Concept:** Evaluation of immunohistochemical and/or molecular biomarkers.
3. **Context:** Original studies involving diagnostic, prognostic, predictive, or translational biomarker assessment.
4. **Study type:** Clinical, translational, molecular, or systematic research.
5. **Language:** Published in English.
6. **Availability:** Full-text accessible.

Exclusion criteria:

- Animal or *in vitro* studies;
- Case reports, editorials, commentaries, letters, conference abstracts;
- Studies lacking clear methodology or biomarker assessment;
- Non-original articles unless containing pooled biomarker data.

1.3. Information sources

A comprehensive search was conducted across the following databases:

- PubMed
- Scopus
- Web of Science
- ScienceDirect
- Google Scholar

The search covered the period January 2000 to March 2025. Additionally, reference lists of all eligible studies and recent reviews were manually screened to identify further relevant articles.

1.4. Search strategy

The search strategy combined controlled vocabulary (MeSH terms) and free-text keywords. The full PubMed search string (as required by PRISMA) was: (“endometrial carcinoma” or “endometrial cancer”) and (“biomarker” or “immunohistochemistry” or “molecular classification”) and (“atypical endometrial hyperplasia” or “endometrioid intraepithelial neoplasia”). Reference lists of included studies and relevant reviews were also screened manually to identify additional eligible sources. Equivalent search

terms were adapted for Scopus, Web of Science, ScienceDirect, and Google Scholar. The complete set of search strategies for all databases will be included in **Appendix 1**.

1.5. Selection process

Two independent reviewers (Reviewer A and Reviewer B) screened titles and abstracts for potential eligibility. Full texts were retrieved when eligibility could not be determined from abstracts alone. Disagreements were resolved through discussion and consensus. A PRISMA flow diagram illustrates the selection process, the number of records identified, screened, included, and excluded.

1.6. Data extraction

Data were extracted using a standardized form and included:

- authors and publication year;
- study design and sample size;
- population characteristics;
- biomarker type (IHC, molecular, or combined);
- methodology details;
- molecular classification when available;
- diagnostic, prognostic, and predictive implications.

Extraction was performed independently by two reviewers; discrepancies were resolved by consensus

1.7. Risk of bias assessment

Given the scope and purpose of this review - synthesizing mechanistic and translational biomarker evidence - standardized risk-of-bias tools (ROBINS-I, QUADAS-2, Cochrane RoB) were deemed not applicable. This is consistent with PRISMA 2020 guidelines for reviews that analyze heterogeneous biomarker studies without comparative clinical outcomes.

A narrative appraisal of study quality was performed where applicable.

1.8. Synthesis methods

Due to heterogeneity in study designs, biomarkers evaluated, laboratory methods, antibody clones, and scoring systems, meta-analysis was not feasible. Therefore, a narrative synthesis was conducted, organized by:

- biomarker function (diagnostic, prognostic, predictive);
- molecular subtype (POLE-mutated, dMMR/MSI-H, p53-abnormal, NSMP);
- relevance to precursor lesions (AEH/EIN, EmGD).

Quantitative summaries were provided where possible.

1.9. Certainty of evidence

The GRADE framework was not applicable because no pooled effect estimates or meta-analytic comparisons were performed. Instead, certainty of evidence was addressed descriptively based on study quality, methodological consistency, and reproducibility of biomarker findings.

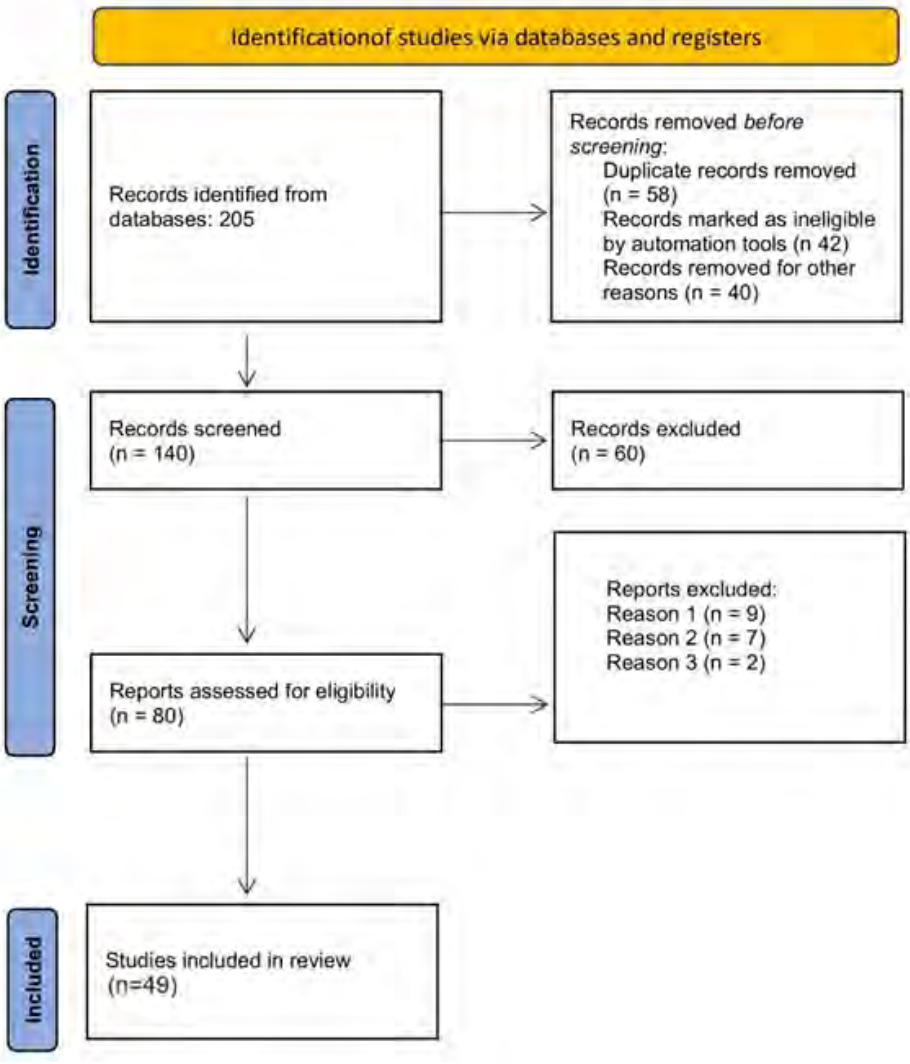

Fig. 1. PRISMA flow diagram summarizing search, screening, inclusion, and exclusion steps. The literature search identified 205 records; after removing duplicates and screening for relevance, 49 studies met inclusion criteria.

2. Data from systematic review

2.1. Study selection

The database search yielded 205 records. After removing duplicates and screening titles and abstracts, 78 articles were retrieved for full-text assessment. Of these, 49

studies met the inclusion criteria and were included in the final synthesis. A PRISMA flow diagram **(Fig. 1)** provides a detailed summary of the identification, screening, eligibility assessment, and inclusion process.

2.2. Study characteristics

The 49 included studies comprised clinical investigations, molecular analyses, immunohistochemical evaluations, and combined IHC–genomic assessments. The most frequently investigated biomarkers included PTEN, PAX2, β-catenin, p53, mismatch repair (MMR) proteins (MLH1, MSH2, MSH6, PMS2), HER2, ER, PR, Ki67, PD-L1, and POLE mutations. The studies covered a wide spectrum of precursor lesions (AEH/EIN, EmGD) and endometrial carcinoma subtypes (endometrioid, serous, mixed, and molecularly annotated EC). **Tables 2 and 3** summarize the principal biomarkers, their clinical applications, key findings, and representative studies.

2.3. Risk of bias in included studies

As detailed in the Methods section, formal risk-of-bias tools (e.g., QUADAS-2, ROBINS-I) were not applicable due to the mechanistic and heterogeneous nature of biomarker studies. Nevertheless, variability across studies was observed in:

IHC antibody clones and staining protocols, scoring thresholds for biomarker positivity, availability of molecular confirmation (e.g., sequencing for POLE, TP53, CTNNB1), reporting completeness.These factors were considered during narrative synthesis.

2.4. Individual study results

2.4.1. Diagnostic biomarkers in precursor lesions (AEH/EIN and EmGD)

PTEN and PAX2 loss were consistently associated with AEH/EIN and early neoplastic transformation. β-catenin nuclear localization was linked to progression risk in EIN. In contrast, EmGD lesions demonstrated aberrant p53 expression and HER2 amplification, mirroring serous carcinoma profiles.

2.4.2. Biomarker distribution across molecular subtypes

The biomarkers aligned with the TCGA classification:

POLE-ultramutated tumors: high TILs, elevated PD-L1, excellent prognosis.

dMMR/MSI-H tumors: loss of MMR proteins, hypermutation, increased immunogenicity.

p53-abnormal tumors: TP53 mutations, HER2 amplification, high-grade serous morphology.

NSMP tumors: PTEN, PIK3CA, and CTNNB1 alterations, often low-grade endometrioid morphology.

2.4.3. Prognostic biomarkers

p53 abnormalities strongly correlated with poor outcomes.

ER/PR loss was associated with dedifferentiation and reduced hormonal responsiveness.

Ki67 index correlated with proliferative activity and tumor aggressiveness.

POLE mutations predicted excellent survival independent of traditional risk factors.

2.4.4. Predictive biomarkers

MMR deficiency and PD-L1 expression predicted response to immune checkpoint inhibitors.

HER2 amplification supported the use of anti-HER2 targeted therapy in serous EC.

AMH/AMHRII remained experimental without sufficient clinical validation.

2.4.5. Quantitative summary

Among the included studies, diagnostic biomarkers were the most freguently investigatedq followed by prognostic and predictive biomarkers, 10 (18%) on predictive markers. Across predictive studies. PD-L1, MMR status, and HER2 amplification demonstrated the strongest correlation with therapeutic responsiveness.

2.5. Synthesis of results

The combined evidence highlights a clear molecular continuum linking AEH/EIN to endometrioid carcinoma and EmGD to serous carcinoma. Immunohistochemical surrogates offer a practical and cost-effective alternative to genomic sequencing for molecular classification. Integration of biomarker expression with TCGA subtypes enhances diagnostic reproducibility, refines risk stratification, and informs tailored therapeutic approaches. **Tables 2, 3 and 4** provide a consolidated overview of biomarker functions, molecular associations, and clinical implications across included studies.

Table 2. Overview of principal immunohistochemical and molecular biomarkers in endometrial carcinoma and their translational relevance across early detection, personalized therapy, and prognostic stratification.

Key benefit / topic	Area of application / Significance	Representative References (updated numbering)
Early detection and diagnosis	Early recognition and histopathologic correlation in precursor and preclinical disease; screening and risk-reducing management; identification of atypical hyperplasia / EIN.	Talhouk A et al. [42]; McConechy MK et al. [26]; Mutter GL [29]; Bagaria M et al. [3]; Cabrera S et al. [9]
Personalized treatment plans	Genomic reclassification of EC and identification of actionable alterations; integration of molecular and IHC markers for post-surgical adjuvant treatment and predictive modelling.	TCGA / Getz G et al. [14]; Stelloo E et al. [39]; Mitric C, Bernardini MQ [27]; Le Gallo M et al. [21]

Key benefit / topic	Area of application / Significance	Representative References (updated numbering)
Improved prognosis	Enhanced prognostic assessment through molecular markers; favorable outcomes associated with POLE exonuclease mutations; validation of grading systems within molecular subtypes.	Raffone A et al. [33]; McConechy MK et al. [26]; León-Castillo A et al. [23]
Targeted therapies	Development and repurposing of hormonal, HER2-targeted and immune therapies; identification of actionable genomic profiles enabling therapy selection and trials.	Ross DS et al. [34]; Buza N, Hui P [7,8]; Aoki D et al. [2]; Getz G et al. [14]
Better risk stratification	Integration of MSI/MMR, PI3K-AKT, Wnt/β-catenin and TP53 pathways for risk assessment; PTEN alterations as early markers for high-risk lesions.	Stelloo E et al. [39]; Zighelboim I / McConechy MK context [26]; Hecht JL, Mutter GL [16,30]
Prevention of disease progression	Optimized management of endometrial hyperplasia to prevent malignant transformation; comparative evaluation of guidelines and long-term surveillance strategies.	Gallos ID et al. [13]; Restaino S et al. [33]; Muñoz Sánchez R et al. [28]

The results demonstrate a clear molecular continuum from precursor lesions to invasive carcinoma. Early alterations such as PTEN and PAX2 loss, frequently observed in AEH/EIN, represent some of the earliest molecular events in endometrioid carcinogenesis and align with previous reports describing their diagnostic utility [25, 30, 46]. Activation of the Wnt/β-catenin pathway, driven by CTNNB1 mutations, was also implicated in the transition from EIN to carcinoma, consistent with earlier molecular and immunohistochemical studies [18, 35, 48].

In contrast, lesions along the serous pathway exhibited aberrant p53 expression and HER2 amplification, consistent with their established roles in serous EC and its precursor, endometrial glandular dysplasia (EmGD) [1, 21, 47]. These biomarker patterns strongly correspond to the four TCGA molecular subtypes—POLE-ultramutated, MMR-deficient/MSI-H, p53-abnormal, and NSMP—each characterized by distinct genetic drivers, immunohistochemical profiles, and prognostic implications [12 ,42, 44].

Table 3. Representative studies evaluating immunohistochemical and molecular biomarkers in endometrial hyperplasia and carcinoma (n = 15)

Biomarker	Study/Year	Study Type	Sample/ Population	Key Findings	Clinical Application
PTEN	Sun et al., 2001 [40]	Clinical	AEH and EC (n=75)	PTEN loss observed in >60% of AEH and 80% of EC; early event in carcinogenesis	Diagnostic / early alteration
β-catenin (CTNNB1)	Travaglino et al., 2019 [46]	IHC + molecular	AEH/EIN (n=82)	Nuclear localization correlates with carcinoma progression	Risk stratification
PAX2	Raffone et al., 2019 [33]	Systematic review	Meta-analysis (10 studies)	PAX2 loss marks early neoplastic change	Diagnostic marker
p53	Jamieson et al., 2021 [19]	Review	EC molecular subtypes	Abnormal p53 defines copy-number-high group; poor prognosis	Prognostic / classification
MMR proteins (MLH1, MSH2, MSH6, PMS2)	McConechy et al., 2015 [26]	IHC	EC (n=97)	MMR loss predicts MSI-High phenotype and immunotherapy response	Predictive marker
HER2	Ross et al., 2022 [35]	IHC + FISH	Serous EC (n=110)	HER2 amplification in ~30% serous EC; targetable alteration	Predictive / therapeutic
ER/PR	Masjeed et al., 2017 [25]	IHC	EC and hyperplasia	ER/PR loss correlates with higher grade and dedifferentiation	Prognostic / therapy guidance
Ki67	Masjeed et al., 2017 [25]	IHC	EC and hyperplasia	High index linked to malignancy risk and poor differentiation	Diagnostic / proliferative index
PD-L1	De Tommasi et al., 2025 [11]	Systematic review	EC (>1000 pooled)	PD-L1 expression highest in POLEmut and MSI-High tumors	Predictive / immunotherapy
POLE	McConechy et al., 2016 [18]	Molecular	EC (n=274)	POLE-mutated EC: ultramutated with excellent prognosis	Prognostic / therapy de-escalation
MSI (Lynch syndrome)	Z Huang et al., 2013 [17]	Clinical	EC with family history	MSI-High linked to Lynch; distinct biomarker pattern	Diagnostic / familial risk
AMH/ AMHRII	Signorile et al., 2014 [37]	IHC	Endometrial tissue (n=60)	AMH modulates proliferation in hyperplastic endometrium	Experimental / diagnostic
PD-1/ Immune checkpoint	Wahba et al., 2024 [47]	Cross-sectional	Egyptian cohort	PD-L1 positivity correlated with MMR deficiency	Predictive biomarker
CTNNB1 mutation	Norimatsu et al., 2007 [31]	IHC + PCR	AEH (n=58)	PTEN loss + nuclear β-catenin predicts carcinoma progression	Combined diagnostic tool
Multigene panels	Mitric & Bernardini, 2022 [27]	Review	TCGA-based	Integration of IHC surrogates improves risk prediction	Translational / classification

2.6. Diagnostic and translational implications

The integration of immunohistochemical markers with molecular classification frameworks greatly enhances diagnostic accuracy:

p53 IHC remains the most reliable surrogate for identifying copy-number–high tumors, with strong prognostic significance [11, 19]. MMR protein loss allows rapid identification of dMMR/MSI-H tumors, which possess high immunogenicity and sensitivity to immune checkpoint blockade [2, 22, 27]. POLE mutations, though less frequent, distinguish tumors with ultramutated profiles and exceptionally favorable prognosis [16, 23]. HER2 amplification in serous carcinoma provides a targetable alteration with increasing therapeutic relevance [8, 47].

Collectively, these biomarkers form the basis of a practical, cost-effective molecular classification system that can be readily implemented in pathology laboratories and aligned with TCGA-guided clinical algorithms [33, 39 ,49].

2.7. Strengths of the evidence

This review demonstrates consistent evidence supporting:

The reproducibility of IHC surrogate markers for molecular subtyping, particularly for p53 and MMR proteins [11, 27, 39].

The strong correlation between PTEN/PAX2 loss and early endometrioid neoplasia, providing robust diagnostic value in distinguishing AEH/EIN from benign hyperplasia [13, 25].

The emerging predictive significance of PD-L1 expression and MMR deficiency in immunotherapy response [2, 43].

The established clinical impact of HER2-targeted therapy in serous carcinoma [8, 47].

2.8. Limitations

Several limitations were identified across included studies:

Methodological heterogeneity was common, including variable IHC protocols, antibody clones, scoring systems, and cut-off thresholds, consistent with prior reviews of biomarker performance [10, 39]. Limited sequencing validation in many studies may affect the accuracy of molecular subtype assignment [22, 26]. Population variability, including geographic and ethnic differences in p53-abnormal and MSI-H frequencies, remains insufficiently explored [43, 48, 49]. Meta-analysis was not feasible due to the substantial heterogeneity in biomarker assessment, study design, and reporting patterns.

2.9. Implications for research

Future studies should focus on:

Standardizing IHC interpretation criteria, particularly for p53, MMR proteins, and β-catenin, to reduce interobserver variability [11 ,18].

Expanding genomic sequencing in diverse populations to clarify suspected ethnic variations in EC molecular profiles [24, 43 49].

Implementing AI-assisted digital pathology for quantitative biomarker assessment [6].

Designing biomarker-driven clinical trials to evaluate tailored therapies, including HER2-targeted and immunotherapy regimens [2, 8].

2.10. Implications for clinical practice

The clinical utility of these biomarkers is substantial:

Incorporating IHC surrogates (p53, MMR, ER/PR, HER2) into routine diagnostics supports rapid and accurate molecular classification aligned with TCGA [33, 39].

MMR and PD-L1 testing enhances identification of candidates for immunotherapy, now a standard component in the management of MMR-deficient EC [2, 22].

HER2 testing is increasingly crucial in high-grade serous carcinoma, enabling targeted treatment strategies with demonstrated benefit [8, 47].

Identification of POLE mutations supports therapy de-escalation in selected patients with excellent prognosis [16, 23].

2.11. Conclusions

The integration of immunohistochemical and molecular biomarkers into contemporary EC diagnostics represents a paradigm shift in gynecologic oncology. By linking traditional morphology with genomic insights, these biomarkers refine diagnosis, enhance reproducibility, guide tailored therapy, and ultimately improve patient outcomes. Continued refinement of biomarker assessment and adoption of standardized molecular classification systems are essential for advancing precision medicine in endometrial carcinoma.

Conclusions from the systematic review

Immunohistochemical and molecular biomarkers provide essential insights into the pathogenesis, diagnostic stratification, prognostic assessment, and therapeutic guidance of endometrial carcinoma. Early alterations such as PTEN and PAX2 loss delineate the development of atypical endometrial hyperplasia/endometrioid intraepithelial neoplasia (AEH/EIN), while aberrant p53 expression and HER2 amplification characterize serous carcinoma and its precursors. The integration of these biomarker profiles with the TCGA molecular classification enables more precise characterization of tumor biology, allowing clinicians to tailor management strategies to individual patient risk.

Predictive biomarkers—including mismatch repair (MMR) deficiency, PD-L1 expression, and HER2 amplification—have emerged as key determinants of response to immunotherapy and targeted therapies, marking a significant shift toward personalized treatment approaches. Although predictive biomarker availability remains limited, their incorporation into routine practice represents a critical advancement in precision oncology.

Table 4. Molecular classification of endometrial carcinoma based on TCGA framework.

Molecular Subtype	Defining Molecular Feature	Typical IHC Surrogates	Representative Biomarkers	Clinicopathologic Features	Prognosis / Therapeutic Implications
POLE ultramutated	Pathogenic *POLE* exonuclease-domain mutation	High PD-L1, high TILs, wild-type p53	*POLE*, *MSH6*, PD-L1	Often endometrioid, low grade, early stage	**Excellent prognosis**, may allow therapy de-escalation
MMR-deficient (MSI-high)	Loss of MMR proteins (MLH1, MSH2, MSH6, PMS2)	MMR IHC loss, high PD-L1	*MLH1*, *MSH2*, *MSH6*, *PMS2*, *PD-L1*	Variable grade, associated with Lynch syndrome	**Good prognosis**, responds to immune checkpoint inhibitors
p53-abnormal (copy-number high)	TP53 mutation or HER2 amplification	Aberrant p53 IHC (overexpression or null), HER2+	*TP53*, *ERBB2*	Serous or mixed histology, older age	**Poor prognosis**, potential benefit from HER2-targeted therapy
NSMP (no specific molecular profile)	Lacks alterations above	p53 wild-type, MMR intact, *POLE* WT	*PTEN*, *CTNNB1*, *PAX2*	Usually low-grade endometrioid	**Intermediate prognosis**, hormone-responsive

Despite variability in methodologies across studies, the collective evidence demonstrates that standardized biomarker assessment improves diagnostic reproducibility and refines risk stratification. Continued advancements in molecular diagnostics, integration of genomic data with immunohistochemical surrogates, and the development of biomarker-driven treatment pathways are essential for further improving outcomes in endometrial carcinoma.

Acknowledgement: Contract No. BG-RRP-2.004-0007-C01 "Program for strategic research and innovation for the development of MU-Plovdiv (SRIPD-MUP)", Pillar 2: Creation of a network of research higher schools of the Program for Accelerating Economic Recovery and Transformation through Science and Innovation from the "Innovative Bulgaria" component of the National Plan for Recovery and Sustainability, funded by the European Union-NextGenerationEU.

References

1. Ambros, R. A., R. J. Kurman. Preinvasive carcinoma of the endometrium. – *Am. J. Surg. Pathol.*, **39**, 2015, 151-160.

2. Aoki, D., F. Amant, C. Creutzberg, N. Colombo, D. Cibula, et al. Endometrial carcinoma: New molecular-driven therapies. – *Ann. Oncol.,* **35**, 2024, 876-889.

3. Bagaria, M., E. Shields, J. N. Bakkum-Gamez. Novel approaches to early detection of endometrial cancer. – *Curr. Opin. Obstet. Gynecol.,* **29**, 2017, 40-46.

4. Bendifallah, S., L. Ouldamer, V. Lavoué, C. Canlorbe, C. Raimond, et al. Patterns of recurrence and outcomes in surgically treated women with endometrial cancer according to ESMO-ESGO-ESTRO risk groups. – *Eur. J. Surg. Oncol.*, **43**, 2017, 882–889.

5. Bokhman, J. V. Two pathogenetic types of endometrial carcinoma. – *Gynecol. Oncol.*, **15**, 1983, 10-17.

6. Bulten, W., J. van der Laak, C. Hulsbergen-van de Kaa, G. Boven, H. Vreuls, et al. Artificial intelligence for histopathologic biomarker quantification in endometrial carcinoma. – *Histopathology*, **82**, 2023, 230–243.

7. Buza, N., P. Hui, N. Singh, T. Bosse, A. McCluggage, et al. HER2 overexpression in serous endometrial carcinoma and targeted therapy perspectives. – *Mod. Pathol*., 36, 2023, 100-112.

8. Buza, N., P. Hui. HER2 testing and implications in uterine serous carcinoma. – *Mod. Pathol.,* **36**, 2023, 100-112.

9. Cabrera, S., I. de la Calle, S. Baulies, A. Gil-Moreno, E. Colas. Screening strategies to improve early diagnosis in endometrial cancer. – *J. Clin. Med.,* **13**, 2024, 5445.

10. Colombo, N., C. Creutzberg, F. Amant, D. Bosse, A. González-Martín, et al. ESMO-ESGO-ESTRO consensus on endometrial cancer management. – *Ann. Oncol.,* **33**, 2022, 860-877.

11. De Tommasi, O., N. Buza, P. Hui, N. Singh, T. Bosse, et al. PD-L1 expression in endometrial carcinoma: A systematic review and meta-analysis. – *J. Clin. Med.*, **14**, 2025, 401.

12. Galant, N., J. Hubert, D. Van den Broeck, A. Talhouk, T. Bosse, et al. Molecular classification of endometrial carcinoma in clinical practice: Diagnostic and prognostic relevance. – *Int. J. Mol. Sci.*, **25**, 2024, 5893.

13. Gallos, I. D., J. Yap, M. Rajkhowa, A. Luesley, A. Coomarasamy, et al. Fertility-sparing therapy in endometrial carcinoma and atypical hyperplasia: A systematic review and meta-analysis. – *Lancet Oncol.*, **23**, 2022, 141-151.
14. Getz, G., D. A. Levine, S. B. Gabriel, R. C. Carter, M. S. Lawrence, et al. Comprehensive genomic characterization defines molecular subtypes in endometrial carcinoma. – *Nature*, **497**, 2013, 67-73.
15. Guan, Y., J. Guo, T. Ma, H. Wang, L. Chen, et al. Prognostic value of Ki-67 in endometrial carcinoma: A systematic review and meta-analysis. – *Gynecol. Oncol.*, **157**, 2020, 602-610.
16. Hecht, J. L., G. L. Mutter. Molecular and pathologic features of endometrial carcinoma: New insights into PTEN and p53 pathways. – *Hum. Pathol.,* **37**, 2006, 1165-1172.
17. Huang, Z., Y. Xu, E. J. Peng, H. Liu, X. Zhang, et al. A functional variomics tool for discovering drug-resistance genes and drug targets. – *Cell Rep.*, **3**, 2013, 577-585.
18. Inoue, S., H. Yoshida, R. Saito, K. Horie, Y. Suzuki, et al. Activation of the Wnt/β-catenin pathway in endometrial carcinoma progression. – *Am. J. Pathol.*, **190**, 2020, 1521-1532.
19. Jamieson, A., N. Singh, S. Kommoss, T. Bosse, R. Salvesen, et al. p53-abnormal endometrial carcinoma: Morphologic spectrum and clinical significance. – *Histopathology*, **78**, 2021, 849-859.
20. Kurnit, K. C., G. N. Kim, B. M. Fellman, A. Urbauer, K. Mills, et al. Genomic profiling of endometrial carcinoma across diverse populations. – *Cancer Med.*, **11**, 2022, 4829-4843.
21. Lax, S., E. S. Pizer, B. M. Ronnett, R. J. Kurman. Endometrial glandular dysplasia and its relationship to serous carcinoma of the endometrium. – *Am. J. Surg. Pathol.*, **35**, 2011, 1887–1893.
22. Le Gallo, M., M. S. Anglesio, D. W. Bell. Emerging predictive biomarkers in endometrial carcinoma immunotherapy. – *Cancer Res.*, **83**, 2023, 512-523.
23. León-Castillo, A., H. Britton, M. K. McConechy, T. Kommoss, C. Gilvazquez, et al. Clinicopathological and molecular features of POLE-mutated endometrial carcinomas: An international study. – *J. Pathol.*, **250**, 2020, 377-386.
24. Li, Y., S. Chen, J. Guo, X. Zhao, H. Wang, et al. Germline–somatic interactions and therapeutic responses in endometrial carcinoma. – *Cancers (Basel)*, **15**, 2023, 3117.
25. Masjeed, N. M. A., M. R. Khan, O. Fadare. Proliferation and hormone receptor biomarkers in endometrial carcinoma and hyperplasia. – *J. Clin. Diagn. Res.*, **11**, 2017, EC31–EC35.
26. McConechy, M. K., J. Ding, J. Senz, C. Yang, A. Melnyk, et al. Molecular heterogeneity of endometrial carcinoma reflects underlying clinicopathologic diversity. – *Clin. Cancer Res.*, **21**, 2015, 276-287.
27. Mitric, C., M. Q. Bernardini. Integrating molecular markers into clinical decision-making in endometrial carcinoma. – *Curr. Oncol.*, **29**, 2022, 741-757.
28. Muñoz Sánchez, R., S. Bigardi, N. Teixeira, T. Ramon y Cajal Asensio, R. Rovira Negre, et al. Prevention of endometrial cancer: The role of immunohistochemistry in optimizing treatment strategies for endometrial hyperplasia. – *Int. J. Gynecol. Cancer,* **34**, 2024, A449.
29. Mutter, G. L., M. C. Lin, J. T. Fitzgerald, J. Kum, J. P. Baak, et al. Endometrial intraepithelial neoplasia: Morphologic and molecular correlates. – *Int. J. Gynecol. Pathol.*, **20**, 2001, 1–12.
30. Mutter, G. L., R. J. Zaino, J. P. Baak, R. C. Bentley, S. J. Robboy, et al. Endometrial intraepithelial neoplasia: Diagnostic criteria for a premalignant lesion of the endometrium. – *Int. J. Gynecol. Pathol.*, **20**, 2001, 1-12.
31. Norimatsu, Y., M. Shimizu, T. K. Kobayashi, M. Moriya, H. Tsukayama, et al. β-Catenin expression in atypical endometrial hyperplasia and carcinoma: Correlation with PTEN. – *Pathol. Int.*, **57**, 2007, 480-486.

32. Page, M. J., J. E. McKenzie, P. M. Bossuyt, I. Boutron, T. C. Hoffmann, et al. The PRISMA 2020 statement: An updated guideline for reporting systematic reviews. – *BMJ*, **372**, 2021, n71.
33. Raffone, A., A. Travaglino, D. Raimondo, G. Maletta, G. Santoro, et al. Reconsidering endometrial carcinoma taxonomy in the molecular era. – *Cancers (Basel)*, **14**, 2022, 2214.
34. Restaino, S., C. Paglietti, M. Arcieri, A. Biasioli, M. Della Martina, et al. Management of patients diagnosed with endometrial cancer: Comparison of guidelines. – *Cancers (Basel)*, **15**, 2023, 1091.
35. Ross, D. S., R. Ali-Fehmi, N. Singh, T. Bosse, A. McCluggage, et al. HER2 amplification in serous endometrial carcinoma: A target for personalized therapy. – *Mod. Pathol.*, **35,** 2022, 962-971.
36. Siegel, R. L., K. D. Miller, N. S. Wagle, A. Jemal. Cancer statistics, 2024. – *CA Cancer J. Clin.*, **74**, 2024, 7-33.
37. Signorile, P. G., R. Viceconte, A. Baldi. Expression of anti-Müllerian hormone (AMH) and its receptor (AMHRII) in human endometrium and endometrial pathologies. – *J. Exp. Clin. Cancer Res.*, **33**, 2014, 46.
38. Singh, N., A. M. Piskorz, T. Bosse, A. Jimenez-Linan, E. Rous, et al. New molecular taxonomy and histopathologic correlation in endometrial carcinoma. – *Int. J. Gynecol. Pathol*., **41**, 2022, 1-12.
39. Stelloo, E., A. León-Castillo, R. A. Nout, T. Bosse, C. Creutzberg, et al. Practical guidance for implementing molecular classification in endometrial carcinoma. – *Histopathology*, 82, 2023, 281-293.
40. Sun, H., T. Enomoto, M. Fujita, K. Wada, T. Yoshino, et al. Altered expression of PTEN and PIK3CA in endometrial hyperplasia and carcinoma. – *Am. J. Clin. Pathol.*, **115**, 2001, 32-38.
41. Sung, H., J. Ferlay, R. L. Siegel, M. Laversanne, I. Soerjomataram, et al. Global cancer statistics 2024: GLOBOCAN estimates of incidence and mortality worldwide for 36 cancers in 185 countries. – *CA Cancer J. Clin.,* **74**, 2024, 13-42.
42. Talhouk, A., J. N. McAlpine. Molecular classification of endometrial carcinoma: Translating theory into practice. – *Br. J. Cancer*, **124**, 2021, 1613-1622.
43. Talseth-Palmer, B. A., R. J. Scott. Lynch syndrome and endometrial carcinoma risk: Genetic and environmental interactions. – Int. J. Biomed. Sci., 7, 2011, 158-166.
44. The Cancer Genome Atlas Research Network. Integrated genomic characterization of endometrial carcinoma. – *Nature,* **497**, 2013, 67-73.
45. Travaglino, A., A. Raffone, M. Mascolo, G. Guida, F. Insabato, et al. Role of CTNNB1 mutations in the progression of endometrioid carcinoma: A systematic review. – *Int. J. Mol. Sci.*, **21**, 2020, 8095.
46. Travaglino, A., A. Raffone, G. Saccone, G. Mollo, F. De Placido, et al. Diagnostic and prognostic value of PTEN and PAX2 loss in endometrial precancers and carcinomas. – *APMIS*, **127**, 2019, 699-709.
47. Wahba, M. G., R. M. Elshafiey, A. M. Khalil, H. A. Ahmed, M. S. Abdelrahman, et al. Mismatch repair deficiency and PD-L1 expression correlation in Egyptian endometrial cancer patients. – *Asian Pac. J. Cancer Prev*., **25**, 2024, 1441-1450.
48. Wang, X., J. Li, S. Zhou, H. Liu, Q. Zhang, et al. Population-based variations in molecular subtypes of endometrial carcinoma. – *Int. J. Mol. Sci.*, **25**, 2024, 5079.
49. Zhang, L., Y. Yu, Y. He. Ethnicity and biomarker expression in endometrial carcinoma: A systematic evaluation. – *Front. Oncol.*, **14**, 2024, 1198.

Institute of Experimental Morphology, Pathology and Anthropology with Museum
Bulgarian Anatomical Society

Acta Morphologica et Anthropologica, 33 (1-2)
Sofia ● 2026

Angiogenesis in Bone Healing Stimulated by Simvastatin: A Review

Nadezhda Kadreva[1], Nadya Penkova[1], Petar Hrischev[2]*

[1] Department of Anatomy, Histology and Embryology, Faculty of Medicine, Medical University – Plovdiv
[2] Department of Physiology, Faculty of Medicine, Medical University – Plovdiv

*Corresponding author e-mail: nadezhda.kadreva@mu-plovdiv.bg

Simvastatin, a widely used HMG-CoA reductase inhibitor, has pleiotropic effects on bone tissue beyond lipid lowering. It promotes osteoblast proliferation and differentiation through upregulation of BMP-2 and activation of Ras/Smad/Erk signaling, while inhibiting osteoclast activity via MAPK/AKT and Src modulation. Simultaneously, simvastatin enhances angiogenesis by increasing VEGF and VEGFR-2 expression, stimulating endothelial proliferation, migration, tube formation, and pro-angiogenic cytokine release from macrophages. The combined osteogenic and angiogenic effects facilitate coordinated bone regeneration and accelerate healing of skeletal defects. These findings highlight the potential of simvastatin as a pharmacological agent for promoting bone repair and provide a mechanistic framework for developing therapeutic strategies targeting healing of bone defects.

Key words: Simvastatin, Osteogenesis, Angiogenesis, Bone Regeneration, VEGF, BMP-2

Angiogenesis in bone

One of the fundamental principles underlying each layer of tissue regeneration is the physiological mechanism that supplies oxygen and nutrients to the tissue and facilitates the removal of waste products during the process of tissue repair or regeneration. Angiogenesis is a complex process that is driven by a number of mechanisms. It is a process that is subject to a number of factors, including factors that are extrinsic to the organism and factors that are intrinsic to the organism. These factors can be categorised into two groups: promoting the process of angiogenesis and promoting the formation of new vessels (vasculogenesis). In the study by Risau et al., the author presents a pioneering analysis of the formation of the vascular systems during the process of embryogenesis as a dual-stage process [19]. In the initial phase, the formation of angioblastic cells occurs, which subsequently differentiate

into endodermal cells. The second stage is the formation of primitive vascular structures from the angiogenic cells in the vicinity of the site of origin of the tissue. As demonstrated in the preceding section, the process that leads to vascularisation is characterised by the formation of new blood vessels. [20-21]. In adults, the process of vasculogenesis is initiated during the process of wound healing or tumour growth. As stated by Rouwkema et al., endothelium-specific progenitor cells (EPCs) located on the vessel wall undergo a process of differentiation, resulting in the formation of primitive endothelial cells (PEC), which subsequently develop into primitive vascular smooth muscle cells (PVSMC) [22]. Angiogenesis, from another perspective, is the formation of blood vessels in a subject of advanced age. This process is distinct from the formation of blood vessels in a subject of younger age, which are typically characterised by the presence of pathological factors. The process of angiogenesis is driven by various intrinsic and extrinsic factors, including vascular endothelial growth factor (VEGF), an extracellular matrix-derived growth factor, and additional growth factors, as well as cytokines, pre-fibroblast cells, stellate cells, and platelet-derived factors. These factors, in turn, regulate the migration of cells and the formation of new blood vessels, contributing to the development of neoplastic lesions [2, 3, 4]. Specific cell adhesion molecules and transcription factors, as well as mechanical forces and vascular regression and remodeling are involved in the subsequent events of endothelial cell differentiation, apoptosis, and angiogenesis [5, 18].

Alternatively, new blood vessels are formed through a process called vasculogenesis, without a pre-existing vascular component. Vasculogenesis is initiated by local differentiation of endothelial progenitor cells, or alternatively, by the involvement of circulating endothelial progenitor cells (EPCs) in the process [28]. Angiogenesis is maintained and regulated by a variety of growth factors, essentialy vascular endothelial growth factor (VEGF) group, which are products of inflammatory cells and stromal cells to induce blood vessel in-growth. It is the primary process of tissue growth and one of the first processes to occur in tissue repair [9].

Angiogenesis during osteogenesis

There is a indissoluble bond between osteogenesis and angiogenesis during the process of bone repair. Neovascularization within the bone defects not only provides nutrients, oxygen, calcium and phosphate but also transports mesenchymal stem cells to facilitate bone regeneration [27]. Therefore, the development of biomaterials and pharmacological substances coupling the enhancement of osteogenesis and angiogenesis has attracted increasing attention in recent years.

Angiogenesis plays a critical role in bone development and regeneration and is closely coordinated with osteogenesis through complex interactions within the bone microenvironment [11]. During skeletal development and fracture healing, the formation of new blood vessels provides both structural support and biochemical signals that facilitate the recruitment, proliferation, and differentiation of osteoblast precursors [10]. Among the principal molecular regulators of this process is vascular endothelial growth factor (VEGF), which promotes endothelial cell proliferation, migration, and

vascular sprouting, while also influencing the osteogenic differentiation of mesenchymal stem cells [29]. Hypoxia-inducible factors, particularly HIF-1α, represent another key regulatory mechanism by enhancing VEGF expression under hypoxic conditions commonly present in developing or healing bone tissue [13]. In addition, endothelial cells actively contribute to bone formation by releasing angiocrine signals, including bone morphogenetic proteins (BMPs), which stimulate osteoblast differentiation and extracellular matrix deposition [16]. This bidirectional communication between vascular endothelial cells and osteogenic cells establishes a coordinated signaling network that ensures the synchronization of vascular development and bone formation during skeletal growth, repair, and regeneration [10].

Angiogenesis and osteogenesis provided by Simvastatin

In recent years, increasing attention has been directed toward the biological effects of statins beyond their well-established role in lowering serum cholesterol levels. Among these additional effects, their potential influence on bone metabolism has attracted particular interest. Early work by Gregory R. Mundy and colleagues demonstrated that statins stimulate bone formation in vivo in rodent models and increase the volume of newly formed bone in cultures derived from mouse calvaria. Subsequent studies have further confirmed the beneficial effects of statins on bone tissue in both in vitro and in vivo experimental settings [15]. The present study investigates the biphasic, dose-dependent effect of HMG-CoA reductase inhibition on angiogenesis. The findings demonstrate that this effect is lipid independent and associated with alterations in endothelial apoptosis and vascular endothelial growth factor signalling. Statins have been observed to exert proangiogenic effects at low therapeutic concentrations, while at higher concentrations, they demonstrate angiostatic properties, which can be reversed by geranylgeranyl pyrophosphate. At clinically relevant doses, statins have been observed to modulate angiogenesis in humans via effects on geranylated proteins [29].

Specifically, investigations examining the effects of simvastatin on osteoblastic differentiation have shown that this statin exerts an anabolic effect on bone, primarily through the promotion of osteoblast differentiation [32].

Statins, inhibitors of the competitive 3-hydroxy-3-methyl coenzyme A (HMG-CoA) reductase, have been widely used to treat hyperlipidemia and hypercholesterolemia. It has been demonstrated that statins, including simvastatin, can induce osteoblastic differentiation of bone marrow mesenchymal stem cells and improve the osteogenesis of human or animal osteoblastic cell lines [11-13, 23-26]. Moreover, statins have been demonstrated to enhance angiogenesis through up-regulation of gene expression of vascular endothelial growth factor (VEGF) and basic fibroblast growth factor (FGF-2) [33]. Statins stimulate VEGF expression in osteoblasts via reduced protein prenylation and the phosphatidylinositide-3 kinase pathway, promoting osteoblastic differentiation [13]. Both VEGF and FGF-2 have been shown to induce BMP-2 expression and stimulate osteoblast differentiation indirectly. Same study reported that locally applied simvastatin promoted critical-sized calvarial defects healing by recruitment of autogenous osteogenic stem cells and endothelial progenitor cells [7].

Statins act on the mevalonate pathway in osteoblasts and enhance the expression of the bone morphogenic protein-2 (BMP-2), which is an important growth factor for osteoblast differentiation. It is believed that BMP-2 upregulation mediates the bone forming effect of statins. Additionally, statins act on the same pathway upstream of the bisphosphonates in osteoclasts via the inhibition of 3-hydroxy-3-methylglutaryl-coenzyme A (HMG-CoA) reductase, leading to decreased protein prenylation which is essential for a normal osteoclast function [1].

Over the last decade, increasing attention has been directed toward the local application of simvastatin due to its pleiotropic effects that extend beyond lipid lowering. Locally administered simvastatin demonstrates pronounced anti-inflammatory, osteogenic, angiogenic, and regenerative properties, making it particularly attractive for applications in tissue engineering, periodontology, bone regeneration, and wound healing. One of the major advantages of local simvastatin delivery over systemic administration is the ability to achieve high drug concentrations directly at the target tissue while minimizing systemic exposure and associated adverse effects. Systemic simvastatin therapy is associated with dose-dependent risks such as hepatotoxicity, elevated liver enzymes, myopathy, and rhabdomyolysis, primarily due to extensive hepatic metabolism and systemic circulation. In contrast, local administration substantially reduces these risks by limiting systemic absorption. Experimental and clinical studies have demonstrated that locally applied simvastatin stimulates bone formation through upregulation of bone morphogenetic protein-2 (BMP-2), vascular endothelial growth factor (VEGF), and osteoblastic differentiation markers. Additionally, simvastatin suppresses inflammatory cytokines and promotes angiogenesis, thereby accelerating tissue repair and regeneration. These effects are particularly beneficial in periodontal defects, extraction sockets, implant osseointegration, and bone healing models. Another important advantage of local delivery is the possibility of controlled and sustained release using biomaterials such as hydrogels, scaffolds, nanoparticles, or collagen membranes. Such systems improve drug retention at the application site and enhance therapeutic efficacy while avoiding first-pass hepatic metabolism [30-33].

Therefore, local simvastatin administration represents a promising therapeutic strategy that preserves the beneficial regenerative and anti-inflammatory effects of the drug while minimizing the systemic adverse reactions commonly associated with oral statin therapy.

It has been demonstrated by Yamashita M et al. that simvastatin exerts its inhibitory effect on the mRNA expression of the key markers for osteoclastic differentiation, including TRAP, RANK and cathepsin-K. A novel inhibitory mechanism of simvastatin on the expression of osteoclast differentiation markers was demonstrated in two different cell lines. The first cell line was osteoclast-like MLC 6 cells, and the second was human osteoclast precursor cells. Both of these cell lines expressed BMP receptors and Smad signalling machinery. The study demonstrated that simvastatin activated MAPK/AKT pathways and inactivated Src phosphorylation in human osteoclasts differentiated by M-CSF and RANKL treatments. Bioassays demonstrated that the inhibition of TRAP and RANK expression by simvastatin was reversed by MAPK/AKT inhibition, whereas Src inhibitor enhanced simvastatin-induced suppression of osteoclast markers [30].

Simvastatin can promote osteoblast viability and differentiation via membrane-bound Ras/Smad/Erk/BMP-2 pathway. In study by Ho et al. Simvastatin promotes osteoblast viability and differentiation via Ras/Smad/Erk/bone morphogenic protein (BMP)-2 signaling pathway. The results of this study demonstrate that simvastatin stimulation promotes membrane localization and GTP loading of Ras, indicating activation of small GTPase signaling molecules involved in Ras regulation [8]. Simvastatin treatment was also associated with increased levels of membrane-bound active phospho-RasGRF1, suggesting that Ras activation may contribute to the regulation of BMP-2 transcription. Furthermore, the activation of Ras signaling was supported by the observed up-regulation of downstream signaling molecules, including phosphorylated Smad (phospho-Smad) and phosphorylated extracellular signal-regulated kinase (phospho-Erk). Together, these findings indicate that simvastatin activates Ras-dependent signaling pathways that may regulate BMP-2 expression and promote osteoblastic activity (**Fig.1**) [6].

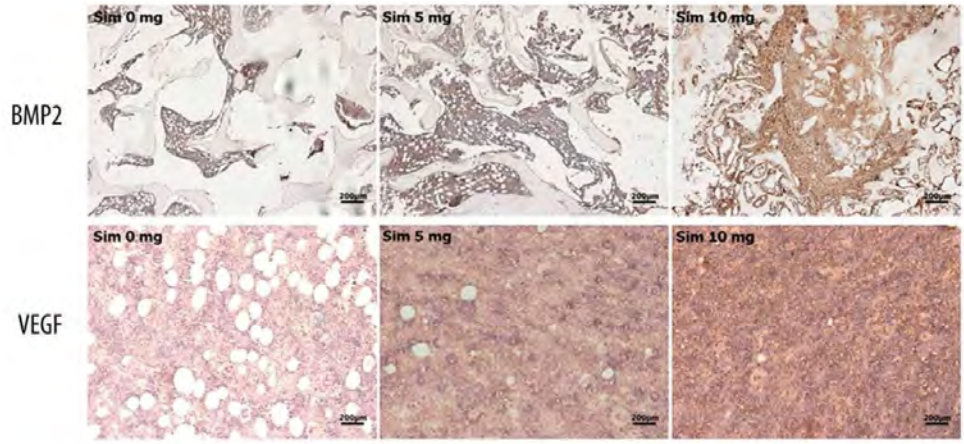

Fig. 1. Immunohistochemistry for BMP-2 and VEGF. Increased BMP-2 and VEGF expression was observed in the simvastatin-treated groups compared with the control group [28].

Simvastatin has been shown to support BMP-induced osteoblast differentiation by antagonizing the cytokine-to-MAPK signaling pathway while simultaneously enhancing BMP–Smad signaling. These mechanisms suggest that simvastatin exerts dual biological functions in bone metabolism, including anti-resorptive effects on osteoclasts as well as stimulatory and anabolic effects on osteoblasts. Consequently, statins with a high affinity for bone tissue may represent promising therapeutic agents for the prevention or treatment of osteoporosis associated with inflammatory cytokines [31].

Recent research has elucidated that simvastatin modulates angiogenic processes that are intrinsically linked to bone regeneration, extending its pleiotropic effects beyond lipid lowering to the vascular compartment of bone healing. Local administration of simvastatin has been shown to significantly enhance neovascularization in osteoporotic

bone, as evidenced by increases in vascular number, volume, and expression of key angiogenic markers such as vascular endothelial growth factor (VEGF) and its receptor VEGFR2 in ovariectomized rat models, concomitant with improvements in bone formation and implant fixation [28]. Moreover, simvastatin's influence on the immune microenvironment has been shown to promote proregenerative cytokine expression, including VEGF, in macrophages, thereby enhancing angiogenic gene expression in endothelial cells and suggesting an immunomodulatory mechanism that supports coordinated angiogenesis and osteogenesis [17]. These proangiogenic effects are consistent with observations in nonskeletal tissues, where simvastatin increases endothelial proliferation and tube formation through activation of signaling pathways such as VEGFR2/Akt/endothelial nitric oxide synthase [14]. Collectively, these findings support a model wherein simvastatin facilitates bone regeneration not only by stimulating osteoblastic differentiation but also by enhancing vascular ingrowth through upregulation of angiogenic signals, thus reinforcing the functional coupling between angiogenesis and osteogenesis that is critical for effective skeletal repair (**Fig.2**).

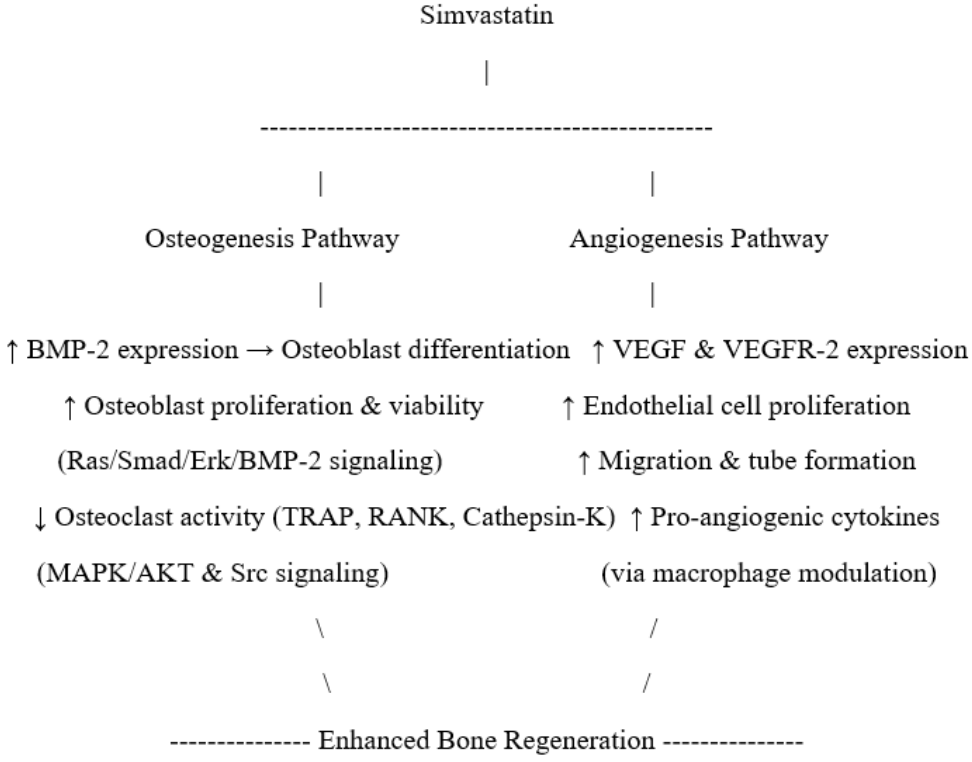

Fig. 2. Simvastatin promotes bone regeneration via dual pathways. On the osteogenic side, it enhances BMP-2 expression, osteoblast proliferation, and inhibits osteoclast activity. On the angiogenic side, it stimulates VEGF/VEGFR-2 signaling, endothelial proliferation and migration, and pro-angiogenic cytokine expression, resulting in coupled angiogenesis and osteogenesis.

Conclusion

Simvastatin exerts dual modulatory effects on bone metabolism by simultaneously promoting osteogenesis and angiogenesis, thereby enhancing bone regeneration. Mechanistically, simvastatin stimulates osteoblast differentiation and proliferation through BMP-2 upregulation and activation of the Ras/Smad/Erk signaling pathway, while inhibiting osteoclast activity via MAPK/AKT and Src signaling modulation. Concurrently, it enhances angiogenic processes by upregulating VEGF/VEGFR-2 signaling, stimulating endothelial proliferation, migration, tube formation, and pro-angiogenic cytokine expression. These interconnected pathways underscore the functional coupling between osteogenesis and angiogenesis, highlighting simvastatin as a promising pharmacological agent for bone healing and regeneration. The integration of osteogenic and angiogenic responses provides a robust biological framework for the development of therapeutic strategies targeting skeletal defects and osteoporosis.

References

1. **Baek, K. H., W. Lee, K. Oh, H. Tae, J. Lee, E. Lee, J. Han, M. Kang, B. Cha, K. Lee, H. Son, S. Kang.** The effect of simvastatin on the proliferation and differentiation of human bone marrow stromal cells. – *J. Korean Med. Sci.*, **20**, 2005, 438-444.
2. **Bryan, B. A., P. D'Amore.** What tangled webs they weave: Rho-GTPase control of angiogenesis. – *Cell. Mol. Life Sci.*, **64**, 2007, 2053-2065.
3. **Carmeliet, P.** Angiogenesis in health and disease. – *Nat. Med.*, **9**, 2003, 653-660.
4. **Carmeliet, P.** Angiogenesis in life, disease and medicine. – *Nature*, **438**, 2005, 932-936.
5. **Carmeliet, P.** Manipulating angiogenesis in medicine. – *J. Intern. Med.*, **255**, 2004, 538-561.
6. **Chen, P. Y., J. Sun, Y. Tsuang, M. Chen, P. Weng, F. Lin**. Simvastatin promotes osteoblast viability and differentiation via Ras/Smad/Erk/BMP-2 signaling pathway. – *Nutr. Res.*, **30**, 2010, 191-199.
7. **Choi, K. Y., H. Kim, M. Lee, T. Kwon, H. Nah, T. Furuichi, T. Komori, S. Nam, Y. Kim, H. Kim, H. Ryoo.** Runx2 regulates FGF2-induced Bmp2 expression during cranial bone development. – *Dev. Dyn.*, **233**, 2005, 115-121.
8. **Ho, M. L., Y. Chen, H. Liao, C. Chen, S. Hung, M. Lee, Y. Fu, Y. Wang, G. Wang, J. Chang.** Simvastatin increases osteoblasts and osteogenic proteins in ovariectomized rats. – *Eur. J. Clin. Invest.*, **39**, 2009, 296-303.
9. **Hu, K., B. Olsen.** Vascular endothelial growth factor control mechanisms in skeletal growth and repair. – *Dev. Dyn.*, **246**, 2016, 227-234.
10. **Kusumbe, A. P., S. Ramasamy, R. Adams.** Coupling of angiogenesis and osteogenesis by a specific vessel subtype in bone. – *Nature*, **507**, 2014, 323-328.
11. **Maeda, T., A. Matsunuma, I. Kurahashi, T. Yanagawa, H. Yoshida, N. Horiuchi.** Induction of osteoblast differentiation indices by statins in MC3T3-E1 cells. – *J. Cell. Biochem.*, **92**, 2004, 458-471.
12. **Maeda, T., A. Matsunuma, T. Kawane, N. Horiuchi.** Simvastatin promotes osteoblast differentiation and mineralization in MC3T3-E1 cells. – *Biochem. Biophys. Res. Commun.*, **280**, 2001, 874-877.

13. **Maeda, T., T. Kawane, N. Horiuchi.** Statins augment vascular endothelial growth factor expression in osteoblastic cells via inhibition of protein prenylation. – *Endocrinology*, **144**, 2003, 681-692.
14. **Matsuno, H., M. Takei, H. Hayashi, K. Nakajima, A. Ishisaki, O. Kozawa.** Simvastatin enhances the regeneration of endothelial cells via VEGF secretion in injured arteries. – *J. Cardiovasc. Pharmacol.*, **43**, 2004, 333-340.
15. **Mundy, G., R. Garrett, S. Harris, J. Chan, D. Chen, G. Rossini, B. Boyce, M. Zhao, G. Gutierrez.** Stimulation of bone formation in vitro and in rodents by statins. – *Science*, **286**, 1999, 1946-1949.
16. **Murasawa, S., T. Asahara.** Endothelial progenitor cells for vasculogenesis. – *Physiology*, **20**, 2005, 36-42.
17. **Niu, Y., Z. Wang, Y. Shi, L. Dong, C. Wang.** Modulating macrophage activities to promote endogenous bone regeneration: Biological mechanisms and engineering approaches. – *Bioact. Mater.*, **6**, 2020, 244-261.
18. **Ribatti, D., A. Vacca, B. Nico, M. Presta, L. Roncali.** Angiogenesis: basic and clinical aspects. – *Ital. J. Anat. Embryol.*, **108**, 2003, 1–24.
19. **Risau, W.** Angiogenesis is coming of age. – *Circ. Res.*, **82**, 1998, 926-928.
20. **Risau, W.** Mechanisms of angiogenesis. – *Nature*, **386**, 1997, 671-674.
21. **Risau, W., I. Flamme.** Vasculogenesis. – *Annu. Rev. Cell Dev. Biol.*, **11**, 1995, 73-91.
22. **Rouwkema, J., N. Rivron, C. van Blitterswijk.** Vascularization in tissue engineering. – *Trends Biotechnol.*, **26**, 2008, 434-441.
23. **Ruiz-Gaspa, S., X. Nogués, A. Enjuanes, J. Monllau, J. Blanch, R. Carreras, L. Mellibovsky, D. Grinberg, S. Balcells, A. Díez-Pérez, J. Pedro-Botet.** Simvastatin and atorvastatin enhance gene expression of collagen type 1 and osteocalcin in primary human osteoblasts and MG-63 cultures. – *J. Cell. Biochem.*, **101**, 2007, 1430-1438.
24. **Song, C., Z. Guo, Q. Ma, Z. Chen, Z. Liu, H. Jia, G. Dang.** Simvastatin induces osteoblastic differentiation and inhibits adipocytic differentiation in mouse bone marrow stromal cells. – *Biochem. Biophys. Res. Commun.*, **308**, 2003, 458-462.
25. **Sonobe, M., K. Hattori, N. Tomita, T. Yoshikawa, H. Aoki, Y. Takakura, T. Suguro.** Stimulatory effects of statins on bone marrow-derived mesenchymal stem cells. Study of a new therapeutic agent for fracture. – *Bio-Med. Mater. Eng.*, **15**, 2005, 261-267.
26. **Stegen, S., N. van Gastel, G. Carmeliet.** Bringing new life to damaged bone: the importance of angiogenesis in bone repair and regeneration. – *Bone*, **70**, 2015, 19-27.
27. **Street, J., M. Bao, L. deGuzman, S. Bunting, F. Peale Jr., N. Ferrara, H. Steinmetz, J. Hoeffel, J. Cleland, A. Daugherty, N. van Bruggen, H. Redmond, R. Carano, E. Filvaroff.** Vascular endothelial growth factor stimulates bone repair by promoting angiogenesis and bone turnover. – *Proc. Natl. Acad. Sci. USA*, **99**, 2002, 9656-9661.
28. **Tan, J., N. Yang, X. Fu, Y. Cui, Q. Guo, T. Ma, X. Yin, H. Leng, C. Song.** Single-dose local simvastatin injection improves implant fixation via increased angiogenesis and bone formation in an ovariectomized rat model. – *Med. Sci. Monit.*, **21**, 2015, 1428-1439.
29. **Weis, M., C. Heeschen, A. Glassford, J. Cooke.** Statins have biphasic effects on angiogenesis. – *Circulation*, **105**, 2002, 739-745.
30. **Yamashita, M., F. Otsuka, T. Mukai, R. Yamanaka, H. Otani, Y. Matsumoto, E. Nakamura, M. Takano, K. Sada, H. Makino.** Simvastatin inhibits osteoclast differentiation induced by bone morphogenetic protein-2 and RANKL through regulating MAPK, AKT and Src signaling. – *Regul. Pept.*, **162**, 2010, 99-108.

31. Yazawa, H., B. Zimmermann, Y. Asami, J.-P. Bernimoulin. Simvastatin promotes cell metabolism, proliferation, and osteoblastic differentiation in human periodontal ligament cells. – *J. Periodontol.*, **76**, 2005, 295-302.

32. Yu, W. L., T. Sun, C. Qi, H. Zhao, Z. Ding, Z. Zhang, B. Sun, J. Shen, F. Chen, Y. Zhu, D. Chen, Y. He. Enhanced osteogenesis and angiogenesis by mesoporous hydroxyapatite microspheres-derived simvastatin sustained release system for superior bone regeneration. – *Sci. Rep.*, **7**, 2017, 44129.

33. Yueyi, C., X. Hu, J. Wang, Q. Su, J. Tian, X. Fu, Y. Xu, C. Song. Calvarial defect healing by recruitment of autogenous osteogenic stem cells using locally applied simvastatin. – *Biomaterials*, **34**, 2013, 9373-9380.

Institute of Experimental Morphology, Pathology and Anthropology with Museum
Bulgarian Anatomical Society

Acta Morphologica et Anthropologica, 33 (1-2)
Sofia ● 2026

Green tea‘s Potential Benefits for Metabolic Syndrome

Sabri Sabri[1], Nicole Kirchev[2] Nadya Penkova[1], Petar Hrischev[3]*

[1] *Department of Anatomy, Histology and Embryology, Faculty of Medicine, Medical University – Plovdiv, Bulgaria*
[2] *Student, Faculty of Dental Medicine, Medical University – Plovdiv, Bulgaria*
[3] *Department of Physiology, Faculty of Medicine, Medical University – Plovdiv, Bulgaria*

*Corresponding author e-mail: Sabri.Sabri@mu-plovdiv.bg

Metabolic syndrome is a combination of related disorders, such as insulin resistance, hyperglycemia, dyslipidemia, high blood pressure and abdominal obesity, which significantly increase the risk of cardiovascular disease and type 2 diabetes. The development of this syndrome involves the interaction of genetic factors, diet and environment. Physical activity and nutrition are no less important than pharmacological therapy. Green tea is prepared from leaves which are subjected to minimal oxidation during processing. It contains bioactive compounds such as polyphenols, the amino acid L-theanine, caffeine, alkaloids, B vitamins. In the present study, we summarize the literature data on the role of different components of green tea in the low-grade chronic inflammation of the intestinal tract, found in metabolic syndrome. The inclusion of appropriate foods and nutritional supplements, such as green tea and its extract, in the dietary regimen would inhibit endotoxin-mediated inflammatory reactions, which are the basis of the metabolic syndrome symptoms.

Key words: Green tea, metabolic syndrome, low-grade chronic inflammation, intestines, intestinal microbiota

Introduction

Metabolic syndrome is a growing problem in modern healthcare, which also carries a huge economic burden. It represents a complex of physiological, biochemical, clinical, and metabolic factors that increase the risk of cardiovascular disease, type 2 diabetes mellitus, etc. It includes a combination of central obesity (abdominal fat accumulation), hyperglycemia, reduced glucose tolerance, insulin resistance, hypertension, dyslipidemia (high triglyceride levels, low HDL cholesterol levels) [16]. The development of this syndrome is determined by the interaction between genetic factors, diet, and the environment. Although effective clinical, surgical, and

pharmacological methods have been developed to treat symptoms associated with metabolic syndrome, these treatments can be expensive and have potential adverse effects [6, 7, 24]. The development of dietary agents for the prevention or treatment of one or more of the symptoms of metabolic syndrome, alone or in combination with lifestyle changes and pharmaceutical agents, could represent a cost-effective and safe approach to the problem [25].

Green tea is made from the leaves of Camellia sinensis, which undergo minimal oxidation during processing. It contains bioactive compounds such as polyphenols, the amino acid L-theanine, caffeine, alkaloids (such as theobromine and theophylline), and B vitamins. The preventive effects of green tea and its ingredients on metabolic syndrome are being studied in both animal models and humans.

Effects of green tea on risk factors for metabolic syndrome

With regard to the various risk factors for metabolic syndrome, the ingredients of green tea have both an independent effect as dietary supplements and a synergistic effect when green tea is consumed (as a beverage or dietary supplement).

• Intestinal microbiota

Metabolic syndrome is a combination of related disorders, such as insulin resistance, hyperglycemia, dyslipidemia, high blood pressure, and abdominal obesity, which significantly increase the risk of cardiovascular disease and type 2 diabetes [16]. The development of this syndrome involves an interaction between genetic factors, diet, and the environment.

One of the key factors in the pathogenesis of metabolic syndrome is low-grade chronic inflammation induced by the intestinal microbiota.

By altering the composition of the gut microbiota, including an increase in Akkermansia, green tea reduces inflammatory markers and improves metabolic parameters [22]. The Firmicutes/Bacteroidetes (F/B) ratio is a measure of the balance between two dominant types of bacteria in the human gut microbiome. A high ratio (more Firmicutes) is associated with obesity [29]. L-theanine modulates the gut microbiota by reducing the Firmicutes/Bacteroidetes ratio, which is associated with obesity, and increases the concentration of short-chain fatty acids (SCFA), which support energy metabolism and regulate inflammatory processes in the intestine, as well as improve insulin sensitivity [13] (**Fig. 1**).

Changes in bacterial composition and intestinal lumen can induce metabolic disorders, regardless of caloric intake and body weight [2]. The transfer of microbiota from obese humans to germ-free mice shows that gut bacteria alone can cause glucose intolerance, insulin resistance, and vascular dysfunction without changing the body weight of the animals [33].

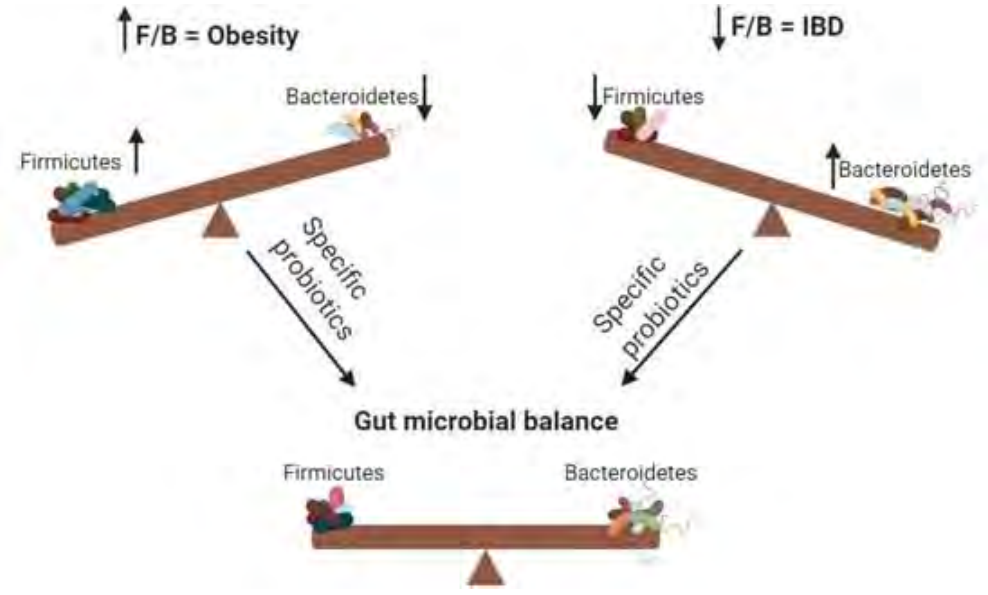

Fig. 1. Changes in the Firmicutes/Bacteroidetes (F/B) ratio

Stojanov, S., Berlec, A., & Štrukelj, B. (2020). https://doi.org/10.3390/microorganisms8111715

• Diet, obesity, and metabolic syndrome

The type of diet, composition, and proportions of the main components of food: proteins, carbohydrates, and lipids are of great importance for the pathogenesis of metabolic syndrome.

Green tea has a beneficial effect on metabolic syndrome induced by a high-calorie diet in mice, as the addition of 2% and 4% significantly reduces weight gain and lipid mass, as well as reducing inflammatory changes compared to the group fed only with high-fat diet (HFD). By altering the composition of the gut microbiota, including an increase in Akkermansia, green tea reduces inflammatory markers and improves metabolic parameters [22]. The HFD complicates the picture of metabolic syndrome by activating TLR4-dependent inflammatory pathways and leading to systemic inflammation, which is associated with visceral hypersensitivity and changes in metabolism [32]. HFD causes intestinal inflammation, which precedes and correlates with the development of obesity and insulin resistance, showing that the interaction between diet and bacteria plays a critical role in metabolic syndrome. Changes in bacterial composition lead to the activation of inflammatory signals and changes in the local immune response, which promotes the disruption of glucose and lipid metabolism [5]. Even short-term exposure to HFD affects immune function by disrupting macrophage activity, maintaining local inflammation, and enhancing systemic metabolic effects. Acute dietary changes and associated dysbiosis can rapidly induce metabolic disturbances and inflammatory responses that undermine normal

glucose and vascular homeostasis [14]. Dysbiosis in a high-fat diet is also characterized by reduced bacterial diversity, an increased Firmicutes/Bacteroidetes ratio, and an increase in LPS-producing taxa [5] (**Fig. 2**).

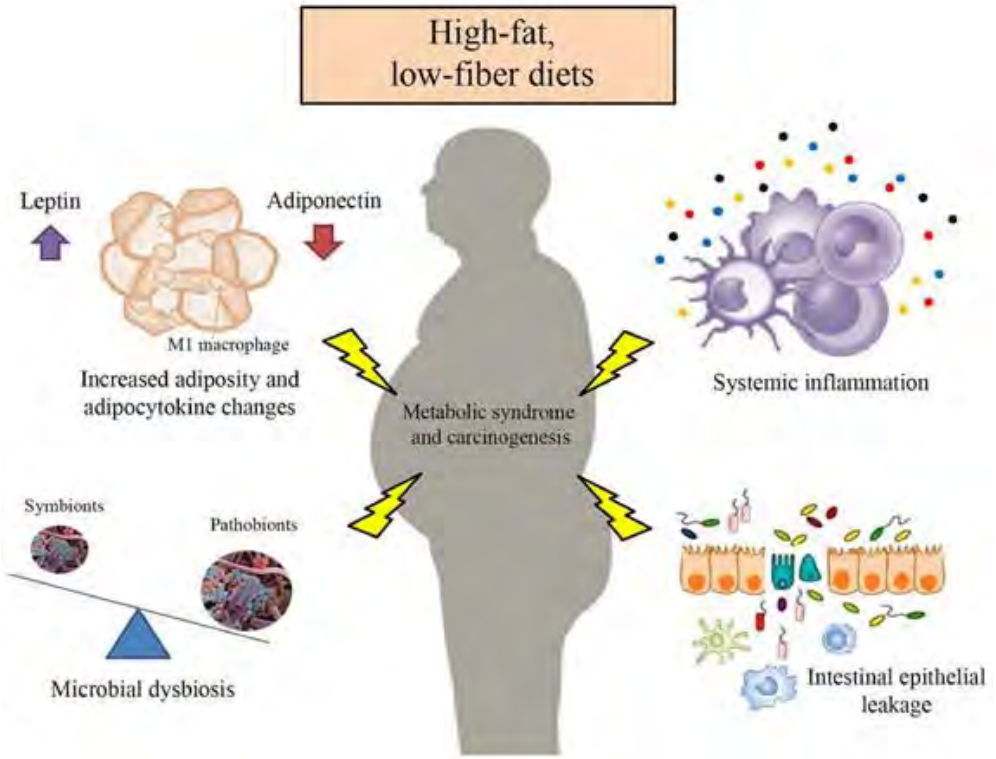

Fig. 2. Obesity and metabolic syndrome.

Saetang, J., & Sangkhathat, S. (2017). https://doi.org/10.3892/or.2017.5385

• Catechins and metabolic syndrome

Catechins are monomeric polyphenols characteristic of green tea. They constitute 25–40% of its dry weight [4, 11]. The most common catechin in green tea is epigallocatechin-3-gallate (EGCG), which has been found to perform various biological functions, including antioxidant and anti-inflammatory effects [12]. EGCG is one of the most potent polyphenolic compounds in green tea due to its effects on glucose and lipid metabolism and insulin resistance [35]. Li et al. showed that EGCG alleviates peripheral insulin resistance caused by free fatty acids (FFA) through insulin signaling and AMPK activation [19]. Many studies have focused on the effects of purified tea catechin preparations or pure EGCG. It has been found that supplements of high-fat-fed C57BL/6J mice fed 0.2 and 0.5% tea catechin reduce body weight gain, visceral fat mass (44–87% reduction), and liver triglycerides (53–75% reduction) [23, 31]. Treatment with tea catechin also reduced total plasma cholesterol and plasma

glucose under fasting conditions [23]. Treatment of C57BL/6J mice fed a high-fat diet with 0.32% EGCG for 16 weeks reduced body weight gain by 33–41% compared to control groups fed a high-fat diet [3] (**Fig. 3**).

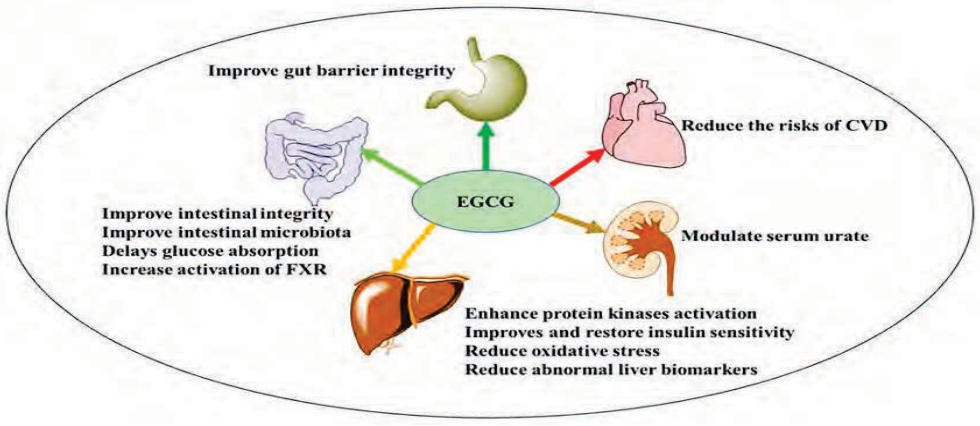

Fig. 3. EGCG and metabolic syndrome.

James, A., Wang, K., & Wang, Y. (2023). https://doi.org/10.3390/nu15133022

- **Caffeine and metabolic syndrome**

The best-known molecule in the fruit of coffee plant is alkaloid methylxanthine caffeine (1,3,7 trimethylxantin) which is a toxin protecting the plant from herbivores [28]. Caffeine is also found in the leaves of Camellia sinensis, with an average content of 3.8%, but this can vary depending on the time of harvest, storage, fermentation, and method of preparation [8].

Caffeine acts as an adenosine antagonist, thereby reducing norepinephrine levels. At the same time, it inhibits phosphodiesterase and increases protein kinase activity. The mixture of catechins and caffeine in green tea activates a signaling cascade that stimulates the sympathetic nervous system, along with hormone-sensitive lipase and upregulation of uncoupling protein, leading to increased energy expenditure and fat oxidation [15]. It was shown that caffeine decreased food intake and increased thermogenesis and this thermogenic effect leads to weight loss. Furthermore, it has been found that caffeine-induced thermogenesis is synergistically enhanced by catechins in the adipose tissue of rats [38].

- **L-Theanine and metabolic syndrome**

L-theanine is an amino acid found in green tea. L-theanine (L-gamma-glutamyl ethyl amide or N5-ethyl-L-glutamine) is a non-proteinogenic amino acid similar to L-glutamate and L-glutamine. It is produced by certain plants, such as Camellia sinensis (the tea plant), as well as by some fungi. As an important component of green tea, L-theanine has attracted the attention of scientists due to its positive role in metabolic syndrome.

L-theanine also modulates the gut microbiota by reducing the Firmicutes/Bacteroidetes ratio, which is associated with obesity, and increases the concentration of short-chain fatty acids (SCFAs), which support energy metabolism, regulate inflammatory processes in the gut, and improve insulin sensitivity [13].

L-theanine exhibits antioxidant and anti-inflammatory properties that can counteract the low-grade inflammation observed in metabolic syndrome, as well as in functional bowel disorders [20]. In the gastrointestinal tract, L-theanine enhances the antioxidant capacity of the intestine via the Nrf2 signaling pathway, which plays a crucial role in cellular antioxidant defenses. As a regulator of antioxidant genes, activation of the Nrf2 signaling pathway reduces oxidative stress in intestinal epithelial cells exposed to the cytotoxic effects of hydrogen peroxide. [20, 26]. In a cellular model of porcine intestinal enterocytes from the jejunum (IPEC-J2 cells) exposed to hydrogen peroxide, L-theanine increases the expression of antioxidant enzymes such as superoxide dismutase and glutathione peroxidase, thereby reducing oxidative stress.

Green tea and its components, including L-theanine, have a direct antibacterial effect on the gut microbiota by destroying the exopolysaccharides and membranes of a number of pathogenic anaerobic and Gram-negative gut bacteria: Staphylococcus sp., Clostridium botulinum, Bacillus cereus, Escherichia coli, Klebsiella pneumoniae, and Salmonella. [1, 36] Exosome-like nanoparticles derived from tea leaves (TELN), which contain L-theanine, significantly improve the barrier function of the intestinal epithelium. [10]. In an in vitro experiment, TELN protect the rat intestinal epithelium from damage caused by lipopolysaccharides. In an in vivo experiment on stressed rats, oral administration of TELN improved the barrier function of the intestinal epithelium by preventing the translocation of bacteria from the intestinal lumen into the submucosa of the intestinal mucosa. TELN improve the function of the intestinal immune barrier through the mediation of interleukin-22 and increased secretion of the antimicrobial peptide Reg3g [9]. (**Fig. 4.**).

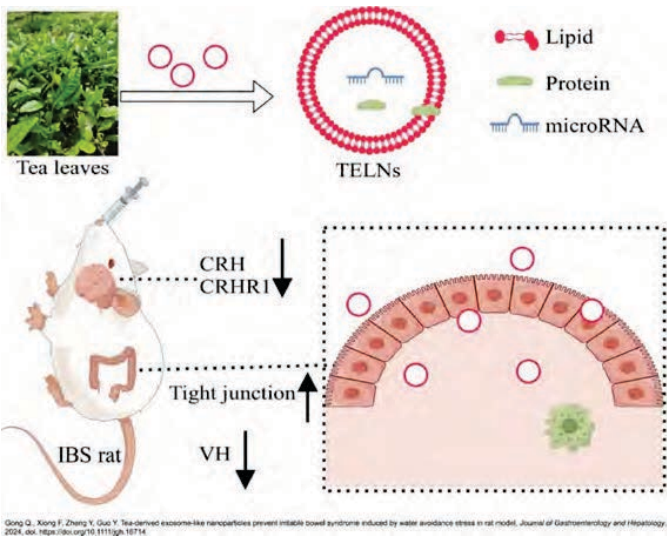

Fig. 4. L-theanine in the form of TELN exosomes—nanoparticles in green tea with a protective effect on intestinal permeability. (Gong et al., 2024). https://doi.org/10.1111/jgh.16714.

L-theanine affects not only intestinal permeability but also has a positive effect on resorptive processes in the small intestine. An improved balance of ingested nutrients is of great importance for metabolic syndrome.

Studies in a mouse model with L-theanine administration at doses of 300 and 400 mg/kg show that L-theanine is also involved in absorptive processes in the small intestine. Through intercellular signaling mechanisms, it influences the synthesis of transport proteins in the duodenum and jejunum. By activating the mTOR (mechanistic target of rapamycin) signaling pathway and the phosphorylation of the mTOR downstream proteins S6 and S6K1, L-theanine participates in the synthesis and modulation of a large number of transporters for various amino acids. In this way, L-theanine improves protein uptake and promotes protein metabolism by increasing intestinal absorption of amino acids and nitrogen utilization. [21]. An experimental rat model administered L-theanine at doses of 0, 50, 200, and 400 mg/kg per day for two weeks also demonstrated its modulatory role in nutrient absorption in the small intestine. In this experiment, the authors observed inhibition of the expression of SGLT3 and GLUT5 carbohydrate transporters, as well as GPR120 and FABP2 fatty acid transporters, while the expression of SLC7a1 and SLC7a9 essential amino acid transporters was increased. Serum glucose and high-density lipoprotein levels were also reduced [34]. Fat accumulation in mice is suppressed by the administration of green tea powder [27], and it is specifically L-theanine that is responsible for this suppressive effect [38].

Metabolic syndrome is also associated with high levels of stress. Chronic stress triggers persistent activation of the hypothalamic-pituitary-adrenocortical axis and the sympathetic nervous system, leading to elevated cortisol levels. In this way, the key components of metabolic syndrome—central obesity, insulin resistance, hypertension, and low-grade chronic inflammation—can be triggered. Stress is also a cause of unhealthy behaviors such as comfort eating and reduced physical activity [37, 38].

L-theanine has a proven calming effect on the nervous system, reducing stress and anxiety while improving cognitive function and memory. As a dietary supplement, this amino acid acts as a natural relaxant [18]. Experiments with oral administration of L-theanine to rats demonstrate its good absorption in the small intestine, and 15 to 30 minutes after administration, between 0.23% and 0.39% of its blood level is detected in the brain [30]. It has been found that in mice, L-theanine increases serotonin levels and decreases levels of dopamine, norepinephrine, and corticotropin in the cerebral cortex, striatum, and hippocampus [17].

Conclusion

Metabolic syndrome, as a borderline condition with various subclinical complications, is largely influenced by lifestyle. Physical activity and nutrition are no less important than pharmacological therapy. The inclusion of green tea in the diet would have a positive effect on the prevention and development of metabolic syndrome due to the various pathogenetic pathways of action of its components.

References

1. **Ahn, Y. J., S. Sakanaka, M. J. Kim, T. Kawamura, T. Fujisawa, T. Mitsuoka.** Effect of green tea extract on growth of intestinal bacteria. – *Microbial Ecology in Health and Disease*, **3**, 1990, 335-338.
2. **Alveirinho, M., P. Freitas, M. L. Faleiro.** Role of gut microbiota in metabolic syndrome: a review of recent evidence. – *Porto Biomedical Journal*, ***5***, 2020, e105.
3. **Bose, M., J. D. Lambert, J. Ju, K. R. Reuhl, S. A. Shapses, C. S. Yang.** The major green tea polyphenol, (-)-epigallocatechin-3-gallate, inhibits obesity, metabolic syndrome, and fatty liver disease in high-fat-fed mice. – *The Journal of Nutrition*, ***138***, 2008, 1677-1683.
4. **Braicu, C., M. R. Ladomery, V. S. Chedea, A. Irimie, I. Berindan-Neagoe.** The relationship between the structure and biological actions of green tea catechins. – *Food Chem.,* **141**, 2013, 3282-3289.
5. **Ding, S., M. M. Chi, B. P. Scull, R. Rigby, N. M. Schwerbrock, S. Magness, C. Jobin, P. K. Lund.** High-fat diet: bacteria interactions promote intestinal inflammation which precedes and correlates with obesity and insulin resistance in mouse. – *PloS one*, ***5***, 2010, e12191.
6. **Filippatos T. D., C. S. Derdemezis, I. F. Gazi, E. S. Nakou, D. P. Mikhailidis, M. S. Elisaf.** Orlistatassociated adverse effects and drug interactions: A critical review. – *Drug Saf.,* **31**, 2008, 53-65.
7. **Graham, D. J., R. Ouellet-Hellstrom, T. E. MaCurdy, F. Ali, C. Sholley, C. Worrall, J. A. Kelman.** Risk of acute myocardial infarction, stroke, heart failure, and death in elderly medicare patients treated with rosiglitazone or pioglitazone. – *Jama*, **304**, 2010, 411-418.
8. **Gramza-Michałowska, A.** Caffeine in tea Camellia sinensis--content, absorption, benefits and risks of consumption. – *The Journal of Nutrition, Health & Aging,* **18**, 2014, 143-149.
9. **Gong, Q., Y. Sun, L. Liu, C. Pu, Y. Guo.** Oral administration of tea-derived exosome-like nanoparticles protects epithelial and immune barrier of intestine from psychological stress. – *Heliyon*, **10**, 2024, e36812.
10. **Gong, Q., F. Xiong, Y. Zheng, Y. Guo.** Tea-derived exosome-like nanoparticles prevent irritable bowel syndrome induced by water avoidance stress in rat model. –*Journal of Gastroenterology and Hepatology,* **39**, 2024, 2690-2699.
11. **Gopal, J., M. Muthu, D. Paul, D. H. Kim, S. Chun.** Bactericidal activity of green tea extracts: The importance of catechin containing nano particles. – *Sci. Rep.*, **6**, 2016, 19710.
12. **Han, X. D., Y. Y. Zhang, K. L. Wang, Y. P. Huang, Z. B. Yang, Z. Liu.** The involvement of Nrf2 in the protective effects of (-)-Epigallocatechin-3-gallate (EGCG) on NaAsO(2)-induced hepatotoxicity. – *Oncotarget*, **8**, 2017, 65302-65312.
13. **He, J., J. Chen, Q. He, S. Li, L. Jian, F. Xie, C. Dong, G. Bai, Z. Wang, T. Zou, J. You.** Oral L-theanine administration promotes fat browning and prevents obesity in mice fed high-fat diet associated with the modulation of gut microbiota. – *Journal of Functional Foods,* **85**, 2021, 104476.
14. **Hill, A. A., M. Kim, D. F. Zegarra-Ruiz, L. C. Chang, K. Norwood, A. Assié, W. H. Wu, M. C. Renfroe, H. W. Song, A. M. Major, B. S. Samuel, J. M. Hyser, R. S. Longman, G. E. Diehl.** Acute high-fat diet impairs macrophage-supported intestinal damage resolution. – *JCI insight*, **8**, 2023, e164489
15. **Janssens, P. L., R. Hursel, M. S. Westerterp-Plantenga.** Nutraceuticals for body-weight management: The role of green tea catechins. – *Physiology & Behavior*, **162**, 2016, 83–87.
16. **Kaur, J.** A comprehensive review on metabolic syndrome. – *Cardiology Research and Practice,* 2014, 943162.

17. Lee, W. K., T. I. Kim, S. K. Park, H. K. Park, J. T. Hong. Anxiolytic Effect of a Combination of Green Tea Extract and L-theanine. – *Lab. Anim. Res.,* **26**, 2010, 63-68.
18. Li, M. Y., H. Y. Liu, D.T. Wu, A. Kenaan, F. Geng, H. B. Li, A. Gunaratne, H. Li, R. Y. Gan. L-Theanine: A unique functional amino acid in tea (Camellia sinensis L.). With multiple health benefits and food applications. – *Front. Nutrition*, **9**, 2022,853846.
19. Li, Y., S. Zhao, W. Zhang, P. Zhao, B. He, N. Wu, P. Han. Epigallocatechin-3-O-gallate (EGCG) attenuates FFAs-induced peripheral insulin resistance through AMPK pathway and insulin signaling pathway in vivo. – *Diabetes Research and Clinical Practic*e, **93**, 2011, 205-214.
20. Li, Z., L. Chen, Z. Huang, G. Jia, H. Zhao, G. Liu, X. Chen. Supplementation with L-theanine promotes intestinal antioxidant ability via Nrf2 signaling pathway in weaning piglets and H2O2-induced IPEC-J2 cells. – *Journal of Functional Foods,* **121**, 2024, 106433.
21. Liu, K., Y. Peng, L. Lin, Z. Gong, W. Xiao, Y. Li. L-Theanine regulates the abundance of amino acid transporters in mice duodenum and jejunum via the mTOR signaling pathway. – *Nutrients,* **15**, 2022, 142.
22. Mei, H., J. Li, S. Liu, A. Jeyaraj, J. Zhuang, Y. Wang, X. Chen, Q. Yuan, X. Li. The role of green tea on the regulation of gut microbes and prevention of high-fat diet-induced metabolic syndrome in mice. – *Foods (Basel, Switzerland)*, **12**, 2023, 2953.
23. Murase, T., A. Nagasawa, J. Suzuki, T. Hase, I. Tokimitsu. Beneficial effects of tea catechins on diet-induced obesity: stimulation of lipid catabolism in the liver. – International journal of obesity and related metabolic disorders. – *Journal of the International Association for the Study of Obesity*, **26**, 2002, 1459-1464.
24. Pories, W. J. Bariatric surgery: Risks and rewards. – *J. Clin. Endocrinol. Metab.,* **93**, 2008, 89-96.
25. Sae-tan, S., K. A. Grove, J. D. Lambert. Weight control and prevention of metabolic syndrome by green tea. – *Pharmacol. Res*., **64**, 2011, 146-154.
26. Saeed, M., M. Naveed, M. Arif, MU. Kakar, R. Manzoor, ME. Abd El-Hack, M. Alagawany, R. Tiwari, R. Khandia, A. Munjal, K. Karthik, K. Dhama, HMN. Iqbal, M. Dadar, C. Sun. Green tea (Camellia sinensis) and l-theanine: Medicinal values and beneficial applications in humans-A comprehensive review. – *Biomed Pharmacotherapy,* **95**, 2017, 1260-1275.
27. Sayama, K., S. Lin, G. Zheng, I. Oguni. Effects of green tea on growth, food utilization and lipid metabolism in mice. – *In Vivo*, **14**, 2000, 481-484.
28. Sirotkin, A. V., A. Kolesárová. The anti-obesity and health-promoting effects of tea and coffee. – *Physiological Research*, **70**, 2021, 161-168.
29. Stojanov, S., A. Berlec, B. Štrukelj. The influence of probiotics on the firmicutes/bacteroidetes ratio in the treatment of obesity and inflammatory bowel disease. – *Microorganisms*, **8**, 2020, 1715.
30. Terashima, T., J. Takido, H. Yokogoshi. Time-dependent changes of amino acids in the serum, liver, brain and urine of rats administered with theanine. – *Biosci. Biotechnol. Biochem.,* **63**, 1999, 615-8.
31. Tokimitsu, I. Effects of tea catechins on lipid metabolism and body fat accumulation. – *BioFactors (Oxford, England)*, **22**, 2004, 141-143.
32. Tramullas, M., B. C. Finger, T. G. Dinan, J. F. Cryan. Obesity takes its toll on visceral pain: High-fat diet induces Toll-like receptor 4-dependent visceral hypersensitivity. – *PloS one,* **11**, 2016, e0155367.

33. Trikha, S. R. J., D. M. Lee, K. E. Ecton, S. D. Wrigley, A. R. Vazquez, N. S. Litwin, K. N. Thomas, Y. Wei, M. L. Battson, S. A. Johnson, K. A. Kuhn, S. P. Colgan, C. L. Gentile, T. L. Weir. Transplantation of an obesity-associated human gut microbiota to mice induces vascular dysfunction and glucose intolerance. – *Gut Microbes,* **13**, 2021, 1940791.

34. Yan, Q., H. Tong, S. Tang, Z. Tan, X. Han, C. Zhou. L-theanine administration modulates the absorption of dietary nutrients and expression of transporters and receptors in the intestinal mucosa of rats. – *Biomed. Res. Int.*, 2017, 9747256.

35. Yang, C. S., J. Zhang, L. Zhang, J. Huang, Y. Wang. Mechanisms of body weight reduction and metabolic syndrome alleviation by tea. – *Molecular Nutrition & Food Research*, **60**, 2016, 160–174.

36. Yoda, Y., Z.Q. Hu, W.H. Zhao, T. Shimamura. Different susceptibilities of Staphylococcus and Gram-negative rods to epigallocatechin gallate. – *J. Infect. Chemotherapy,* **10**, 2004, 55-8.

37. Zhang, J., W.-Z. Zhang. Stress-induced metabolic disorders: Mechanisms, pathologies, and prospects. – *Am. J. Biomedical Sci. Res.,* **26 (6)**, 2025**,** 2025041086.

38. Zheng, G., K. Sayama, T. Okubo, L.R. Juneja, I. Oguni. Anti-obesity effects of three major components of green tea, catechins, caffeine and theanine, in mice. – *In Vivo*, **18**, 2004, 55-62.

Institute of Experimental Morphology, Pathology and Anthropology with Museum
Bulgarian Anatomical Society

Acta Morphologica et Anthropologica, 33 (1-2)
Sofia ● 2026

Molecular Tools for Diagnosing Wildlife Infections Caused by Some of Most Studied Lung and Gastrointestinal Nematodes

Mariana Panayotova-Pencheva[1], Delka Salkova[1], Rasa Binkienė[2], Gražina Stanevičiūtė[2], Virmantas Stunžėnas[2]*

[1]*Institute of Experimental Morphology, Pathology and Anthropology with Museum, Bulgarian Academy of Sciences, Sofia, Bulgaria*
[2]*Nature Research Centre, Lithuanian Academy of Sciences, Vilnius, Lithuania*

* Corresponding author e-mail: marianasp@abv.bg

This study presents a brief review of current molecular methodologies used to characterise some of the most popular gastrointestinal and lung nematodes in various wildlife hosts. Data from recent scientific developments were systematically compared, focusing on key parameters such as parasite life stages, host range, DNA extraction protocols, and target genomic regions. Attention is also given to primer selection and resulting amplicon sizes. Analysis of the compiled data highlights a primary reliance on ribosomal DNA markers (partial 18S and 28S rRNA genes, and ITS1-5.8S-ITS2 sequences), the MSP1 gene, and mitochondrial genes (e.g., COI, 12S) for species-level identification. Various PCR-based approaches and extraction techniques optimised for both non-invasive faecal samples and lung tissue specimens are summarised. These standardised molecular tools are essential for improving our understanding of nematode diversity and transmission dynamics, providing a practical guide for wildlife parasitology research.

Key words: Wildlife diseases, Molecular diagnostics, Gastrointestinal nematodes, Lungworms, PCR primers

Introduction

Parasitism is a complex interspecific relationship in which one organism, the parasite, lives on or within another, the host, typically at the host‘s expense [23]. Parasites can impact their hosts to varying degrees, leading to clinical conditions known as parasitoses.

The spread of parasitic diseases, including helminthoses, among wildlife populations carries significant ecological and economic implications. High parasite burdens can lead to substantial morbidity and mortality [4, 17]. In subclinical or mild infections, these diseases often remain asymptomatic or present with non-specific symptoms such as decreased appetite, weight loss, growth retardation, and reproductive failure [20, 21]. Collectively, these effects can trigger population declines, resulting in the loss of biodiversity and negatively affecting the game breeding and hunting industries. Furthermore, the shared use of habitats by wild and domestic animals facilitates the interspecific exchange of pathogens [18]. Animal migrations and translocations also serve as significant drivers for parasite dispersal and the emergence of novel parasitoses in wild populations [5]. This exchange is particularly pronounced in zoological gardens, where high animal density and close cohabitation between diverse species create ideal conditions for transmission [11].

Timely and accurate diagnosis is a cornerstone of effective disease management. Traditionally, the diagnosis of helminthoses has relied on the morphological identification of adult specimens. However, diagnostic accuracy based solely on the morphology of eggs and larvae is often limited and, in some cases, unreliable. This challenge is further compounded by a frequent lack of morphological expertise regarding the parasitofauna of exotic and endangered species. According to Gasser [8], many parasites previously categorised as single species with broad host ranges have been redefined as complexes of host-specific cryptic species. This distinction is critical for disease control: a parasite strictly specific to a wild host may pose no risk to livestock, and vice versa. In such contexts, molecular taxonomy has become an indispensable tool for differential diagnosis and epidemiological surveillance.

In light of these considerations, the present study reviews molecular research on some groups of selected nematodes in wildlife, aiming to provide a preliminary overview that may assist in future investigations.

Relevant literature was retrieved from the Scopus, Web of Science, and Google Scholar databases. The present study synthesizes data from the reviewed publications, with key parameters—including sample sources, parasite life stages, and the specific molecular tools used for identification— systematised and presented in comprehensive tables.

Molecular studies on lung nematodes

Gajadhar et al. [7] developed the first reliable molecular diagnostic tool to differentiate morphologically indistinguishable dorsal-spined first-stage larvae (L1) and other developmental stages of the subfamily Elaphostrongylinae. A PCR assay was designed to selectively amplify the rDNA ITS2 region. Based on the lengths of the resulting fragments, the assay successfully differentiated between the genera *Elaphostrongylus* and *Parelaphostrongylus*. While one primer set was capable of distinguishing all three *Parelaphostrongylus* spp. in a single reaction, the authors recommended a second set for routine diagnostic confirmation. Furthermore, two of the three primer sets

successfully amplified DNA from all six elaphostrongyline species, allowing for the specific identification of *Elaphostrongylus alces* and *Parelaphostrongylus odocoilei*. However, while *E. cervi* and *E. rangiferi* produced distinct fragments, they could not be differentiated from each other based on size alone. The study demonstrated the reliability of these primers across all life stages, including L1, L3, and adult worms, using various nematode, host, and faecal controls.

Lungworm infections are prevalent in North American bighorn sheep (*Ovis canadensis*), with *Protostrongylus stilesi* and *P. rushi* being the predominant species. Historically, *Muellerius capillaris* had only been documented in bighorns from South Dakota, USA. However, at the National Bison Range (NBR) in Montana, Ezenwa et al. [6] reported that 100% of surveyed sheep across six sampling periods shed first-stage dorsal-spined larvae (DSL) morphologically consistent with *M. capillaris*. In contrast, *Protostrongylus* larvae prevalence remained at or below 39%. Using molecular techniques, the authors confirmed the DSL as *M. capillaris*, marking the first definitive record of this parasite in a free-ranging bighorn sheep population outside South Dakota.

Dorsal-spined protostrongylid larvae (Nematoda: Protostrongylidae) were recovered from the faeces of the endangered pampas deer (*Ozotocerus bezoarticus celer*) in the Campos del Tuyú Wildlife Reserve, Argentina [3]. Partial sequences of the 28S rRNA gene and the ITS2 rDNA region were amplified, cloned, and analyzed. Phylogenetic analysis of the 28S rDNA sequences indicated a close relationship to *Parelaphostrongylus* spp., while ITS2 analysis placed the nematode within a clade containing both *Parelaphostrongylus* and *Elaphostrongylus* spp. Although these sequences exhibited considerable divergence from known protostrongylids, they remained most similar to these two genera. Consequently, the authors suggest that this parasite represents an undescribed species, likely belonging to the subfamily Elaphostrongylinae.

Lesage et al. [15] conducted pathological examinations of lungs from European hares in Southeast France. Morphological characterisation of adult male worms was confirmed via molecular analysis of the 28S (D2 domain) and ITS2 rDNA regions. Two species were identified: *Protostrongylus pulmonalis*, which was identical to haplotypes previously deposited in GenBank, and *P. oryctolagi*. The latter was identified based on the morphology of the copulatory bursa, specifically spicule length and gubernaculum structure. This study represents the first report of *P. oryctolagi* in both European hares and rabbits in France.

Pyziel et al. [24] developed a multiplex PCR assay designed to detect and differentiate *Dictyocaulus* species in cattle and wild ruminants using both adult and larval DNA. The assay employed four novel primers targeting species-specific regions of the ITS2 rDNA, designed from original and GenBank sequence data. Following amplification of samples from European bison (*Bison bonasus*), cattle (*Bos taurus*), moose (*Alces alces*), red deer (*Cervus elaphus*), and roe deer (*Capreolus capreolus*), gel electrophoresis revealed three distinct, species-specific bands: approximately 560 bp for *D. viviparus*, 400 bp for *D. capreolus*, and 660 bp for *Dictyocaulus* sp. from red deer and moose. Notably, *D. eckerti* (expected at 714 bp) was not observed. This

multiplex method yielded consistent results across samples from Sweden and Poland, overcoming the morphological limitations of traditional identification at various life stages.

Saidi et al. [25] investigated the prevalence and abundance of gastrointestinal parasites in three antelope species: the dorcas gazelle (*Gazella dorcas*), the scimitar-horned oryx (*Oryx dammah*), and the addax (*Addax nasomaculatus*). A total of 180 faecal samples were analysed using the Baermann technique for morphological examination, followed by molecular identification via PCR amplification and sequencing of the rDNA second internal transcribed spacer (ITS2) region. Two protostrongylid species, *Muellerius capillaris* and *Neostrongylus linearis*, were identified across all three antelope populations.

Bangoura et al. [1] described a lung nematode infection in a Rocky Mountain elk (*Cervus canadensis nelsoni*) from Wyoming, USA, which presented with severe bronchitis and pneumonia. Numerous large nematodes were recovered from the bronchi and trachea; female specimens were morphologically and molecularly identified as *Dictyocaulus* spp. based on mitochondrial *cox1* and 18S rRNA genes. Maximum likelihood phylogenetic analysis revealed that these parasites formed a subclade with *D. cervi*, nested within a larger clade including *D. eckerti*. Notably, both eggs and free first-stage larvae were observed within the adult females – a feature previously undescribed for *Dictyocaulus* spp. The authors concluded that the infection was caused by a *D. cervi*-like lungworm, marking its first report in North America.

Kuchboev and Krücken [13] characterised the diversity of *Metastrongylus* spp. in wild boars and identified the earthworm intermediate hosts contributing to the parasite‘s life cycle. Following parasitological necropsies, the authors identified three lungworm species in wild boars–*M. pudendotectus*, *M. salmi*, and *M. elongatus*–which were confirmed via ITS2 sequencing and phylogenetic analysis. Earthworms collected from wild boar habitats were screened for larvae, with three of the six investigated species testing positive for metastrongyloid larvae. While phylogenetic analysis clearly resolved *M. pudendotectus*, it provided limited resolution for the other species. The authors suggest that additional sequence data are required to resolve potential cryptic species, while deep sequencing approaches could offer deeper insights into species-specific epidemiology and pathology.

Karaer et al. [12] investigated helminth diversity in captive and free-ranging mountain gazelles (*Gazella gazella*) in Hatay, Türkiye, while assessing potential zoonotic risks. A total of 188 fresh faecal samples were analysed using DNA metabarcoding to determine helminth composition and seasonal diversity. The study identified eight taxa, two of them – lung nematodes. Significant seasonal variations in helminth abundance and composition were observed. These findings underscore the efficacy of advanced molecular techniques in characterising parasite diversity within wild ungulate populations.

Dictyocaulus spp. recovered from red deer lungs in Spain were identified through morphological examination and molecular barcoding [10]. The study confirmed the presence of three distinct genetic groups, supported by significant Φ_{ST} values. While

D. cervi and *D. viviparus* exhibited separate matrilineal ancestries, *D. eckerti* and *D. cervi* showed evidence of matrilineal sharing. These findings highlight the necessity of evaluating potential introgression between the latter two species.

Molecular studies on gastrointestinal nematodes

Despite their public health significance, few ascarid species from wild animals have been characterised at the molecular level [16]. To address this gap, the authors investigated the classification and phylogenetic relationships of roundworms from 21 captive wild animal species by sequencing partial 18S and 28S rDNA, along with the mitochondrial (mt) 12S gene. Phylogenies were inferred using Neighbor-Joining (NJ), Maximum Parsimony (MP), and Maximum Likelihood (ML) methods based on both single-gene and concatenated datasets. Sequence analysis indicated that the 18S region was highly conserved across all 21 species, whereas the 28S gene exhibited significant interspecific variability. Divergence levels in the 12S gene suggested both intra- and interspecific variation. Phylogenetic reconstruction resolved the isolates into two families, four genera, and seven species, with robust bootstrap support for each clade. Furthermore, concatenated trees suggested that *Baylisascaris ailuri* is more closely related to *B. transfuga* than to *B. schroederi*. This study identifies valuable molecular markers for the classification, phylogenetics, and epidemiological surveillance of ascarids in wildlife.

It remains debatable whether *Trichuris trichiura* is a multi-host parasite with a broad taxonomic range or a complex of host-specific species infecting closely related hosts [9]. To address this, the authors investigated the phylogenetic structure of whipworms within a multi-species community of non-human primates and humans in Western Uganda. A novel nested PCR method, applied to non-invasively collected faecal samples, demonstrated 100% sensitivity and 97% specificity compared to traditional microscopy. Phylogenetic analysis of the ribosomal DNA internal transcribed spacer regions (ITS1 and ITS2) revealed three co-circulating *Trichuris* lineages. Notably, one group was restricted to humans, whereas another infected all screened host species, indicating active transmission between wild primates and humans. These findings suggest that the host range within the genus *Trichuris* varies, with some lineages exhibiting strict host specificity and others showing host generality. Specifically, the identification of a multi-host *Trichuris* taxon challenges previous assumptions regarding helminth host-specificity and underscores significant concerns for both wildlife conservation and public health.

Moudgil et al. [19] performed faecal screening of Asiatic lions (*Panthera leo leo*) in an Indian zoo, identifying nematode eggs morphometrically and molecularly as *Toxascaris leonina*. Molecular confirmation was achieved via PCR targeting the internal transcribed spacer (ITS) sequences. Following identification, an anthelmintic treatment was implemented involving the administration of fenbendazole and ivermectin. The authors conclude that their study underscores the importance of molecular tools in validating morphological diagnoses and demonstrates the successful management of *T. leonina* in captive Asiatic lions.

Uakhit et al. [26] investigated the helminth fauna of wolves in Kazakhstan using a combination of classical parasitological and molecular techniques. The study identified several taxa, including *Echinococcus granulosus*, *Taenia krabbei*, *Dipylidium* spp., *Mesocestoides* spp., *Toxascaris leonina*, *Trichinella nativa*, and *Dirofilaria repens*. Prevalence and intensity of infection were evaluated, and helminth identification was further confirmed through amplification and sequencing of the cytochrome oxidase (*cox1*) marker gene.

To assess the prevalence of gastrointestinal parasites in a Chinese zoo, Cai et al. [2] analysed faecal samples from birds, primates, and non-primate mammals. Two ascarid species were molecularly characterized; sequence analysis of the ITS2 and *cox1* regions identified eggs from the African lion (*Panthera leo*) as *Toxascaris leonina* and those from the brown bear (*Ursus arctos*) as *Baylisascaris transfuga*. The authors emphasize that the zoonotic potential of these agents warrants increased public health attention. Furthermore, these findings provide a theoretical framework for the development of targeted prevention and control strategies for parasitic diseases in captive wildlife populations in China.

Parasitic nematodes of the superfamily Ascaridoidea infect a wide range of vertebrates, with certain taxa, particularly *Toxocara* spp., posing significant zoonotic risks. Kuchboev et al. [14] identified and characterised ascarids from wild and stray canids and felids in Uzbekistan. Specimens recovered from stray dogs, jackals, and stray cats were examined via light microscopy and molecular analysis of the partial ITS1-5.8S-ITS2 rDNA region. Morphological findings identified *Toxocara canis* and *Toxascaris leonina* in dogs and jackals, while *Toxocara cati* was identified in cats. BLAST analysis of the ITS sequences showed 99–100% identity with respective reference sequences. Maximum likelihood phylogenetic analysis confirmed that *T. canis* and *T. cati* clustered according to their known host families (Canidae and Felidae). Notably, *T. leonina* was partitioned into subclades based on host origin, suggesting a species complex with distinct host-associated infectivity.

Vafaei et al. [27] investigated the role of wild herbivores as reservoirs for helminth infections in western Iran, focusing on the goitred gazelle (*Gazella subgutturosa*, n = 36) and the wild goat (*Capra aegagrus*, n = 14). Faecal samples were microscopically screened for gastrointestinal helminth eggs, followed by genomic DNA extraction and PCR amplification of the ribosomal ITS2 region. Phylogenetic analysis of the resulting nucleotide sequences confirmed the species identities. The most prevalent circulating species were *Teladorsagia circumcincta*, *Marshallagia* spp., and *Nematodirus oiratianus*, all of which were reported for the first time in wildlife from this region. The authors concluded that these findings underscore the necessity of continuous parasite surveillance in both wildlife and domestic environments to effectively detect and manage potentially zoonotic parasitic agents.

Methodological and genetic parameters

The primary methodological and genetic parameters from the reviewed studies are synthesized and presented in **Table 1** and **Table 2**. Organised in this manner, the data may serve as a practical reference for researchers engaged in the molecular identification of pulmonary and gastrointestinal nematodes in wildlife.

The analysis of the data from the **Table 1** shows that recent studies on lung nematodes cover various wild ungulates, such as deer and musk oxen [7], chamois and bighorn sheep [1, 6], wild boar [13], and gazelles [14]. Many of these parasites, especially from the family Protostrongylidae, have life cycles that include intermediate hosts like snails [7] or earthworms [13]. This requires specific methods to collect and identify the parasite larvae from the tissues of these invertebrates.

The data show that molecular diagnostics are used for various biological materials. These include first-stage larvae (L1) from faecal samples [6, 14), third-stage larvae (L3) from intermediate hosts [7, 13], and adult worms from lung tissue [1, 13]. The use of L1 from faeces reflects a growing trend toward non-invasive monitoring of wild animal populations.

DNA extraction protocols and sample preparations also differ depending on the type of material. In some cases, enzymatic digestion is used, such as extracting L3 from snails using pepsin-HCl [7]. Other studies involve mechanically breaking down adult worms with micropestles to improve DNA release [1]. The DNA extraction kits vary as well. For faecal samples, kits for complex materials like GeneMatrix [14] are used, while for larvae and adults, tissue kits like Nucleon HT [1] or standard Qiagen kits are preferred [13].

Ribosomal DNA (rDNA) is the main diagnostic marker, with the ITS2 region being most frequently used to differentiate species within the Protostrongylidae and Metastrongylidae families [6, 7, 13]. More conservative genes, such as 18S and 28S, help determine the phylogenetic position of new or unknown parasites [6, 14]. These markers are also used in metabarcoding studies to analyse parasite communities [14]. Additionally, mitochondrial genes like *cox1* and the *MSP1* gene are used as markers to better distinguish between closely related species [1].

The reviewed studies most often use universal primers, such as the NC1/NC2 combination for the ITS2 region, which is widely applied to identify different genera [6, 7, 13]. To accurately distinguish species with similar amplicon sizes, specific primer pairs have been developed. For example, ECP1 and PTP1 are used to differentiate small lungworms of the family Protostrongylidae [7], while newly designed primers for the *cox1* and *MSP1* genes help identify large lungworms of the family Dictyocaulidae [1].

The size of the amplified DNA fragments is important for diagnostic accuracy. For example, the ITS2 region varies between species, ranging from 445 bp in *Umingmakstrongylus* sp. to 597 bp in *Elaphostrongylus* sp. [7], which allows for visual differentiation on a gel. In contrast, the 18S rRNA gene produces much longer fragments (about 1750 bp) suitable for detailed phylogenetic analysis [1]. The *MSP1* markers are shorter (328–393 bp) and are useful for rapid detection [1].

Table 1. Molecular diagnostic workflows and genetic parameters for the identification of lung nematodes in wildlife.

Nematode Species	Hosts	Sample Type & Life Stage	Extraction Protocol, Pre-treatment & Other specificities	Genetic Marker & Target Region	Primer & Specificity	Amplicon Size (bp)	References
Parelaphostrongylus tenuis; P. andersoni; P. odocoilei; Elaphostrongylus cervi; E. alces; Umingmakstrongylus pallikuukensis	Deer; Muskox (*Ovibos moshatus*); Snails	Faeces (L1); Gastropods (L3)	Pepsin-HCl digestion (for extraction of L3 from snails); Three sets of primers designed and used successfully to distinguish larvae at the species level.	ITS2 rDNA	Universal: NC1 / NC2	*P. t.(576); P.a.(566); P.o.(571); E.c. (597); E.a. (581); U.p. (445)*	Gajadhar et al., 2000
					Specific: ECP1, PTP1, PTP2 (Designed for species-level differentiation)	Size differs across universal and newly designed primer sets.	
Muellerius capillaris	Bighorn sheep (*Ovis canadensis*)	Faeces (L1)	-	ITS2 rDNA	Universal: NC1 / NC2	425 bp	Ezenwa et al., 2010
Unknown protostrongylid (genetically clustered with *Parelaphostrongylus*/ *Elaphostrongylus* group)	Pampas deer (*Ozotocerus bezoarticus celer*)	Faeces (L1)	PCR amplification, cloning, and direct sequencing for comparative analysis and species identification.	28S rDNA (D2–D3 domains)	391 F / 501 R	950 bp	Carreno et al., 2012
				ITS2 rDNA	Universal: NC1 / NC2	Not reported (Expected: ~ 400–500 bp)	

Protostrongylus oryctolagi; P. pulmonalis	European hare (*Lepus europaeus*); Rabbit (*Oryctolagus cuniculus*)	Defrosted pulmonary tracts (adult male worms & L1)	Pre-treatment: Lungworms isolated via lung tissue dissection and vigorous shaking in water (sedimentation).; Mechanical lysis of adult worms (piston pellet).; QIAamp DNA Mini Kit (Qiagen)	28S rDNA (D2 domain)	C2 / D2	Not specified; Species identified by sequencing and phylogenetic analysis.	Lesage et al., 2014
				ITS2 rDNA	Universal: NC1 / NC2		
Dictyocaulus viviparous; D. capreolus; Dictyocaulus sp.; *D. eckerti*	European bison (*B. bonasus*), Red deer (*Cervus elaphus*); Roe deer (*Capreolus capreolus*); Moose (*Alces alces*)	Adult worms; Single larva	Nucleospin Tissue DNA Extraction Kit (Macherey–Nagel, Germany); Multiplex PCR protocol for simultaneous detection of multiple species.; Multiplex PCR for species differentiation based on diagnostic band sizes.	ITS2 rDNA	4 novel species-specific primers (Multiplex set), newly designed for ITS-2 regions	560 bp (*D. viviparus*); 400 bp (*D. capreolus*); 660 bp (*Dictyocaulus* sp.); 714 bp (*D. eckert i* expected, but not found)	Pyziel et al., 2015

Muellerius capillaris; Neostrongylus linearis	Dorcas gazelle (*Gazella dorcas);* Addax *(Addax nasomacculatus);* Scimitar-horned oryx *(Oryx dammah)*	Faeces (L1)	QIAamp DNA Mini Kit (Qiagen, Germany); Protocol modified for tissue/ faecal samples.	ITS2 rDNA	Universal for nematodes: NC1 / NC2	ITS2 (+ flanking regions) – 425 bp	Saidi et al., 2020
Dictyocaulus spp.	Rocky mountain elk (*Cervus canadensis nelsoni*)	Adult worms	Tissue grinding: BioMasher II (micro pestle); Nucleon HT Genomic DNA Kit (GE Healthcare, USA)	mtDNA (*cox1*);	Newly designed: Deap_ COX1F/ Deap_COX1R	373 bp	Bangoura et al., 2020
				SSU rDNA (18S)	Universal: NC18SF1 / NC5BR	1750 bp	
				MSP1 gene	Newly designed: Dspp_ MSP1F/ Dspp MSP1R	328–393 bp	
Metastrongylus spp.	Wild boar (*Sus scrofa*) Earthworms (Lumbricidae)	Adult worms; Earthworms (L3)	Qiagen kit (India); Phusion DNA Polymerase; Earthworms: Pre-killed with 1% formalin; Isolation L3 via dissection, compressor method & artificial gastric juice digestion.	ITS2 rDNA	Universal: NC1 / NC2	Approximately 495 bp for all species.	Kuchboev & Krücken, 2022

Gastrointestinal and lungworm community (full taxonomic list provided)	Mountain gazelle (*Gazella gazella*)	Faeces (L1)	Storage: Samples stored at −20 °C.; Extraction: GeneMatrix Kit (EURx, Poland), optimized for complex faecal matrices.; Library Prep: NEBNext Ultra II.QC: Bioanalyzer/ Qubit.	SSU rDNA (18S) metabar-coding locus	Universal nematode 18S primers (18S F / 18S R)	Metabarcoding: Varies by taxa (NGS library preparation) - NovaSeq 6000	Karaer et al., 2025
Dictyocaulus spp. (*D. cervi, D. eckerti*)	Red deer	Adult worms	End-point PCR; Sequencing used to identify matrilineal groups.	mtDNA (*cox1*)	COX I_F; COX I_R: Self-designed (NCBI Primer-BLAST)	320 bp; 7 unique haplotypes; 100% coverage compared to GenBank entries	González-Velo et al., 2025

NC1: 5'ACGTCTGGTTCAGGGTTGTT; **NC2**: 5'-TTAGTTTCTTTTCCTCCGCT-3'; **ECP1**: 5'GGAATCGTCCGTCTATCGTT'3; **ECP1R**: 5'GTCAAAACGATAGACGGACG'3; **PTP1**: 5'CCGTCGAATACATGTCATCC'3; **PTP2**: 5'TCGTCAAGACGATGATTCCC'3; **391F**: 5′- AGCGGAGGAAAAGAAACTAA); **501R**: 5′-TCGGAAGGAACCAGCTACTA; **C2'**: 5′-GAAAAGAACTTTGRARAGAGA-3′; **D2**: 5′-TCCGTGTTTCAAGACGGG-3; **18S F**: 5′- GGCCGTTCTTAGTTGGTGGA-3′; **18S R**: 5′- CCCGGACATCTAAGGGCATC-3′; **NC5BR:** 5′-GCAGGTTCACCTACAGAT-3′; **Dspp_ MSP1F**: 5′-AGTTCCCCCTGGAGACATCAAC-3′; **Dspp_ MSP1R**: 5′-ATCTCCTTGGAACCACTCGC-3′; **COX I_F**: 5′-TTTTTTTTGGGCATCCTGAGGTTTAT-3′; **COX I_R**: 5′-TAAAGAAAGAAAGAACATAATGAAAAAATG-3′; **Deap_ COX1F**: 5′-CCTTTGATGTTGGGTAGACCTG-3′; **Deap_ COX1R**: 5′-GTATAGTAATAGCACCAGCC-3′; **NC18SF1:** 5′-AAAGATTAAGCCATGCA-3′

Table 2 focuses on gastrointestinal nematodes and shows a wide range of hosts. These include primates and humans [9], zoo animals like pandas and big cats [16], and wild ruminants such as gazelles and chamois [27]. Of particular interest is the identification of *Trichuris* spp. with zoonotic potential in monkeys and humans in Uganda [9]. Additionally, there is a first report of a possible *T. ovis* infection in long-tailed macaques in Thailand [22]. These findings show how molecular diagnostics can detect parasite transmission in areas where humans and wildlife live in close contact.

The primary sources of genetic material in these studies (**Table 2**) are eggs from faecal samples [9, 22, 27] or adult worms collected after deworming [16]. When analysing environmental samples like faeces, identifying nematodes from the order Strongylida is difficult because their eggs look very similar. This makes molecular markers necessary for accurate species differentiation [27]. In these studies, sample preparation and DNA extraction are critical to break through the tough egg shells. A highly efficient method for lysis involves freeze-thaw cycles using liquid nitrogen and a hot bath [9, 27]. For DNA purification, specialised commercial kits like the ZR Faecal DNA MiniPrep [9], GF-1 Tissue Kit [22], and QIAamp DNA Stool Mini Kit [27] are widely used. For adult parasites, a modified phenol-chloroform extraction is still used to obtain sufficient DNA from tissue [16].

Ribosomal DNA (rDNA) is the main marker for diagnosing gastrointestinal nematodes. Internal transcribed spacers (ITS1 and ITS2) are preferred because they vary significantly between species [9, 27]. For broader taxonomic studies, combined analyses of 18S and 28S rDNA, as well as the mitochondrial 12S gene, are used [16]. When the ITS2 region fails to amplify, 18S rRNA is a reliable alternative for confirming the genus [22]. Nested PCR with outer and inner primers is used to increase sensitivity when DNA concentrations are low [9]. Most authors rely on established universal primers, such as NC1/NC2 for the ITS region [22, 27], or specific pairs like 18S965F/18S1573R for the genus *Trichuris* [22]. Using universal primers followed by Sanger sequencing is a standard approach for distinguishing species that live in the same area, such as *Teladorsagia* sp., *Marshallagia* sp., and *Haemonchus* sp. [27].

The sizes of the PCR products vary depending on the study‘s goal. Short fragments of about 320–330 bp are typical for ITS2 diagnostics [22, 27]. In contrast, nested PCR protocols generate longer amplicons (between 895 bp and 1088 bp for ITS1), providing more genetic information for phylogenetic analysis [9]. Variations in 18S rRNA length (416 to 680 bp) are also used for precise clustering of isolates [22].

The final step in these studies is bioinformatic analysis. Software platforms like MEGA 11 are used to build phylogenetic trees, often applying the Maximum Likelihood [22] or Neighbor-Joining methods [27]. To ensure the statistical reliability of the results, 1000 bootstrap replicates are typically used [22, 27].

Conclusions

The reviewed studies demonstrate that molecular diagnostics have become an essential tool for identifying both pulmonary and gastrointestinal nematodes in wildlife. While

Table 2. Molecular diagnostic workflows and genetic parameters for the identification of gastrointestinal nematodes in wildlife.

Nematode species	Hosts	Sample type & Life stage	Extraction protocol, Pre-treatment & Other specificities	Genetic marker & Target region	Primer & Specificity	Amplicon Size (bp)	References
Ascarid nematodes	Giant panda (*Ailuropoda melanoleuca*); Red panda (*Ailurus fulgens*); Ursids; Primates; Canids; Felids	Adult worms	Adult worms collected following routine deworming of zoo inhabitants. Modified phenol/chloroform extraction of DNA.	rDNA (18S, 28S) & mtDNA (12S)	12SF / 12SR	490 bp	Li et al., 2012
					18SF / 18SR	750 bp	
					28SF / 28SR	1700 bp	
Trichuris sp.	Black-and-white colobus (*Colobus guereza*); Blue monkeys (*Cercopithecus mitis*); Grey-cheeked mangabeys (*Lophocebus albigena*); L'hoest monkeys (*Cercopithecus lhoesti*); Olive baboons (*Papio anubis*); Red colobus (*Procolobus rufomitratus*); Red-tailed guenons (*Cercopithecus ascanius*); Human (*Homo sapiens*)	Faeces (eggs)	ZR Faecal DNA MiniPrep Kit (Zymo Research Corporation, Irvine, CA, USA); Nested PCR	rDNA (ITS1 & ITS2)	ITS1 Region: External Primers 1417F / 2505R & Internal Primers: 1567F / 2462R	Expected size: 1088 bp / 895 bp	Ghai et al., 2014
					ITS2 Region: External Primers: 2462F / NC2 & Internal Primers: 2560F / NC2	Expected size: ~584 bp / 486 bp	

Toxascaris leonina	Asiatic lions (*Panthera leo persica*)	Faeces (eggs)	Sheather's sugar flotation; Concentrated eggs subjected to repetitive freeze-thaw cycles for disruption.; QIAamp DNA Stool Mini Kit (Qiagen, Germany)	rDNA (ITS-1 & ITS-2)	ITS-F / ITS-R	380 bp	Moudgil et al., 2017
Toxascaris leonina	Wolf (*Canis lupus*)	Adult worms	Homogenization with pistils in extraction buffer; Phenol-chloroform method	mtDNA (***cox1***)	JB3_F / JB4.5_R	320 bp (100% coverage)	Uakhit et al., 2022
Toxascaris leonina; Baylisascaris transfuga	African lion (*Panthera leo*); Brown bear (Ursus arctos)	Faeces (eggs)	~100 eggs ground 5 times in liquid nitrogen; MiniBEST Universal Genomic DNA Extraction Kit Ver.5.0 (TaKaRa, Japan).	rDNA (ITS-2)	*Toxascaris leonina*: TleoF / NC2R; *Baylisascaris transfuga*: NITSF / NITSR	300 bp (*Tl*) / 301 bp (*Bt*)	Cai et al., 2024
				mtDNA (*cox1*)	Generic: JB3F / JB4.5R	450 bp	
Toxocara canis	Golden jackal (*Canis aureus*)	Adult worms	GeneJET Genomic DNA Purifi-cation Kit (Thermo Fisher, USA)	rDNA (ITS1-5.8S-ITS2)	Universal for ascaridoid nematodes: TW81F' / AW28R	614–675 bp	Kuchboev et al., 2025

Trichuris spp.	Long-tailed macaques (*Macaca fascicularis*)	Faeces (eggs)	GF-1 Tissue Kit (Vivantis Technologies, Malaysia)	18S rRNA (Successful)	Genus-specific (*Trichuris* spp.): 18S965F / 18S1573R	727 bp (expected); 416 – 680 bp (final analyzed)	Phosuk et al., 2025
				ITS2 (Unsuccessful)	According previous study.	325 bp (expected) Failed (final analyzed)	
Teladorsagia circumcincta; Marshallagia spp.*; Nematodirus oiratianus*	Gazelle (*Gazella subgutturosa*); Wild goat (*Capra aegagrus*)	Faeces (eggs)	QIAamp DNA Stool Mini Kit (Qiagen, Germany); Faecal samples were frozen/thawed (3 cycles) in liquid nitrogen and 95°C water bath to rupture egg shells.	ITS-2	Universal primers: NC1 (F) / NC2 (R)	~320 bp (ranging 280–330 bp depending on species)	Vafaei et al., 2025

JB3_F: 5′-TTTTTTGGGCATCCTGAGGTTTAT-3; **JB4.5_R**: 5′-TAAAGAAAGAACATAATGAAAATG-3′; **TW81F**: 5’-GTTTCC GTAGGTGAACCTGC-3’; **AW28R**: 5’-ATATGC TTAAGTTCAGCGGGT-3’; **28SF:** 5′-CCCGATTGATTCTGTCGGC-3′; **28SR:** 5′-TGATCCTTCTGCAGG TTCACCTAC-3′; **18SF**: 5′-AGCGGAGGAAAAGAAACTAA-3′; **18SR:** 5′-TGATCCTTCTGCAGG TTCACCTAC-3′; **12SF:** 5′-AGCGGAGGAAAAGAAACTAA-3′; **12SR:** 5′-TGATCCTTCTGCAGGTTCACCTAC-3′; **ITS-F**: 5’-ATATCGGAAAAGGACGCACA-3’; **ITS-R**: 5’-TTA GTT TCT TTT CCT CCG CT-3’; **TleoF**: 5’-CGAACGCTCATATAACGGCATACTC-3′; **NC2R**: 5’-TTAGTTTCTTTTCCTCCGCT-3′; **NITSF**: 5’-TTATGAATTTTCAACATGGC-3′; **NITSR**: 5’-GTTAGATGCTTAAATTCAGC-3′; **JB3F**: 5’-TTTTTTGGGCATCCTGAGGTTTAT-3′; **JB4.5R**: 5’-TAAAGAAAGAACATAATGAAAATG-3′; **D769:** 5′-GAGTAATTTTTATAATRCGRGAAGT-3′; **D770:** 5′-AATTTTCAGG RTCTCTRCTTCAAT-3′; **CORA:** 5′-ACYACATAGTAGGTRTCATG-3′; **HC02198F:** 5′-TGATTTTTTGGTCACCCTGAAGTTTA-3′; **1417F**: 5’-AGGGACCAGCGACACTTTC-3’; **2505R**: 5’-GAGTGTCACGTCGTTCTTCAAC-3’; **1567F**: 5’-GTTCTCGTGACTGGGAC-3’; **2462R:** 5’-CTACGAGCCAAGTGATCC-3’; **2462F**: 5’-GGATCACTTGGCTCGTAG-3’; **NC2:** 5’-TTAGTTTCTTTTCCTCCGCT-3’; **2560F:** 5’-CTTGAATACTTTGAACGCACATTG-3’; **18S965F**: 5’-GGCGAAACCGCGAATGGCTC-3’; **18S1573R**: 5’-CCATGCTGAAGTATGCTTG-3’

traditional morphological methods often struggle with similar-looking eggs and larvae, molecular markers—particularly the rDNA (ITS1, ITS2, and 18S) and mitochondrial genes—provide the precision needed for accurate species differentiation. Key advancements, such as nested PCR and specialized DNA extraction protocols, have successfully addressed the challenges of working with low-concentration environmental samples and robust egg shells. Furthermore, the transition toward Next-Generation Sequencing (NGS) and metabarcoding marks a significant shift from studying individual species to analyzing entire parasite communities. These molecular approaches not only improve diagnostic accuracy but also enhance our understanding of interspecies transmission and zoonotic risks in regions where humans and wildlife coexist.

Acknowledgements: The financial support from the Bulgarian Academy of Sciences (Bilateral agreement between BAS and LAS, № IC-LT/01/2025-2027) is gratefully acknowledged. Project: "An integrative taxonomic approach to studying etiology of helminthoses in wild animals in Bulgaria and Lithuania".

References

1. Bangoura, B., B. Brinegar, T. E. Creekmore. *Dictyocaulus cervi*–like lungworm infection in a rocky mountain elk (*Cervus canadensis nelsoni*) from Wyoming, USA. - *J. Wildl. Dis.*, **57,** 2021, 71-81.

2. Cai, W., Y. Zhu, F. Wang, Q. Feng, Z. Zhang, N. Xue, X. Xu, Z. Hou, D. Liu, J. Xu et al. Prevalence of gastrointestinal parasites in zoo animals and phylogenetic characterization of *Toxascaris leonina* (Linstow, 1902) and *Baylisascaris transfuga* (Rudolphi, 1819) in Jiangsu Province, Eastern China. - *Animals*, 2024, 14, 375.

3. Carreno, R.A., D. Caporossi, M. S. Beade, C. A. Marull, M. M. Uhart, D. D. Markwardt, S. A. Nadler. Discovery of an undescribed protostrongylid nematode from the endangered pampas deer (*Ozotoceros bezoarticus celer*) in Argentina. – *J. Wildl. Dis.*, **48**, 2012, 724-31.

4. Cigler, P., P. Kvapil, M. Kastelic, M. Gombač, T. Švara**, J. Vobr, J. Račnik, E. Bartova**. Retrospective study of causes of animal mortality in Ljubljana Zoo 2005–2015. - *J. Zoo Wildl. Med.,* **51**, 2020, 571–577.

5. Demiaszkiewicz, A.W. Migrations and the introduction of wild ruminants as a source of parasite exchange and emergence of new parasitoses. - *Ann. Parasitol*., **60**, 2014, 25–30.

6. Ezenwa, V. O., A. M. Hines, E. A. Archie, E. P. Hoberg, I. M. Asmundsson, J. T. Hogg. *Muellerius capillaris* dominates the lungworm community of bighorn sheep at the National Bison Range, Montana. – *J. Wildl. Dis.,* **46**, 2010, 988-993.

7. Gajadhar, A., T. Steeves-Gurnsey, J. Kendall, M. Lankester, M. Stéen. Differentiation of dorsal-spined Elaphostrongyline larvae by polymerase chain reaction amplification of ITS-2 of rDNA. – *J. Wildl. Dis.*, **36**, 2000, 713-722.

8. Gasser, R. B. Advances in molecular tools for parasitic nematodes of animals – From genetic markers to metabarcoding and genomics. - *Biotechnology Advances,* **85***,* 2025, 108688.

9. Ghai, R.R., N. D. Simons, C. A. Chapman, P. A. Omeja, T. J. Davies et al. Hidden population structure and cross-species transmission of whipworms (*Trichuris* sp.) in humans and non-human primates in Uganda. – *PLOS Negl. Trop. Dis*., **8**, 2014, e3256.

10. **González-Velo, M., A. Espinosa-Sánchez, A. Ripa, M. A. Hurtado-Preciado, M. Martínez-Estéllez, J. Fernández-García, C. Bazo-Pérez**. Contributions to knowledge of the *Dictyocaulus* infection of the red deer. - *Vet. Sci.*, **12**, 2025, 595.
11. **Kaandorp, J.** Veterinary challenges of mixed species exhibits. - *Fowler's Zoo and Wild Animal Medicine*, 2012, 24–31.
12. **Karaer, M. C., B. Karataş, E. Madak, et al**. Characterizing the helminth community of the mountain gazelle (*Gazella gazella* Pallas, 1766) through DNA metabarcoding. - *Acta Parasit.,* **70**, 2025, 82.
13. **Kuchboev, A. E., J. Krücken**. Prevalence, infection intensity and molecular diagnosis of mixed infections with *Metastrongylus* spp. (Metastrongylidae) in wild boars in Uzbekistan. – *Pathogens*, **11**, 2022, 1316.
14. **Kuchboev, A. E., A. G. Sotiboldiyev, B. K. Ruziev, A. A. Safarov**. Molecular identification and phylogenetic positioning of nematodes *Toxocara canis, T. cati* (Ascarididae) and *Toxascaris leonina* (Toxocaridae) from domestic and wild carnivores in the Fergana Valley, Uzbekistan. - *Biosystems Diversity*, **33**, 2025, e2538.
15. **Lesage, C., D. Jouet, C. Patrelle, J. S. Guitton, A. Decors, H. Ferté**. *Protostrongylus pulmonalis* (Frölich, 1802) and *P. oryctolagi* Baboš, 1955 (Nematoda: Protostrongylidae), parasites of the lungs of European hare (*Lepus europaeus* L.) in France: morphological and molecular approaches. – *Parasitol. Res*., **113**, 2014, 2103-2011.
16. **Li, Y., L. Niu, Q. Wang, Z. Zhang, Z. Chen, X. Gu, Y. Xie, N. Yan, S. Wang, X. Peng, G. Yang**. Molecular characterization and phylogenetic analysis of ascarid nematodes from twenty-one species of captive wild mammals based on mitochondrial and nuclear sequences. – *Parasitology*, **139**, 2012, 1329-1338.
17. **Lim, Y. A. L., R. Ngui, J. Shukri, M. Rohela, H. R. Mat Nairn.** Intestinal parasites in various animals at a zoo in Malaysia. - *Vet. Parasitol.*, **157**, 2008, 154–159.
18. **Martin, C., P. Pastoret, B. Brochier, M. Humblet, C. Saegerman.** A survey of the transmission of infectious diseases/infections between wild and domestic ungulates in Europe. – *Vet. Res*., **42**, 2011, 70.
19. **Moudgil, A. D., L. D. Singla, M. P. Singh**. Internal transcribed spacer sequence based molecular confirmation and drug efficacy assessment against *Toxascaris leonina* (Linstow, 1909) infection in Asiatic lions (*Panthera leo persica*). – *Helminthologia*, **54**, 2017, 152-156.
20. **Panayotova-Pencheva, M.** Parasites in captive animals: A review of studies in some European zoos. - *Der Zoolog. Garten*, **82**, 2013, 60–71.
21. **Panayotova-Pencheva, M. S.** Strongyloides sp. infection in a brown capuchin (*Sapajus apella* L.): Case report. - *Acta Morphol. Anthropol*., **30**, 2023, 116-121.
22. **Phosuk, I., T. Thanchomnang, J. Banglua, S. Laymanivong, D. Puangpronpitag, J. Jongthawin**. Molecular identification of *Trichuris* species in long-tailed macaques from Dong Ling Don Chao Pu Park and Kumphawapi Monkey Garden, Northeast Thailand: First report suggesting possible *Trichuris ovis* infection in non-human primates. - *Int. J. Parasitol.: Paras. Wildl*., **27**, 2025, 101063.
23. **Poulin, R.** Evolutionary ecology of parasites. Princeton University Press, 4-5. ISBN 978-0-691-12085-0. 2007.
24. **Pyziel, A.M., Z. Laskowski, J. Höglund**. Development of a multiplex PCR for identification of *Dictyocaulus lungworms* in domestic and wild ruminants. – *Parasitol. Res.*, **114**, 2015, 3923-3926.

25. Saidi, A., R. Mimouni, F. Hamadi, W. Oubrou. Coprological survey of protostrongylid infections in antelopes from Souss-Massa National Park (Morocco). – *Helminthologia*, **57**, 2020, 306-313.

26. Uakhit R. S., A. M. Smagulova, L. A. Lider, S. V. Leont'ev, A. P. Berber, V. S. Kiyan. Species composition of wolf (Canis lupus) helminth fauna in Kazakhstan. – *Euras. J. Appl. Biotechnol.*, **1**, 2022, 49-58.

27. Vafaei, M. R., M. Safaie, E. Kazemirad, H. Mirjalali, Z. Askari, M. Mohebali, G. Mowlavi. Molecular identification of nematodes (superfamily: Strongylida) traced in herbivores excrement found in wildlife from western Iran. - *Iran. J. Parasitol*., **20**, 2025, 573-583.

Institute of Experimental Morphology, Pathology and Anthropology with Museum
Bulgarian Anatomical Society

Acta Morphologica et Anthropologica, 33 (1-2)
Sofia ● 2026

ANTHROPOLOGY AND ANATOMY 33 (2)

Original Articles

Correlations between Some Cardiac and Anthropometric Parameters in Male Patients from South Bulgaria with Arterial Hypertension

Kristian Argirov[1], Atanas Baltadjiev[1], Bistra Dobreva-Yatseva[2], Tsvetanka Petleshkova[1]*

[1]Department of Anatomy, Histology and Embryology, Faculty of Medicine, Medical University of Plovdiv, Bulgaria
[2]First Department of Intermal Disease, Section of Cardiology, Faculty of Medicine, Medical University of Plovdiv, Bulgaria

* Corresponding author e-mail: kristian.argirov@mu-plovdiv.bg

This study aims to evaluate the relationships between anthropometric parameters and echocardiographic markers of left ventricular structure and geometry in Bulgarian men with arterial hypertension. Anthropometric indices reflecting overall and central adiposity were assessed, and transthoracic echocardiography was used to measure interventricular septal thickness, posterior wall thickness and left ventricular internal diameter in diastole. Left ventricular mass, left ventricular mass index, and relative wall thickness were calculated. Correlation analysis demonstrated significant positive associations between most anthropometric measurements: particularly body weight, body mass index, waist and hip circumference, and body surface area as well as echocardiographic indices of left ventricular wall thickness, chamber dimensions, and myocardial mass. Waist-to-height ratio and body roundness index were also significantly associated with several echocardiographic parameters. These findings indicate that anthropometric parameters, especially those reflecting overall and central adiposity, are closely associated with left ventricular remodeling in men with arterial hypertension.

Key words: Bulgarians, arterial hypertension, cardiac measurements, anthropological parameters, correlations

Introduction

Arterial hypertension is one of the most prevalent cardiovascular disorders worldwide and remains a leading risk factor for cardiovascular morbidity and mortality, contributing substantially to the development of heart failure, ischemic heart disease, and stroke [15]. Sustained elevation of arterial pressure imposes chronic hemodynamic overload on the myocardium, leading to structural and geometric alterations of the left ventricle collectively described as left ventricular remodeling [5]. These alterations include increased myocardial wall thickness, left ventricular hypertrophy, chamber dilatation, and changes in ventricular geometry, all of which have been known to have independent prognostic significance [11].

Echocardiography is the preferred non-invasive imaging modality for the assessment of left ventricular structure and geometry, allowing accurate quantification of interventricular septal thickness, posterior wall thickness, left ventricular internal diameter from which left ventricular mass, left ventricular mass index, and relative wall thickness can be calculated [9]. Increased left ventricular mass and abnormal ventricular geometry have been consistently associated with adverse cardiovascular outcomes, independent of blood pressure levels and other common risk factors [4].

Anthropometric characteristics have been increasingly recognized as important determinants of left ventricular remodeling in patients with arterial hypertension [14]. Traditional measures such as body weight, body mass index, waist circumference, and hip circumference reflect overall and regional adiposity and have been shown to correlate with left ventricular mass and myocardial wall thickness in hypertensive populations [7]. Excess adiposity contributes to cardiac structural changes through complex mechanisms involving increased circulating blood volume, neurohormonal activation, insulin resistance, and chronic low-grade inflammation [10].

In recent years, novel anthropometric indices, including waist-to-height ratio, body roundness index, body surface area, and a body shape index, have been proposed as alternative markers of cardiometabolic risk that may better capture the effects of body fat distribution than traditional indices [8]. However, the associations between these newer anthropometric measures and echocardiographic markers of left ventricular remodeling remain insufficiently studied, particularly in patients with established arterial hypertension [1]. Moreover, available data comparing the relative predictive value of classical and novel anthropometric indices for specific echocardiographic parameters are limited and inconsistent [6].

Furthermore, sex-related differences influence the relationship between anthropometry and cardiac remodeling. Men with arterial hypertension more frequently exhibit increased left ventricular mass and larger chamber dimensions compared with women at similar blood pressure levels [13]. These differences may be attributed to variations in body composition, fat distribution, and hormonal milieu, as well as differences in myocardial adaptive responses to pressure overload [12]. Considerable number of hypertension-focused studies have demonstrated that left ventricular hypertrophy is highly prevalent in hypertensive men and can be important prognostic predictor [2].

Identifying anthropometric parameters that are most strongly associated with left ventricular wall thickness, chamber dimensions, mass, and geometry may improve early risk stratification and facilitate the individualized management of patients with arterial hypertension [3].

The present study **aims** to evaluate the relationship between anthropometric parameters and echocardiographic markers of left ventricular structure and geometry in Bulgarian men with arterial hypertension.

Materials and Methods

The study included 60 male patients with arterial hypertension. The research was conducted at medical center "Tonus" in the city ot Pazardjik, Bulgaria. ***The inclusion criteria*** for the patients were Bulgarian origin, age between 40 and 70 years, a history of arterial hypertension (Systolic blood pressure ≥ 140 mmHg and/or Diastolic blood pressure ≥ 90 mmHg measured on at least two separate occasions**)** of at least five years duration, and good pharmacological blood pressure control. Patients with a previous history of acute coronary syndrome (ACS) were ***excluded from the study***. The study was perfomed between May 2025 and December 2025.

All patients provided written informed consent following the principles of the 1964 Declaration of Helsinki.

The following four anthropometric parameters were measured: height, body weight, waist circumference, and hip circumference. All measurements were performed according to the Martin–Saller methodology. The following anthropometric indexes – BMI (body mass index), Waist/Hip ratio, Waist/Height ratio, ABSI (a body shape index), ABSI z-score, BRI (body roundness index) and BSA (body surface area) were calculated using corresponding formulas, as follows- $BMI=weight/height^2$, $ABSI=waist\ circumference/BMI^{2/3}x\ height^{1/2}$, $BRI= 364.2- 365.5\times\sqrt{[1-((waist\ circumfrence/2\pi)^2/(0.5\times height)^2)]}$, $BSA=0.007184\times Height^{0.725}\times Weight^{0.425}$.

In all examined patients, a standard transthoracic echocardiographic evaluation was performed. For the purposes of the study, the following echocardiographic parameters were optained: interventricular septum thickness in diastole (IVSd), left ventricular posterior wall thickness in diastole (LVPWd), and left ventricular internal diameter in end-diastole (LVIDd). In addition, left ventricular mass (LV mass), left ventricular mass index (LVMI), and relative wall thickness (RWT) were calculated by the corresponding formulas, as follows- $LVM=0.8\times[1.04(\ (IVSd+LVIDd+PWTd)^3-(LVIDd)^3)]+ 0.6$, $LVMI=LVM/BSA$, $RWT=(2xLVPWd)/LVIDd$.

Statistics. Pearson's correlation was used to assess the correlations between the variables, and Pearson's correlation coefficient (PC) was calclated as well. The value of the coefficient was used to estimate the correlation's strength: low correlation 0.01–0.30; moderate 0.30–0.50; strong 0.50–0.70; high 0.70–0.90, and very high correlation >0.90. A level of statistical significance $p < 0.05$ was used. Data processing and statistical analyses were performed using SPSS Statistics version 23.0.

Results

The obtained results of the studied anthropometric and cardiological parameters are presented in **Tables 1 and 2**.

Table 1. Anthropometric parameters in male Bulgarian patients with arterial hypertension

Parameters	N	Mean	SE	SD
WC (cm)	60	109.74	2.19	13.85
HC (cm)	60	107.32	1.63	10.29
Weight (kg)	60	90.45	2.92	18.44
Height (cm)	60	171.42	1.11	7.03
BMI (kg/m²)	60	30.82	0.88	5.56
WHR	60	1.02	0.01	0.08
WHtR	60	0.64	0.01	0.08
ABSI	60	0.10	0.01	0.07
ABSI-z score	60	0.38	0.18	1.13
BRI	60	6.54	0.32	2.04
BSA (m²)	60	2.07	0.03	0.22

WC-waist circumference; HC- hip circumference; BMI- body mass index; WHR ratio-waist to hip ratio; WHtR waist to height ratio; ABSI- a body shape index; BRI- body roundness index; BSA-body surface area.

Table 2. Cardiac parameters in male Bulgarian patients with arterial hypertension

Parameters	N	Mean	SE	SD
IVSd (mm)	60	13.75	0.27	1.70
LVPWd (mm)	60	12.60	0.22	1.41
LVIDd (mm)	60	48.87	1.03	6.52
LVmass (g)	60	261.02	12.85	81.28
LVMI (g/m²)	60	125.52	3.88	24.53
RWT	60	0.52	0.01	0.08

IVSd-intraventricular septum in diatole; LVPWd- left ventricle posterior wall in diastole; LVIDd- left ventricle internal diameter in diastole; LV mass- left ventricle mass; LVMI- left ventricle mass index; RWT- relative wall thickness

Correlations between Interventricular septum thickness in diastole (IVSd) and some anthropometric parameters.

Strong positive significant correlations were detected between IVSd on one hand and body weight (PC 0.517; $p < 0.001$), WC (PC 0.599; $p < 0.001$), BMI (PC 0.662; $p < 0.001$), Waist/Height ratio (PC 0.645; $p < 0.01$) and BRI (PC 0.662; $p < 0.001$) on the

other hand. Moderate positive significant correlations were discovered between IVSd and HC (PC 0.492; $p < 0.001$), waist/ hip ratio (PC 0.398; $p < 0.001$) and BSA (PC 0.455; $p < 0.001$).

Correlations between Left ventricular posterior wall thickness in diastole (LVPWd) and some anthropometric parameters.

Strong positive significant correlations were observed between LVPWd and body weight (PC 0.582; $p < 0.001$), WC (PC 0.605; $p < 0.001$), HC (PC 0.513; $p < 0.001$) BMI (PC 0.662; $p < 0.001$), Waist/Height ratio (PC 0.619; $p < 0.001$) and BRI (PC 0.631; $p < 0.001$) and BSA (PC 0.527; $p < 0.001$). A moderate positive significant correlation was discovered between LVPWd and waist/ hip ratio (PC 0.371; $p < 0.01$).

Correlations between left ventricular internal diameter in diastole (LVIDd) and *some anthropometric parameters*

Left ventricular internal diameter in diastole (LVIDd) demonstrated high positive significant correlations with body weight (PC 0.777; p<0.001) and BSA (PC 0.811*;* $p<0.001$), strong positive significant correlatins with height (PC 0.507; $p<0.001$), WC (PC 0.630; p<0.001), HC (PC 0.690; p<0.001), BMI (PC 0.579; p<0.001), and moderately positive once with waist-to-height ratio (PC 0.428; p<0.01), BRI (PC 0.448; p<0.01) (Table 3).

Table 3. Correlations between some cardiac and anthropometric parameters in Bulgarian male patients with arterial hypertension.

Anthropometric parameter	IVSd		LVPWd		LVIDd	
	r (PC)	P	r (PC)	P	r (PC)	P
Height	-.176	0,278	-.105	0,519	**.507**	**0,001**
Weight	**.517**	**0,001**	**.582**	**0,001**	**.777**	**0,001**
WC	**.599**	**0,001**	**.605**	**0,001**	**.630**	**0,001**
HC	**.492**	**0,001**	**.513**	**0,001**	**.690**	**0,001**
BMI	**.662**	**0,001**	**.662**	**0,001**	**.579**	**0,001**
WHR	**.398**	**0,01**	**.371**	**0,02**	.146	0,370
WHtR	**.645**	**0,000**	**.619**	**0,001**	**.428**	**0,001**
ABSI	-.197	0,222	-.207	0,201	.068	0,676
ABSI z-score	.073	0,656	.046	0,779	.046	0,779
BRI	**.662**	**0,001**	**.631**	**0,001**	**.448**	**0,001**
BSA	**.455**	**0,003**	**.527**	**0,001**	**.811**	**0,001**

Correlations between left ventricular mass (LV mass) and some anthropometric parameters

High positive significant correlations were detected between Left ventricular mass and weight (PC 0.893; p<0.001), WC (PC 0.782; p<0.001), HC (PC 0.802; p<0.001),

BMI (PC 0.794; p<0.001) and BSA (PC 0.882 p<0.001). Strong positive significant correlations were detected with waist to height ratio (PC 0.639; p<0.001) and BRI (PC 0.663; p<0.001). A moderate positive significant correlation was detected with the height (PC 0.318; p<0.05) (**Table 4**).

Correlations between left ventricular mass index (LVMI) and some anthropometric parameters

High positive significant correlations were detected between Left ventricular mass index and weight (PC 0.786; p<0.001), WC (PC 0.755; p<0.001), HC (PC 0.709; p<0.001), BMI (PC 0.770; p<0.001) and BSA (PC 0.763; p<0.001). Strong positive significant correlations were discovered with waist to height ratio (PC 0.670; p<0.05) and BRI (PC 0.689; p<0.001). A moderate positive correlation was revealed between LVMI and W/H ratio (PC 0.359; p<0.05) (**Table 4**).

Correlations between RWT (relative wall thickness) and some anthropometric parameters

The relative wall thickness showed a moderate negative significant correlation with heigh (PC -0.488; p<0.001) only (**Table 4**).

Table 4. Correlations between LV mass, LVMI, RWT cardiac parameters and some anthropometric parameters in Bulgarian male patients with arterial hypertension

Anthropometric parameter	LV mass		LVMI		RWT	
	r (PC)	P	r (PC)	P	r (PC)	P
Height	**.318**	**0,05**	.165	0,308	**-.488**	**0,001**
Weight	**.893**	**0,001**	**.786**	**0,001**	-.161	0,321
WC	**.782**	**0,001**	**.755**	**0,001**	-.017	0,919
HC	**.802**	**0,001**	**.709**	**0,001**	-.155	0,340
BMI	**.794**	**0,001**	**.770**	**0,001**	.073	0,655
WHR	.272	0,089	**.359**	**0,04**	.197	0,223
WHtR	**.639**	**0,001**	**.670**	**0,001**	.156	0,336
ABSI	-.074	0,648	-.134	0,410	-.206	0,203
ABSI z-score	.043	0,791	.078	0,633	.028	0,866
BRI	**.663**	**0,001**	**.689**	**0,001**	.148	0,362
BSA	**.882**	**0,001**	**.763**	**0,001**	-.233	0,147

Discussion

The present study demonstrates significant and clinically relevant associations between anthropometric parameters and echocardiographic markers of left ventricular structure and geometry in men with arterial hypertension. These findings highlight the important

role of body size and adiposity in modulating hypertensive cardiac remodeling and support the concept that anthropometric characteristics contribute substantially to myocardial structural adaptation beyond the effects of elevated blood pressure alone.

A consistent positive relationship was observed between traditional anthropometric measures, including body weight, body mass index, waist circumference, and hip circumference, and echocardiographic indices of left ventricular wall thickness, such as interventricular septal thickness and posterior wall thickness in diastole. These findings align with previous evidence demonstrating that excess body mass is a major determinant of myocardial hypertrophy in hypertensive patients [7, 14]. The observed correlations likely reflect the combined impact of increased hemodynamic load, augmented circulating volume, and obesity-related metabolic and inflammatory pathways that promote myocardial growth and fibrosis [10].

Left ventricular internal diameter in diastole showed strong correlations with body weight and body surface area and moderate associations with indices reflecting central adiposity. This pattern suggests that increased body size in hypertensive men is associated not only with concentric wall thickening but also with chamber enlargement, indicative of eccentric remodeling. Such remodeling patterns have been linked to a higher risk of progression to heart failure and adverse cardiovascular outcomes [5, 11]. The particularly strong correlation between body surface area and left ventricular internal diameter emphasizes the importance of accounting for body size when interpreting echocardiographic dimensions [3].

Left ventricular mass and left ventricular mass index demonstrated the strongest correlations with anthropometric parameters, particularly body weight, body mass index, waist circumference, hip circumference, and body surface area. These findings are consistent with prior studies indicating that obesity is a powerful independent determinant of left ventricular mass in hypertensive individuals [4, 14]. The magnitude of these associations in the present male cohort suggests that excess body mass may substantially amplify the structural cardiac effects of arterial hypertension.

In contrast, relative wall thickness showed limited associations with anthropometric indices, with a significant inverse relationship observed only with height. These findings suggest that relative wall thickness may be less sensitive to adiposity-related influences and more reflective of intrinsic ventricular geometry and pressure-loading conditions. Previous research has indicated that relative wall thickness and left ventricular mass may vary independently, particularly in individuals with larger body size, which may explain the weaker correlations observed [5, 9].

The examined anthropological indices waist-to-height ratio and body roundness index demonstrate significant correlations with several echocardiographic parameters, whereas a body shape index and its z-score were not significantly related to left ventricular structure. These findings suggest that not all emerging anthropometric indices are equally informative in the context of hypertensive cardiac remodeling. Indices incorporating both body size and central adiposity may better reflect the hemodynamic and metabolic burden imposed on the myocardium, whereas a body shape index appears to have limited applicability in this clinical setting [1, 8, 6].

Hypertensive men are more likely to develop increased left ventricular mass and altered ventricular geometry compared with women, even at comparable blood pressure levels [13, 12]. Major hypertension-focused studies have further demonstrated that left ventricular hypertrophy is highly prevalent in men and represents a strong predictor of adverse cardiovascular outcomes [2]. The findings of the present study therefore provide clinically relevant insight into a population at particularly high risk of hypertensive heart disease.

The results suggest that simple anthropometric measures obtained during routine examination may provide valuable information regarding the likelihood of adverse left ventricular remodeling in men with arterial hypertension as a clinical perspective. Patients with increased body mass and central obesity may benefit from closer echocardiographic surveillance and more aggressive lifestyle and therapeutic interventions aimed at weight reduction and cardiovascular risk modification.

The cross-sectional design precludes causal inference, and additional longitudinal studies are required to determine whether changes in anthropometric parameters directly influence the progression or regression of left ventricular remodeling. Additionally, potential confounding factors such as duration of hypertension, type of antihypertensive therapy, and metabolic variables were not accounted for and may have influenced the observed relationships. Nevertheless, the consistency and biological plausibility of the observed associations support the validity of the findings.

Conclusion

Anthropometric parameters are closely related to echocardiographic markers of left ventricular structure and remodeling in men with arterial hypertension. Measures reflecting overall and central adiposity, including body weight, body mass index, waist and hip circumference, waist-to-height ratio, body roundness index, and body surface area, demonstrated consistent associations with left ventricular wall thickness, chamber dimensions, and myocardial mass. In contrast, a body shape index showed limited utility in characterizing hypertensive cardiac remodeling. Relative wall thickness was largely independent of adiposity-related measures, with height being the only significant determinant. These findings highlight the importance of comprehensive anthropometric assessment in the evaluation of hypertensive patients and suggest that simple, routinely obtained body measurements may facilitate identifying individuals at increased risk of adverse left ventricular remodeling.

References

1. **Ashwell M, P. Gunn, S. Gibson.** Waist-to-height ratio is a better screening tool than waist circumference and BMI for adult cardiometabolic risk factors: systematic review and meta-analysis**. -** *Obesity Reviews,* **13**(3), 2012, 275–286.
2. **Cuspidi C, M. Rescaldani, C. Sala, G. Grassi.** Left-ventricular hypertrophy and obesity: a systematic review and meta-analysis of echocardiographic studies**.** – *J. Hypertens*., **32**, 2014, 16–25.

3. de Simone, G., S. R. Daniels, R. B. Devereux, R. A. Meyer, M. J. Roman, O. de Divitiis, M. H. Alderman. Left ventricular mass and body size in normotensive children and adults: assessment of allometric relations and impact of overweight**.** – *J. Am. College of Cardiology*, ***20*** **(5),** 1992, 1251-1260.

4. Devereux, R. B., K. Wachtell, E. Gerdts. Prognostic significance of left ventricular mass change during treatment of hypertension**.** – *ACC Current Journal Review,* **14 (3)**, 2005, 26-27.

5. Ganau, A., R. B. Devereux, M. J. Roman, G. De Simone, T. G. Pickering, P. S. Saba, J. H. Laragh. Patterns of left ventricular hypertrophy and geometric remodeling in essential hypertension**. -** *J. Am. College of Cardiology,* **19**(7), 1992, 1550–1558.

6. Goh, L. G., S. S. Dhaliwal, T. A. Welborn, A. H. Lee, P. R. Della, Anthropometric measurements of general and central obesity and the prediction of cardiovascular disease risk in women**:** a cross-sectional study**.** – *BMJ Open*., **4**, 2014, e004138.

7. Kotsis, V., S. Stabouli, S. Papakatsika, Z. Rizos, G. Parati. Mechanisms of obesity-induced hypertension**. -** *Hypertension Research,* **33**(5), 2010, 386–393.

8. Krakauer, N. Y., and J. C. Krakauer. A new body shape index predicts mortality hazard independently of body mass index. – *PLoS ONE*, **7**(7), 2012, e39504.

9. Lang, R. M., L. P. Badano, V. Mor-Avi, J. Afilalo, A. Armstrong, L. Ernande, J. U. Voigt. Recommendations for cardiac chamber quantification by echocardiography in adults: an update from the American Society of Echocardiography and the European Association of Cardiovascular Imaging**. –** *Eur. Heart J. – Cardiovascular Imaging***, 16**(3), 2015, 233–271.

10. Lavie C. J., R. V. Milani, H. O. Ventura. Obesity and cardiovascular disease: risk factor, paradox, and impact of weight loss**.** – *J. Am. College of Cardiology,* **63**(14), 2014, 1345–1354.

11. Levy, D., R. J. Garrison, D. D. Savage, W. B. Kannel, W. P. Castelli. Prognostic implications of echocardiographically determined left ventricular mass in the Framingham Heart Study**.** – *New England J. Med.,* **322**(22), 1990, 1561–1566.

12. Olivetti G, M. Melissari, J. M. Capasso, P. Anversa. Cardiomyopathy of the aging human heart: myocyte loss and reactive cellular hypertrophy. *Circulation Res.,* **68**(6), 1995, 1560–1568.

13. Regitz-Zagrosek, V., S. Oertelt-Prigione, E. Prescott, F. Franconi, V. Stangl, EUGenMed, Cardiovascular Clinical Study Group. Gender in cardiovascular diseases: impact on clinical manifestations, management, and outcomes**.** – *Eur. Heart J.,* **37**(1), 2016, 24–34.

14. Verdecchia, P., F. Angeli, C. Borgioni, R. Gattobigio, G. De Simone, R. B. Devereux, C. Porcellati. Changes in cardiovascular risk by reduction of left ventricular mass in hypertension: a meta-analysis**.** – *Am. J. Hypertension.* **16**(11), 2003, 895–899.

15. Williams, B., G. Mancia, W. Spiering, E. A. Rosei, M. Azizi, et al. 2018 ESC/ESH Guidelines for the management of arterial hypertension**.** – *Eur. Heart J.,* **39**(33), 2018**,** 3021–3104.

Institute of Experimental Morphology, Pathology and Anthropology with Museum
Bulgarian Anatomical Society

Acta Morphologica et Anthropologica, 33 (1-2)
Sofia ● 2026

Age and Gender-Related Differences in Anthropometric Foot Indices within the Bulgarian Population

Meglena Angelova, Desislava Marinova, Veselina Zhekova

Department of Anatomy and Cell Biology, Medical University "Prof. Dr P. Stoyanov" – Varna, Bulgaria

*Corresponding author e-mail: angelovameglena@gmail.com

The human foot is designed for multi-functional performance, providing essential stability while standing, seamless adaptability to varied terrain, and the mechanical leverage necessary for movement. Foot characteristics show significant regional and ethnic differences. The characteristics of the foot change throughout the ontogenetic development. This determines the different frequency of high and low arch cases in different age groups. Within the Bulgarian population, the prevalence of low-arched feet (pes planus) is significantly higher in individuals under the age of 40 compared to those over 40. Furthermore, the incidence of the Greek foot (Morton's toe) is lower in the cohort under 40 years of age. Our study shows that foot morphology in Bulgaria is changing over time. This shift is most evident in men, where younger generations are more likely to have low arches, significantly changing the balance between high-arched and low-arched foot types in the population.

Key words: foot, plantograms, foot arch

Introduction

The human foot is designed for multi-functional performance, providing essential stability while standing, seamless adaptability to varied terrain, and the mechanical leverage necessary for movement. There is a broad consensus that morphological variations in anatomical structures directly impact biomechanical function, thereby predisposing individuals to an increased risk of musculoskeletal pathologies and injury [14, 17].

Plantograms or foot prints, obtained by inking the plantar surface of the foot or by using digital plantogrphs, reflect the shape and orientation of this surface of the lower limb during standing or locomotion. Measurements of various distances, angles, and

areas on plantograms are considered a simple and objective method for foot typing.

Because foot characteristics are heavily influenced by regional and ethnic factors, using external population data for local clinical assessments can be problematic [9, 12]. Our study addresses this gap by characterizing the Bulgarian population, where we observed distinct morphological trends - specifically, a high frequency of the 'Greek foot' variant and a relatively high incidence of high arch foot [2, 6].

The Greek foot, or Morton's toe, is a morphological variation where the second digit surpasses the hallux in length. This condition - described by American surgeon Dudley Morton—is primarily attributed to an abnormally short first metatarsal (brachymetatarsia) [8].

The characteristics of the foot change throughout the ontogenetic development. This determines the different frequency of high and low arch cases in different age groups [13, 15], and such differences have been reported in many populations. Using these literature data, we also examined the distribution of foot types in different age groups in Bulgarian population.

Material and Methods

Footprints (plantograms) of randomly selected 210 Bulgarian men and women, without malformations, surgery or traumas of the foot, aged 18 to 60 years were collected after their written consent. The female participants were 115, and the male ones – 95. According to their age the participants under 40-years were 125, and these over 40-years age were 85. The study was approved by the Research Ethics Committee at the Medical University "Prof. Dr. P. Stoyanov" with protocol №140/01.07.2021. All participants filled out a survey in which they also noted their height and weight. The Body Mass Index (BMI) was calculated based on this data. Each plantogram was studied using different measurements - Clarke angle (CA), the Chippaux-Smirak Index (CSI) and the Arch Index (AI).

CA is the angle between the tangent line connecting the most medial points of the forefoot (1st metatarsal head) and the hindfoot (heel), and the line connecting that same forefoot point to the deepest part of the arch curve. If the CA value is between 42° and 54° the foot is normal. High-arched foot presents with CA more than 54° and the low-arched one with CA value less than 41°.

CSI is calculated as the ratio between the minimum midfoot width and the maximum forefoot width. First, a line is drawn across the widest part of the metatarsals. A second, parallel line is then measured at the narrowest point of the arch. The index is defined as the ratio of the arch width to the metatarsal width. In the cases with CSI between 25% and 45% the foot was considered as normal. If the CSI was more than 45% the foot was described as flat or low-arched foot (pes planus) and when the index was less than 25% - as high arched foot.

AI represents the ratio of the middle third of the footprint to the total footprint area (excluding the toes). To determine this, a longitudinal axis is drawn from the center of the heel to the base of the second toe. The footprint is then segmented into three equal

sections by lines perpendicular to this axis. The area of the middle part and the area of the entire footprint were measure with ImageJ software and AI was calculated The normal foot was defined by AI scores between 0,21 and 0,28. The high-arched foot had AI value less than 0,21, and the low-arched foot – more than 0,28.

Cases with a longer second toe and a difference of at least 2 mm with the first toe on the plantogram were defined as Greek foot or Morton's toe.

The study participants were first divided by age into two groups: under and over the age of 40. The average age of each group was respectively 26,5 and 48,8 years. Each of these groups was subdivided by gender into women and men. The t-test and chi-square test were used to analyze the data.

Results

We compared the frequency of Greek foot in people under and over 40 years of age, and we found a significant difference. In the group under 40 years the incidence of Morton's toe was 37.7% but in the group over 40 years it was 49.4%. Statistical significance was confirmed by chi-square test ($p<0.0001$).

When analyzing the prevalence of the Greek foot (Morton's toe) across both age and gender, our data revealed a significant higher frequency among older cohorts. Specifically, women over 40 demonstrated a higher prevalence of Morton's toe compared to those under 40 ($p < 0.001$). A similar age-related trend was confirmed in men, with the Greek foot being significantly more common in the over-40 demographic ($p < 0.001$). While no gender-based differences were observed in participants under 40, a notable disparity emerged in the older group: the frequency of Greek foot in women over 40 was significantly higher than in their male counterparts—exceeding 50% compared to 32%, respectively ($p < 0.001$) (**Fig. 1**).

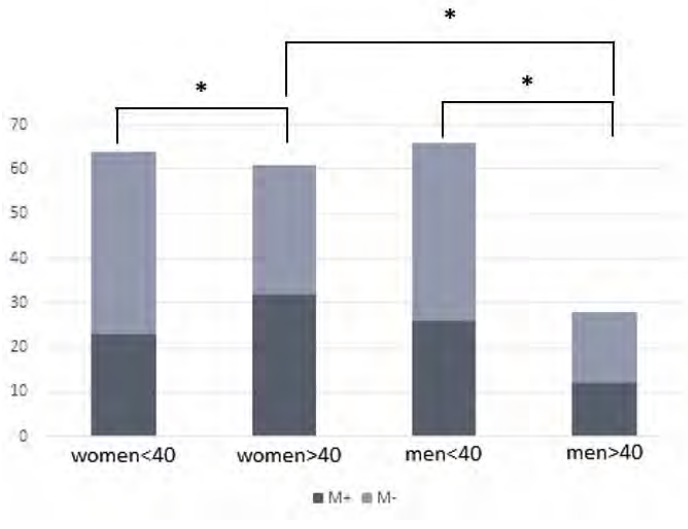

Fig. 1. Number of participants by gender and age group, with (M+) and without (M-) Morton's toe. <40 – under 40 years of age; >40 - over 40 years of age. * - statistically confirmed difference

We analized the values of CA, CSI and AI in both described age groups. According to the values of each

of the anthropometric indices, the plantograms were divided into three groups: 1) with normal values, 2) with high foot arch 3) with low foot arch. Statistical analysis confirmed the difference in the distribution of foot types in the two groups with $p< 0.001$ in both the t-test and the chi-square test. We found a different ratio of cases of high and low arch in the two age groups. In the group under 40 years of age, more cases of flatfoot are observed, and this difference is reported in all three indices (CA, CSI and AI) with $p<0.001$ (**Fig. 2**).

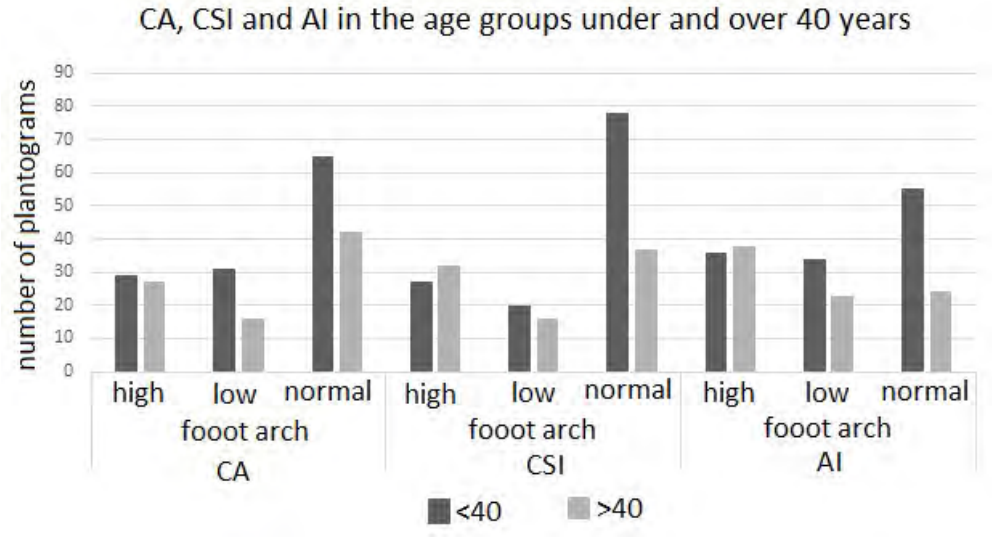

Fig. 2. Number of participants with different foot types (high-arched foot, normal-arched foot, low-arched foot) in the groups under and over 40 years of age according to used anthropometric indices (CA, CSI, AI)

We studied the distribution of foot types according to the values of each anthropometric index by gender in both age groups. Statistical analysis using the chi-square test confirmed significant differences in the distribution of foot types across age groups for both sexes. While this age-related variation was evident in both cohorts, it was more pronounced in men ($p < 0.001$) than in women ($p < 0.01$) (**Fig. 3**).

We analyzed the constitutional characteristics of the participants using height, weight, and BMI data. Independent t-tests revealed no statistically significant differences ($p > 0.5$) between the male and female cohorts across these metrics.

Discussion

Our data show that the anthropometric indicators characterizing the foot in the Bulgarian population are not static. The shifting distribution of foot types across different age groups highlights a distinct morphological trend, particularly among men.

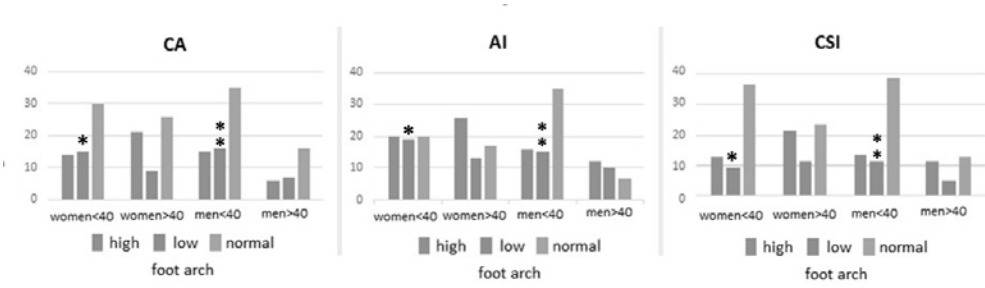

Fig. 3. Number of participants with different foot types according to used anthropometric indices (high-arched foot, normal-arched foot, low-arched foot), grouped by age and gender. * - statistically confirmed difference with p<0,01; ** - statistically confirmed difference with p<0,001.

Notably, younger male participants show a higher prevalence of low arches, resulting in a significant shift in the ratio between high-arched and low-arched individuals compared to older cohorts. The data should also be interpreted with the knowledge that in general the arches of the foot decrease with age within the framework of individual lifespan. This decrease according to literature data is particularly pronounced in the female gender, where it is associated with pregnancy and hormonal changes during the woman‘s life, as well as with socio-economic factors, such as the type of shoes [7, 10 11]. However, in the Bulgarian women population over 40 years of age, the frequency of flat feet is not higher compared to the group under 40 years of age.

The formation of the arches of the feet occurs during the first years of life, and is completed around 9-10 years of the age (slightly later for boys) [15]. A number of studies have attempted to answer the question of which factors have the greatest influence. Most of them assume that barefoot walking is essential in this early childhood [3]. Furthermore, research comparing orthopedic and regular shoes has reported no significant impact of either footwear type on the eventual height of the foot‘s arch [16].

Undoubtedly, socio-economic factors, such as living in the city or in the countryside, such as walking style and shoes worn in early childhood, such as the terrain on which one walks, have their importance in the formation of different foot types and the frequency of high and low arches in the population. These factors complement hereditary and genetic ones. The latter are unclear, and it is assumed that they act through a complex inheritance mechanism [5].

Our data clearly show that the hereditary factors act and modify the frequency of foot types in the Bulgarian population. If the cases of high and low arch are the result of a combination of external and internal factors, then the frequency of Greek foot depends only on genetic ones [1].

Data on the distribution of foot types in a population are important for sports medicine, physiotherapy, orthopedic practice and for industries such as footwear manufacturing [4]. Due to the complex set of social, economic and genetic factors that

determine the formation of the arches of the feet, significant regional, geographical, ethnic and racial characteristics are observed. This does not allow the free use of data obtained in the study of one population to characterize another and determines the need for local studies as ours.

Conclusions

1. Within the Bulgarian population, the prevalence of low-arched feet (pes planus) is significantly higher in individuals under the age of 40 compared to those over 40.
2. The incidence of the Greek foot (Morton's toe) is lower in the cohort under 40 years of age
3. Bulgarian males exhibit more pronounced shifts in anthropometric foot indices when comparing age groups under and over 40 years.

References

1. Aigbogun, E. O., A. Alabi, B. Didia, K. Ordu. Morton's Toe: Prevalence and inheritance pattern among Nigerians. – *Int. J. Applied & Basic Med. Res.,* **9 (2),** 2019, 89.

2. Angelova, M., D. Marinova, V. Zhekova, St. Pavlov. Association between foot arch index and other morphometric indices. - *Acta Morphol. Anthropol.,* **30 (3-4),** 2023, 61-66.

3. Echarri, J. J. and Fr. Forriol. The development in footprint morphology in 1851 Congolese children from urban and rural areas, and the relationship between this and wearing shoes. – *J. Pediatric Orthopedics, Part B,* **12 (2)**, 2003, 141-46.

4. Fernández-Seguín, L. M., J. Mancha, R. S. Rodríguez, E. E. Martínez, B. G. Martín, J. R. Ortega. Comparison of plantar pressures and contact area between normal and cavus foot. - *Gait & Posture,* **39 (2)**, 2014, 789-792.

5. He, Y., M. Verleyen, B. Callewaert, A. Burssens, E. Audenaert. Unraveling the genetic landscape of foot arch morphology: A systematic review of single nucleotide polymorphisms. – *Clin. Genet.,* **107 (5)**, 2025, 485-494.

6. Marinova, D., M. Angelova, V. Zhekova. Morton's Toe frequency among the Bulgarian population and its association with high arched foot. - *Acta Morphol. Anthropol.,* **29,** 2022.

7. Matsumoto, Y., N. Ogihara, S. Kosuge, H. Hanawa, T. Kokubun, N. Kanemura. Sex differences in the kinematics and kinetics of the foot and plantar aponeurosis during drop-jump. – *Sci. Reports*, **13 (1)**, 2023, 12957.

8. Morton, D. J. Structural factors in static disorders of the foot. – *The Am. J. Surgery,* **9 (2),** 1930, 315-328.

9. Munro, B. J., and J. R. Steele. Foot-care awareness. A survey of persons aged 65 years and older. – *J. Am. Pediatric Med. Association* **88 (5),** 1998, 242-248.

10. Nozaki, S., K. Watanabe, T. Kamiya, M. Katayose, N. Ogihara. Sex- and age-related morphological variations in the talar articular surfaces of the calcaneus. – *Ann. Anatomy,* **229,** 2020, 151468.

11. Otsuka, R., H. Yatsuya, Y. Miura. Association of flatfoot with pain, fatigue and obesity in Japanese over sixties. – *Nihon Koshu Eisei Zasshi Japanese J.Public Health,* **50 (10),** 2003, 988-998.

12. **Pita-Fernandez, S., C. Gonzalez-Martin, F. Alonso-Tajes.** Flat foot in a random population and its impact on quality of life and functionality. – *J. Clin. Diagn. Res.,* **11 (4),** 2017, 22-27.
14. **Scott, G., H. B. Menz, L. Newcombe.** Age-related differences in foot structure and function. – *Gait & Posture,* **26 (1),** 2007, 68-75.
15. **Spörndly-Nees, S., B. Dåsberg, R. O. Nielsen, M. I. Boesen, H. Langberg**. The navicular position test - a reliable measure of the navicular bone position during rest and loading. – *Int. J. Sports Physical Therapy,* **6 (3),** 2011, 199-205.
16. **Stavlas, P., T. B. Grivas, C. Michas, E.Vasiliadis, V. Polyzois.** The evolution of foot morphology in children between 6 and 17 years of age: A cross-sectional study based on footprints in a Mediterranean population. – *The J. Foot & Ankle Surgery,* **44 (6),** 2005, 424-428.
17. **Vangara, S.V., P. Vv. Gopichand, M. Bedi, N. Puri**. Effect of barefoot walking on foot arch structure in tribal children. – *Asian J. Med. Sci.,* **7 (5),** 2016, 108-116.
18. **Williams, D. S., I. S. McClay, J. Hamill.** Arch structure and injury patterns in runners. – *Clin. Biomechanics (Bristol, Avon),* **16 (4),** 2001, 341-347.

Institute of Experimental Morphology, Pathology and Anthropology with Museum
Bulgarian Anatomical Society

Acta Morphologica et Anthropologica, 33 (1-2)
Sofia ● 2026

Agenesis of the Celiac Trunk with Absence of the Common Hepatic Artery. A Cadaveric Observation

K. Topalova[1], Ts. Petleshkova[1], S. Novakov[1], R. Novakov[2]*

[1]*Department of Anatomy, Histology, and Embryology, Faculty of Medicine, Medical University of Plovdiv, Plovdiv, Bulgaria*
[2]*Clinic of Plastic Reconstructive and Esthetic Surgery, University Hospital „St. George"- Plovdiv, Medical University of Plovdiv, Plovdiv, Bulgaria*

*Corresponding author e-mail: Katerina.Topalova@mu-plovdiv.bg

Existing classifications of the different variations of the celiac trunk confirm that its absence is the rarest of them, occurring in a very small percentage according to different authors. A cadaver examination of a 71-year-old male revealed the independent separation of three arteries from the abdominal aorta: the left gastric artery (LGA), which gave rise to the replaced left hepatic artery (rLHA), the splenic artery (SA), and the hepatomesenteric trunk (HMT), which split into the superior mesenteric artery (SMA) and the replaced right hepatic artery (rRHA). The dissected cadaver was donated to the Department of Anatomy, Histology and Embryology for educational purposes. Understanding variations in the celiac trunk is of significant clinical importance when performing surgical procedures in the field of abdominal vascular surgery.

Key words: absent celiac trunk, variations, cadavers

Introduction

The classical anatomy of the celiac trunk (CT) is typically described as a trifurcation into the left gastric (LGA), splenic (SA), and common hepatic (CHA) arteries [13]. However, the complete absence of a typical celiac trunk is an exceptionally rare vascular variation. Current literature reports a very low incidence of this variation, with documented values ranging from 0.24% to 0.76% [5, 8, 12]. Triantafyllou et al. [14] noted an incidence of 0.43%, observing that this condition is significantly more prevalent in radiological imaging studies compared to cadaveric dissections. According to Bergman [16], the incidence of a missing celiac trunk varies between 0.1% and 4%. In such cases, the

arterial origins shift significantly: the CHA may arise from the superior mesenteric artery (SMA), while the LGA and SA originate independently from the aorta; alternatively, the SA may arise from the SMA. To further categorize these branching patterns, Mao et al. [6] proposed a classification into five distinct types based on the origin of the three main branches and the SMA. According to this framework, a celiac trunk is considered absent when no single trunk contains at least two of its primary branches. The types are defined as follows: Type I: Independent origin of LGA, CHA, SA, and SMA from the aorta; Type II: Presence of a hepatomesenteric trunk (HMT) with independent LGA and SA; Type III: A splenomesenteric trunk (SMT) with independent LGA and CHA; Type IV: A gastromesenteric trunk (GMT) with independent CHA and SA; Type V: Any other variation meeting the criteria for CT absence.

Case Report

During routine anatomical dissection of a 71-year-old male cadaver, a rare vascular configuration was identified, characterized by the complete agenesis of the celiac trunk. The left gastric artery (LGA) and the splenic artery (SA) arose independently from the abdominal aorta. The common hepatic artery was absent. Instead, a split hepatic supply was observed: a replaced left hepatic artery (rLHA) arising from the LGA and a replaced right hepatic artery (rRHA) originating from the superior mesenteric artery at the level of the middle colic artery. The LGA, measuring 7 mm in diameter, originated directly from the abdominal aorta at the level of Th12, subsequently giving rise to the replaced left hepatic artery (rLHA), and then coursed to the lesser curvature of the stomach. The SA, with a diameter of 9 mm, arose from the abdominal aorta at 10 mm from the LGA. The HMT is 8.5 mm in diameter and originated from the abdominal aorta 5 mm

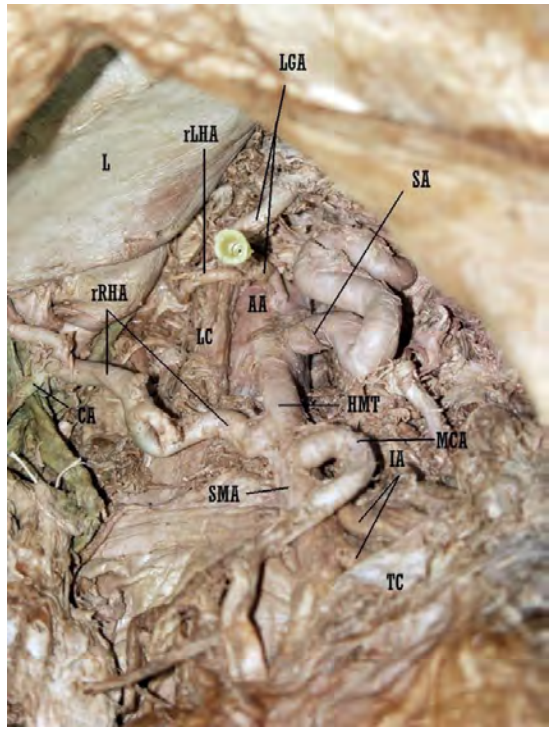

Fig. 1. Anatomical dissection of the supracolic compartment demonstrating the absence of a common celiac trunk. **AA:** abdominal aorta; **LGA:** left gastric artery; r**LHA:** replaced left hepatic artery; **SA:** splenic artery; **HMT:** hepatomesenteric trunk; r**RHA:** replaced right hepatic artery; **CA:** cystic artery; **SMA:** superior mesenteric artery; **MCA:** middle colic artery; **IA:** intestinal artery; **L:** liver; **LC:** left crus of diaphragm; **TC:** transverse colon.

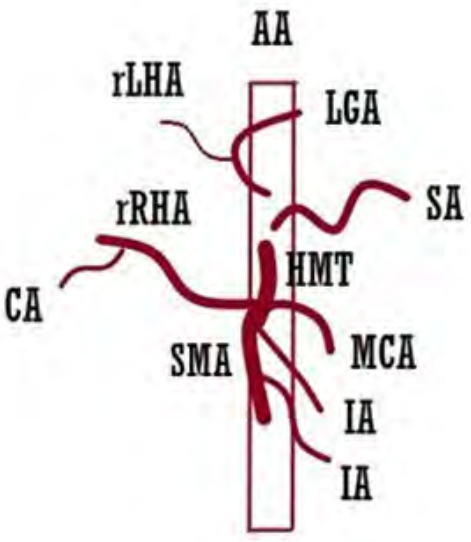

Fig. 2. Schematic representation of the dissected cadaver showing the celiac trunk variation. **AA:** abdominal aorta; **LGA:** left gastric artery; r**LHA:** replaced left hepatic artery; **SA:** splenic artery; **HMT:** hepatomesenteric trunk; r**RHA:** replaced right hepatic artery; **CA:** cystic artery; **SMA:** superior mesenteric artery; **MCA:** middle colic artery; **IA:** intestinal artery.

inferior to the origin of the SA. At 11 mm from its origin, the HMT gave off the replaced right hepatic artery (rRHA, 7.5 mm) and continued as the SMA. In summary, the absence of the celiac trunk was represented by the following vessels: rLGA+LHA; SA; HMT, which gave rise to the rRHA and SMA (**Fig. 1, Fig. 2**).

Discussion

The vitelline arteries, which are pairs of vessels responsible for supplying the yolk sac, gradually merge and form the arteries located in the dorsal mesentery of the intestine. In adults, these are the unpaired branches of the abdominal aorta - the celiac trunk, the superior mesenteric artery, and the inferior mesenteric artery. These vessels supply the anterior, middle, and posterior parts of the intestine, respectively. During embryological development, various anatomical variations of these vessels may occur [10].

This specific configuration, characterized by a hepatomesenteric trunk alongside independent aortic origins of the left gastric and splenic arteries, is exceptionally rare. Mao et al. reported a prevalence of only 0.36% (9 cases) in their extensive study [6] Although rare, this configuration of the celiac trunk was also reported by Ramanand et al. [9] and Hemalini et al. [2]. Ye et al. [18] described the same type of variation – LGA, SA, and HMT, with the difference that they identified an accessory left hepatic artery (aLHA) branching from the LGA. Unlike the authors mentioned above, in our case there was agenesis of the celiac trunk and an absent common hepatic artery (CHA). Replacement branches separating from the LGA and the SMA take over its function.

A similar variation was described by Zhang et al. [19], in which the LGA, SA, and gastroduodenal artery (GDA) originated directly from the abdominal aorta (AA) in the absence of the CHA. In their report, the replacement left hepatic artery (rLHA) branched from the LGA, and the replacement right hepatic artery (rRHA) originated from the SMA, which is completely consistent with our findings. Sheta [11] also identified cases with altered configuration of the celiac trunk and variable pattern of the hepatic arteries. In his first case, the SA arose directly from the AA, while the

RHA and SMA branched from a common trunk. In the second case, the SA originated from the AA, and the CHA and SMA emerged from a common hepatomesenteric trunk (HMT), with the CHA branching into four segments: RHA, LHA, MHA, and GDA. Although Michels and Hiatt's classifications described hepatic variations in detail, they did not include cases of complete agenesis of the celiac trunk. Our case corresponded to Type IV (double replacement hepatic supply), but with atypical direct separation of the LGA, SA, and SMA from the aorta [7, 3]. Türkyılmaz et al. [17] reported a double replacement blood supply combined with an additional left hepatic artery (a LHA) from the aorta and GDA from the splenic artery – a configuration present in only 0.21% of cases and classified by them as type IV a.

A similar rare clinical case of the celiac trunk and common hepatic artery was published by Bulgarian authors, with the difference that there was a common hepatic artery that gave rise to the left hepatic artery (LHA), middle hepatic (MHA), right hepatic (RHA), cystic (CA), right gastric (RGA), and gastroduodenal arteries (GDA). The celiac trunk is also subject to variation [15]. Notably, despite the documented cases in neighboring regions like Romania and Moldova [4, 1], to the best of our knowledge, this is the first reported case of a absent celiac trunk within the Bulgarian population.

These rare cases reveal the great variety of arterial patterns in celiac trunk absence, highlighting the need for detailed morphological analysis.

Conclusion

Understanding the variations in the celiac trunk is of great clinical importance in abdominal surgical procedures such as liver transplantation, acute mesenteric occlusion, laparoscopic surgery, and in radiological procedures (interventional angiography and computed tomography) in the upper abdomen.

References

1. **Covantsev, S., R. Uzdenov, N. Mazuruc-Gladcova, D. Turovets, O. Belik.** Absent celiac trunk and unusual arterial anatomy of the upper abdomen: into the deep. – *Folia Med. (Plovdiv)*, **65**(3), 2023, 500-507.
2. **Hemamalini.** Variations in the branching pattern of the celiac trunk and its clinical significance. – *Anat. Cell Biol.*, **51**(3), 2018, 143-149.
3. **Hiatt, J. R., J. Gabbay, R. W. Busuttil.** Surgical anatomy of the hepatic arteries in 1000 cases. – *Ann. Surg.,* **220**(1), 1994, 50–52.
4. **Iacob, N., I. Sas, S. C. Joseph, H. Pleş, G.D. Miclăuş et al.** Anomalous pattern of origin of the left gastric, splenic, and common hepatic arteries arising independently from the abdominal aorta. – *Rom. J. Morphol. Embryol*., **55**(4), 2014, 1449-1453.
5. **Iezzi, R., A. R. Cotroneo, D. Giancristofaro, M. Santoro, M.L. Storto.** Multidetector-row CT angiographic imaging of the celiac trunk: anatomy and normal variants. – *Surg. Radiol. Anat.*, **30**(4), 2008, 303-310.

6. Mao, Y., Y. Yao, X. Li, X. Chen, C. Zhang et al. Absence of the celiac trunk: Definition, classification, multidetector computed tomography angiographic findings, and their probable embryological mechanisms. – *Vascular*, **31**(6), 2023, 1214-1221.
7. Michels, N. A. *Blood supply and anatomy of the upper abdominal organs with a descriptive* Atlas. Philadelphia, JB Lippincott, 1955, 136–147.
8. Panagouli, E., D. Venieratos, E. Lolis, P. Skandalakis. Variations in the anatomy of the celiac trunk: a systematic review and clinical implications. – *Ann. Anat.*, **195**, 2013, 501-511.
9. Ramanand, G., C. A. Singh, C. K. Rana, K. Ramesh, S. I. Singh. Slice CT evaluation of anatomical variations of main arteries arising from the abdominal aorta and their branching pattern. – *J. Med. Sci. Clin. Res.*, **6**(6), 2018, 576-588.
10. Sadler, T. W. *Langman's Medical Embryology.* 12th ed., Philadelphia, Lippincott Williams & Wilkins, 2012, 188.
11. Sheta, A. A. Prevalence of anatomical variants in the branches of celiac and superior mesenteric arteries among Egyptians. – *Anat. Cell Biol.*, **57**(3), 2024, 353-362.
12. Song, S. Y., J. W. Chung, Y. H. Yin, H.J. Jae, H.C. Kim et al. Celiac axis and common hepatic artery variations in 5002 patients: systematic analysis with spiral CT and DSA. – *Radiology*, **255**(1), 2010, 278-288.
13. Standring, S. *Gray's Anatomy: The Anatomical Basis of Clinical Practice.* 41st ed., Elsevier Limited, 2016.
14. Triantafyllou, G., N. Belimezakis, O. Lyros, A. Węgiel, N. Arkadopoulos et al. Prevalence of coeliac trunk variants: A systematic review with meta-analysis. – *Ann. Anat.*, **259**, 2025, 152385.
15. Trifonov, S., M. Dobrev, P. Hristova, I. Bogeva-Tsolova. Rare variation of the branches of the coeliac trunk and the common hepatic artery in human cadaver: a case report. – *Ann. Med. Surg. (Lond)*, **87**(4), 2025, 2477-2483.
16. Tubbs, R. S., M. M. Shoja, M. Loucas. *Bergman's Comprehensive Encyclopedia of Human Anatomic Variation.* New Jersey, John Wiley & Sons, 2016.
17. Türkyılmaz, Z., O. Kula, A. O. Çelik, T. Demirel, B. Günay. Evaluation of celiac artery and common hepatic artery variations by CT-angiography and new classification model. – *Surg. Radiol. Anat.*, **45**(8), 2023, 1037-1047.
18. Ye, Z., S. Ye, D. Zhou, W. Wang. A rare variation of celiac trunk and hepatic artery complicating pancreaticoduodenectomy: A case report and literature review. – *Medicine (Baltimore)*, **96**(48), 2017, e8969.
19. Zhang, Z., S. Wang, M. Ye, F. Tao, D. Guo. Rare variation: the absence of both the celiac trunk artery and the common hepatic artery. – *World J. Surg. Oncol.*, **20**(1), 2022, 388.

Institute of Experimental Morphology, Pathology and Anthropology with Museum
Bulgarian Anatomical Society

Acta Morphologica et Anthropologica, 33 (1-2)
Sofia ● 2026

Most Often Injured Anatomical Locations and Injury Prevention of CrossFit Athletes

*Dilyana Zaykova**

Department of Heavy Athletics, Boxing, Fencing and Sport for All", National Sports Academy "Vassil Levski", Sofia Bulgaria

* Corresponding autor e-mail: dilyana.zaykova@nsa.bg

The study aimed to analyze acute injuries and their localizations amongst people practicing CrossFit and provide some guidelines and possibilities for prevention. The research included 54 participants practicing CrossFit in Bulgaria. The participants filled out a questionnaire, which included open and closed questions about type, severity, location, and the reasons for the appearance of injuries. The results showed 61 acute injuries among the participants. The most prevalent injuries for both sexes were the lumbar spine (24.6%), knee (16.4%) and shoulder (14.8%). Slight injuries (29.5%) and minimal injuries (27.9%) were the most frequently reported. The main reasons for the injuries were overtraining (42.9 %) and fatigue (36.4 %). Most participants (74.1%) had not trained with a licensed CrossFit instructor, and 66.7% had not taken precautions. The distribution of the injuries according to their number and location was similar to the one described in the scientific literature.

Key words: CrossFit, musculoskeletal injuries, acute injuries, anatomical locations

Introduction

Approximately 74% of all athletes who practice some sport (even unprofessionally) suffer a moderate or severe injury yearly [8]. CrossFit is often associated with a risk of musculoskeletal injuries as a result of the high intensity of the training load [15] and the complexity of execution of the training sets of exercises in combination with little or no breaks between the sets [18]. Weisenthal [22] provides the following definition of musculoskeletal injuries in CrossFit: "any muscle, tendon, bone, joint, or ligament injury sustained while doing CrossFit that resulted in your consultation with a physician, or health care provider, and that caused you to stop or reduce your usual physical activity, your typical participation in CrossFit, or caused you to have

surgery." In sports practice, to prevent injuries, warm-up and stretching exercises are done before the main load [13] which aims to increase the range of motion, activate blood circulation, and prepare the muscles and joints for the forthcoming load [9]. The specialists in CrossFit emphasize instructors' competence and their personal work with athletes in injury prevention [12, 20].

This study aimed to analyze acute injuries and their localizations amongst people practicing CrossFit and provide some guidelines and possibilities for prevention.

Material and Methods

In order to assess the level of injuries in the previous year (12 months), we had the participants fill out a online questionnaire, which included open and closed questions about severity, location, and the reasons for the appearance of injuries in the following anatomical locations: head, neck, shoulder, upper arm, elbow, forearm, wrist and hand, chest, abdomen, thoracic spine, lumbar spine, pelvis and buttock (bones), hip and groin (muscles), thigh, knee, lower leg, ankle, foot. Participants could point to more than one injured location [17, 24, 25]. According to the severity of injuries and the time needed for recovery, the injuries were divided into slight (1/2 days), minimal (1-3 days), mild (4-7 days), moderate (8-28 days), and severe (over 28 days) [6]. The study was conducted in accordance with the principles set forth in the Declaration of Helsinki for research on humans [23].

For the purposes of the analysis, we used Chi-square and Z-test to determine the differences in the distribution of injuries, their incidence, location, and severity. We used frequency analysis as well. The statistical processing of the data was done with the software package SPSS V.25. The accepted statistical significance level was $p < 0.05$. In the tables and in the text, the values are presented as numbers and percentages of total injuries or cases.

Results

The survey was conducted among 54 participants practicing CrossFit in Bulgaria. Injuries for the study period have been reported by 27 people practicing CrossFit in their free time - 15 men (mean age 30.8 ± 3.53 years), with an average training experience of 3.6 ± 2.05 years, with an average of 3.7 ± 0.75 training sessions per week and 12 women (mean age 32.9 ± 2.03 years), with an average training experience of 3.7 ± 1.12 years, with an average of 3.6 ± 0.71 training sessions a week.

The total number of injuries reported by the participants was 61 (**Table 1**). The men reported 33, and the women reported 28 acute injuries over a year, without significant differences between them ($p > 0.05$). Since we found no significant sex-related differences in injuries across anatomical locations, we analyzed the data for the combined group. The distribution of the injuries was relatively equal for both genders. The men reported injuries in another two anatomical locations - thigh and the forearm.

The most frequently injured anatomical locations of the whole researched group were the lumbar spine with 15 injuries (24.6%), the knee with 10 injuries (16.4%), the shoulder with 9 injuries (14.8%), and the ankle with 6 injuries (9.8%) (**Table 1**). The total number of injuries in the anatomical location lumbar spine was significantly higher than the ones reported in the anatomical locations ankle ($p < 0.05$), elbow ($p < 0.05$), lower leg ($p < 0.05$), neck ($p < 0.05$), foot ($p < 0.01$), thigh ($p < 0.05$), and forearm ($p < 0.05$). Regarding the anatomical location of the knee, we found significant differences between the injuries reported in this anatomical location and the forearm ($p < 0.05$).

The slight injuries were the most frequent for the whole researched group -18, which were significant more than the eight moderate injuries ($p < 0.05$) and the five severe injuries ($p < 0,01$). The women reported 11 slight injuries, significant more than the eight slight injuries reported by the men ($p < 0.05$) (**Table 1**).

Table 1. Most often injured anatomical locations and severity of injuries

	Total (n=61)	**Men (n=33)**	**Z test**	**Women (n=28)**
Anatomical locations	**N (%) of injuries**	**N (%) of injuries**		**N (%) of injuries**
lumbar spine	15 (24.6%)	8 (13.1%)	$p > 0.05$	7 (11.5%)
knee	10 (16.4%)	6 (9.8%)	$p > 0.05$	4 (6.6%)
shoulder	9 (14.8%)	5 (8.2%)	$p > 0.05$	4 (6.6%)
ankle	6 (9.8%)	3 (4.9%)	$p > 0.05$	3 (4.9%)
elbow	5 (8.2%)	2 (3.3%)	$p > 0.05$	3 (4.9%)
lower leg	5 (8.2%)	2 (3.3%)	$p > 0.05$	3 (4.9%)
neck	3 (4.9%)	1 (1.6%)	$p > 0.05$	2 (3.3%)
foot	3 (4.9%)	1 (1.6%)	$p > 0.05$	2 (3.3%)
thigh	3 (4.9%)	3 (4.9%)		
forearm	2 (3.3%)	2 (3.3%)		
Severity of injuries	**N (%) of injuries**	**N (%) of injuries**		**N (%) of injuries**
slight	18 (29.5%)	7 (11.5%)	**$p < 0.05$**	11 (18%)
minimal	17 (27.9%)	7 (11.5%)	$p > 0.05$	10 (16.4%)
mild	13 (21.3%)	9 (14.8%)	$p > 0.05$	4 (6.6%)
moderate	8 (13.1%)	6 (9.8%)	$p > 0.05$	2 (3.3%)
severe	5 (8.2%)	4 (6.6%)	$p > 0.05$	1 (1.6%)

Both genders reported severe injuries (over 28 days) in the anatomical locations of the lumbar spine. The men also reported injuries in the knee and shoulder. Men reported moderate injuries (8-28 days) in the anatomical locations of the lumbar spine (2) and knee (2) and one injury in the anatomical locations of the shoulder and thigh.

The women reported two moderate injuries in the anatomical locations of the lumbar spine and knee over the research period. The distribution of the injuries regarding the other severity types was relatively the same for both genders (**Table 2**).

Table 2. Injury distribution according to severity and anatomical location

	Injured anatomical locations									
CrossFit participants	**Lumbar spine**	**Knee**	**Shoulder**	**Ankle**	**Elbow**	**lower leg**	**Foot**	**Neck**	**Thigh**	**Forearm**
Male (n=15)	1^{b}, 3^{c}, 2^{d}, 2^{e}	2^{b}, 1^{c}, 2^{d}, 1^{e}	1^{b}, 2^{c}, 1^{d}, 1^{e}	1^{a}, 1^{b}, 1^{c}	1^{a}, 1^{b}	2^{a}	1^{b}	1^{a}	1^{a}, 1^{c}, 1^{d}	1^{a}, 1^{c}
Female (n=12)	2^{a}, 2^{b}, 1^{c}, 1^{d}, 1^{e}	1^{b}, 2^{c}, 1^{d}	1^{a}, 2^{b}, 1^{c}	1^{a}, 2^{b}	1^{a}, 2^{b}	2^{a}, 1^{b}	2^{a}	2^{a}		

Legend: slight ½ days symptoms – **a**; minimal 1-3 days symptoms – **b**; mild 4-7 days symptoms – **c**; moderate 8-28 days symptoms – **d**; severe over 28 days symptoms – **e**

The leading reason for injuries was overtraining, which differs significantly from a skipping a warm-up ($p < 0.05$) and the technical fault ($p < 0.01$). The accumulation of fatigue was the next most frequently reported, which similarly differs significantly from a warm-up ($p < 0.05$) and the technical fault ($p < 0.05$). The researched individuals were able to give more than one correct answer (**Table 3**).

Table 3. Reasons for injuries

Reasons	**Total n (%)**	**Men n (%)**	**Women n (%)**
Overtraining	33 (42.9 %)	18 (54.6%)	15 (45.5%)
Fatigue	28 (36.4 %)	12 (42.9%)	16 (57.1%)
Skipping a warm-up	10 (13 %)	7 (70%)	3 (30%)
Technical fault	6 (7.8 %)	4 (66.7%)	2 (33.3%)

Most of the participants in the research reported they had not used safety measures (a belt, knee pads, wrist braces, swath) in CrossFit training sessions. Their number was significantly higher than that of the participants who used safety measures occasionally ($p < 0.05$) and that of the participants who used safety measures in each training session ($p < 0.05$). (**Table 4**). Twenty of the researched athletes had not used a licensed

CrossFit instructor's services. Their number was significantly higher than those who trained with a CrossFit instructor ($p < 0.05$) (**Table 4**).

Table 4. Safety measures and training sessions with an instructor

Safety Measures	**Total n (%)**	**Men n (%)**	**Women n (%)**
Do not use	18 (66.7%)	8 (44.4%)	10 (55.6%)
Occasionally	4 (14.8%)	2 (50%)	2 (50%)
Use	5 (18.5%)	5 (100%)	
Training session with an instructor	**Total n (%)**	**Men n (%)**	**Women n (%)**
No	20 (74.1%)	13 (65%)	7 (35%)
Yes	7 (25.9%)	2 (28.6%)	5 (71.4%)

Discussion

The summary analysis of traumatism in power sports is 1-2 injuries per athlete a year or 2-4 injuries per 1000 training hours [14]. The average number of injuries among the participatnts in our survey was 1.1 annually.

The most common acute injuries in both sexes were those in the lumbar spine (24.6%), knee (16.4%) and shoulder (14.8%) (**Table 1**), similar to the injuries found in other CrossFit athletes [5, 15, 22]. The injuries in the anatomical location of the shoulder most often appear as a result of gymnastics exercises, and those in the anatomical locations of the lumbar spine and knees – as a result of the strength exercises [7, 10, 15].

Pain in the lumbar spine is one of the major injuries reported by 32% of active athletes [1]. It could be provoked by insufficiently developed muscles, an impaired technique of execution of the movements, overtraining, abrupt or twisting movements, weight lifting, and holding a static, strenuous posture for a more extended period [11]. Some of the exercises used in CrossFit training sessions that could lead to injuries in the area of the waist are deadlifts, squats, medicine ball throws, and variations in the execution of abdominal crunches.

The knee is another very often injured location in sports because knees take part in executing many multi-joint movements and functional loads. A survey on traumatism in sports [12] found that injuries in the anatomical location of the knee were approximately 15% of all CrossFit injuries. Knee injuries due to CrossFit training sessions can often be provoked by the execution of various squats, step-ups, leg extensions, box jumps, and running.

The shoulder was the third most often traumatized anatomical location in our study (**Table 1**). Shoulders play a crucial role in executing various complex multijoint exercises performed with a significant amplitude and rotation, holding the weight or achieving stability in a particular phase of the execution of the exercise [4]. Exercises such as snatch and muscle-ups increase the risk of injury due to the high compression the movements exert on the supporting shoulder joint [16]. Almost all CrossFit exercises include those with shoulder strain. Combined with the longer duration of the training and shorter rest and recovery periods, CrossFit increases the risk of injury [5]. Although the training of elite athletes in CrossFit includes up to 7 workouts per week lasting up to 2-3 hours, the injury to the shoulder joints is no different from that of other sports [22]. Other CrossFit exercises that can provoke pain in the shoulders and the rotation cuff are throwing exercises, shoulder fly's, rope slams, pullups, bench presses, and shoulder presses.

The ankle injuries (9.8%) were the next most frequent among the groups we researched (**Table 1**). Many sets of CrossFit exercises are related to landing after a jump, a subsequent rotation, and a twist in the ankle joint when performing gymnastics exercises [3]. The fast and frequent change of direction requires strength, stability, and mobility of the ankles. Improper technique, overtraining, and insufficient balance when running various distances, box jumps, lateral agility drills, and others may also provoke ankle injuries.

The injuries in the anatomic location of the elbow take from 3rd to 5th place (up to 12% of the total injuries) in frequency in CrossFit [19]. They took the 4th place in the group we researched, with a total of 8.2% of the injuries (**Table 1**). During CrossFit training sessions, elbows usually perform repetitive movements, which can be dynamic when flexing the elbow joint or static when holding and carrying weights. The injuries in this anatomical location appear due to overtraining, hyperextension, or because of another injury (a hit, for example). They are often provoked when performing gymnastics exercises and movements from Olympic weight lifting [19].

The researched men and women reported 61 injuries over the research period. Regarding the severity of injuries, slight injuries (29.5%) and minimal injuries (27.9%), requiring shorter recovery periods, were the dominant ones (**Table 1**).

The primary reasons for the injuries were overtraining (42.9%) and fatigue in 36.4% of the cases of traumatism (**Table 3**). One of the leading causes of musculoskeletal injuries in CrossFit is the extensive training loads that exceed the athlete's capacity [2].

Most of the CrossFit athletes we researched did not use safety measures (66.7%) and did not train with a licensed CrossFit instructor (74.1%) (**Table 4**). The role of CrossFit instructors is to observe the adequate and dosed load during training [12, 20, 21], especially for beginners practicing CrossFit less than a year and less than three workouts per week, to prevent injuries [12].

We recommend that CrossFit training sessions emphasize the gradual development of the motor qualities of strength and endurance, which will ensure the optimal time for the organism to get ready for the continuous increase in the intensity of the workload. That requires the stricter observation of the principle of progressive overload, which

enables the organism to adapt adequately to the increasing load requirements. The pain appearing in some anatomic locations should not be neglected but be perceived as a limiting factor. When it is impossible to work with a particular daily intensity, training should be reduced to the state adequate to the momentary functional state of the organism, especially in group training sessions.

Conclusions

The number and location of injuries among athletes in this study is similar to that described in the scientific literature for CrossFit athletes. The severity of injuries in our study group was low. Further research among CrossFit practitioners is highly recommended to prevent musculoskeletal injuries regarding using protective equipment (such as belts, knee pads, shoulder protectors, etc.), proper warm-up and stretching, and training sessions with a licensed instructor.

Limitations

The limitations of this study include the small sample size and the study's retrospective nature based on self-reported data. In its current form, this questionnaire study provides indicative data on injuries in this sport. Further standardized and more extensive studies are needed to provide sufficient data on injuries suffered by CrossFit practitioners to take adequate measures to reduce them.

References

1. **Alekseyev, K., A. John, A. Malek, M. Lakdawala, N. Verma, C. Southall, A. Nikolaidis, S. Akella, S. Erosa, R. Islam, E. Perez-Bravo, M. Ross.** Identifying the most common CrossFit injuries in a variety of athletes. – *Rehabil Process Outcome*. **9**, 2020, eCollection 2020
2. **Bergeron, M. F., B. C, Nindl, P.A. Deuster, N. Baumgartner, S.F. Kane, W. J. Kraemer, L. R. Sexauer, W. R. Thompson, F. G. O'Connor.** Consortium for health and military performance and American College of Sports Medicine consensus paper on extreme conditioning programs in military personnel. – *Curr Sports Med Rep*., **10** (6), 2011, 383-9.
3. **Caine, D., M. L. Harringe**. Epidemiology of Injury in Gymnastics. – In: *Gymnastics* (eds D.J. Caine, K. Russell and L. Lim), Lausanne, International Olympic Committee, 2013, 109-124.
4. **Campos, Y.A.C., J. M. Vianna, M. P. Guimarães, J. L. D. Oliveira, C. Hernández-Mosqueira, S. F. da Silva, P. H. Marchetti.** Different shoulder exercises affect the activation of deltoid portions in resistance-trained individuals. – *J Hum Kinet.,* **75**, 2020, 5-14.
5. **Carbone, S., V. Candela, S. Gumina, S.** High rate of return to CrossFit training after arthroscopic management of rotator cuff tear. – *Orthop J Sports Med*, **8** (4), 2020, eCollection 2020 Apr.
6. **Clarsen, B., O. Rønsen, G. Myklebust, T. W. Flørenes, R. Bahr.** The Oslo Sports Trauma Research Center questionnaire on health problems: a new approach to prospective monitoring of illness and injury in elite athletes. – *Br J Sports Med*., **48** (9), 2014, 754-760.

7. Claudino, J., T. Gabbett, F. Bourgeois, H. Souza, R. Miranda, B. Mezêncio, R. Soncin, C. Filho, M. Bottaro, A. Hernandez, A. Amadio, J. Serrão. CrossFit overview: Systematic review and meta-analysis. – *Sports Med Open*., **4** (1), 2018, 11.

8. Daoud, A. I., G. J. Geissler, F. Wang, J. Saretsky, Y. A. Daoud, D. E. Lieberman. Foot strike and injury rates in endurance runners: A retrospective study. – *Medicine & Science in Sports & Exercise,* **44**, 2012, 1325-1334.

9. Decoster, L. C., J. Cleland, C. Altieri, P. Russell. The effects of hamstring stretching on range of motion: a systematic literature review. – *J Orthop Sports Phys Ther*., **35** (6), 2005, 377–87.

10. Dominski, F., T. Siqueira, T. Serafim, A. Andrade. Injury profile in CrossFit practitioners: systematic review. – *Fisioter Pesqui*., **25** (2), 2018, 229-239.

11. Fares, M.Y., J. Fares, H. A. Salhab, H. H. Khachfe, A. Bdeir, Y. Fares. Low back pain among weightlifting adolescents and young adults. – *Cureus*., **12** (7), 2020, e9127.

12. Feito, Y., E. K. Burrows, L. P. Tabb. A 4-Year analysis of the incidence of injuries among CrossFit-trained participants. – *Orthop J Sports Med*., **6** (10), 2018, eCollection 2018 Oct.

13. Fradkin, A., B. Gabbe, P. Cameron. Does warming up prevent injury in sports?. – *Journal of Science and Medicine in Sport,* **9** (3), 2006, 214–220.

14. Keogh, J., P. Winwood, The epidemiology of injuries across the weight-training sports. – *Sports Med*. , **47** (3), 2017, 479-501.

15. Klimek, C., C. Ashbeck, A. J. Brook, C. Durall. Are injuries more common with CrossFit Training than other forms of exercise? – *J Sport Rehabil*., **27** (3), 2018, 295-299.

16. Kolber, M.J., K. S. Beekhuizen, M. S. Cheng, et al. Shoulder injuries attributed to resistance training: a brief review. – *J Strength Cond Res*, **24** (6), 2010, 1696–1704.

17. Konchev, M., D. Zaykova. Epidemiology of injuries of the Bulgarian national team of Olympic weightlifting. – *Journal of Environmental Protection and Ecology*, **24** (1), 2023, 17-26.

18. Kozub, F. M. Using the snatch and CrossFit principles to facilitate fitness. – *JOPERD*, **84**, 2013, 13-16.

19. Nicolay, R. W., L. K., Moore, T. D. DeSena, J. S. Dines. Upper extremity injuries in CrossFit athletes - a review of the current literature. – *Curr Rev Musculoskelet Med*., **15** (5), 2022, 402-410.

20. Tibana, R. A, N. M. F. de Sousa. Are extreme conditioning programmes effective and safe? A narrative review of high-intensity functional training methods research paradigms and findings. – *BMJ Open Sport Exerc. Med*., **4** (1), 2018, e000435.

21. Waryasz, G., V. Suric, A. Daniels, J. Gil, C. Eberson. CrossFit® instructor demographics and practice trends. – *Orthop Rev (Pavia)*, **8** (4), 2016, 6571.

22. Weisenthal, B. M., C. A. Beck, M. D. Maloney, K. E. DeHaven, B. D. Giordano. Injury rate and patterns among CrossFit athletes. – *Orthop J Sports Med*., **2** (4), 2014, eCollection 2014 Apr.

23. World Medical Association, Declaration of Helsinki - Ethical principles for medical research involving human subjects. – *WMJ*, **54** (4), 2008, 122-125.

24. Zaykova, D., M. Konchev. Injury profile of Bulgarian male Olympic weightlifters. – *Series on Biomechanics*, **37** (1), 2023, 25-30.

25. Zaykova, D., M. Konchev, I. Yanev, L. Dimitrova. Epidemiology profile of injuries of elite and sub-elite male artistic gymnasts in Sofia, Bulgaria. – *Proceedings of the International Scientific Congress „Applied Sports Sciences"*, **2**, 2022, 23-30.

Institute of Experimental Morphology, Pathology and Anthropology with Museum
Bulgarian Anatomical Society

Acta Morphologica et Anthropologica, 33 (1-2)
Sofia ● 2026

Relationships between Body Proportions and Maximal and Relative Strength in Strength Sports

Valentin Panayotov[1], Krassimir Petkov[2], Rasho Makaveev[3]*

[1]Department Weightlifting, boxing, fencing and sports for all, National Sports Academy, Sofia, Bulgaria
[2]Department Weightlifting, boxing, fencing and sports for all, National Sports Academy, Sofia, Bulgaria
[3]Department Wrestling and judo, National Sports Academy, Sofia, Bulgaria

*Corresponding author e-mail: v.panayotov@nsa.bg

This study explores the relationships between some specific body proportions and maximal and relative strength of lower extremities, measured by 1 repetition maximum (RM) in a classic resistance exercise – the back squat. 42 athletes in total participate in the study. They were competitors at the national level in bodybuilding, powerlifting and Olympic weightlifting. Linear regression equations were estimated between three relative body measures (Height seated/Height, Length of lower extremity/Height and Height/Thigh circumference) and maximal and relative strength in the back squat. All studied variables reached statistical significance in the models except for height/thigh circumference as a predictor of relative squat strength. The studied relative body measures proved to be reliable predictors of strength and relative strength abilities of lower extremities. These results can find practical application in the process of sports selection and specialization in strength sports.

Key words: maximal strength, strength sports, bodybuilders, powerlifters, Olympic weightlifters

Introduction

Bodybuilding, powerlifting and Olympic weightlifting are popular under the common name of strength sports. Resistance training is one of the oldest sports disciplines. Ancient Egyptians, Greeks and Romans exercised with heavy objects to develop their strength. Many artefacts prove that ancient warriors regularly performed strength exercises and participated in strength tournaments. Athletes in the early Olympic

Games in Ancient Greece also used resistance movements. Weights were used not only for strength demonstrations but also in some track and field disciplines – for example, long jumps were performed while athletes held a weight, which had to be thrown back an instance before landing [21]. All strength sports use similar training means: different types of resistance exercises [14, 15]. However, their training goals and methodologies are quite different. Bodybuilders aim at achieving muscle hypertrophy, decreasing subcutaneous fat and modelling symmetric bodies [27]. Olympic weightlifters and powerlifters use resistance exercises to develop maximal and/or explosive strength and lift heavier weights [31]. Despite these two sports having similar goals, their training methodologies differ in many aspects. Powerlifting encompasses muscle efforts that are positioned on the upper part of the force-velocity curve [1, 34], close to the region of isometric contractions. On the other hand, Olympic weightlifting competitive exercises are technically complex and dynamic and require the development of the so-called strength-speed abilities [30, 35]. Differences in training methodologies of strength sports are the reason for variations in strength abilities and physical development of strength athletes [25, 33]. Powerlifters and Olympic weightlifters aim to increase their strength abilities without gaining excessive body weight [7, 12]. On the other hand, in bodybuilding, the purpose is to maximize muscle hypertrophy irrespective of the development of motor abilities [28]. Nevertheless, generally, muscle strength increases in parallel with muscle size [2, 17]. For these reasons, the three sports are considered similar not only in training means (resistance exercises) but also in outcomes.

We studied one of the most popular strength training exercise – barbell back squat. We should mention that Olympic weightlifters and bodybuilders generally use slightly different technique in the back squat compared to some powerlifters – the so-called high-bar squat [7, 29. 31]. While back squat is a competitive movement only in powerlifting, it is strongly correlated to the results in the snatch and clean-and-jerk and is widely used as an auxiliary exercise in Olympic weightlifting [7, 22]. Results in the squat may seem unimportant for bodybuilders at first glance, as judges assess them based on their visual appearance rather than motor abilities. However, this exercise is one of the most potent means for building muscle size and is widely used in many bodybuilding training routines. As all experienced athletes in strength sports are proficient in the different versions of squat, in this experiment, we standardized the technique for all participants – we used “high bar” squat [26].

The aim of this study was to determine whether some specific relative body proportions give advantages in low extremities strength in competitive athletes in the three strength sports. We studied the relationships between some body proportions and maximal and relative strength measured by the heaviest weight lifted in one of the most popular strength exercises – the back squat. We expect that our findings will be of practical use for coaches, especially in the sports selection process.

Materials and Methods

Participants

The contingent of the study consisted of 42 strength athletes with a competitive experience at National level. Among them: 14 bodybuilders aged 24.7 ± 4.97 years and sports age (duration of practice in sport) of 7.5 ± 4.47 years; 11 powerlifters aged 23.6 ± 3.14 years and sports age of 6.05 ± 25.37 years; and 17 Olympic weightlifters aged 21.29 ± 2.97 years and sports age of 6.56 ± 3.92 years. The studies were approved by the Ethics Commission of the National Sports Academy, Sofia, Bulgaria. The study was conducted in accordance with the local legislation and institutional requirements. All subjects gave written informed consent in accordance with the Declaration of Helsinki.

Procedure

We measured 4 anthropometric parameters, all of them body segment lengths. The measurements were conducted by a standard methodology [24]:

Lengths and circumferences of the body and body segments measured by a standard anthropometer of Martin type [3] with an accuracy of 0.1 cm:

Height – the distance between the floor and the vertex (the highest point on the sagital line of the skull) while the participant is barefoot and standing upright.

Height seated – the distance between surface of seating and the *vertex*.

Length of the lower extremity – the distance between the floor and *spina iliaca anterior superior*.

Thigh circumference – the circumference of the right thigh on the level of the *sulcus glutaeus* in shoulder-width stance.

All measurements were taken by the same investigator who was assisted by a colleague as instructions were given verbally to the participants.

As length of body segments is strongly correlated with body mass, and thus, indirectly, with maximal strength we only used relative variables based on these measurements. Four indices that describe the length of different body parts relative to body height were calculated:

$\frac{Height\ seated}{Height}$ (HSH) – we used this index to calculate the relative length of the torso

$\frac{Length\ of\ lower\ extremity}{Height}$ (LEH) – this index measures the relative length of the lower extremity

$\frac{Height}{Thigh\ circumference}$ (HT) – with this index we measured the muscularity of lower extremity. We corrected for height to obtain a universal measure independent of body dimensions.

Additionally, we calculated an index to estimate the relative strength. As the standard approach of evaluating it as maximal strength per kilogram of body mass suffers from significant inaccuracies, we corrected the data in accordance to the equation suggested by Zatsiorsky & Kraemer [34]:

$$Max.strength = a.(Body\ mass)^{\frac{2}{3}}$$

We used an arbitrary value of 1 for the constant ***a***. Despite this approach not being exactly accurate, it captures the essence of the formula – to correct the power of body mass in order to eliminate the inaccuracy due to the positive relationship between maximal strength and body mass. As the constant ***a*** only changes proportionally the slope of the curve (its first derivative) but not its type, we consider this index as an appropriate proxy with relative strength. In both powerlifting and Olympic weightlifting similar approaches (based on variations of this formula) are used to determine the best lifter in a competition [13, 16]. Accordingly, relative strength is an important parameter of training and preparation in strength sports.

The index was calculated as:

$$\frac{Squat}{Body\ mass^{\frac{2}{3}}} \text{ (Relative squat),}$$

and measures the relative strength in the squat.

Test protocol

We used the following test to measure the maximal strength:

Barbell back squat: The bar is placed behind the neck on the top of the back. The grip is wider than shoulder-width. The stance is shoulder-wide. The participant squats to the point when the hip joint is below knee joint.

We modified the Comfort [4] protocol for measuring maximal strength (estimating 1 repetition maximum/RM) [4]. It is relatively easy to perform, has high statistical reliability and is suitable for experienced athletes:

Participants warmed up by performing the exercises with submaximal loads that they were accustomed to from their normal training. Participants were permitted a maximum of 6 progressively increasing loads, for each exercise, although all participants completed the testing within 4–5 attempts. Weight was increased in increments of between 5 and 20 kg starting with larger increments and gradually decreasing them until the maximum was reached.

We specifically chose this exercise because it is widely used in training routines of all strength sports and accordingly, all subjects were well acquainted with the technique of execution. Maximal strength is defined as one's ability to exert maximal force against an external resistance and requires a maximal voluntary contraction [32]. All participants used lifting belts and shoes. No other accessory equipment was allowed.

Statistical analysis

We used the following statistical methods to interpret the results of the study:

- *Variation analysis.* The following parameters were calculated: mean value, standard deviation, minimum value and maximum value.
- *Correlation analysis.* We studied the relationships between the measured variables by calculating Pearson correlation coefficients at a level of significance of $p<0.05$. We tested our data set for normality by the Kolmogorov-Smirnov test [10].
- *Stepwise regression analysis*. A stepwise regression analysis was performed with a forward multiple linear regression approach to estimate the value of the studied variables as predictors of each of the maximal strength tests [11, 23].

All statistical analyses were conducted on the IBM SPSS Statistics for Windows software package (version 21).

Results

The variation analysis of the data is presented and the results of Kolmogorov-Smirnov test for normality of each variable are presented in **Table 1**. Pearson linear correlation coefficients of the studied variables are shown in **Table 2**. We found statistically significant correlations between both squat and relative squat and all studied variables with the exception of only this between relative squat and HT. These results (although expected) set the basis for the search for quantifying these relationships by regression models. The correlation coefficient between HSH and LEH is also statistically significant. No statistically significant correlations were calculated between HT and HSH or LEH. Accordingly, the regression models derived for HSH and LEH may provide overlapping information to some extend (due to the correlation between them) while LH carries independent predictive value.

Table 1. Variation analysis of obtained data

	Minimum	Maximum	Mean	Std. Deviation	K-S test
Height	1.580	1.855	1.729	0.061	0.747
Height seated	0.840	1.010	0.920	0.040	0.129
Upper extremity length	65.000	83.000	74.900	4.230	0.071
Lower extremity length	87.000	105.000	98.33	4.315	0.449
HSH	0.500	0.562	0.426	0.187	0.309
LEH	52.352	59.195	56.871	1.486	0.994
HT	0.722	0.897	0.814	0.049	0.495
Squat	120.000	320.000	206.845	45.9290	0.389
Relative squat	7.873	16.540	10.758	2.057	0.913

Abbreviations: HSH – height seated/height; LEH – length of lower extremity/height; HT – height/thigh circumference; K-S test – Kolmogorov-Smirnov test

Table 2. Correlation matrix of studied variables

	HSH	LEH	HT	Squat	Relative squat
HSH	-				
LEH	-0584*				
HT	0.187	0.163			
Squat	-0.543*	0.459*	-0.385*		
Relative squat	-0.519*	0.507*	0.089	0.886*	-

Statistically significant correlations ($p<0.05$) are marked with *

Abbreviations: HSH – height seated/height; LEH – length of lower extremity/height; HT – height/thigh circumference

The parameters of the models of linear regression are presented in **Tables 3** and **4**. For the squat, all of them are statistically significant with Adjusted R squared values varying between 0.148 (for HT) to 0.277 (for HSH). Prima facie, each of the models taken separately explains a relatively small portion of data variance, but the combined information of the three may be a powerful tool in the training and preparation process of athletes. Interestingly, for the relative squat, only two of the models (for HSH and LEH) show statistical significance of the estimated parameters with higher values of Adjusted R squared – 0.253 and 0.256 respectively. Although somewhat unexpected, these findings are consistent with the lack of correlation between relative squat and HT (**Table 2**).

Table 3. Linear regression models of studied variables vs. Squat

Model B		Unstandardized Coefficients		t	Sig.	Adjusted R Squared
		Std. Error				
Squat	Constant	918.506	174.126	5.275	0.000	0.277
	HSH	-1335.359	326.534	-4.089	0.000	
Squat	Constant	-411.161	189.433	-2.170	0.036	0.191
	LEH	1427.125	437.199	3.264	0.002	
Squat	Constant	463.231	97.523	4.750	0.000	0.148
	HT	-9567.536	3630.865	-2.635	0.012	

Abbreviations: HSH – height seated/height; LEH – length of lower extremity/height; HT – height/thigh circumference

Table 4. Linear regression models of studied variables vs. Relative squat

Model B		Unstandardized Coefficients		t	Sig.	Adjusted R Squared
		Std. Error				
Relative Squat	Constant	41.516	8.076	5.140	0.000	0.253
	HSH	-57.657	15.131	-3.811	0.000	
Relative Squat	Constant	-19.585	8.290	-2.362	0.023	0.256
	LEH	70.114	19.144	3.662	0.001	
Relative Squat	Constant	13.277	4.756	2.792	0.008	0.007
	HT	-93.865	176.832	-.531	0.599	

Abbreviations: HSH – height seated/height; LEH – length of lower extremity/height; HT – height/thigh circumference

Discussion

According to the common wisdom among strength training coaches, certain specific body proportions can provide advantages in basic resistance exercises (e.g., front and back squats or deadlifts) and are therefore beneficial for developing strength in competitive lifting. For instance, relatively long hands are considered advantageous for conventional or sumo deadlift and short lower extremities for squat [31]. In our study, all anthropometric parameters analysed proved to be statistically significant predictors of maximal and relative strength in the squat, with the exception of HT and relative squat. Irrespective of the fact that adjusted R-squared values (the variance explained by the model) are not high, the significance of the statistical models is for all constants and predictors (**Tables 3** and **4**). These findings indicate that other (unidentified) predictors exist that explain the variation of the results. Interestingly, the parameters of the regression model for HT as a predictor of squat strength are not statistically significant. HT is a measure of muscularity (and thus indirectly, strength, as muscle strength is proportional to muscle cross sectional area or volume) of thigh muscles relative to body height. Thus, it is logical HT to be highly correlated to strength of lower limbs. Despite the fact that HT is an indirect indicator of relative strength as it does not measure muscle strength directly, it still provides information on this parameter. According to our findings, muscle volume (of thighs) does not have any predictive value for relative squat strength – i. e., athletes with different levels of thigh hypertrophy would have similar strength per kilogram body mass in the squat. However, relative squat is a measure of a specific muscle quality – strength per kilogram and it is logical for it to be uncorrelated with the amount of muscle mass measured – both absolutely or relatively (HT). In this regard, our results are not unexpected, especially considering the fact that we studied athletes in strength sports with similar body compositions.

Not many authors have explored relationships between anthropometric measures and performance in strength sports and logically, no systemized unanimous opinions and conclusions on the topic exist among the scientific community. Keogh et al. [17] studied anthropometric profiles and somatotypes of competitive New Zealand powerlifters of different weight classes [18]. These authors made a brief comparison of their results with anthropometric measures of bodybuilders and Olympic weightlifters (reported by other researchers). The same researchers analysed the relationships between anthropometric parameters and strength abilities in powerlifters [19]. They found no differences in body segment lengths between weaker and stronger athletes. Differences in body lengths were observed between powerlifters of different weight classes. However, unlike the present study, the authors concentrated their attention on determining differences in body proportions and body composition between stronger and weaker athletes.

Ferrari et al. [9] studied the relationships between body composition and maximal strength in powerlifters. The authors derived multiple regression equations using these variables as predictors for the three competitive lifts (and the total) in powerlifting. Vis-a-vis our study, their results are focused on body circumferences. The only reported statistically significant relationship was between the length of the upper limb/height and performance.

Similarly, Ebada [5] studied the relationships between anthropometric measures and results in Olympic weightlifting [10]. However, the only body length the authors measured was maximal height, which makes their results incomparable to ours.

Lovera & Keogh [19] studied 31 anthropometric measures of Argentinean competitive powerlifters [20]. Irrespective of the fact that the study was focused primarily on measuring body composition, the authors also did not find any statistically significant relationships between body segment lengths and results in the competitive lifts. Our study differs in methods, as we aimed at establishing universal relationships between strength and body proportions and accordingly, only examined relative body segment lengths.

Our study corroborates some of the conclusions of a previous experiment, which studied experienced powerlifters [9]. The authors used a stepwise multinomial regression approach to derive equations predicting maximal strength in squat, bench press and deadlift based on anthropometric data. Although in addition to the lengths of the body segments, they also measured the circumferences, their results demonstrate that relative torso length is an important factor of performance in powerlifting. Following a similar protocol, Ferland et al. [7] studied junior competitive powerlifters and compared their maximal strength abilities to those of American football players. They derived similar multiple regression equations to their previous study. Regrettably, we cannot compare their results to ours as they only report data on the combined group of subjects – powerlifters and American football players.

Conclusions

The most important practical use of our results is the opportunity the models can give to coaches to access athletes' potential to excel in one of the most popular strength exercises that is competitive in powerlifting – the back squat. This is a powerful tool (which is based on simple sometometric measurements that can be easily done on

site) in the process of sports selection and specialization. Additionally, the models can quantify the expected gains in these exercises, especially regarding their relative variants. This is important for predicting athlete's potential for better ranking in the absolute category in powerlifting events.

Admittedly, the study has limitations. Most importantly, due to the specifics of the studied sample (highly qualified strength athletes), our results most probably are not directly applicable to competitors in other sports or the general population. The same holds true for female and youth athletes in strength sports. It is also important to mention that the exercise we used for testing (back squat) is technically complex and requires enough time for technique perfecting. In this regard, it is not appropriate for use by inexperienced athletes. Additionally, the testing protocol for estimating 1 RM is also taxing and requires training experience.

Acknowledgments: We extend our sincere appreciation to the participants whose willingness to share their valuable experiences made this study possible. Their contributions were critical to the successful completion of our research. We also appreciate the National Sports Academy support for the publication. The authors declare that no financial support was received for the research, authorship, and/or publication of this article.

References

1. **Alcazar, J., R. Csapo, I. Ara, L. Alegre**. On the shape of the force-velocity relationship in skeletal muscles: The linear, the hyperbolic, and the double-hyperbolic. - *Frontiers in Physiology*, **10**, 2019, 769.
2. **Baechle, T. R., R. W. Earle**. *National Strength and Conditioning Association. Essentials of strength training and conditioning.* 3rd ed. Champaign, IL, Human Kinetics, Albany, 2008.
3. **Cameron, N**. *Measurement of human growth*. Dobbs Ferry, New York, Sheridan House, 1984.
4. **Comfort, P., J. J. McMahon**. Reliability of maximal back squat and power clean performances in inexperienced athletes. – *J. Strength Cond. Res.,* **29**(11), 2015, 3089-3096.
5. **Ebada, K**. Relative strength, body mass and height as predictors of Olympic weightlifting players performance. – *Journal of Physical Education And Sports Science*, **13**(2), 2011, 166-171.
6. **Everett, G.** *Olympic weightlfting,* Second edition. USA, Catalyst Athletics, San Francisco, 2016.
7. **Ferland, P. M., A. Laurier, A. S. Comtois.** Relationships between anthropometry and maximal strength in male classic powerlifters. - *International journal of Exercise Science*, **13**(4), 2020, 1512–1531.
8. **Ferland, P. M., A. Pollock, R. Swope, M. Ryan, M. Reeder, K. Heumann, A. S. Comtois.** The relationship between physical characteristics and maximal strength in men practicing the back squat, the bench press and the deadlift. - *International Journal of Exercise Science*, **13**(4), 2020, 281–297.
9. **Ferrari, L., A. L. Colosio, M. Teso, S. Pogliaghi.** Performance and anthropometrics of classic powerlifters: Which characteristics matter? - *Journal of Strength and Conditioning Research,* **36**(4), 2022,1003–1010.
10. **Freud, J. E.** *Mathematical statistics.* New Jersey: Prentice-Hall, Inc. Englewood Cliffs, 1962.

11. **Hatfield, F. C**. *Powerlifting: A scientific approach. Chicago: Contemporary Books*, 1981
12. IPF, IPF PL formula, 2020. Available at: https://www.powerlifting.sport/rules/codes/info/ipf-formula
13. **Issurin, V.** *Block Periodization: Breakthrough in sports training*. Muskegon, MI, Ultimate Athlete Concepts, 2008, 1-213.
14. **Issurin, V**. New horizons for the methodology and physiology of training periodization. - *Sports Med*., **40**, 2010, 189-206.
15. IWF. *Sinclair coefficient*, 2021. Available at: https://iwf.sport/weightlifting_/sinclair-coefficient/
16. **Katch, L., F. Katch, R. Moffatt, M. Gittleson**. Muscular development and lean body weight in body builders and weight lifters. – *Med. Sci. Sports Exercise*, 1980, **12**(5), 340-344
17. **Keogh, J., P. Hume, S. Pearson, P. Mellow.** Anthropometric dimensions of male powerlifters of varying body mass. - *Journal of Sports Sciences*, **25**(12), 2007, 1365–1376.
18. **Keogh, J., P. Hume, S. Pearson, P. Mellow**. Can absolute and proportional anthropometric characteristics distinguish stronger and weaker powerlifters? – *J. Strength Cond. Res.*, **23**, 2009, 2256–2265.
19. **Lovera, M., J. Keogh.** Anthropometric profile of powerlifters: differences as a function of bodyweight class and competitive success. - *The Journal of Sports Medicine and Physical Fitness*, **55**(5), 2015, 478-487.
20. **Panayotov, V**. Study of morphological characteristics and their impact on strength abilities of competitors in bodybuilding, powerlifting and Olympic weightlifting. *PhD Thesis*, National Sports Academy, 2007, 88 p. [In Bulgarian]
21. **Panayotov, V.** Relationships between body dimensions and strength abilities in experienced Olympic weightlifters, powerlifters and bodybuilders. - *Series on Biomechanics*, **34**(4), 2020, 52-58.
22. **Papoulis, A.** *Probability, random variables and stochastic processes*. Texas, McGraw -Hill Inc., 1991.
23. **Preedy, V.** *Handbook of anthropometry physical measures of human form in health and disease*. New York, Springer, 2012.
24. **Ratamess, N.** *ACSM's Foundations of strength training and conditioning*. Indianapolis: American College of Sports Medicine, 2012.
25. **Rippetoe, M., L. Kilgore.** *Starting strength,* 2nd ed. Texas, The Aasgaard Company, 2007.
26. **Schoenfeld, B.** The Mechanisms of muscle hypertrophy and their application to resistance training. - *Journal of Strength and Conditioning Research*, **24**, 2010, 2857-2872.
27. **Schwarzenegger, A., B. Dobbins.** *The New encyclopedia of modern bodybuilding*. New York, Simon and Schuster, 1998.
28. **Sheiko, B.** Powerlifting: foundations and methods. Ufa, Russia, 2018.
29. **Siff, M.** *Biomechanical Foundations of Strength and Power Training, Biomechanics in sport.* Oxford, Blackwell Science, 2000.
30. **Simmons, L.** *The Westside barbell book of methods*. Texas, Action Printing, 2007.
31. **Thompson, S. W., D. Rogerson, A. Ruddock, A. Barnes**. The effectiveness of two methods of prescribing load on maximal strength development: *A systematic review.* - *Sports Medicine (Auckland, N.Z.),* **50**(5), 2020, 919–938.
32. **Verkhoshansky, Y., C. Siff.** *Supertraining*, 6th ed. – *Expanded version*. USA, Verchoshansky.com, 2009.
33. **Zatsiorsky, V., W. Kraemer.** *Science and practice of strength training,* 2nd ed. Illinois, Human Kinetics, 2006.
34. **Zatsiorsky, V**. *Biomechanics in sport. New Jersey, Blackwell Science*, 2000.

Institute of Experimental Morphology, Pathology and Anthropology with Museum
Bulgarian Anatomical Society

Acta Morphologica et Anthropologica, 33 (1-2)
Sofia ● 2026

Garré's Sclerosing Osteomyelitis of the Tibia in a Male from Nor Armavir (6th–5th centuries BC), Armenia

Anahit Yu. Khudaverdyan[1], Margar S. Hmayakyan[1], Shota A. Vardanyan[2], Vardan V. Margaryan[3], Nvart G. Tiratsyan[1], Anna P. Antonyan[3], Yurii M. Cherepennikov[3], Vahan R. Kocharyan[3], Simon G. Hmayakyan[1]

[1]*Institute of Archaeology and Ethnography, National Academy of Science, Yerevan, Republic of Armenia*
[2]*Department of Forensic Medicine, Yerevan Mkhitar Heratsi State Medical University, Yerevan, Republic of Armenia*
[3]*Institute of Applied Problems of Physics of National Academy of Science, Republic of Armenia*

*Corresponding author e-mail: ankhudaverdyan@gmail.com

At the Nor Armavir site, dated to the Late Iron Age, skeletal remains of adult male, aged 40–45 years, showing pathological alterations of the lower leg, were recovered. Macroscopic analysis was utilized to estimate sex and age, followed by a paleopathological differential diagnosis. Three-dimensional computed microtomography and analysis of bone microelement composition were performed to conduct a detailed examination of the tibia and to assess pathological versus post-depositional changes, thereby supporting the differential diagnosis. Our study suggests the presence of Garre's sclerosing osteomyelitis. This disease could have caused abnormal Sc content. The diagnosis of Garre's sclerosing osteomyelitis is supported by the presence of pronounced cortical thickening of the tibial diaphysis, concentric periosteal bone apposition, narrowing of the medullary cavity, and the absence of sequestra or cloacae, as demonstrated by macroscopic examination and 3D microtomographic analysis. This represents the first documented case identified among ancient inhabitants of Armenia.

Key words: Armenia, Late Iron Age, 3D computed microtomography, Garre's sclerosing osteomyelitis, scandium (Sc)

Introduction

Osteomyelitis is an inflammatory process of bone tissue that develops in response to infection, usually of bacterial origin [20]. It arises under the influence of various pathogenic microorganisms and spreads within the bone tissue. In this condition,

inflammatory bone remodeling characterized by concurrent osteolytic and osteosclerotic processes occurs, with the degree of each process depending on the virulence of the pathogenic microorganisms and the reactivity of the host organism. The most common causative agent is *Staphylococcus aureus*; less frequently, hemolytic streptococci, *Streptococcus albus*, pneumococci, *Bact. pyocyaneus*, typhoid and paratyphoid bacilli, and other pathogens are involved [27].

Osteomyelitic lesions may originate in the surrounding soft tissues, the periosteum enveloping the bone, or the bone marrow, which occupies the medullary cavity of long tubular bones as well as the spaces and sinuses between trabeculae and lamellae of the osseous tissue. Cases of osteomyelitis originating from the periosteum are relatively benign, with a slower clinical course and without extensive bone destruction. In contrast, lesions arising from the bone marrow are characterized by a more aggressive course and are associated with substantial destruction of bone tissue [30].

In 1893, the Swiss surgeon Carl Garré first provided a detailed description of ten clinical variants of acute osteomyelitis. One of these was characterized by aseptic osteosclerosis accompanied by thickening of the bone and periosteum [5, 25]. Garré's sclerosing osteomyelitis is a rare and specific form of chronic osteomyelitis, characterized by cortical thickening and obliteration of the medullary canal [32]. It predominantly affects children and young individuals [5, 12], although cases involving individuals aged 50 years and older have also been reported [35]. The scientific literature indicates that the disease primarily affects the mandible and only rarely involves the metaphysis of long bones [32], whereas other studies report a predominance of lesions in the diaphysis of the tibia (approximately 70% of cases) and the femur (27.5%) [34]. To date, the precise etiology of this condition remains unclear [5, 35].

This disorder is more frequently discussed in the dental literature, where the mandible is reported as the most commonly affected bone [12]. It is known that the chronic process may be maintained by a persistent, low-grade infection and may persist even after treatment; therefore, the role of bacterial infection in the development of this condition has not been conclusively established [5, 26]. Isotope scans may reveal increased uptake of radiotracers at the affected site [32]. Garré's osteomyelitis most frequently affects males [34, 35]. The predominant morphological feature of this rare chronic condition is fusiform thickening of the cortical layer of the affected bone. The disease is usually confined to a single bone, although multiple regions of the same bone may be involved.

The present study provides anthropological data for an individual recovered from a 6^{th}–5^{th} century BC burial at the Nor Armavir cemetery. The village of Nor Armavir is located northwest of the "Fortress of Saint David." The aim of this study is to present a detailed description of a case of tibial osteomyelitis identified in an individual from the Nor Armavir site (Armenia), to conduct a differential diagnosis, and to assess other possible conditions that may produce symptoms similar to those observed in this study.

Material and Methods

The investigation of the archaeological site of Nor Armavir (Argishtikhinili) is associated with the establishment of the capital of Greater Armenia, Armavir, in the eastern citadel of the city in the 4th century BC. Argishtikhinili is located in the Armavir Province of the Republic of Armenia. The city was founded on two hills in 776 BC by King Argishti I. Both hills – Armavir and the so-called "Fortress (or Hill) of Saint David" – have remained places of worship up to the present day. The city is mentioned in Urartian cuneiform inscriptions dating to the 8th century BC and was later described in detail in the 5th century AD by Movses Khorenatsi [17].

An important role in the early investigation of Armavir was played by the learned monks of Echmiadzin, who repeatedly surveyed the area over many years. In the second half of the 19th century, the Echmiadzin scholar Mesrop Smbatyants discovered two cuneiform inscriptions of Argishti I and Rusa III in the vicinity of Armavir. The first reconnaissance and survey excavations were organized in 1880 by A. D. Yeritsov and A. S. Uvarov [22].

Over different periods, the Armavir Archaeological Expedition was led by N.Ya. Marr, S.V. Ter-Avetisyan, S. Ter-Hakopyan, B.N. Arakelyan, A.A. Martirosyan, R.M. Torosyan, G.A. Tiratsyan, I.A. Karapetyan, and S.G. Hmayakyan. The Nor Armavir cemetery was excavated during the 2021 field season under the direction of S.G. Hmayakyan, and the burial analyzed in the present study dates to the 6th–5th centuries BC. The present study provides bioarchaeological data on an individual from this burial. The village of Nor Armavir is located to the northwest of the "Fortress of Saint David." More than 50 burials dating to the 8th–6th centuries BC were discovered and excavated within household plots in the village (**Fig. 1**), 17 of which were karas burials (interments in large ceramic vessels or pithoi) [13].

The bioarchaeological material from the Nor Armavir burial complex was excavated in Sector 3 ("Levon's Gardens") by the archaeological expedition of the Institute of Archaeology and Ethnography of the National Academy of Sciences of the Republic of Armenia, under the direction of S.G. Hmayakyan (archaeologists M.S. Hmayakyan and N.G. Tiratsyan). The article analyzes the skeletal remains from burial No. 6 of the Nor Armavir cemetery, which was excavated in 2021 (**Fig. 1**). This burial is unusual in that three individuals were interred in each layer, arranged one above the other. The skeleton from grave No. 6 were dated using relative (archaeological) methods. Other burials at the Nor Armavir cemetery exhibit comparable structural features, including grave type and skeletal positioning. The anthropological materials are curated in the Physical Anthropology Laboratory of the Institute of Archaeology and Ethnography, National Academy of Science, Republic of Armenia (Yerevan).

---

[1] 40°09′N 44°03′E

Fig. 1. Map of Armenia showing the location of Nor Armavir (drawing by A.Yu. Khudaverdyan), with the burial analyzed in this study shown at the top (drawing by S.G. Hmayakyan).

Detailed examination of the skeleton was conducted to evaluate preservation and completeness and to estimate the sex and age at death of the individual. Morphological characteristics of the pelvis and skull were used for sex determination [4, 28]. Age at death for the adult individual was estimated using a combination of pubic symphysis morphology [10, 15, 23], changes to the auricular surface [19], degree of epiphyseal fusion [4], dental wear [1], and cranial suture closure [23].

Diagenetic changes were evaluated macroscopically and through spectrometric analysis and were distinguished from pathological bone responses based on their distribution, structural organization, and relationship to the original cortical architecture.

A noninvasive X-ray study of human bone was conducted using experimental facilities for X-ray fluorescence (XRF) spectral analysis and microtomography (MicroCT) imaging at the Institute of Applied Problems of Physics (Yerevan, Armenia). XRF was employed to determine the elemental composition of the sample. Measurements were performed using a custom-designed setup comprising a BSV-25 X-ray tube and a silicon drift detector (AMPTEK-SDD). The X-ray beam was collimated using two narrow slits to achieve a beam size of 1 mm (vertical) × 0.1 mm (horizontal). XRF spectra were collected from four distinct points on the sample. The X-ray tube operated at 33 kV and 10 mA, with an exposure time of 300 seconds, kept constant across all measurements. Potential measurement errors inherent to the X-ray system were acknowledged and controlled by repeating measurements and maintaining consistent acquisition parameters across all samples.

Microtomographic imaging was carried out using a specialized system that included an XRB150PN6004009 X-ray source (Spellman High Voltage Electronics) and a Care View 750MT flat-panel detector (CareRay Digital Medical Technology). System control, data acquisition, and image reconstruction were managed using the T4 software platform, developed at Tomsk Polytechnic University (available at https://rsp.tpu.ru/tech/). This configuration enabled the capture of high-resolution X-ray images with a spatial resolution of approximately 60 μm. The X-ray tube operated at 70 kV and 1 mA, and the emitted beam was filtered through a 1 mm thick aluminum foil to optimize image contrast and reduce beam hardening effects.

Results

Skeleton 6 belonged to an adult male, aged approximately 40–45 years at the time of death. Sex was determined based on pelvic and cranial morphology. Age at death was estimated using a combination of changes to the auricular surface, degenerative bone conditions, dental wear, and cranial suture closure. Based on these features, the individual's age at death is estimated at 40–45 years. The skeleton is moderately well preserved, with most elements present; some bones exhibit post-mortem damage (**Fig. 2**).

The tibia shows marked enlargement involving the proximal metaphysis and the upper half of the diaphysis. A transverse section of the bone, resulting from post-mortem breakage, reveals pronounced cortical thickening and complete sclerotic obliteration of the medullary cavity by newly formed spongy bone. A large subcortical cavitation is present in the superolateral portion of the bone (**Fig. 3**). Plaque-like areas of new bone formation are observed on both the medial and lateral surfaces of the distal metaphysis. Bone sequestra and drainage channels (cloacae) are absent.

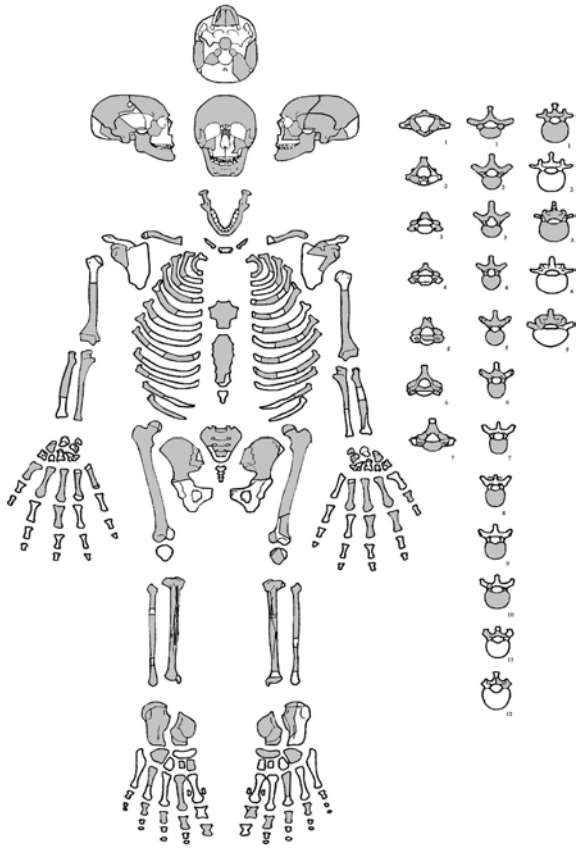

Fig. 2. Completeness of the human skeleton (grey colour – skeletal elements present, white – absent)

Radiographic examination demonstrates a thickened cortex in the diaphyseal region of the right tibia, accompanied by progressive narrowing of the medullary cavity. Computed tomography (CT) sections obtained at different levels provide clearer visualization of partial (**Fig. 4**) and complete obliteration of the medullary canal, as well as localized circumferential cortical thickening and the presence of bone lacunae. All bones were carefully cleaned prior to scanning, and the medullary cavities were free of soil or other extraneous material. The diaphysis exhibits a characteristic fusiform expansion. The narrowing of the medullary cavity is due to the formation of endosteal bone deposits along the inner cortical surface, reflecting a pathological response.

In some areas, against the background of cortical thickening and osteosclerosis, zones of osteodestruction are observed in the form of polymorphic, partially coalescing resorption cavities, producing a characteristic "moth-eaten" appearance of the dense bone tissue (**Figs. 4, 5**). The affected region exhibits increased radiodensity, consistent with osteosclerosis. Diagenetic changes were excluded by examining bone microstructure, evaluating the distribution of mineral deposits, and confirming that the cortical thickening followed anatomical patterns rather than irregular post-mortem mineralization.

Fig. 3. The cortical layer along the anterior medial surface of the tibia is thickened, areas of heterogeneous density are noted.

Multiple regions of the tibia are involved in the pathological process. Areas of bone necrosis (bone marrow infarction) were identified, resulting from insufficient blood supply and leading to the death of bone marrow and trabecular bone. This process contributed to narrowing and eventual obliteration of the medullary canal (**Fig. 3**). The fibula is unaffected and appears normal.

Computed tomography of the tibia revealed pronounced cortical thickening, narrowing, and obliteration of the medullary canal (**Fig. 5**). Extensive bone sclerosis is

clearly visible in both longitudinal and cross-sectional views, confirming pathological endosteal bone growth rather than taphonomic filling.

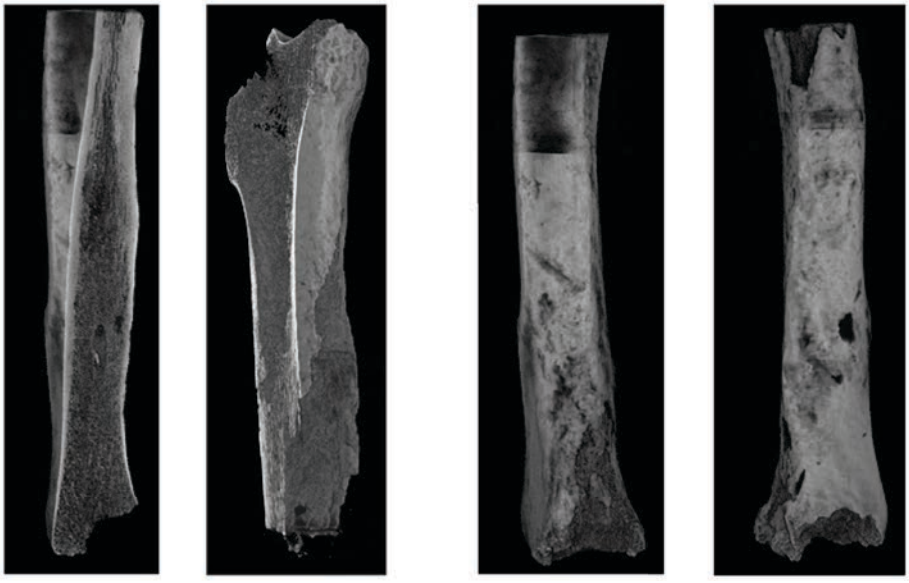

Fig. 4. On the surface of the tibia, areas of non-uniform density are observed, including ground glass opacity; a zone of bone marrow infarction is observed.

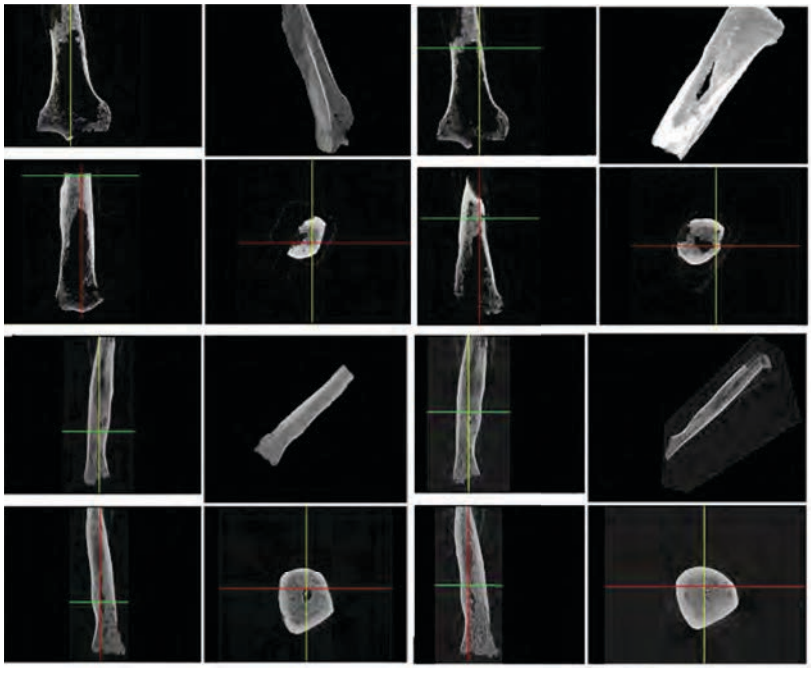

Fig. 5. X-ray fluorescence spectrometric analysis of several areas of the tibia.

Calcium (Ca) values in the tibia ranged from 77.662 % to 99.463 %, indicating post-mortem diagenetic alteration rather than the original biogenic composition of the bone **(Table 1)**. Similarly, strontium (Sr) concentrations likely reflect diagenetic uptake. Manganese (Mn) and iron (Fe) levels were relatively low, amounting to 2.056 µg/g and 13.171 µg/g, respectively. In contrast, the concentration of scandium (Sc) was notably elevated, reaching 12.839 µg/g. For comparison, the average scandium content in human skeletal bone is approximately 1–2 µg/kg, with a commonly cited mean value of about 1.5 µg/kg [5]. Given the unusual Sc enrichment, this observation may reflect unique environmental or pathological incorporation, and warrants further discussion.

Fig. 6. Dimensions of the tibia (upper transverse (1, 3: right 32,9 mm: 2, 44: left 32 mm), upper sagittal (1, 3: right 31 mm: 2, 44: left 21 mm); lower transverse (1, 3: right 31,5 mm: 2, 44: left 29 mm), upper sagittal (1, 3: right 33 mm: 2, 44: left 24 mm). Post-cranial skeleton without evidence of pathological changes (2, 4, 5-8).

No bone lesions or traumatic injuries were observed in the left tibia (**Fig. 6)**. Other elements of the cranial and post-cranial skeleton showed no additional evidence of pathological changes, including trauma.

Discussion

In the individual from Nor Armavir, several pathological features were documented – including pronounced cortical thickening in the anterior midshaft region of the tibia, narrowing and obliteration of the medullary canal, and extensive bone sclerosis. The medullary canal was thoroughly cleaned of soil and other debris prior to examination, and CT imaging confirmed that the cavity was filled with endosteal bone rather than post-mortem material, suggesting that the obliteration reflects a pathological process rather than taphonomic accumulation. This condition has been described in the literature under various terms, including chronic osteomyelitis with proliferative

periostitis and non-suppurative sclerosing osteomyelitis [25, 33, 34. 31]. In the present case, the pathological changes are predominantly endosteal, affecting the medullary cavity rather than the periosteal surface. The generally accepted term for this entity is Garré's sclerosing osteomyelitis.

Garré's osteomyelitis is classically characterized by fusiform enlargement of the affected bone, marked thickening and sclerosis of the cortical layer (dense compact bone), and narrowing or complete obliteration of the medullary canal. The differential diagnosis of Garré's osteomyelitis requires exclusion of other skeletal pathologies, including chronic suppurative osteomyelitis, fibrous dysplasia, malignant bone tumors (osteosarcoma, Ewing sarcoma), benign lesions (osteoid osteoma, eosinophilic granuloma, osteoblastoma), Paget's disease, as well as syphilitic bone disease [8, 11, 14, 18, 24].

Although Garré's osteomyelitis represents a form of chronic osteomyelitis, classic chronic osteomyelitis typically presents with foci of bone destruction, sequestra, and draining sinuses. In contrast, Garré's osteomyelitis is dominated by hyperostosis and sclerosis, rather than suppurative lesions. Fibrous dysplasia may show overlapping features with Garré's osteomyelitis; however, Garré's osteomyelitis is associated with a characteristic spiculated ("needle-like") periosteal reaction, whereas fibrous dysplasia more often exhibits a diffuse, "ground-glass" or hazy radiographic appearance. A similar sclerotic pattern may be observed in malignant bone tumors, such as osteosarcoma and Ewing sarcoma. Nevertheless, these neoplasms typically demonstrate more aggressive cortical destruction and permeative bone loss [6], features that are absent in Garré's osteomyelitis. Ewing sarcoma is also rare in individuals older than 30 years. Radiologically, it is characterized by an aggressive lytic lesion with a prominent periosteal reaction, often described as an "onion-skin" pattern. In the present case, the age at death, the absence of extensive cortical destruction, and preservation of the original diaphyseal architecture argue strongly against a diagnosis of Ewing sarcoma. In syphilitic bone disease, the pathological process is typically polyostotic, affecting multiple skeletal elements simultaneously. Deformation of the affected bones lacks the regular fusiform configuration characteristic of Garré's osteomyelitis, and the external contours are often irregular, undulating, or serrated, as seen in crest-like or circular periostitis. Although both syphilitic lesions and Garré's osteomyelitis are associated with hyperostosis and sclerosis, syphilis is usually accompanied by well-demarcated, rounded destructive foci of varying size, surrounded by sclerotic rims, corresponding to gummatous lesions – features not observed in the present case.

Benign bone lesions, such as osteoid osteoma and eosinophilic granuloma, typically display less extensive sclerosis or a more specific anatomical localization than that observed in Garré's osteomyelitis. Osteoblastoma, although classified as a benign tumor, is locally aggressive and shows a marked predominance in males (approximately 2:1), most frequently affecting adolescents and young adults, with the majority of cases reported between 10 and 25 years of age. The posterior elements of the vertebral column represent the most common site of involvement; long bones, particularly the femur and tibia, may also be affected, usually involving the medullary cavity and diaphysis, with

epiphyseal localization being rare. Osteoblastoma is characterized by a central lesion typically exceeding 2 cm in diameter and surrounded by a reactive sclerotic rim [2]. In the present case, the age of the individual falls outside the most commonly reported range for osteoblastoma. In addition, the affected bone segment is substantially larger, and the morphology and distribution of internal cavitations differ from those typically described for osteoblastoma, making this diagnosis unlikely.

Paget's disease of bone is a metabolic skeletal disease, characterized by excessive resorption followed by excessive formation of bone, with abnormal bone remodeling. A critical element in the differential diagnosis concerns the condition of the medullary cavity. Involvement is usually polyostotic and asymmetric, and the most affected bones are the pelvis, spine, skull, femur, and tibia. In Garré's osteomyelitis, progressive endosteal bone apposition commonly leads to marked narrowing or even complete obliteration of the medullary canal. Moreover, Paget's disease frequently involves overall bone expansion and polyostotic distribution, features that further distinguish it from the localized, obliterative sclerosis observed in Garré's osteomyelitis.

Taken together, the macroscopic, radiological, and differential diagnostic evidence - while acknowledging the presence of post-depositional diagenetic alterations - suggests that the tibial pathology may represent a form of Garré's sclerosing osteomyelitis.

The lesion is best understood as a long-standing, localized, non-suppurative inflammatory process dominated by excessive bone formation and sclerosis, features that cannot be adequately explained by diagenetic processes alone. Post-depositional diagenetic alterations are indeed present and are evident in both the macroscopic appearance of the specimen and the spectrometric data. The extremely high calcium (Ca) values recorded in the tibia (77.662–99.463%) markedly exceed the expected range for archaeological bone with preserved collagen (26–38%) [4]. Such elevated Ca concentrations clearly reflect advanced post-depositional diagenetic mineral alteration of the bone tissue. Accordingly, the spectrometric data are interpreted as evidence of diagenetic overprint rather than as a direct indicator of pathological bone metabolism. Similarly, strontium (Sr) concentrations likely reflect diagenetic uptake. Manganese (Mn) and iron (Fe) levels were relatively low.

Given the unusual Sc enrichment, this finding may reflect specific geochemical conditions of the burial environment or a pathological alteration in bone metabolism that facilitated the atypical incorporation of trace elements. Scandium is not typically reported in elevated concentrations in archaeological bone, and its biogenic role remains poorly understood. Therefore, the detected enrichment is unlikely to represent a random fluctuation and may instead indicate selective uptake or post-depositional chemical interaction under particular environmental conditions. At the same time, chronic inflammatory processes and sustained bone remodeling – such as those inferred in the present case - could potentially influence trace element distribution and retention within newly formed bone tissue. While scandium has been discussed in modern medical literature as potentially associated with sclerosing osteomyelitis [9, 12, 16], the evidence remains limited. Although the available data do not allow us to conclusively distinguish between diagenetic and biogenic pathways, the unusual Sc signal warrants further targeted geochemical and histological investigation.

Importantly, while diagenetic processes may modify bone surface texture and mineral composition, they do not adequately account for the extent, distribution, and organization of the excessive bone formation and sclerosis observed in the tibia. These features are therefore interpreted as primarily pathological in origin and consistent with Garré's sclerosing osteomyelitis rather than post-depositional alteration alone.

Importantly, no pathological alterations were observed in the contralateral (left) tibia or in other elements of the cranial and post-cranial skeleton. This localization of the pathological and elemental changes to a single bone favors a localized chronic process rather than a systemic metabolic disorder.

Cases of sclerosing osteomyelitis with morphology comparable to that described by Garré in modern clinical literature have been reported in ancient populations. Manchester [21] documented cases of chronic osteomyelitis with pronounced periosteal appositions on long bones but did not distinguish Garré's osteomyelitis as a separate entity. Ortner [27] noted that Garré's osteomyelitis may be misinterpreted as nonspecific chronic osteomyelitis with periosteal reaction. Similarly, Roberts & Manchester [30] described periosteal reactions and sclerotic processes without defining Garré's osteomyelitis as a distinct diagnostic category. Dutour et al. [7] reported cases of cortical thickening with periosteal apposition in ancient Egyptian skeletons; although these changes may correspond to Garré's osteomyelitis, no definitive identification was proposed.

Within the paleopathological literature, only two cases of Garré's sclerosing osteomyelitis - a chronic form of osteomyelitis characterized by intense periosteal reaction with minimal or absent suppuration - have been explicitly reported [11, 29]. One case involves a tibia recovered from an archaeological site in Poland and dated to the medieval period [29]. The other documents sclerosing osteomyelitis of the tibia from the medieval church cemetery of Monte di Croce in Tuscany, Italy [11].

Conclusions

1. The pathological changes observed in the tibia from Nor Armavir are characterized by pronounced cortical thickening, extensive sclerosis, and near-complete obliteration of the medullary canal due to endosteal bone formation.
2. Macroscopic and CT data demonstrate that the obliteration of the medullary cavity represents a true pathological process rather than post-mortem sediment infill or taphonomic alteration.
3. Differential diagnostic analysis excludes a wide range of alternative conditions, including chronic suppurative osteomyelitis, fibrous dysplasia, malignant and benign bone tumors, Paget's disease, and syphilitic bone involvement, based on the absence of characteristic destructive, polyostotic, or neoplastic features.
4. The combination of morphological and radiological features is most consistent with Garré's sclerosing osteomyelitis, a localized, chronic, non-suppurative inflammatory condition dominated by bone sclerosis and hyperostosis.

5. Spectrometric analysis indicates significant post-depositional diagenetic alteration, as reflected by elevated calcium and altered trace element composition; however, these changes do not account for the structural organization and extent of pathological bone formation.

6. The unusual enrichment in scandium may reflect either specific burial geochemistry or altered bone metabolism associated with chronic inflammation, although its origin remains unresolved and requires further investigation.

7. The restriction of pathological changes to a single bone element supports the interpretation of a localized process rather than a systemic metabolic disorder.

8. This case represents a rare example of Garré's sclerosing osteomyelitis in the paleopathological record and contributes to the limited number of securely identified cases reported in archaeological populations.

References

1. **AlQahtani, S. J., M. P. Hector, H. M. Liversidge.** Brief communication: the London atlas of human tooth development and eruption. - *American Journal of Biological Anthropology*, **142** (3), 2010, 481–490.
2. **Atesok, K. I., B. A. Alman, E. H. Schemitsch, A. Peyser, H. Mankin.** Osteoid osteoma and osteoblastoma. - *Journal of the American Academy of Orthopaedic Surgeons*, **19**, 2011, 678–689.
3. **Evaristo, B., M. Claudio, A. Tiziana.** Sclerosing osteomyelitis of Garré periostitis ossificans. - Journal of Craniofacial Surgery, **13** (6), 2002, 765–768.
4. Buikstra, J., D. D. Ubelaker. *Standards for the data collection from human Skeletal remains*, Fayetteville: Arkansas Archaeological Survey Research Series, 1994.
5. **Burton, J. H.** *Bone chemistry and trace element analysis*, in: Katzenberg M. A., Saunders, S. R. (eds.) Biological Anthropology of the Human Skeleton. Wiley-Liss, USA, 2008, pp. 443–460.
6. **de Moraes, F. B., M. T. Motta, A. A. Severin, D. de Alencar Faria, F. de Oliveira César, S. de Souza Carneiro**. Garré's sclerosing osteomyelitis: case report. - *Revista Brasileira de Ortopedia*, **49**, 2014, 401-404.
7. **Dorfman, H., B. Cerniak.** *Ewing Sarcoma and Related Entities*, Mosby, St Louis, 1998, pp. 607–642.
8. **Dutour, O., G. Pálfi, J. Bérato, J-P. Brun.** Paleopathology of the spine and ribs. In Diseases in Antiquity: A Survey of the Diseases, Injuries, and Surgery of Early Populations (Eds. D. E. Brothwell & A. T. Sandison), Springfield, IL: Charles C. Thomas, 1994, pp. 635–650.
9. **Fadil, M., A. Farouki, R. Saouab, H. En-Nouali, J. E. Fenni, Z. Toufga.** Garré's chronic sclerosing osteomyelitis: An overview of clinical and radiologic features. - *Oxford Medical Case Reports*, **12**, 2025, 1058-1061
10. **Gilbert, B. M., T. W. Mckern.** *A method for aging the female os pubis*. - American Journal of Physical Anthropology, **38**, 1973, 31-38.
11. **Giuffra, V., A. Vitiello, S. Giusiani, D. Caramella, G. Fornaciari.** A possible case of Garre's sclerosing osteomyelitis from Medieval Tuscany (11th–12th centuries). - International Journal of Paleopathology, **11**, 2015, 51–55.

12. **Ghazali, F. R., A. H. Z. Samsudin.** Sclerosing osteomyelitis of Garré: A Clinico radiological correlation. – *Cureus,* **14** (7), 2022, e26866.
13. **Hmayakyan, S. G., N. V. Tiratsyan, M. S. Hmayakyan.** Karasnoye and "clay box" burials from the 2016 excavations in Argishtikhinili. Preliminary report, in: On the other side of Aragats: archaeological research dedicated to the memory of Telemak Khachatryan. Yerevan, 2018, pp. 175–181. [in Armenian]
14. **Kashima, T. G., N. G. Gamage, U. Dirksen, C. L. Gibbons, S. J. Ostlere, N. A. Athanasou**. Localized Ewing sarcoma of the tibia. - **Clinical Sarcoma Research**, **3**, 2013, 2.
15. **Katz, D., J. M. Suchey.** Age determination of the maleos pubis. - American Journal of Physical Anthropology, **69**, 1986, 427-435.
16. **Khan, A. G. S., H. Ahsin, S. Khan, A. Rafique, R. Kamal.** Garre's osteomyelitis of long bone in adult. - *Journal of Ayub Medical College Abbottabad,* **36** (3), 2024, 674-677.
17. **Khorenatsi, M.** *Istoriya Armenii* / Per. N. O. Emina [*History of Armenia* / Translated by N. O. Emin], Moscow, 1893. [in Russian]
18. **Lee, C. H., S. H. Han, B. Y. Yoon, Y. W. Lee.** Monostotic Paget's disease of the tibia in Korea. - Clinical Rheumatology, **23**, 2004, 381–382.
19. **Lovejoy, C. O., R. S. Meindl, T. R. Pryzbeck, R. P. Mensforth.** Chronological metamorphosis of the auricular surface of the ilium: A new method for the determination of adult skeletal age at death. - American Journal of Physical Anthropology, **68**, 1985, 15-28.
20. **Macnicol, M. F., A. C. Watts.** Haematogenous osteomyelitis. - Surgery (Oxford), **23** (1), 2005, 25-30.
21. **Manchester, K.** *The archaeology of discase*. Bradford, 1983.
22. **Martirosyan, A. A.** Argishtikhinili. Arkheologicheskiye pamyatniki Armenii. Urartskiye pamyatniki [Argishtikhinili. Archaeological Monuments of Armenia. Urartian Monuments], Yerevan, 1974. [in Russian]
23. **Meindl, R. S., C. O. Lovejoy, R. P. Mensforth, L. D. Carlos.** Accuracy and direction of error in the sexing of the skeleton: Implications for paleodemography. - American Journal of Physical Anthropology, **68**, 1985, 79-85.
24. **Moraes, de F. B., T. M. Motta, A. A. Severin, D. de Alencar Faria, F. de Oliveira César, S. de Souza Carneiro**. Garré's scle rosing osteomyelitis: case report. - *Revista Brasileira de Ortopedia,* **49**, 2014, 401-404.
25. **Nasir, N., K. Aquilina, D. Q. Ryder, C. J. Marks, C. Keohane.** Garré's chronic diffuse sclerosing osteomyelitis of the sacrum: a rare condition mimicking malignancy. - *British Journal of Neurosurgery,* **20**, 2006, 415-419.
26. **Nikomarov, D., M. Zaidman, A. Katzman, Y. Keren, M. Eidelman.** New treatment option for sclerosing osteomyelitis of Garré. - *Journal of Pediatric Orthopaedics B*, **22**, 2013, 577-582.
27. **Ortner, D. J.** *Identification of pathological conditions in human skeletal remains.* Academic Press, 2003.
28. **Phenice, T. W.** A newly developed visual method of sexing the os pubis. - *American Journal of Physical Anthropology*, **30**, 1969, 297-302.
29. **Prejzner, W., J. J. Gladykowska-Rzeczycka.** An attempt to evaluate the criteria for diagnosing nonspecifica inflammatory diseases observed on ancient skeletons. - *Przeglad Antropologiczny*, **60**, 1997, 103–109.
30. **Roberts, C., K. Manchester.** *The archaeology of disease.* Cornell University Press, 2007.

31. **Silva, A. J. S. G., J. A. Correia, F. Salvado, J. C. Romeu.** Garrè's Osteomyelitis regarding a clinical case and literature review: Garrè's Osteomyelitis a review. - European Journal of Stomatology, Oral and Facial Surgery, **2** (1), 2025, 02:01.
32. **Song, S., H. J. Jeong, H. K. Shin, E. Kim, S. J. Park, J. H. Park.** Sclerosing osteomyelitis of Garré: A confusing clinical diagnosis. - *Journal of Orthopaedic Surgery (Hong Kong)*, **27**, 2019, 2309499019874704
33. **Suma, R., C. Vinay, M. C. Shashikanth, V. V. Subba Reddy**. Garré's sclerosing osteomyelitis. - *Journal of Indian Society of Pedodontics and Preventive Dentistry,* **1**, 2007, 30-33.
34. **Vannet, N. B., H. L. Williams, B. Healy, R. Morgan-Jones.** Sclerosing osteomyelitis of Garré: management of femoral pain by intramedullary nailing. - *BMJ Case Reports* 2014: 10.1136/bcr-2014-206533.
35. **Volodina, V. D., A. A. Babkova, N. S. Serova, D. S. Bobrov, V. V. Zuev.** Garre's sclerosing osteomyelitis. – *Russian Electronic Journal of Radiology*, **12** (4), 2022, 153-158.

Table 1. X-ray fluorescence spectrometry analysis of several sections of the tibia (Figure 5)

Elt	Line	Intensity	Conc.
Precinct 1			
Ar	Ka	0.01	0.162
K	Ka	0.09	0.832
Ca	Ka	9.92	77.662
Ti	Ka	0.14	1.395
Mn	Ka	0.53	2.056
Fe	Ka	4.35	13.171
Sr	Ka	1.61	1.786
Nb	Ka	0.99	2.935
Tb	La	0.00	0.000
Total:			100.000
Precinct 2			
P	Ka	0.00	0.356
Ar	Ka	0.00	0.000
K	Ka	0.03	0.243
Ca	Ka	10.79	99.401
Mn	Ka	0.00	0.000
Fe	Ka	0.00	0.000
Sr	Ka	0.00	0.000
Zr	Ka	0.00	0.000
Nb	Ka	0.00	0.000
Tb	La	0.00	0.000
Total:	100.000		
Precinct 3			
P	Ka	0.00	0.000
Ar	Ka	0.00	0.000

Ca	Ka	9.45	87.051
Sc	Ka	0.54	12.839
Mn	Ka	0.00	0.000
Fe	Ka	0.00	0.000
Cu	Ka	0.00	0.000
Sr	Ka	0.08	0.110
Y	Ka	0.00	0.000
Nb	Ka	0.99	2.935
Tb	La	0.00	0.000
Total:	100.000		
Precinct 4			
Ar	Ka	0.00	0.000
Ca	Ka	21.18	99.463
Ti	Ka	0.03	0.221
Mn	Ka	0.00	0.000
Fe	Ka	0.00	0.000
Sr	Ka	0.45	0.316
Total:	100.000		

Institute of Experimental Morphology, Pathology and Anthropology with Museum
Bulgarian Anatomical Society

Acta Morphologica et Anthropologica, 33 (1-2)
Sofia ● 2026

Review Articles

An Overview of Proprioceptive Concepts of the Human Foot: Morphological, Neurophysiological, and Anthropological Perspectives

*Atanas Katsarov**

Institute of Experimental Morphology, Pathology and Anthropology with Museum, Bulgarian Academy of Sciences, Sofia, Bulgaria

*Corresponding author e-mail: zanasko@gmail.com

The human foot is increasingly recognized as a proprioceptive organ, integrating morphology, neurophysiology and cultural adaptation to regulate balance and locomotion. Recent studies highlight that plantar mechanoreceptors, intrinsic muscles, and ligamentous structures form an interconnected sensory system that dynamically adjusts to posture, load and environment. Neurophysiological findings demonstrate that cutaneous and muscular receptors redundantly maintain proprioceptive acuity, with plasticity evident through interventions such as robotic training, proprioceptive insoles and minimal footwear. Clinical applications include improved balance, reduced falls, and enhanced rehabilitation outcomes in older adults and neurological patients, while athletes benefit from sharper agility and reduced injury incidence. Anthropological perspectives show that barefoot populations maintain superior acuity compared with shod groups, suggesting an evolutionary role of proprioception in bipedal endurance. Collectively, these findings redefine the foot not as a passive support structure but as a dynamic sensory platform with broad clinical, athletic, and anthropological implications.

Key words: proprioceptive, human, foot, proprioception

Introduction

Proprioception - the ability to perceive body position and movement - is central to motor control and human adaptation. While muscles and joints are widely recognized as major proprioceptive contributors, the role of the human foot as a sensory organ

has only recently gained attention [4, 5, 11, 13, 18]. The plantar sole contains one of the highest concentrations of mechanoreceptors in the body, providing continuous feedback about surface interaction, stability, and posture [3, 10, 14, 17]. Recent studies have highlighted three critical dimensions of this phenomenon. First, morphological plasticity allows structural tissues of the foot - including arches, fascia, and intrinsic muscles - to act as both mechanical stabilizers and sensory modulators. Second, neurophysiological adaptability ensures that cutaneous, muscular, joint, and ligamentous receptors work redundantly to preserve function under varying loads and postures. Third, anthropological insights reveal that barefoot populations maintain superior proprioceptive acuity compared with shod groups, illustrating how cultural practices shape sensory pathways [6, 20]. In addition to these natural mechanisms, clinical and athletic interventions now leverage proprioceptive training, robotic devices, and textured insoles to enhance sensory function [7, 15, 16]. By synthesizing these perspectives, the present review provides an updated framework for understanding the foot not as a passive base of support but as an active proprioceptive system with evolutionary, clinical, and medico-anthropological significance.

Systematic approach in proprioception studying

A narrative systematic review was performed with analysis of contemporary literature published between 2019 and 2025. Searches were performed in PubMed, Scopus, Web of Science and Google Scholar databases using the following keywords: foot proprioception, plantar sensitivity, insoles, robotic training, gait biomechanics, barefoot populations, anthropological locomotion.

Inclusion criteria: peer-reviewed studies investigating morphological structures and proprioceptive mechanisms of the foot; experimental and clinical studies evaluating proprioceptive training or interventions; and anthropological research comparing barefoot and shod populations.

Exclusion criteria: works published before 2019 unless essential for conceptual background; case studies unrelated to proprioception; purely mechanical gait models lacking neurophysiological or sensory data.

A total of 23 studies met inclusion criteria. Morphological data included imaging and cadaveric research on fascia, arches, and postural influence [3, 10, 14, 17]. Neurophysiological studies included microneurography, afferent mapping, robotic training, and insole trials [2, 8, 16, 20, 22]. Anthropological works addressed barefoot locomotion, footwear effects, and evolutionary developments [20, 21, 23]. Findings were synthesized across these domains into an integrated account of foot proprioception.

Clinical findings and proprioception relations

Findings demonstrate that the human foot functions as a complex proprioceptive system where structure, receptors, and cultural practices converge. Postural variations alter afferent thresholds: dorsiflexion increases mechanoreceptor sensitivity in the heel and midfoot, while plantarflexion enhances responsiveness in the forefoot [3, 14].

Intrinsic muscles show anticipatory activation before ground contact, stiffening the arch and refining feedback accuracy [9]. The plantar fascia, traditionally considered mechanical, emerges as a sensorimotor bridge where strain deformation correlates with afferent thresholds [10]. Imaging studies reveal uneven distribution of fascial strain, strongest along the medial arch, underscoring its dual stabilizing and sensory role (**Fig. 1**). Minimal footwear studies show that morphology is adaptable: even three minutes of use enhances acuity [4], while long-term adaptation significantly improves plantar thresholds and reduces gait variability [17].

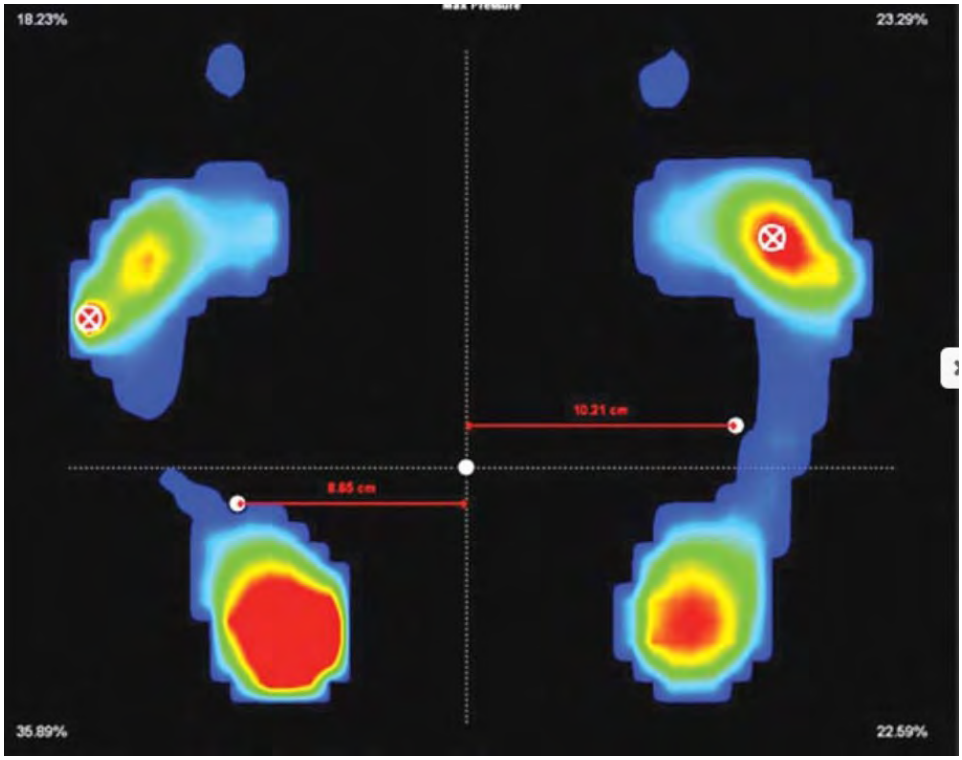

Fig. 1. Evaluation of pressure distribution in orthostatic condition.

Proprioception arises from the integration of multimodal sensory inputs, primarily derived from muscle spindles and Golgi tendon organs, with additional contributions from joint and cutaneous receptors. Muscle spindles are widely considered the dominant source of afferent information for proprioceptive acuity, particularly in fine motor control. Golgi tendon organs complement this by encoding muscle force, while articular and cutaneous receptors serve as modulators, particularly at movement extremes or when muscle spindle input is reduced. The vestibular system, while not strictly proprioceptive, is integral to the central nervous system's construction of body schema and postural orientation (**Table 1**).

Table 1. Major receptor types and their relative contribution to proprioception

Receptor Type	Anatomical Location	Principal Function in Proprioception	Approximate Relative Contribution
Muscle spindles (Ia and II afferents)	Intrafusal fibers within skeletal muscles	Encode dynamic and static changes in muscle length; provide fine-grained information regarding limb position and movement	**50–70%**
Golgi tendon organs (Ib afferents)	Myotendinous junctions	Monitor muscle tension and force generation, contributing to load detection and protective reflexes	**10–20%**
Joint capsule and ligament receptors	Articular capsules and periarticular tissues	Signal extremes of joint movement and contribute to joint position sense, particularly under high strain	**~10%**
Cutaneous mechanoreceptors (e.g., Ruffini endings, Merkel cells, Pacinian corpuscles)	Dermis and subcutaneous tissues surrounding joints	Provide supplementary proprioceptive feedback through skin stretch and pressure changes	**~10%**
Vestibular apparatus (otolith organs and semicircular canals)	Inner ear labyrinth	Supplies information on head position and motion; interacts synergistically with proprioceptive signals but is not classically categorized as a proprioceptor	*Not a direct proprioceptor; ~5% influence in integrated body schema*

The receptor network of the foot comprises cutaneous, muscular, joint, and ligament receptors. Merkel discs and Meissner corpuscles in the toe pads detect contact and slip, Ruffini endings in the dermis sense sustained stretch, and Pacinian corpuscles respond to high-frequency vibration and micro-slips [3, 11]. Microneurography confirms that the hallux and medial forefoot are sensory "hot spots," while anesthesia studies show postural sway increases 30–50% when plantar sensitivity is partially blocked [18]. Intrinsic muscle spindles monitor toe and arch position, while tendon organs in extrinsic muscles regulate tension for mediolateral stability [8, 9]. Fatigue studies show reduced spindle sensitivity leads to impaired ankle joint sense, confirming

their importance. Joint and ligament receptors further secure function, responding at extremes of motion and deformation, with finite element models linking ligament strain directly to afferent activation (**Fig. 2**).

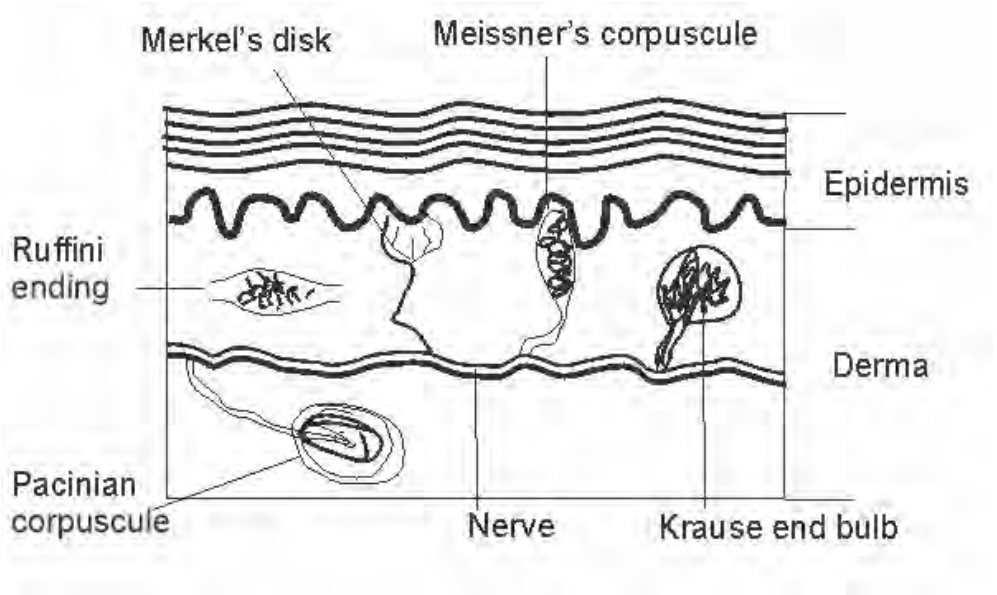

Fig. 2. Primary mechanoreceptors of the skin

Neurophysiological adaptability is supported by experimental modulation. Thermal stimulation of the sole enhances reflex amplitudes in leg muscles [8], whereas electrical stimulation has yielded mixed outcomes [19]. More effective are robotic ankle-foot interventions. Park et al. [16] reported that robot-assisted training improved walking speed by 25% and reduced balance errors by nearly a third in post-stroke patients, with associated cortical reorganization, demonstrating proprioceptive plasticity even after injury.

Proprioceptive insoles represent one of the most practical and effective interventions. Textured or contoured designs continuously stimulate plantar mechanoreceptors during gait. Alfuth et al. [2] documented reduced double-support phase and altered plantarflexion mechanics, while D'Aout et al. [7] showed posture-specific changes in lower-leg muscle activity. Clinical evidence demonstrates improved stability in older adults and enhanced sensory thresholds in neuropathic and post-stroke populations [3, 16]. In athletes, insoles sharpen agility, landing mechanics, and reduce injury incidence (**Table 2**.).

Zech et al. [22] found martial artists improved response times by 15%, while systematic reviews confirm broader reductions in ankle sprains and improved agility [1, 15]. Importantly, individual variability exists: some users benefit immediately, others require habituation. Factors include baseline plantar acuity, footwear history, and

neuromuscular conditioning. Insoles should therefore be viewed as active modulators of sensory input; not passive orthotic supports.

Table 2. The effects of proprioceptive insoles across populations

Population	Reported Effects	Key Studies
Older adults / fall risk	Reduced sway, improved symmetry, enhanced stability	Altfuth et al. (2); D'Aout et al. (7)
Neurological patients	Better balance, faster walking, cortical reorganization	Park et al. (16); Alshehri et al. (3)
Athletes	Improved agility, faster responses, reduced injury incidence	Zech et al. (22); Meng et al. (15); Acar (1)
Habitually shod adults	Enhanced plantar feedback, reduced double-support time	Liu et al. (12); Park et al. (19)
Habitually barefoot groups	Already high acuity, little added benefit	Mace et al. (14); O'Neill et al. (18)

Anthropological research reveals the role of culture in proprioception. Barefoot populations outperform shod groups in balance and sensitivity, exhibiting 25% less postural sway [6, 20]. Minimal footwear restores some of this acuity in industrialized populations [12]. Fossil evidence suggests that the development of the medial arch and hallux alignment represented not just mechanical innovations but sensory refinements for endurance locomotion [21, 22]. Cultural practices such as barefoot running and martial arts maintain this evolutionary heritage, sustaining high proprioceptive capacity even in modern contexts.

Conclusion

The evidence reviewed here positions the foot as an organ of proprioception as much as of locomotion. Morphologically, its structures adapt continuously, transforming load-bearing tissues into sensory mediators. Neurophysiological, redundancy among receptor classes ensures robust input even when one pathway is compromised. Anthropologically, the evolution of the arch and hallux, and the persistence of barefoot practices in recent time, highlight the deep roots of proprioception in human adaptation.

Clinical implications are substantial. Proprioceptive enhancement through training, insoles, and robotic devices consistently improves balance, gait efficiency, and cortical reorganization in older adults and neurological patients [2, 3, 16]. These non-invasive interventions address fall risk, stroke rehabilitation, and neuropathy. Athletic populations demonstrate parallel benefits: improved agility, sharper reaction times, and reduced injuries [1, 15, 22]. Proprioceptive conditioning therefore links rehabilitation and performance optimization, bridging medical and sports domains.

Anthropologic insights reveal that cushioned footwear diminishes sensory capacity, while barefoot and minimal practices preserve it [6, 12, 14].

Future research must prioritize personalized interventions, wearable technologies, and longitudinal cross-cultural studies to assess proprioceptive trajectories over the lifespan (**Fig. 3**).

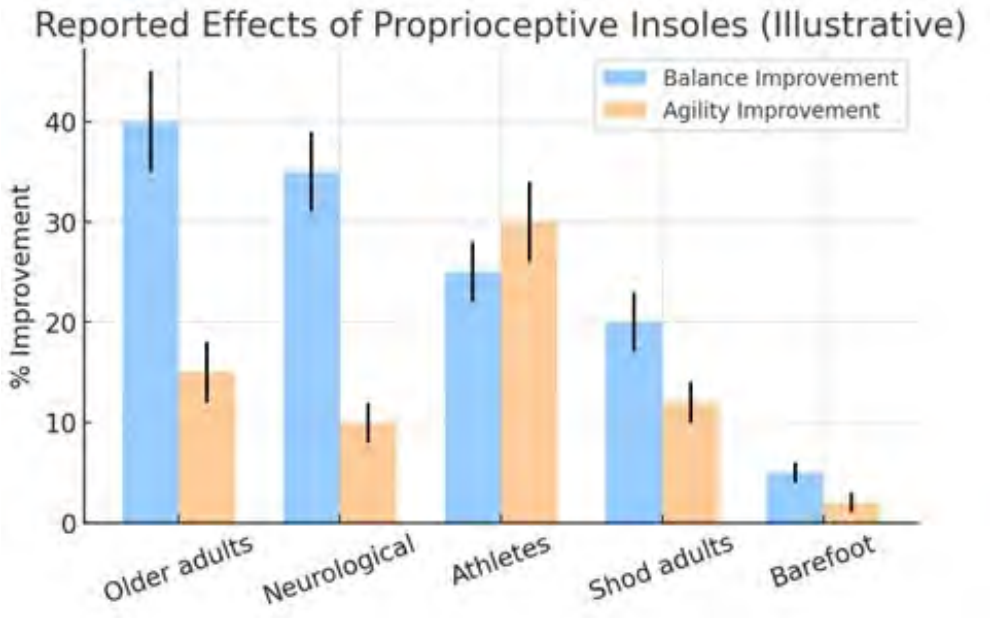

Fig. 3. Boxplot comparison of postural sway in barefoot vs shod groups

The conceptual shift is evident: the foot should not be regarded merely as a mechanical support structure, but rather as a dynamic sensory organ. This reconceptualization carries significant implications for rehabilitation, athletic training, and anthropological analysis, ensuring that one of humanity's most fundamental anatomical structures is appreciated in its full functional and adaptive complexity.

References

1. **Acar, G., S. Seyhan, K. Cimen, H. Sinen, S. Ekentok et al.** The Effect of Customised Insoles on Performance in Athletes. – *Int. J. Holistic Health, Sports and Recreation*, **4** (1), 2025, 79-86.
2. **Alfuth, M., D.** Rosenbaum. Effects of changes in plantar sensory feedback on human gait characteristics: a systematic review. - *Footwear Science*, **4 (**1), 2012, 1-22.
3. **Alshehri, S., M. S. Alshahrani, S. Y. Al Yadal, F. M. Alyazedi, H. Hasan et al.** An examination of ankle joint position sense, postural control and associated neuromuscular deficits in patients with plantar fasciitis: a cross-sectional analysis with advanced biomechanical and psychosocial correlates. – *J. Orthop. Surg. Res.*, **20**, 2025, 67.

4. **Biscarini, A., A. Calandra, A. Marucci, R. Panichi, A. Belloti.** Enhanced foot proprioception through 3-minute walking bouts with ultra-minimalist shoes on surfaces that mimic highly rugged natural terrains. - *Biomimetics*, **9**(12), 2024, 741.
5. **Collins, D. F., K. M. Refshauge, G. Todd, S. C. Gandevia.** Cutaneous receptors contribute to kinesthesia at the index finger, elbow, and knee. – *J. Neurophysiol.*, **94**(3), 2005, 1699-1706.
6. **Cudejko, T., J. Gardiner, A. Akpan, K. D'Août.** Minimal footwear improves stability and physical function in middle-aged and older people compared to conventional shoes. - *Clinical Biomechanics*, **71**, 2020, 139-145.
7. **D'Août, K. and P. Aerts.** The evolutionary history of the human foot. In: *Advances in Plantar Pressure Measurements in Clinical and Scientific Research* (Eds. K. D'Août, K. Lescrenier, B. Van Gheluwe, D. De Clercq), Maastricht, Shaker Publishing BV, 2008, 44–68,
8. **De Santis, D., J. Zenzeri, M. Casadio, L. Masia, A. Riva et al.** Robot-assisted training of the kinesthetic sense: enhancing proprioception after stroke. - *Front. Hum. Neurosci*., **8**, 2014, 1037.
9. **Futrell, E., Y. Golightly, Y. Haddad, A. Carmichael, D. Taylor.** The effects of intrinsic foot muscle strengthening interventions for adults over age 65: a randomized controlled trial protocol. - *Front Aging*, **6**, 2025, 1622232.
10 **Futrell, E., R. Kaufman, J. Chevan.** Long-term effects and impressions of minimal footwear in older adults. - *Gerontology*, **70**(11), 2024, 1137–1147.
11. **Hai, S., M. Driller, I. Ghai.** Effects of joint stabilizers on proprioception and stability: A systematic review and meta-analysis. - *Physical Therapy in Sport*, **25**, 2017, 65-75.
12. **Hatton, A. L., J. Dixon, D. Martin, K. Rome.** The effect of textured surfaces on postural stability and lower limb muscle activity. - *Journal of Electromyography and Kinesiology*, **19**(5), 2009, 957-964.
13. **Hijmans, J. M., W. Zijlstra, J. H. B. Geertzen, A. L. Hof, K. Postema**. Effects of vibrating insoles on standing balance in diabetic neuropathy. - *Journal of Rehabilitation Research & Development*, **45**, 2008, 1442–1450.
14. **Ma, C., N. Rao, S. Muthukrishnan, A. S. Aruin.** A textured insole improves gait symmetry in individuals with stroke. – *Disabil. Rehabil.*, **40**(23), 2018, 2798-2802.
15. **Meng, L., B. Porr, K. Macleod, H. Gollee.** A functional electrical stimulation system for human walking inspired by reflexive control principles. – *J. Engineering in Medicine*, **231**(4), 2017, 315–325.
16. **Park, J. H., H. S. Jeon, Ji-H. Kim, H. B. Yoon, O. B. Lim et al**. Immediate effect of insoles on balance in older adults. - *The Foot*, **47**, 2021, 101768.
17. **Ren, W., L. Xu, X. Zheng, F. Pu, D. Li et al.** Effect of different thermal stimuli on improving microcirculation in the contralateral foot. - *BioMed Eng OnLine*, **20**, 2021, 14.
18. **Richard, M., E. G. Spaich, M. Serrao, O. K. Andersen.** Stimulation site and phase modulation of the withdrawal reflex during gait initiation. - *Clinical Neurophysiology*, 1**26** (12), 2015, 2282-2289.
19. **Robbins, S. E., E. Waked, J. Mcclaran.** Proprioception and stability: Foot position awareness as a function of age and footware. - *Age and Ageing*, **24**, 1995, 67-72.
20. **Schiftan, G. S., L. A. Ross, A. J. Hahne.** The effectiveness of proprioceptive training in preventing ankle sprains in sporting populations: a systematic review and meta-analysis. – *J. Science and Medicine in Sport*, **18 (3)**, 2015, 238-244.

21. **Trinkaus, E., H. Shang**. Anatomical evidence for the antiquity of human footwear: Tianyuan and Sunghir. – *J. Archaeological Science*, **35** (7), 2008, 1928-1933.
22. **Trinkaus, E.** Anatomical evidence for the antiquity of human footwear use. – *J. Archaeological Science*, **32**, 2005, 1515-1526.
23. **Zech, A., S. Meining, K. Hötting, D. Liebl, K. Mattes et al.** Effects of barefoot and footwear conditions on learning of a dynamic balance task: a randomized controlled study. – *Eur. J. Appl. Physiol.*, **118**, 2018, 2699–2706.
24. **Zipfel, B., L. R. Berger.** Shod versus unshod: The emergence of forefoot pathology in modern humans? - *The Foot*, **17**, 2007, 4, 205-213.

Institute of Experimental Morphology, Pathology and Anthropology with Museum
Bulgarian Anatomical Society

Acta Morphologica et Anthropologica, 33 (1-2)
Sofia ● 2026

Anatomical Variations of the Brachial Plexus Cords and Their Clinical Relevance to the Infraclavicular Block: A Literature Review

Petar-Preslav Petrov[1], Delyan Dimitrov[2], Pavel Timonov[3], Tanya Kitova[1], Antoaneta Fasova[1], Darina Barbutska[1]*

[1] Department of Human Anatomy, Histology and Embryology, Medical University of Plovdiv, Plovdiv, Bulgaria
[2] Faculty of Medicine, Medical University of Plovdiv, Plovdiv, Bulgaria
3 Department of Forensic Medicine and Deontology, Medical University of Plovdiv, Plovdiv, Bulgaria

*Corresponding author e-mail: Petar-Preslav.Petrov@mu-plovdiv.bg

Anatomical variations of the brachial plexus are frequently encountered during anatomical dissections and clinical procedures. Among its components, the cords represent a structurally complex and developmentally dynamic segment, making them particularly prone to morphological deviations. The present review summarizes and systematizes the anatomical variations of the lateral, medial, and posterior cords of the brachial plexus as reported in the literature from 1918 to 2025. Variations include alterations in cord formation, atypical contributions from roots and trunks, absence or fusion of cords, anomalous communications between cords, and variations in terminal branching patterns. Particular attention is given to deviations in the segmental composition and structural organization of the cords. Understanding these variations is essential for accurate anatomical interpretation and for preventing iatrogenic injury during surgical and anesthetic procedures involving the axillary region. This review aims to provide a morphological overview of cord variations and to contribute to the field of variation anatomy.

Key words: Brachial plexus; anatomical variations; lateral cord; medial cord; posterior cord

Introduction

Anatomical variability is a well-recognized phenomenon in human morphology. Although classical anatomical descriptions present a standardized structural pattern,

numerous deviations from the classical configuration occur during embryological development. These anatomical variations are generally non-pathological and present at birth, yet they may significantly influence surgical approaches, regional anesthesia, and the interpretation of neurological deficits.

The brachial plexus is one of the most complex peripheral nerve networks in the human body. Due to its intricate developmental formation and segmental organization, it exhibits a broad spectrum of anatomical variations. While many studies have described variations of the roots and trunks, relatively less systematic attention has been directed specifically toward the cords of the brachial plexus.

The cords — lateral, medial, and posterior — represent the infraclavicular portion of the plexus and serve as the origin of the major terminal branches supplying the upper limb. Variations in their formation, fiber composition, and branching pattern may alter the classical anatomical relationships around the axillary artery.

A structured literature search was conducted using PubMed and Scopus databases covering the period from 1918 to 2025. The following keywords and combinations were used: “brachial plexus”, “cords”, “lateral cord”, “medial cord”, “posterior cord”, “anatomical variation”, “infraclavicular” and “infraclavicular block”.

Inclusion criteria comprised cadaveric studies and case reports describing variations of the brachial plexus cords. Studies focusing exclusively on roots, trunks, or divisions without cord-level analysis were excluded unless relevant to infraclavicular organization.

Additional sources were identified through manual screening of reference lists of selected articles.

The aim of the present review is to analyze and systematize the anatomical variations of the cords of the brachial plexus reported in the literature, with particular emphasis on their morphological patterns, structural classification, and clinical relevance to infraclavicular block.

Anatomical Variations

During embryological development, structural variations may arise in individual anatomical components. It has long been recognized in anatomical science that the human body exhibits a spectrum of morphological deviations from the most commonly described structural pattern, commonly referred to as anatomical variation [39]. An anatomical variation represents a normally developed body structure whose morphological characteristics differ from the classical description and from the configuration observed in the majority of individuals.

Such variations may involve a wide range of anatomical structures, including muscles, ligaments, vascular branches, and nerves, and may extend to entire neural networks such as the brachial plexus [3]. In most cases, these variations are congenital and present at birth. They are generally non-pathological and do not significantly impair function.

Despite their non-pathological nature, anatomical variations possess considerable clinical relevance. They may influence diagnostic interpretation, modify surgical

landmarks, and necessitate adapted clinical approaches during interventional or anesthetic procedures [35]. For this reason, variation anatomy represents an important field within the morphological sciences, aiming to identify, document, and systematize deviations in human structural organization.

Variations are frequently encountered during surgical interventions and radiological examinations, where unexpected anatomical configurations may complicate clinical management. Therefore, knowledge of variation anatomy is essential not only for anatomists but also for clinicians. In a study conducted in 2015, Raikos and Smith [33] reported that clinicians encounter anatomical variations regularly in practice — monthly (39%), weekly (25%), and even daily (21%), underscoring their practical significance.

Normal Anatomy of the Brachial Plexus

The brachial plexus is a complex neural network responsible for the motor and sensory innervation of the upper limb [40]. It is classically formed by the ventral rami of the spinal nerves C5, C6, C7, C8, and T1 [5]. In certain cases, additional contribution from C4 results in a prefixed brachial plexus, whereas participation of T2 defines a postfixed brachial plexus [29].

The ventral rami unite to form three trunks: the superior, middle, and inferior trunks. The superior trunk is formed by the ventral rami of C5 and C6; the middle trunk represents the continuation of the ventral ramus of C7; and the inferior trunk is formed by the ventral rami of C8 and T1 [23, 40].

Each trunk divides into anterior and posterior divisions. These divisions reorganize in the infraclavicular region to form three cords, which are named according to their relationship to the axillary artery: the lateral cord, medial cord, and posterior cord [40].

The lateral cord is formed by the anterior divisions of the superior and middle trunks and typically contains fibers from C5–C7. The medial cord arises from the anterior division of the inferior trunk and contains fibers from C8–T1. The posterior cord is formed by the posterior divisions of all three trunks and therefore contains fibers from C5–T1 [30].

Topographically, the brachial plexus is divided into supraclavicular (roots and trunks) and infraclavicular (divisions and cords) parts. The cords are located in the infraclavicular region and surround the axillary artery [28].

The lateral cord gives rise to the lateral pectoral nerve, the musculocutaneous nerve, and the lateral root of the median nerve. The medial cord gives rise to the medial pectoral nerve, the medial cutaneous nerve of the arm, the medial cutaneous nerve of the forearm, the ulnar nerve, and the medial root of the median nerve. The posterior cord gives rise to the subscapular nerves, the thoracodorsal nerve, the axillary nerve, and the radial nerve.

The schematic representation of the normal anatomy of the brachial plexus is shown in **Figure 1**.

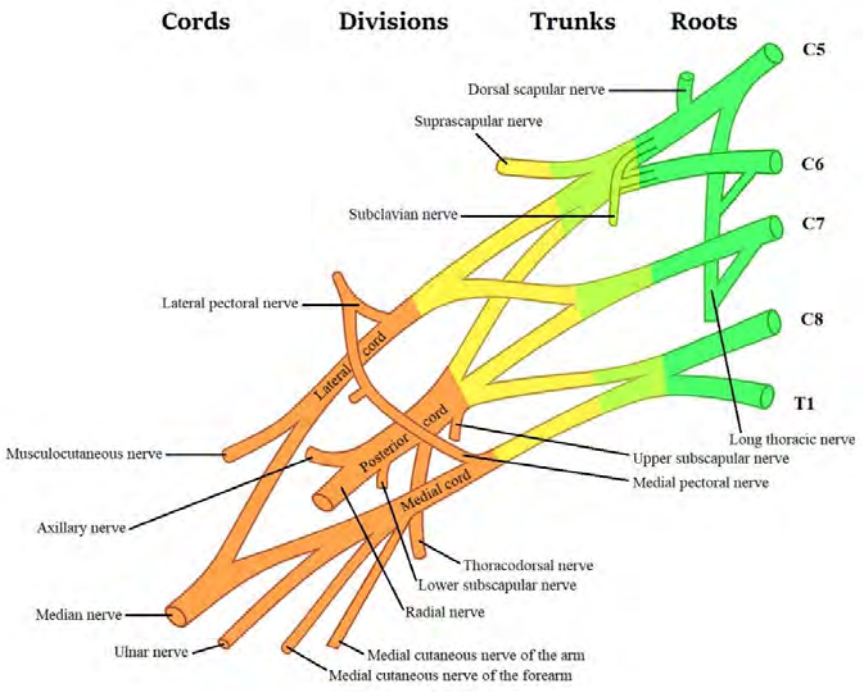

Fig. 1. Schematic representation of the normal anatomy of the brachial plexus. Modified from Wikimedia Commons, licensed under CC BY-SA 4.0.

Classification of Brachial Plexus Variations

The brachial plexus represents a hierarchically organized neural structure composed of roots, trunks, divisions, cords, and terminal branches. Variations may occur at any **level** of th**is** anatomical **organization**. From a structural perspective, brachial plexus variations can therefore be categorized into five principal groups:

(1) root variations;
(2) trunk variations;
(3) division variations;
(4) cord variations;
(5) terminal nerve variations.

While such a level-based classification provides a general anatomical framework, more detailed **classifications have** been proposed specifically for **patterns of cord formation.**

Cord-Level Classification According to Benes et al. (2021) **[6]**

A comprehensive meta-analysis conducted by Benes et al. (2021) identified six principal subtypes of variation in the formation of the brachial plexus cords from the anterior and posterior divisions of the trunks:

1. Standard cord formation pattern

• Classical configuration with three cords formed in the usual manner.

2. Rearranged merging of divisions

• Abnormal redistribution or splitting of anterior/posterior divisions leading to atypical cord composition. This includes:

• Splitting of the anterior division of the middle trunk with contributions to both lateral and medial cords.

• Absence of contribution of the anterior division of the middle trunk to the lateral cord.

• Absence of contribution of the posterior division of the inferior trunk to the posterior cord.

• Abnormal participation of the posterior division of the superior trunk in medial cord formation.

3. Variations in trunk number with preservation of three cords

• Altered number of trunks (two or four trunks) with subsequent formation of three anatomically recognizable cords.

4. Qualitative changes in cord configuration

• Structural reorganization such as:

• Single common cord,

• Two-cord configuration (anterior and posterior),

• Temporary fusion of cords with subsequent separation,

• Post-formation splitting of the posterior cord.

5. Absence of cord formation

• Partial or complete failure of cord development, with divisions continuing directly as terminal nerves.

6. Unclassified or rare patterns

• Variants not fitting into the above categories.

This meta-analytic classification provides a structured framework for understanding variability **in cord formation** and highlights the considerable morphological plasticity of the infraclavicular brachial plexus.

Scope of the Present Review

The present review focuses exclusively on cord-level variations, analyzing published cases in relation to:

• alterations in cord formation,

• **changes in** segmental composition,

• topographic deviations relative to the axillary artery,

• intercord communications, and

• variations in branching patterns.

By adopting a morphology-oriented analytical approach, this review aims to expand upon existing classifications and to integrate developmental and clinical perspectives into cord-level variations.

Embryological Basis of Variations of the Brachial Plexus

The development of the brachial plexus begins during the fourth week of embryogenesis, when motor axons emerging from the ventral horns of the spinal cord extend toward the developing upper limb bud. Shortly thereafter, sensory fibers from the dorsal root ganglia join these motor axons, forming the primitive neural network that later differentiates into the definitive brachial plexus [5, 10].

Plexus formation involves sequential processes of axonal growth, redistribution, fusion, and separation. Initially, ventral rami establish a primitive neural meshwork, directing fibers toward the dorsal and ventral muscle masses of the developing limb. From this early arrangement arise the anterior and posterior divisions of the trunks, followed by secondary reorganization into the three cords.

The patterning of this neural network is regulated by highly coordinated molecular signaling between mesenchymal cells and axonal growth cones. Axonal extension is guided by the expression of chemoattractant and chemorepellent molecules in a spatially and temporally controlled manner. Disruptions in these signaling pathways may alter axonal trajectory and fiber redistribution, resulting in variations in trunk division or cord formation [9, 34].

Following initial formation, selective apoptosis and remodeling of transient neural connections occur. Some early embryonic communications regress, whereas others persist. Persistence of such temporary connections may explain accessory roots of the median nerve, atypical intercord communications, or abnormal segmental participation within specific cords. Once established, these anatomical variations persist after birth [9].

Vascular development in the axillary region may further influence plexus organization. Variations in the formation of the axillary vessels can mechanically affect fusion patterns and spatial relationships between plexus components [40].

From an evolutionary perspective, the organization of the brachial plexus demonstrates considerable phylogenetic plasticity. Lower vertebrates lack a clearly defined trunk-and-cord arrangement, whereas primates exhibit progressive structural specialization. This evolutionary variability may partly account for the relatively high frequency of brachial plexus variations in humans.

Thus, variations in cord formation may be attributed to:

- Alterations in axonal migration and guidance signaling
- Persistence of transient embryonic neural connections
- Atypical trunk fusion or division
- Vascular developmental influences
- Evolutionary morphological variability.

The embryological complexity of this secondary reorganization stage explains why the cords of the brachial plexus demonstrate considerable morphological variability.

Anatomical Variations of the Brachial Plexus Cords

1. Variations of the Lateral Cord

The lateral cord demonstrates considerable variability in its formation, segmental composition, intercord communications, branching pattern, and topographic relations.

Early documentation of lateral cord anomalies dates back to Kerr (1918), who reported absence and atypical configurations of the lateral cord in his large anatomical series [19].

1.1. Variations in Formation

Altered formation of the lateral cord is among the most frequently described infraclavicular variations. Uysal et al. [41], in a fetal series, described cases in which the lateral cord was formed solely from the anterior division of the superior trunk, without contribution from the middle trunk. **This is presented in Figure 2.** Similar observations were reported by Wozniak et al. [44], who identified several plexuses in which the lateral cord was formed only by the anterior division of the superior trunk. In such cases, the typical C7 contribution through

the middle trunk is absent, resulting in altered segmental distribution to the musculocutaneous nerve and the lateral root of the median nerve.

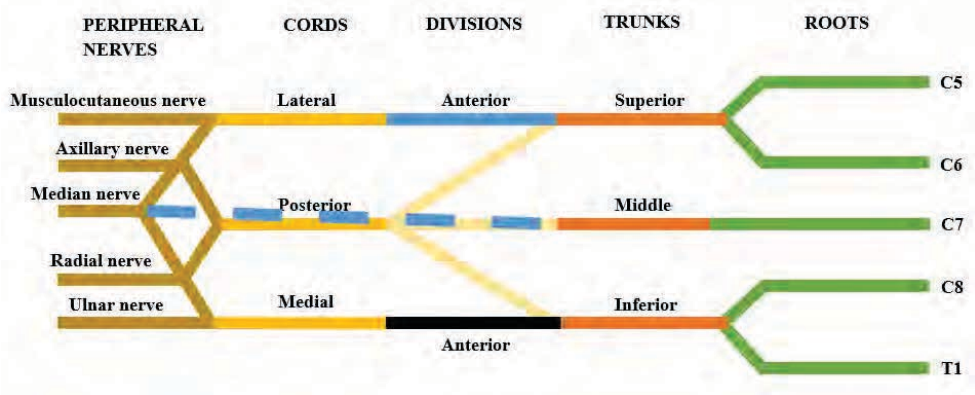

Fig. 2. Formation of the lateral cord from the anterior division of the superior trunk, without contribution from the anterior division of the middle trunk.

More complex rearrangements of cord formation have also been described. Uysal et al. [41] reported a case in which the inferior trunk divided into two anterior and two posterior branches; one anterior and one posterior branch united to form the medial cord, whereas the remaining anterior branch joined the lateral cord and the remaining posterior branch contributed to the posterior cord. This configuration illustrates marked redistribution of fibers between the cords and modification of the classical infraclavicular architecture. This is presented in **Figure 3**.

Failure of superior trunk formation may further alter lateral cord development. In two plexuses described by Uysal et al. [41], the ventral rami of C5 and C6 did not unite into a superior trunk; instead, they divided independently, with the posterior components contributing to the posterior cord and the anterior components joining to form the lateral cord. This arrangement bypasses the classical trunk–division–cord sequence while preserving the expected segmental origin of the fibers. **This is presented in Figure 4.**

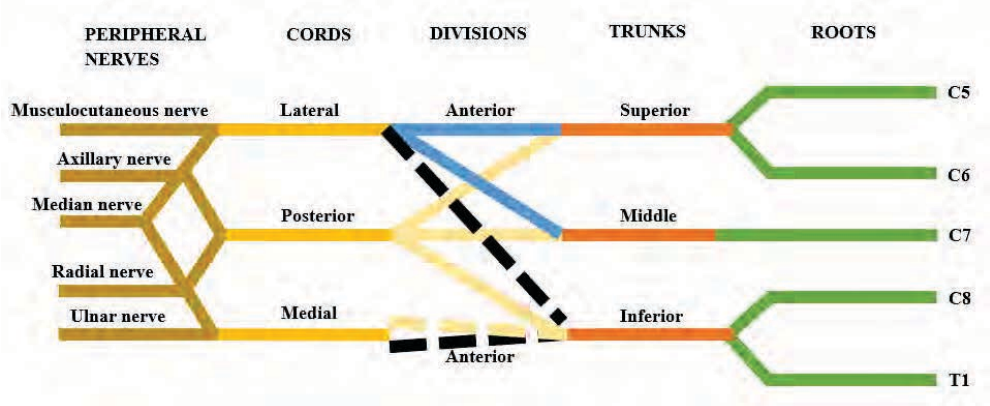

Fig. 3. Formation of the medial cord from one anterior and one posterior branch of the inferior trunk; lateral cord from the anterior branch and anterior divisions of the superior and middle trunks; posterior cord from the posterior branch of the inferior trunk and posterior divisions of the superior and middle trunks.

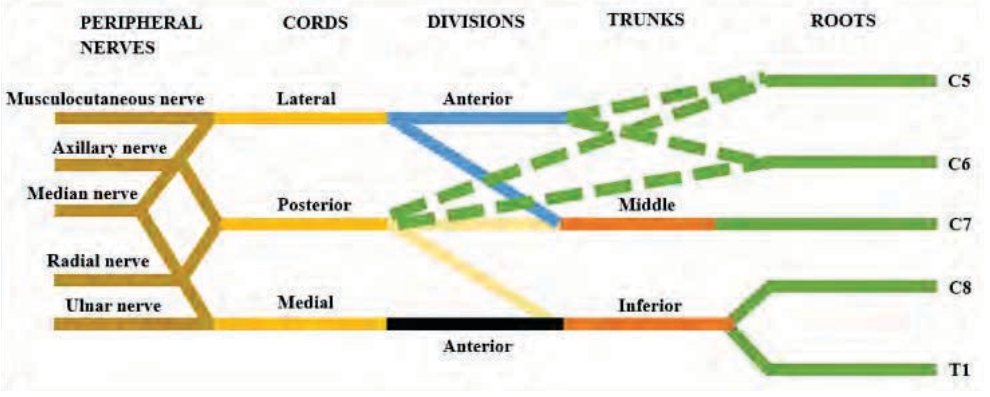

Fig. 4. Lateral cord formed by the anterior components of C5 and C6 ventral rami; posterior cord formed by the posterior components of C5 and C6. Superior trunk is absent.

Large cadaveric studies also support the variability of lateral cord formation. Pandey and Shukla [25], in a series of 172 brachial plexuses, documented abnormal cord formation and location in a notable proportion of specimens, reinforcing the morphological diversity of the infraclavicular plexus.

1.2. Variations in Segmental Contribution

Segmental alterations may significantly affect the fiber composition of the lateral cord. Proximal prefixation has been described, including direct participation of C4 in the superior trunk and subsequent contribution to the lateral cord. Uysal et al. [41] reported a rare case (0.5%) in which the superior trunk was formed by C4 and C5, while C6 divided independently and contributed directly to cord formation. **This is presented in**

Figure 5. Wozniak et al. [44] also described a plexus in which the lateral cord received fibers directly from C4.

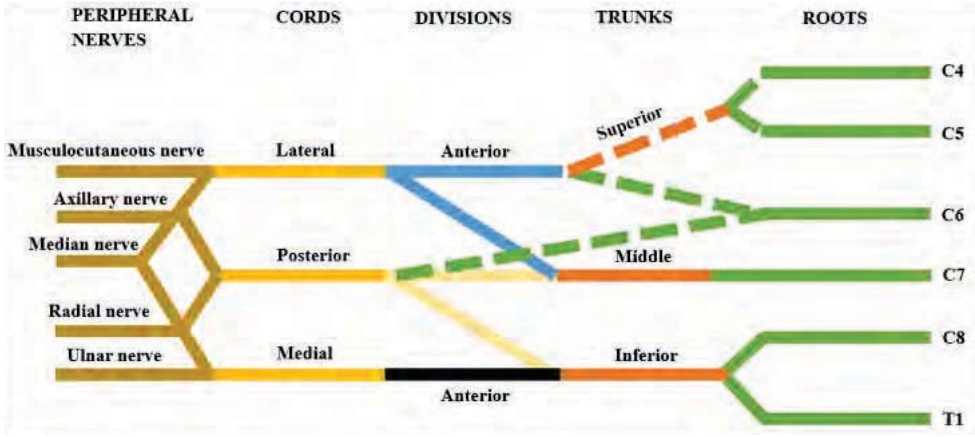

Fig. 5. Rare variant with superior trunk formed by C4–C5 and independent contribution of C6 to cord formation.

Distal postfixation and caudal fiber redistribution have likewise been documented. Prasad and Patel [31] described bilateral variations in which C8 failed to join T1 in the usual manner to form the inferior trunk; instead, C8 contributed to the anterior divisions of the superior and middle trunks, resulting in a lateral cord containing fibers from C5 to C8. **This is presented in Figure 6.** Comparable patterns were noted by Kerr [19], who reported lateral cords receiving fibers from C8 in two cases and from the inferior trunk in one case, as well as a lateral cord with fibers extending from C4 to C7. Fazan et al. [13] also noted segmental redistribution associated with atypical posterior cord formation. Such changes may alter the functional distribution of fibers within lateral cord derivatives and may influence the clinical presentation of plexus lesions.

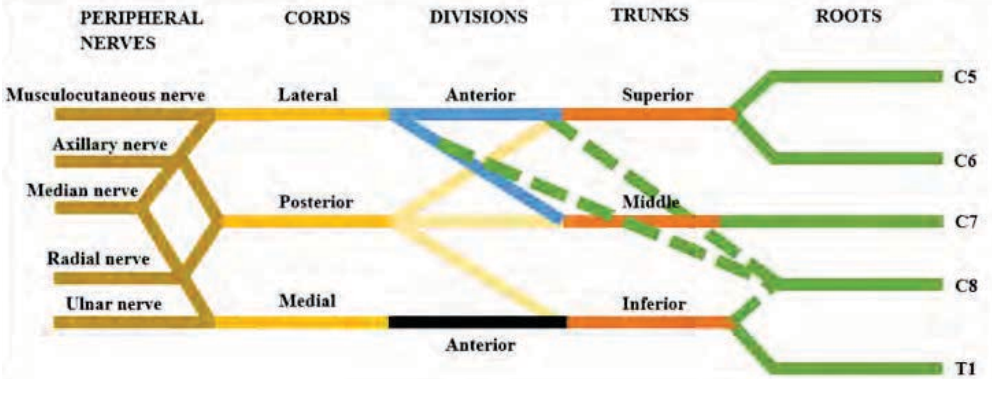

Fig. 6. Variation with C8 bypassing T1, contributing to anterior divisions of superior and middle trunks, forming a lateral cord containing C5–C8 fibers.

Additional rearrangement of middle trunk fibers has also been reported. Uysal et al. [41] described division of the middle trunk into two parts, with the superior portion joining the lateral root of the median nerve and the inferior portion contributing to the medial cord. Although this variant primarily affects median nerve formation, it also reflects redistribution of fibers that would normally contribute to the lateral cord system. **This is presented in Figure 7.**

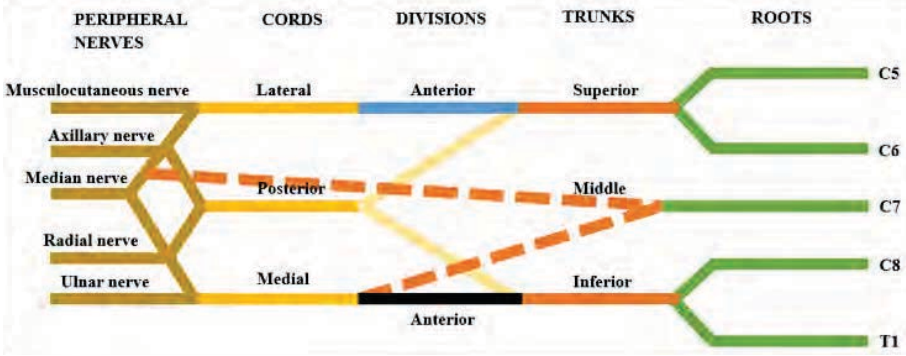

Fig. 7. Division of the middle trunk into superior and inferior portions: superior portion joins the lateral root of the median nerve, while inferior portion contributes to the medial cord, illustrating fiber redistribution that normally contributes to the lateral cord system.

1.3. Absence of the Lateral Cord

Complete absence of a morphologically distinct lateral cord has been documented. Kerr [19] reported seven cases in which the lateral cord was not observed as a separate structure. Wozniak et al. [44] described additional cases in which the anterior division of the superior trunk continued directly as the musculocutaneous nerve, effectively replacing the lateral cord as an anatomically recognizable cord. **This is presented in Figure 8.**

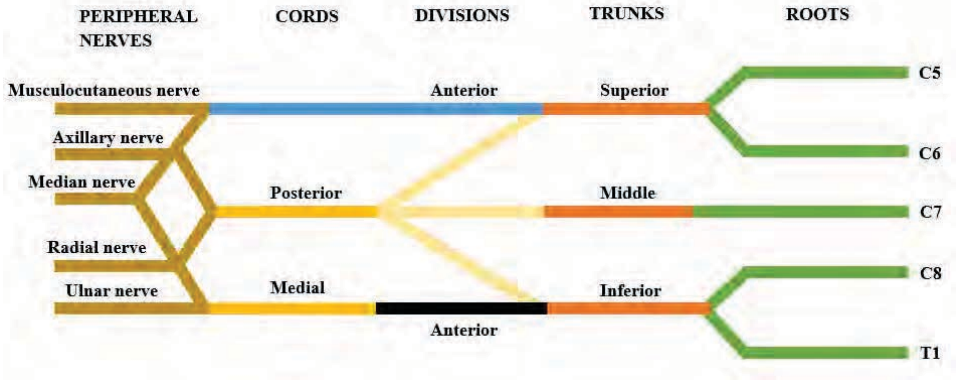

Fig. 8. Anterior division of the superior trunk continuing directly as the musculocutaneous nerve, effectively replacing the lateral cord as an anatomically distinct cord.

1.4. Intercord Communications

Intercord communications involving the lateral cord are among the most commonly reported infraclavicular variations. Wozniak et al. [44] identified the most frequent anomaly as an additional communicating branch between the lateral cord and the medial root of the median nerve, producing a double lateral root configuration; triple lateral contributions were also observed in one plexus. **This is presented in Figure 9.** Similar findings have been reported by Patel and Smit**h** [26], who described cases in which the median nerve was formed by two branches from the lateral cord and one branch from the medial cord, whereas the inverse configuration was rare.

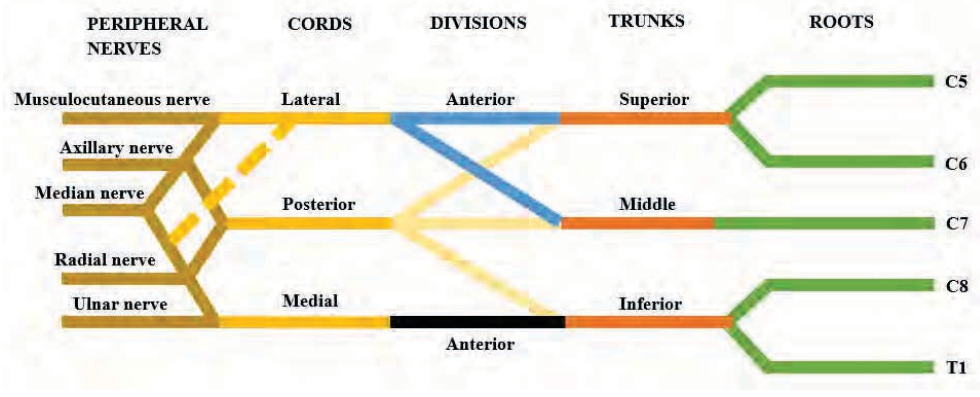

Fig. 9. Additional communicating branch between the lateral cord and the medial root of the median nerve, resulting in a double lateral root configuration.

Pattanshetti et al. [27] described accessory lateral roots of the median nerve in seven limbs (11.67%). Additional communicating branches from the lateral cord to the ulnar nerve or to the medial root of the median nerve have also been reported by Han et al. [15], who documented multiple cord-to-nerve communications in cadaveric material. Ajayi et al. [2] likewise reported a median nerve formed by two lateral roots and one medial root, further illustrating the tendency of the lateral cord to contribute accessory fibers to the median nerve.

Cross-communications and proximal fusion between the lateral and medial cords have also been documented. Malukar et Rathva [22] reported fusion of the lateral and medial cords anterior to the axillary artery, whereas Patel and Smith [26] described proximal cross-connections and fusion of the two cords before the formation of the classical “M”. Such patterns modify the expected topography of the infraclavicular part of the brachial plexus and may complicate both dissection and regional anesthesia.

1.5. Variations in Branching Pattern

Terminal organization of the lateral cord may show substantial variation. Pattanshetti et al. [27] reported absence of the musculocutaneous nerve in four limbs (6.67%), as well as frequent accessory lateral roots of the median nerve. Gupta et al. [14] described

a case in which the anterior division of the middle trunk gave rise to a branch to the coracobrachialis muscle together with an accessory lateral root of the median nerve, functionally approximating middle trunk fibers to lateral cord derivatives.

Han et al. [15] reported cases in which the medial root of the median nerve was absent. In those specimens, the lateral cord divided into the musculocutaneous nerve and a lateral root component, which fused with the medial cord and then bifurcated into the median and ulnar nerves. These patterns emphasize the close developmental relationship between lateral cord formation and median nerve organization.

1.6. Topographic Variations

Topographic deviations relative to the axillary artery have also been documented. Das et Paul [11] described anomalous branches of the lateral cord passing anterior to the axillary artery, a relationship of possible compressive and surgical significance. Malukar et Rathva [22] reported fusion of the lateral and medial cords located anterior to the artery, and in some cases all three cords were positioned lateral to the axillary artery. **This is presented in Figure 10.** Similar positional changes have been described in anomalous two-cord or fused-cord configurations [20].

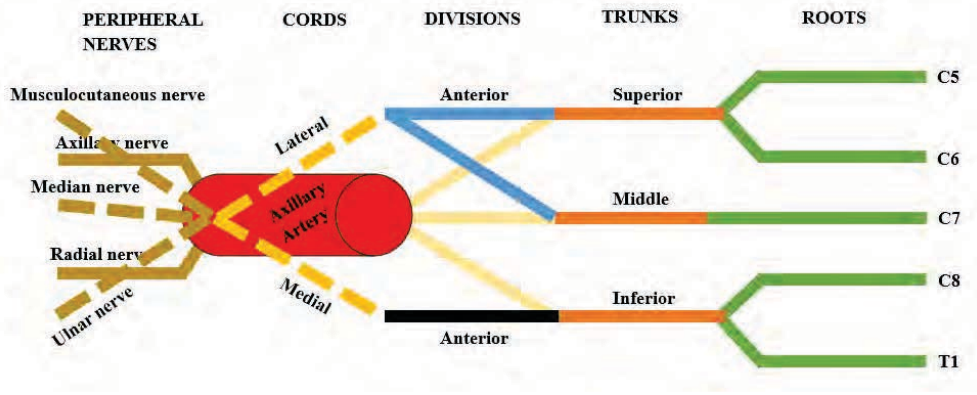

Fig. 10. Fusion of the lateral and medial cords located anterior to the axillary artery

Collectively, these findings indicate that the lateral cord demonstrates marked morphological plasticity, particularly in relation to its formation, segmental contribution, and communications with the medial cord.

2. Variations of the Medial Cord

The medial cord is traditionally described as the continuation of the anterior division of the inferior trunk and normally contains fibers from C8 and T1. Although it is generally considered to be more stable than the lateral and posterior cords, several structural deviations have been documented.

2.1. Variations in Formation

Alterations in the classical formation pattern of the medial cord have primarily been described in fetal and cadaveric series. Uysal et al. [41] reported cases in which a branch from the anterior division of the middle trunk contributed to the formation of the medial cord, thereby introducing C7-derived fibers into a cord that is classically formed by C8–T1. This atypical participation expands the segmental composition of the medial cord beyond its usual pattern. **This is presented in Figure 11.**

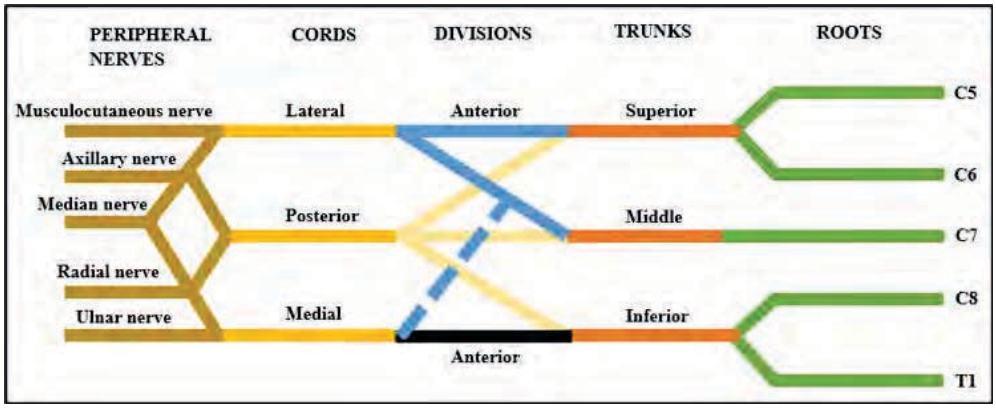

Fig. 11. Contribution of a branch from the anterior division of the middle trunk to the medial cord, introducing C7 fibers into a cord normally formed by C8–T1.

More complex rearrangements have also been described. In one fetal plexus reported by Uysal et al. [41], the inferior trunk divided into two anterior and two posterior branches; one anterior and one posterior branch united to form the medial cord, whereas the remaining anterior branch joined the lateral cord and the remaining posterior branch contributed to the posterior cord. This pattern reflects profound redistribution of fascicles between the cords and a substantial departure from the normal infraclavicular organization.

2.2. Variations Associated with Absence or Reorganization of the Inferior Trunk

Because the medial cord is classically derived from the anterior division of the inferior trunk, anomalies affecting inferior trunk formation directly alter medial cord morphology. Uysal et al. [41] described 18 plexuses (9%) in which the inferior trunk failed to form; under these conditions, the ventral ramus of C8 divided independently, with its posterior part joining the posterior cord and its anterior part uniting with T1 to form the medial cord. This represents a direct root-level reorganization of C8–T1 fibers without an intervening inferior trunk**. This is presented in Figure 12.**

Additional caudal rearrangements have also been documented. In a rare case described by Uysal et al. [41], the inferior trunk was formed by T1 and T2, whereas C8 divided and contributed separately to the medial and posterior cords. **This is presented in Figure 13.** Aragão et al. [4] likewise reported a four-trunk configuration in a fetal plexus in which the medial cord was formed by the anterior divisions of C8 and T1, while the posterior cord received fibers from all posterior divisions. These variants

alter the segmental composition of the medial cord and may influence the clinical expression of lower plexus lesions.

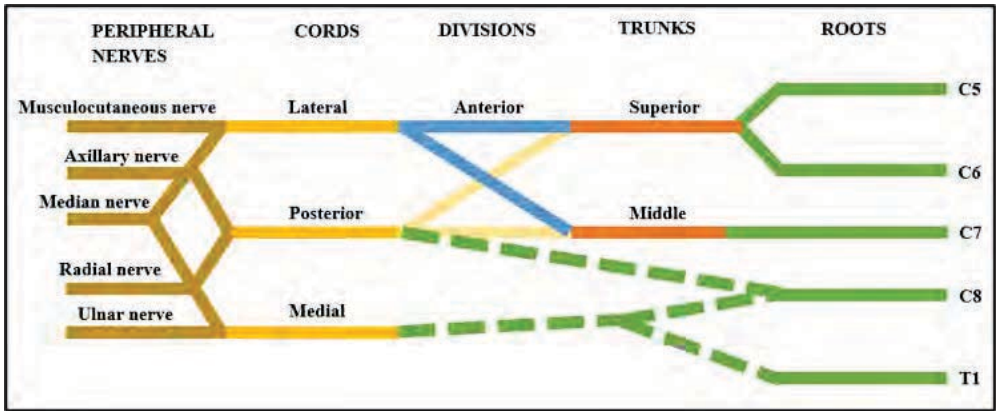

Fig. 12. Absence of the inferior trunk: C8 ventral ramus divides independently, with its posterior part joining the posterior cord and anterior part uniting with T1 to form the medial cord, representing direct root-level reorganization of C8–T1 fibers.

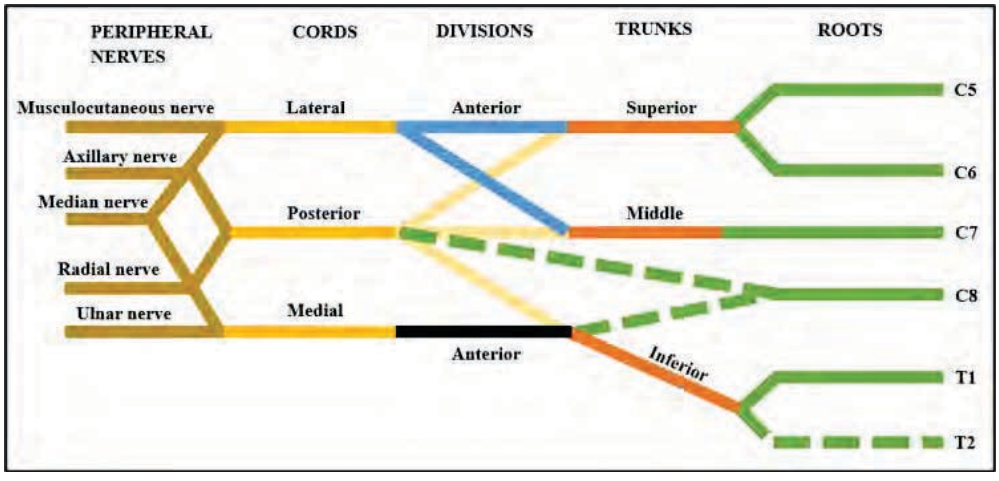

Fig. 13. Inferior trunk formed by T1 and T2, with C8 dividing independently to contribute to the medial and posterior cords.

Prasad and Patel [31] described a bilateral variation in which C8 did not join T1 in the usual manner. On one side, the medial cord was formed mainly by T1 with a minor contribution from C8, whereas on the opposite side T1 fibers passed directly into the medial cord without forming a conventional inferior trunk. Similar patterns were later described by Mchonde et al. [**24**], who reported bilateral multiple variations in which the inferior trunk was effectively represented by T1 alone and continued as the medial cord.

2.3. Redistribution of Middle Trunk Fibers

Uysal et al. [41] further described division of the middle trunk into two portions, with the superior portion joining the lateral root of the median nerve and the inferior portion contributing to the medial cord. This configuration demonstrates simultaneous fascicular and terminal reorganization and shows that fibers usually associated with the lateral cord system may be redistributed to the medial cord.

2.4. Stability and Prevalence

Despite these variants, the medial cord appears comparatively stable. In his extensive anatomical material, Kerr [19] reported that the medial cord was present in all examined plexuses and that in 99.46% of cases it was formed predominantly by the anterior division of the inferior trunk; only two cases showed additional contribution from another division.

Across major cadaveric series, anomalies of the medial cord are reported less frequently than posterior cord variations, reinforcing its relatively consistent anatomical pattern.

2.5. Variations in Relation to the Median Nerve

Terminal organization of the medial cord may also vary. Pattanshetti et al. [27] reported two limbs (3.33%) in which the medial root of the median nerve did not arise from the classical medial cord. Instead, it originated from the first part of the anterior division of fused middle and inferior trunks, whereas the second part functioned as the medial cord proper and gave rise to its remaining branches. **This is presented in Figure 14.**

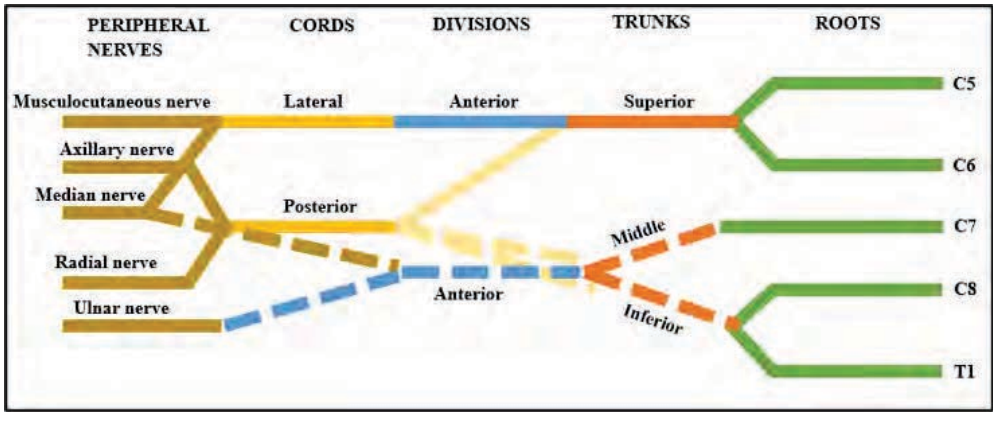

Fig. 14. Medial root of the median nerve originating from the anterior division of fused middle and inferior trunks, while the remaining portion functions as the medial cord proper, illustrating variation in terminal organization of the medial cord.

Han et al. [15] described cases in which the medial root of the median nerve was absent, and the lateral root component fused with the medial cord before dividing into the median and ulnar nerves. Patel and Smith [26] also reported rare cases in which the median nerve received two branches from the medial cord and only one from the

lateral cord, further illustrating variability in the contribution of the medial cord to median nerve formation.

Overall, the medial cord demonstrates comparatively limited variability, with most deviations related to altered inferior trunk formation, redistribution of C8–T1 fibers, and variant participation in median nerve organization.

3. Variations of the Posterior Cord

The posterior cord represents one of the most frequently involved components in infraclavicular variations of the brachial plexus. Most anomalies involve altered contributions of posterior divisions, absence of inferior trunk participation, proximal displacement of branches, duplication or splitting patterns, or reduction of the posterior cord as a distinct morphological entity.

3.1. Variations in Formation

Historical observations by Kerr [19] demonstrated that in 36 of 175 plexuses (20.57%), a true posterior cord was not clearly identifiable unless the radial nerve was regarded as its representative. This early finding illustrates reduction or indistinct formation of the posterior cord as a separate anatomical structure.

A recurring pattern reported in multiple studies is formation of the posterior cord solely from the posterior divisions of the superior and middle trunks, without contribution from the inferior trunk. **This is presented in Figure 15.** Wozniak et al. [44] described this arrangement in four plexuses, and Fazan et al. [13] reported the same configuration in five plexuses (9%), all from male Black cadavers. Singh et al. (2019) [36] likewise observed five plexuses in which the posterior cord was formed by the posterior divisions of the superior and middle trunks alone. Similar configurations were also noted by Priya et al. and by Mchonde et al. [32, 24], in whom the inferior trunk continued as the medial cord without contributing to the posterior cord.

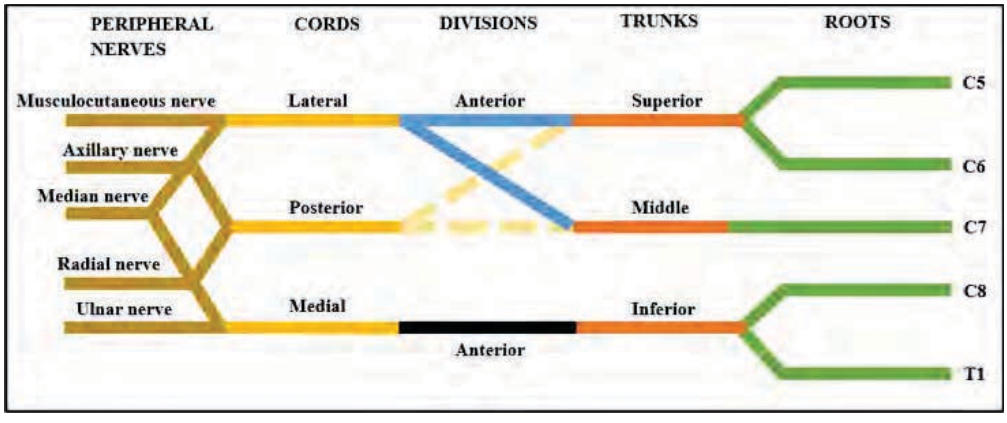

Fig. 15. Posterior cord formed solely from the posterior divisions of the superior and middle trunks, without contribution from the inferior trunk.

Failure or reorganization of trunk formation may further modify posterior cord assembly. Uysal et al. [41] described 18 plexuses in which the inferior trunk did not form; in these cases, the posterior part of C8 joined the posterior cord directly. In additional cases, failure of superior trunk formation led to independent division of C5 and C6, with their posterior components contributing to the posterior cord. Uysal et al. [41] also reported a rare prefixation pattern in which the superior trunk was formed by C4 and C5, while the posterior division of C6 contributed directly to the posterior cord.

More complex rearrangements of trunk organization have also been described. Singh [37] reported cases in which the superior and middle trunks fused into a common trunk that later divided into lateral and posterior cords, whereas the inferior trunk continued as the medial cord. **This is presented in Figure 16.** In related cases, the inferior trunk failed to divide into anterior and posterior divisions and continued directly as the medial cord, leaving the posterior cord to be formed only by posterior divisions of the superior and middle trunks [20, 37]. Cash et al. [8] described a two-trunk variation in which the posterior cord was formed by the posterior divisions of the superior and inferior trunks, reflecting the altered architecture of a two-trunk brachial plexus.

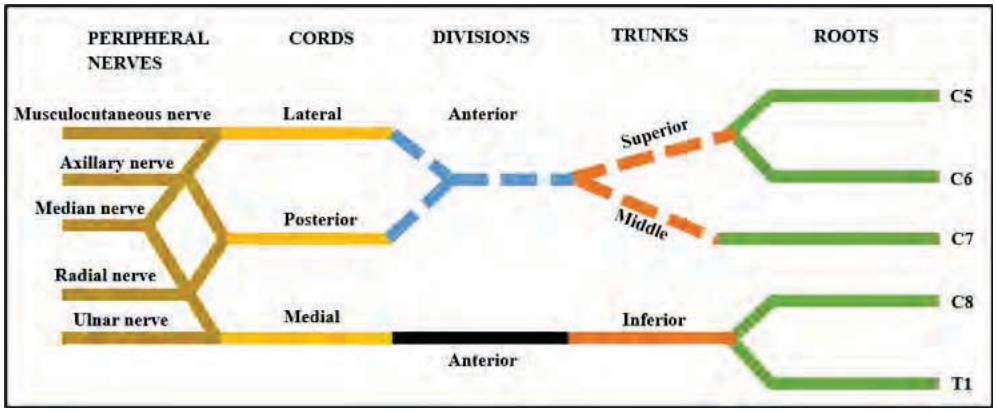

Fig. 16. Fusion of the superior and middle trunks into a common trunk, which divides into lateral and posterior cords, while the inferior trunk continues as the medial cord.

Four-trunk configurations further expand the spectrum of posterior cord variation. Aragão et al. [4] reported a fetal case in which C4–C5, C7, C8, and T1 formed four trunks, and the posterior cord was assembled from the posterior divisions of all participating trunks. Han et al. [15] likewise described several four-trunk patterns, including cases in which the posterior cord was formed by the posterior divisions of three trunks and others in which all four trunks contributed to it.

An extreme variant was reported by Elzawawy [12], in which the posterior cord was effectively replaced by the posterior division of the superior trunk; this branch gave rise to the axillary and upper subscapular nerves and continued as the radial nerve. This represents near-complete proximal substitution of the posterior cord. **This is presented in Figure 17.**

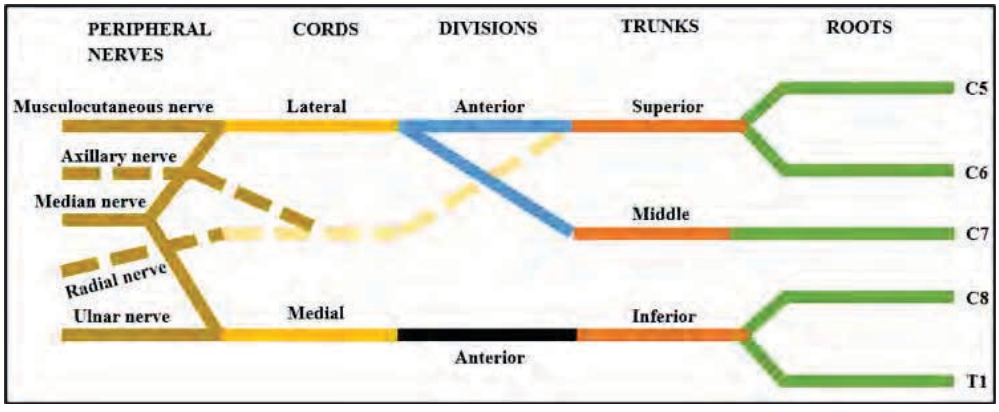

Fig. 17. Posterior cord effectively replaced by the posterior division of the superior trunk, giving rise to the axillary and upper subscapular nerves and continuing as the radial nerve, representing near-complete proximal substitution of the posterior cord.

3.2. Split or Duplicated Posterior Cord Patterns

A distinct morphological variation involves splitting of the posterior cord into two roots that subsequently reunite to form the radial nerve. Bhat and Girijavallabhan (2008) [7] described such a configuration, in which the two roots compressed the subclavian artery before reuniting. **This is presented in Figure 18.** Pattanshetti et al. [28] observed a similar two-root radial origin pattern in one limb (1.67%). These variants are of potential surgical relevance because of their unusual relationship to neighboring vessels.

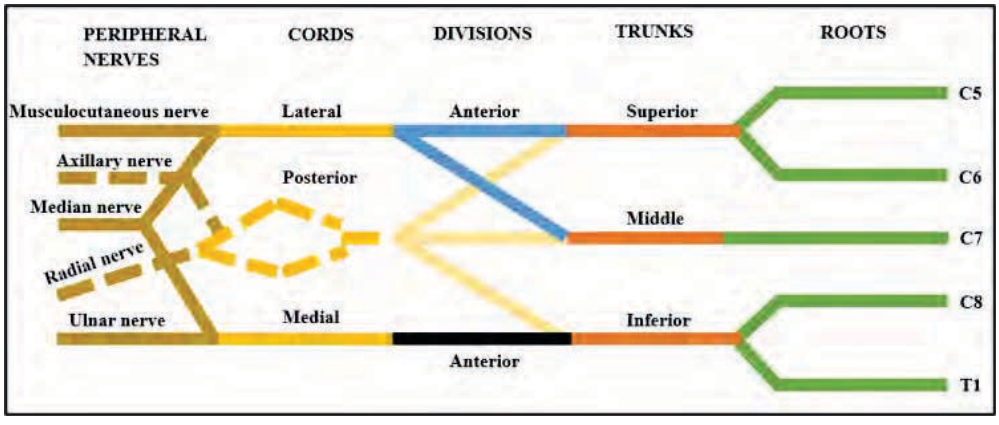

Fig. 18. Two roots of the posterior cord compressing the subclavian artery before reuniting, illustrating a split or duplicated posterior cord configuration.

3.3. Proximal Displacement of Posterior Cord Branches

Several reports describe branches that normally arise from the posterior cord as originating instead from the posterior division of the superior trunk. Kocabiyik et

al. [21] reported a case in which the upper subscapular, thoracodorsal, and lower subscapular nerves arose from the posterior division of the superior trunk, after which the posterior cord continued as the axillary and radial nerves. A similar pattern was noted by Pattanshetti et al. [27], in whom the axillary nerve and subscapular branches occasionally arose proximally from a posterior division rather than from the fully formed posterior cord. Such findings may be interpreted as a proximal shift of posterior cord branches rather than complete absence of the cord.

3.4. Associated Branch Variations and Intercord Redistribution

Branch-level anomalies related to the posterior cord include duplication of the thoracodorsal nerve, as reported by Pattanshetti et al. [27] in two limbs (3.33%), and variations in the origin of the subscapular nerves [36]. In some plexuses, posterior cord fibers also contribute aberrantly to the roots of the median nerve. Wozniak et al. [44] described one case in which two branches from the posterior cord joined the medial and lateral roots of the median nerve. Patel and Smith [26] likewise reported a rare pattern in which fusion involving the medial and posterior cords caused the median nerve to receive fibers indirectly from all three cords. These observations highlight the possibility of intercord redistribution beyond the classical pattern.

3.5. Reduction to Two-Cord or Single-Cord Patterns

More radical reorganizations include reduction of the infraclavicular plexus to two cords or even a single common cord. Han et al. [15] described a case in which only anterior and posterior cords were present, both located lateral to the axillary artery; in that specimen, the anterior cord represented fusion of the lateral and medial cords. Havaldar et al. [17] also reported a two-cord configuration in a two-trunk brachial plexus, with a superior and an inferior cord located lateral to the axillary artery.

Single-cord configurations have been documented by several authors. Priya et al. [32] reported bilateral cases in which two trunks fused and continued as a single cord giving rise to all terminal branches. Similar single-cord patterns were described by Viswanathan et al., Aggarwal et al., Singh et al., and Hasan and Narayan [42, 1, 38, 16]. Although such cases affect the entire infraclavicular plexus rather than the posterior cord alone, they are relevant because they represent the most extreme loss of normal cord differentiation and therefore include functional replacement of the posterior cord within a common neural bundle.

Taken together, these findings show that posterior cord variations are frequently part of broader system-level reorganization rather than isolated anomalies. Among the three cords, the posterior cord appears to be the most susceptible to structural rearrangement.

Collectively, the reviewed studies demonstrate considerable morphological variability in the formation and organization of the brachial plexus cords. Variations most frequently involve the posterior cord, particularly alterations in trunk contributions and proximal displacement of branches. In contrast, the medial cord appears to demonstrate relatively greater structural stability, while the lateral cord commonly participates in intercord communications and variations related to the formation of the median nerve. These findings highlight the developmental plasticity of the infraclavicular brachial plexus.

The principal patterns of cord-level anatomical variations and their clinical implications are summarized in Table 1.

Clinical relevance: Implications for Infraclavicular Block

The cords of the brachial plexus represent the principal neural targets of the infraclavicular block, as they are arranged around the second part of the axillary artery in the infraclavicular region [43]. Classical anatomical descriptions assume a predictable relationship between the lateral, medial, and posterior cords and the axillary artery. However, multiple cadaveric studies demonstrate that this arrangement is subject to considerable variability.

Variations in cord formation, position, and intercord communications may significantly influence the success and safety of infraclavicular anesthesia.

Altered topographic relationships have been described, including:

1. Fusion of lateral and medial cords
2. All three cords positioned lateral to the axillary artery
3. Posterior cord formed only from posterior divisions of the superior and middle trunks
4. Absence or reduction of a morphologically distinct cord

Such variations may modify the expected triangular or circumferential distribution of the cords around the axillary artery under ultrasound guidance. As a result, anesthetic deposition based on classical anatomical assumptions may lead to incomplete blockade, particularly if one cord lies outside the anticipated spread of local anesthetic.

Intercord communications, especially additional connections between the lateral cord and the medial root of the median nerve, may further complicate the clinical picture by producing partial or asymmetric motor blockade.

Because infraclavicular block specifically targets the cords rather than trunks or terminal branches, detailed understanding of cord-level anatomical variability is essential for optimizing needle placement, ensuring adequate anesthetic spread, and minimizing vascular or neural injury.

Conclusion

The cords of the brachial plexus demonstrate considerable anatomical variability. Reported variations include atypical formation from trunks and divisions, altered segmental contributions, absence or fusion of cords, anomalous communications between cords, and deviations in terminal branching patterns. Among the three cords, the posterior cord appears to be most frequently involved in structural rearrangements, followed by the lateral cord, while the medial cord demonstrates relatively greater stability.

These morphological deviations reflect the developmental complexity of the brachial plexus and underline the importance of variation anatomy in both

Table 1. Summary of the principal anatomical variations of the brachial plexus cords and their clinical relevance

Cord	Type of Variation	Morphological Pattern	Representative Sources	Clinical Relevance
Lateral cord	Altered formation	Formation solely from the anterior division of the superior trunk (absence of middle trunk contribution)	Uysal et al.; Wozniak et al.	Altered C7 fiber distribution; possible incomplete block
Lateral cord	Segmental variation	Contribution from atypical roots (C4 or C8) due to prefixation or postfixation	Kerr; Prasad & Patel	Atypical motor and sensory distribution
Lateral cord	Absence	Direct continuation of anterior division as musculocutaneous nerve	Kerr; Wozniak et al.	Misidentification of cord structure; procedural difficulty
Lateral cord	Intercord communication	Additional lateral roots contributing to median nerve formation	Pattanshetti et al.; Patel & Smith	Partial or asymmetric median nerve blockade
Lateral cord	Fusion pattern	Fusion with medial cord forming a common anterior cord	Malukar & Rathva	Altered infraclavicular topography
Medial cord	Altered formation	Contribution from middle trunk (C7 fibers)	Uysal et al.	Expanded segmental composition
Medial cord	Inferior trunk variation	Absence or reorganization of inferior trunk affecting cord formation	Uysal et al.; Mchonde et al.	Altered C8–T1 distribution
Medial cord	Median nerve variation	Absence or atypical origin of medial root of median nerve	Han et al.; Pattanshetti et al.	Atypical nerve formation; anesthetic variability

Table 1. Summary of the principal anatomical variations of the brachial plexus cords and their clinical relevance

Posterior cord	**Altered formation**	**Formation without contribution from posterior division of inferior trunk**	**Fazan et al.; Wozniak et al.; Singh et al.**	**Incomplete posterior cord blockade**
Posterior cord	**Reduction/ absence**	**Radial nerve replacing or representing posterior cord**	**Kerr; Elzawawy**	**Misinterpretation during surgery or dissection**
Posterior cord	**Split pattern**	**Division into two roots forming radial nerve**	**Bhat & Girijavallabhan**	**Risk of vascular compression; surgical relevance**
Posterior cord	**Proximal branching**	**Branches arising from posterior division of superior trunk**	**Kocabiyik et al.; Pattanshetti et al.**	**Altered surgical landmarks**
All cords	**Topographic variation**	**Atypical position relative to axillary artery (e.g., all cords lateral)**	**Das & Paul; Malukar & Rathva**	**Incomplete anesthetic spread; technical difficulty**
All cords	**Two-cord pattern**	**Fusion into anterior and posterior cords**	**Han et al.; Havaldar et al.**	**Modified anesthetic distribution**
All cords	**Single-cord pattern**	**Complete fusion into one common cord**	**Priya et al.; Aggarwal et al.**	**Major deviation from classical anatomy**

anatomical research and clinical practice. A thorough understanding of the possible cord configurations is essential for accurate interpretation of anatomical findings and for minimizing complications during surgical and interventional procedures in the infraclavicular region.

References

1. **Aggarwal, A., N. Puri, A. K. Aggarwal, H. Kaur, D. Sahni**. Anatomical variation in formation of brachial plexus and its branching. – *Surg. Radiol. Anat*., **32**, 2010, 891-894.
2. **Ajayi, N. O., L. Lazarus, K. S. Satyapal.** Multiple variations of the branches of the brachial plexus with bilateral connections between ulnar and radial nerves. – *Int. J. Morphol.*, **30**, 2012, 656-660.
3. **Alraddadi, A**. Literature review of anatomical variations: clinical significance, identification approach, and teaching strategies. – *Cureus*, **13**, 2021, e14451.
4. **Aragão, J. A., L. O. Melo, A. T. F. Barreto, A. T. da Silva Leal.** Variations in the formation of the trunks of the brachial plexus. – *Int. J. Morphol.*, **32**, 2014, 123-127.
5. **Bayot, M. L., A. Nassereddin, M. A. Varacallo**. Anatomy, shoulder and upper limb, brachial plexus. – *In: StatPearls. Treasure Island* (FL), StatPearls Publishing, 2023.
6. **Benes, M., D. Kachlik, M. Belbl, V. Kunc, S. Havlikova, A. Whitley, V. Kunc.** A meta-analysis on the anatomical variability of the brachial plexus: Part I – roots, trunks, divisions and cords. – *Ann. Anat*., **238**, 2021, 151751.
7. **Bhat, K. M. R., V. Girijavallabhan**. Variation in the branching pattern of posterior cord of brachial plexus. – *Neuroanatomy*, **7**, 2008, 10-11.
8. **Cash, C. A., C. Buskey, E. Boateng, A. Maklad, H. Delaviz.** A two-trunked anatomical variance of the brachial plexus: a cadaveric case report. – *Transl. Res. Anat*., **40**, 2025, 100422.
9. **Chaudhary, P., R. Singla, K. Arora, G. Kalsey.** Formation and branching pattern of cords of brachial plexus: a cadaveric study in north Indian population. – *Int. J. Anat. Res*., **2**, 2014, 225-233.
10. **Cole, P., Y. Kaufman, D. A. Hatef, L. H. Hollier**. Embryology of the hand and upper extremity. – *J. Craniofac. Surg*., **20**, 2009, 992-995.
11. **Das, S., S. Paul**. Anomalous branching pattern of lateral cord of brachial plexus. – *Int. J. Morphol.,* **23**, 2005, 289-292.
12. **Elzawawy, E. M.** The brachial plexus: more and more variations. – *Surg. Res*., **3**, 2021, 1-10.
13. **Fazan, V. P. S., A. de S. Amadeu, A. L. Caleffi, O. A. Rodrigues Filho.** Brachial plexus variations in its formation and main branches. – *Acta Cir. Bras.*, **18**, 2003, 14-18.
14. **Gupta, M., N. Goyal, Harjeet.** Anomalous communications in branches of brachial plexus. – *J. Anat. Soc. India*, **54**, 2005, 22-25.
15. **Han, Y., M. An, P. L. M. Zilundu, Z. Zhuang, J. Chen, Z. Jiang, L. Gu, J. Yang, D. Wang, D. Xu, L. Zhou**. Anatomical variations of the brachial plexus in adult cadavers: a descriptive study and clinical significance. – *Microsurgery*, **44**, 2024, e31182.
16. **Hasan, M., D. Narayan**. A single cord human brachial plexus. – *J. Anat. Soc. India,* **13**, 1964, 103-104.
17. **Havaldar, P. P., A. Gupta, H. V. Rajasekhar.** Variation in the formation of cords of brachial plexus and its relation with axillary artery. – *Curr. Neurobiol.*, **3**, 2012, 7-9.

18. **Kachlík, D., I. Varga, V. Báča, V. Musil.** Variant anatomy and its terminology. – *Medicina (Kaunas),* **56**, 2020, 713.
19. **Kerr, A. T.** The brachial plexus of nerves in man, the variations in its formation and branches. – *Am. J. Anat*., **23**, 1918, 285-395.
20. **Khan, G. A., D. Kafle, S. K. Yadav, O. Shrestha, A. Dhakal, S. K. Yadav, R. Guha.** Variation in brachial plexus formation, branching pattern and relation with major vessels.– *Int. J. Res. Med. Sci.*, **2**, 2014, 1591-1594.
21. **Kocabiyik, N., B. Yalçin, N. Candir, H. Ozan.** Re: anatomical variations of the cords of brachial plexus and the median nerve. – *Clin. Anat.*, **20,** 2007, 709; author reply 710.
22. **Malukar, O., A. Rathva.** A study of 100 cases of brachial plexus. – *Natl. J. Community Med.*, **2**, 2011, 166-170.
23. **Martinoli, C., S. Bianchi, E. Santacroce, F. Pugliese, M. Graif, L. E. Derchi.** Brachial plexus sonography: a technique for assessing root level. – *AJR Am. J. Roentgenol*., **179**, 2002, 699-702.
24. **Mchonde, G. J., F. M. Fabian, H. G. Nondoli.** Bilateral multiple variations in the formation of the brachial plexus and its terminal nerves: a case report. – *Int. J. Anat. Res.,* **1**, 2013, 78-82.
25. **Pandey, S. K., V. K. Shukla.** Anatomical variations of the cords of brachial plexus and the median nerve. – *Clin. Anat.*, **20**, 2007, 150-156.
26. **Patel, N. T., H. F. Smith.** Clinically relevant anatomical variations in the brachial plexus. – *Diagnostics (Basel)*, **13**, 2023, 830.
27. **Pattanshetti, S. V., P. S. Jevoor, V. S. Shirol, D. Dixit, S. Bhimalli.** A study of the formation and branching pattern of brachial plexus and its variations in adult human cadavers of north Karnataka. – *J. Sci. Soc.*, **39**, 2012, 70-77.
28. **Paulsen, F., T. M. Böckers, J. Waschke**. *Sobotta Anatomy Textbook*: English Edition with Latin Nomenclature. 1st ed. Munich, Elsevier (Urban & Fischer), 2018.
29. **Pellerin, M., Z. Kimball, R. S. Tubbs, M. Loukas.** The prefixed and postfixed brachial plexus: a review with surgical implications. – *Surg. Radiol. Anat.*, **32,** 2010, 251-260.
30. **Polcaro, L., M. Charlick, D. T. Daly.** Anatomy, head and neck: brachial plexus. – *In: StatPearls. Treasure Island (FL)*, StatPearls Publishing, 2023.
31. **Prasad, S., P. K. Patel.** Study of brachial plexus with regards to its formation, branching pattern and variations and possible clinical implications of those variations. – *IOSR J. Dent. Med. Sci.*, **15**, 2016, 23-28.
32. **Priya, A., C. Gupta, A. S. D'Souza.** Cadaveric study of supraclavicular part of brachial plexus. – *Int. J. Anat. Radiol. Surg.,* **7**, 2018, 41-44.
33. **Raikos, A., J. D. Smith.** Anatomical variations: how do surgical and radiology training programs teach and assess them in their training curricula? – *Clin. Anat.*, **28**, 2015, 717-724.
34. **Sanes, D. H., T. A. Reh, W. A. Harris.** *Development of the Nervous System*. San Diego, Academic Press, 2000.
35. **Sañudo, J., R. Vázquez, J. Puerta.** Meaning and clinical interest of the anatomical variations in the 21st century. – *Eur. J. Anat.*, **7**, 2003, 1-4.
36. **Singh, B. R., A. Sawal, U. Gajbe.** A study to evaluate the variations in brachial plexus and its correlates as observed among adult male and female cadavers of teaching institutes. – *Int. J. Sci. Res*., **8**, 2019, 57-58.
37. **Singh, R.** Variations of cords of brachial plexus and branching pattern of nerves emanating from them. – J. *Craniofac. Surg.*, **28**, 2017, 543-547.

38. **Singh, R., R. S. Tubbs, Raj Kumar.** Abnormal cord formation of brachial plexus. – *Basic Sci. Med.*, **5**, 2016, 1-4.
39. **Smith, H. F.** Anatomical variation and clinical diagnosis. – *Diagnostics (Basel),* **11**, 2021, 247.
40. **Standring, S.** *Gray's Anatomy: The Anatomical Basis of Clinical Practice.* 39th ed. Edinburgh, Elsevier Churchill Livingstone, 2005.
41. **Uysal, I. I., M. Seker, A. K. Karabulut, M. Büyükmumcu, T. Ziylan.** Brachial plexus variations in human fetuses. – *Neurosurgery*, **53**, 2003, 676-684.
42. **Viswanathan, U., V. Madhivadhany, N. Shankar.** Bilateral single cord of the brachial plexus in an adult female cadaver of South Indian origin. – *Anat. Cell Biol.,* **46**, 2013, 223-227.
43. **Williams, L. M., K. Singh, A. Dua, A. Singh, A. Cummings.** Infraclavicular nerve block. – *In: StatPearls. Treasure Island (FL)*, StatPearls Publishing, 2023.
44. **Wozniak, J., A. Kedzia, K. Dudek.** Brachial plexus variations during the fetal period. – *Anat. Sci. Int*., **87**, 2012, 223-233.

Institute of Experimental Morphology, Pathology and Anthropology with Museum
Bulgarian Anatomical Society

Acta Morphologica et Anthropologica, 33 (1-2)
Sofia ● 2026

Women‘s Invaluable Contribution in the Development of Anatomical Knowledge and Education through the Centuries

*Desislava Marinova, Stefan Trifonov**

Department of Anatomy, Histology, Cytology and Biology, Faculty of Medicine, Medical University – Pleven, Pleven, Bulgaria

* Corresponding author e-mail: stefantrifonov@outlook.com

Stereotypes and prejudice have long been significant barriers to women‘s participation in the development of anatomical knowledge and education. Despite these challenges, generations of women have persevered, overcoming numerous obstacles to establish themselves in the field. The history of anatomy is often viewed as male-dominated, yet women have made significant contributions, even when societal norms or legal restrictions sought to limit their involvement. Women excelled as prosectors, anatomists, researchers, and educators – even when such practices were viewed as scandalous or were prohibited. This historical review aims to shed light on the contributions of female anatomists, who were not just scientists but also philosophers, innovators, and visionaries. By documenting their achievements, we seek to raise awareness of their invaluable role in shaping the field of anatomy. Recognizing the history of these women is crucial in understanding both the progress made and the ongoing need for gender equality in science and medicine.

Key words: history of medicine, women anatomists, history of anatomy, dissection, wax modeling

Anatomy is a foundational subject for many fields of study. A deeper exploration of this discipline often inspires admiration in those who choose to pursue it further. However, it is not only the complexity and significance of the subject itself that draws admiration, but also the discoverers who showed courage and boldness in their exploration. As a mark of respect, many anatomical structures and anomalies have been named after their discoverers [12, 21]. What stands out, however, is that most of the well known anatomical terms named after scientists are associated with male names. This raises important questions: What has been the role of women in anatomy and anatomy

education? Did they contribute to the field of science? Were they allowed to participate, and did they have the desire, ambition, and vision to advance the field? In response to these questions, this review seeks to examine the role of women in the development of anatomy and anatomical education throughout history.

1. Before the Early Modern Period

1.1. Ancient History

The earliest historical connections between women and anatomy can be traced back to ancient Greek myths and legends. One such figure is the goddess Iris, daughter of the gods Thaumas and Electra. Iris, the personification of the rainbow and messenger of the gods, served the Olympians, particularly Queen Hera. Later, the colored part of the eye surrounding the pupil was named after her. The term „iris" comes from the Greek word for „rainbow," reflecting both the goddess and the multiple colors found in this part of the eye.

Allesandra Gialini (1307-1326)

Alessandra Giliani is regarded as the world's first female anatomist and prosector [20]. She entered the University of Bologna at the age of 16 and, disguised as a man, worked as a prosector and demonstrator during anatomy lectures (**Fig. 1).** Giliani developed an innovative technique for visualizing blood vessels in cadavers using injected dyes, enabling detailed observation of vascular structures. Her career was brief, ending with her death at the age of 19 in 1326. One theory suggests that she succumbed to an infected wound, while others believe her death was linked to a colleague's romantic feelings, which revealed her true gender. According to some accounts, her exposure led to her being condemned by the Inquisition and burned at the stake as a witch outside the Church of San Pietro e Marcellino in Florence, for daring to work alongside men.

2. The Period Between the 15th and 18th Century

The period between 1400 and 1700 saw advances in the natural sciences, but progress in anatomy and women's participation slowed due to traditional beliefs, religious restrictions, limited scientific methods, and restricted access to medical education. Socioeconomic challenges such as wars, epidemics, and poverty further hindered development. Nevertheless, this period laid the foundation for theories that later flourished during the Enlightenment.

2.1. Early Modern Period – Enlightenment (17th and 18th centuries)

Laura Maria Katerina Bassi (1711-1778)

Laura Bassi began studying biology, natural history, and medicine at the age of 13 (**Fig. 2**). In 1731, she started teaching anatomy at the medical faculty of the University of Bologna, and at 21 earned a doctorate in philosophy and became a professor [17,20]. Despite her family responsibilities, she continued teaching anatomy through private courses and was highly respected in scientific and political circles in Italy.

Anna Morandi Manzolini (1714-1774)

Anna Morandi Manzolini was an internationally renowned anatomist and creator of wax anatomical models at the University of Bologna [13,17,20]. Together with her husband, Giovanni Manzolini, she worked in ceroplasty, initially collaborating with the Bologna Museum and later continuing independently in their home laboratory (**Fig. 3**) [1,17,18]. She served for several years as a professor of anatomy and made significant contributions, including the discovery of the attachment points of the oblique muscles of the eyeball. Morandi Manzolini became widely known for her highly detailed wax models, accurately reproducing fine anatomical structures such as capillaries and nerves (**Fig. 4**). Her collection, the *Supellex Manzoliniana*, was recognized throughout Europe as an important educational resource (**Fig. 5**) and influenced later developments in anatomical modeling.

Marie-Marguerite Biheron (1719-1795)

Marie-Marguerite Biheron was a French anatomist, medical illustrator, and artist renowned for her anatomically precise wax models [7]. Due to the limitations of working with cadavers, she turned to ceroplasty, producing durable models widely used for anatomical education in laboratories, medical schools, and museums. Her innovative techniques gained international recognition; however, restrictions at the Royal Academy of Sciences in Paris prevented her from teaching anatomy, leading her to continue her work in England. In May 1761, she opened an exhibition of her anatomical models in her home on Rue Vieille Estrapade, known as the „Exhibition of Artificial Anatomy".

Maria Petracini (1759 – 1791)

Maria Petracini was an Italian physician and professor of anatomy at the University of Ferrara (**Fig. 6**) [17]. In 1789, she published an influential work on maternal and newborn care, combining medical knowledge with personal experience. Petracini criticized harmful infant swaddling practices and advocated early breastfeeding, while also providing guidance on congenital malformations and infectious diseases (**Fig. 7**).

3. 19th to 20th centuries

Augusta Déjerine-Klumpke (1859 – 1927)

Augusta Déjerine-Klumpke was an American-born French physician noted for her contributions to neuroanatomy and the description of Klumpke paralysis (**Fig. 8**) [26]. She was among the first female hospital interns in Paris, although her medical training was initially hindered by gender-based restrictions [22]. During her externship, she studied neurology under Jean-Martin Charcot and focused on the anatomy of the brachial plexus. Her clinical observations formed the basis of her doctoral thesis, published in 1885, which earned several prestigious academic awards.

Vera Mikhailovna Danchakova (1879 – 1950)

Vera Mikhailovna Danchakova was a prominent Russian anatomist, embryologist, and cell biologist. In 1908, she became the first woman in Russia elected as a professor

of anatomy at Moscow University (**Fig. 9**). In 1915, Danchakova moved to the U.S., working at the Rockefeller Institute and later at Columbia University‘s College of Medicine, teaching anatomy during the early inclusion of women in medical education. In 1916, she proposed that all blood cells develop from a single type of cell, introducing the term „stem cell“ and noting that stem cells could undergo pathological changes [14]. She is recognized as a pioneer in hematopoietic stem cell research, called the „Mother of Stem Cells“ by M. A. Lichman (2001). Between 1934–1937, she worked at the Lithuanian Medical University. In 1938, she conducted experiments exposing female guinea pig foetuses to testosterone, showing it could increase masculine sexual behavior in adulthood.

Mabel Heath Palmer (1885 – 1949)

Mabel Heath Palmer, known as the „First Lady of Chiropractic“ (**Fig. 10**), was an American chiropractor and anatomist [23]. Married to B. J. Palmer, she graduated from the Palmer School of Chiropractic in 1905 and studied anatomy and dissection in Chicago. In 1918, she published *Anatomy*, the first anatomy textbook for chiropractic students. Returning to the Palmer School, she taught anatomy for 40 years and founded Sigma Phi Chi, the first chiropractic sorority.

Katharine Julia Scott Bishop (1889 – 1975)

Katharine Julia Scott Bishop was an anatomist, physician, researcher, and educator, best known for codiscovering Vitamin E (**Fig. 11**) [10, 24]. After graduating from medical school, she taught histology at the University of California Medical School in Berkeley until 1923. Working with Herbert McLean Evans, she studied the reproductive cycle of rats, publishing a monograph on vital staining of connective tissue. Their experiments on dietary deficiencies led to the identification of a factor essential for reproduction, initially called „Factor X,“ later named Vitamin E, derived from lipid extracts of lettuce and wheat germ.

4. Contemporary History (1945 to today)

Marian Diamond (1926 – 2017)

Marian Cleeves Diamond was an American neuroscientist and a pioneer in neuroplasticity (**Fig. 12**) [2,8,9,25]. She was the first female graduate student in the Department of Anatomy at UC Berkeley and taught well into her eighties. In the early 1960s, Diamond provided the first evidence that the cerebral cortex can change structurally in response to enriched or impoverished environments, from prenatal stages to old age. Her experiments showed that rats in enriched environments had a cortex 6% thicker and a greater learning capacity than those in impoverished conditions. Diamond also analyzed preserved blocks of Albert Einstein’s brain, discovering an increased glial cell-to-neuron ratio, particularly in area 39 of the left hemisphere. Her integrative biology lectures became globally popular on YouTube, and the 2017 documentary *My Love Affair with the Brain* highlights her scientific contributions and teaching legacy.

Eva Braak (1939-2000)

Eva Braak was a German anatomist known for her work on neurodegenerative diseases, especially Alzheimer's (**Fig. 13**) [3-6]. As a professor at Johann Wolfgang Goethe University, she and her husband Heiko Braak led a research group studying degenerative brain disorders. In the 1970s, they refined the silver-iodate histological technique to examine thick brain sections, advancing understanding of Alzheimer's and Parkinson's diseases. In 1987, they first described argyrophilic grain disease, a previously misclassified tauopathy. Their 1991 classification system for Alzheimer's, the Braak and Braak stages, delineated six pathoanatomical stages based on neurofibrillary changes. In 1998, Eva Braak became the first female recipient of the Lifetime Achievement Award in Alzheimer's Disease Research.

Carolyn Larabell (1947-)

Carolyn Larabell (**Fig. 14**) is an American scientist pioneering biological imaging through soft X-ray microscopy [11,15,16,19]. Since 1997, she has been at Lawrence Berkeley National Laboratory, advancing X-ray microtomography for 3D visualization of cells. In 2004, she founded the NCXT to develop soft X-ray tomography, including Beamline 2.1 (XM-2), the world's first soft X-ray microscope. Her work enables the study of cellular pathways for clearing misfolded proteins, offering insights into Alzheimer's, Parkinson's, and Huntington's diseases, bridging light and electron microscopy and providing unprecedented views of cellular structures.

Conclusions

"I am among those who think that science has great beauty." ***Marie Curie***

This sentiment, echoed by luminaries such as Marie Curie, encapsulates the profound impact that women have had in the scientific realm, particularly in anatomy and medical research. Throughout history, women have not only contributed groundbreaking discoveries but have also enriched the field with diverse perspectives and innovative approaches that highlight the intricate beauty of biological systems. From the pioneering work of Alessandra Giliani in the 14th century to the contemporary advancements of Carolyn Larabell, women have consistently broken barriers and challenged conventions, illuminating the path for future generations. Their dedication and resilience remind us that the pursuit of knowledge is a collaborative endeavor that thrives on inclusivity and diversity. By recognizing and celebrating the achievements of women in science, we honor the beauty inherent in scientific inquiry and inspire a more equitable future where all voices are heard. In doing so, we gain deeper insight into life's intricacies while embracing the wonder, innovation, and beauty that science has to offer.

References

1. Ballestriero, R. Anatomical models and wax venuses: Art masterpieces or scientific craft works? – *J. Anat.*, **216**, 2010, 223–234.

2. **Bennett, E. L., M. C. Diamond, D. Krech, M. R. Rosenzweig.** Chemical and anatomical plasticity of brain. – *Science*, New Series **146**, 1964, 610–619.

3. **Braak, E., H. Braak.** Silver staining method for demonstrating Lewy bodies in Parkinson's disease and argyrophilic oligodendrocytes in multiple system atrophy. – *J. Neurosci. Methods*, **87**, 1999, 111–115.

4. **Braak, H., E. Braak.** Argyrophilic grains: Characteristic pathology of cerebral cortex in cases of adult onset dementia without Alzheimer changes. – *Neurosci. Lett.*, **76**, 1987, 124–127.

5. **Braak, H., E. Braak.** Neuropathological stageing of Alzheimer-related changes. – *Acta Neuropathol.*, **82**, 1991, 239–259.

6. **Braak, H., E. Braak.** Staging of Alzheimer's disease-related neurofibrillary changes. – *Neurobiol. Aging*, **16**, 1995, 271–278; discussion 278–284.

7. **Dacome, L.** Intimate connections: Marie Marguerite Biheron and her "Little Boudoir". – *Bull. Hist. Med.*, **95**, 2021, 315–349.

8. **Diamond, M. C., A. B. Scheibel, G. M. Murphy, T. Harvey.** On the brain of a scientist: Albert Einstein. – *Exp. Neurol.*, **88**, 1985, 198–204.

9. **Diamond, M. C., D. Krech, M. R. Rosenzweig.** The effects of an enriched environment on the histology of the rat cerebral cortex. – *J. Comp. Neurol.*, **123**, 1964, 111–119.

10. **Evans, H. M., K. S. Bishop.** On the existence of a hitherto unrecognized dietary factor essential for reproduction. – *Science*, **56**, 1922, 650–651.

11. **Guo, J., C. A. Larabell.** Soft X-Ray tomography: Virtual sculptures from cell cultures. – *Curr. Opin. Struct. Biol.*, **58**, 2019, 324–332.

12. **Habbal, O.** The science of anatomy: A historical timeline. – *Sultan Qaboos Univ. Med. J.*, **17**, 2017, e18–e22.

13. **Hildebrandt, S.** The lady anatomist. – *J. Clin. Invest.*, **121**, 2011, 2532–2532.

14. **Keung, A. J., S. Kumar, D. V. Schaffer.** Presentation counts: Microenvironmental regulation of stem cells by biophysical and material cues. – *Annu. Rev. Cell Dev. Biol.*, **26**, 2010, 533–556.

15. **Larabell, C. A., M. A. Le Gros.** X-Ray Tomography generates 3-D reconstructions of the yeast, *Saccharomyces cerevisiae*, at 60-nm resolution. – *Mol. Biol. Cell.*, **15**, 2004, 957–962.

16. **Larabell, C. A., K. A. Nugent.** Imaging cellular architecture with X-Rays. – *Curr. Opin. Struct. Biol.*, **20**, 2010, 623–631.

17. **Logan, G. B.** The desire to contribute: An eighteenth-century Italian woman of science. – *Am. Histor. Review*, **99**, 1994, 785.

18. **Maraldi, N. M., G. Mazzotti, L. Cocco, F. A. Manzoli.** Anatomical waxwork modeling: The history of the Bologna anatomy museum. – *Anat. Rec.*, **261**, 2000, 5–10.

19. **McDermott, G., M. A. Le Gros, C. G. Knoechel, M. Uchida, C. A. Larabell.** Soft X-ray tomography and cryogenic light microscopy: The cool combination in cellular imaging. – *Trends Cell. Biol.*, **19**, 2009, 587–595.
20. **Narlieva, N., D. Dardanov.** *Anatomiyata i anatomite prez vekovete.* Pleven, Bulgaria, Izd. "Iztok-Zapad", 2018. [in Bulgarian]
21. **Narlieva, N., S. Marinova-Todorova, D. Dardanov.** *Rechnik na anatomichnite imena*; Pleven, Bulgaria, Izd. Tsentar MU-Pleven, 2005. [in Bulgarian]
22. **Nogueira, E. de A.G., V. M. de Carvalho, M. V. de Queiroz, G. R. Rosa, Y. D. Fragoso.** Augusta Marie Déjerine-Klumpke: Much more than just Déjerine's Wife. – *Arq. Neuropsiquiatr.*, **76**, 2018, 117–119.
23. **Palmer College of Chiropractics.** Available at: https://www.palmer.edu/palmer-blog/mabel-palmer/ (accessed on 15 October 2024).
24. **Rizvi, S., S. T. Raza, F. Ahmed, A. Ahmad, S. Abbas, F. Mahdi.** The role of vitamin E in human health and some diseases. – *Sultan Qaboos Univ. Med. J.*, **14**, 2014, e157–e165.
25. **Squire, L. R., M. C. Diamond.** In *The History of Neuroscience in Autobiography*. – Oxford Univ. Press, **6**, 2009, 63–96.
26. **Ulgen, B. O., H. Brumblay, L. J. S. Yang, S. M. Doyle, K. C. Chung.** Augusta Déjerine-Klumpke, M.D. (1859–1927): A Historical perspective on Klumpke's Palsy. – *Neurosurgery*, **63**, 2008, 359–367.

Figure 1. Anathomia corporis humani title page (Leipzig edition dated 1493).

Figure 2. Portrait of Laura Bassi by unknown author.

Figure 3. Anna Morandi Manzolini (1714-1774), Italian anatomist and sculptor, from a drawing of Cesare Bettini.

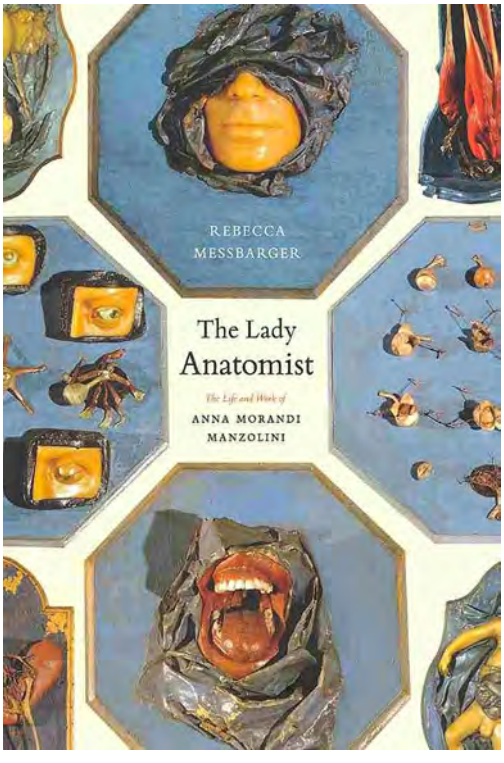

Figure 4. The front cover of the book: The Lady Anatomist, The Life and Work of Anna Morandi Manzolini by Rebecca Messbarger. The University of Chicago Press.

Figure 5. Anna Morandi and Giovanni Manzolini, muscles of the forearm. Courtesy of Museo di PalazzoPoggi, Universita di Bologna.

Figure 6. Portrait of Maria Petracini by unknown author.

Figure 7. Maria Maddalena Petraccini, Memoria per servire alla fisica educazione de‘ Bambini, Ferrara, 1789.

Figure 8. Augusta and Jacqueline Dejerine-Klumpke. Author Andre-Thomas.

Figure 9. Vera Mikhailova Danchakova (Unknown author - http://www.sbras.ru/HBC/article.phtml?nid=656&id=3).

Figure 10. The bronze bust of Mabel Heath Palmer in Heritage Courtyard on the Davenport Campus of Palmer College of Chiropractic.

Figure 11. Katharine J. Scott Bishop. Smithsonian Institution Archives. Image SIA2009-3085.

Figure 12. Dr Marian Diamond smiles, standing in her laboratory, 28 December 2022.

Figure 13. Photograph of Eva Braak

Figure 14. Carolyn A. Larabell (https://biosciences.lbl.gov/profiles/carolyn-a-larabell/)

Institute of Experimental Morphology, Pathology and Anthropology with Museum
Bulgarian Anatomical Society

Acta Morphologica et Anthropologica, 33 (1-2)
Sofia ● 2026

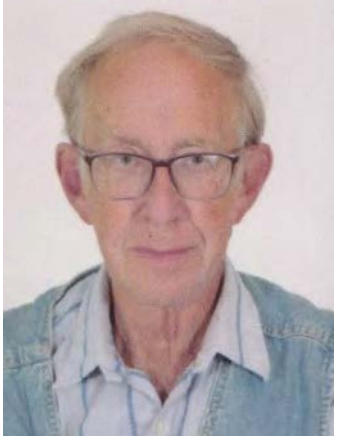

IN MEMORIAM

Associated Professor Racho Stefanov Stoev, PhD

(17.04.1956 - 05.11.2025)

Racho Stefanov Stoev was born on April 17, 1956 and passed away on November 5, 2025 at his home in Sofia after a short illness.

Racho Stoev studied at the Department of Biology (Biology and Environment Protection) of the Sofia University "St. Kliment Ohridski" where he graduated with honors in 1983. Due to his excellent achievements as a university student he was appointed directly as a research associate in the Institute of Morphology in the Bulgarian Academy of Sciences (predecessor of IEMPAM-BAS) without any entrance competition.

A great part of his research work is focused on the investigation of the processes of growth and development as well as sexual maturation and the influence of social and economic conditions and living standards of the family such as income, education, employment, etc. His research on the topic formed the basis of his PhD thesis "Anthropological characteristics of adolescents – physical development and sexual maturation in conditions with the socio-familial environment" which he defended successfully in 2007 at IEMA-BAS.

In 2012 he was promoted in Associated Professor in the Department of Anthropology and Anatomy, which he headed in the period 2015 – 2022. He was a member of the Editorial Board of the scientific journal "Acta Morphologica et Anthropologica".

A particular interest in his research was the characterization of the various anthropological types inhabiting the territories of Bulgaria and the Balkans. In these studies, Assoc. Prof. Stoev successfully applies the methods of mathematical taxonomy and contributes significantly to deepening the knowledge and understanding of the processes related to biological and cultural diversity in the region. His research interests includes also human ecology, historical anthropometry and secular trend, ethnic anthropology, including anthropogenesis and ethnic dermatoglyphics, demography. This led him to specialize in many anthropological centers abroad during his scientific career - in the USSR, Poland, Greece, Russia.

His intellectual curiosity and interest in knowledge and science did not wane over the years, and in 2024 he enrolled in History at Sofia University, which unfortunately he did not manage to complete.

Associated Professor Racho Stefanov Stoev was respected and recognised anthropologist in Bulgarian and European scientific societies. He is the author and coauthor of over 50 scientific publications. He participated in many national and international scientific forums and maintained good personal and working relations with colleagues from Russia, Belarus, Poland, Greece, Hungary, Serbia, etc. He was a member of the European Anthropological Association, Bulgarian Anthropological Society, Bulgarian Anatomic Society, Polish Anthropological Society (1989-1990).

Assoc. Prof. Racho Stoev was young at heart, an excellent scientist, colleague and friend, known with his humility and humanity, devoted his life to understanding the man as biological and social being.

Yanitsa Zhecheva

Author Guidelines

Acta Morphologica et Anthropologica is an open access peer review journal published by Bulgarian Academy of Sciences, Prof. Marin Drinov Publishing House.

Corporate contributors are Bulgarian Academy of Sciences, Institute of Experimental Morphology, Pathology and Anthropology with Museum and Bulgarian Anatomical Society.

Acta Morphologica et Anthropologica is published in English, 4 issues per year.

The journal accepts manuscripts in the following **fields**: experimental morphology, cell biology and pathology, anatomy and anthropology.

Publication types: original articles, short communications, case reports, reviews, Editorial, letters to the Editors.

Acta Morphologica et Anthropologica is the continuation of Acta cytobiologica et morphologica

The **aim** of the Journal is to disseminate current interdisciplinary biomedical research and to provide a forum for sharing new scientific knowledge and methodology. The general editorial policy is to optimize the process of issuing and distribution of *Acta Morphologica et Anthropologica* in line with modern standards for scientific periodicals focusing on content, form, and function.

Scope - experimental morphology, cell biology and pathology (neurobiology, immunobiology, tumor biology, environmental biology, reproductive biology, etc.), new methods, anatomy and pathological anatomy, anthropology and paleoanthropology, medical anthropology and physical development.

Acta Morphologica et Anthropologica is published twice a year as one volume with 4 issues. For the first two issues (1-2) the deadline for manuscript submission is March 15th and for the next two issues (3-4), the deadline is September 15th. Electronic version for issues 1-2 is uploaded on the website till June 30th and for issues 3-4 – till December 30th.

Contact details and submission

Manuscript submission is electronical only. The manuscripts should be sent to the Managing Editor's e-mail address ama.journal@iempam.bas.bg, ygluhcheva@hotmail.com with copy to iempam@bas.bg

All correspondence, including notification for Editor's decision, requests for revision, is sent by e-mail.

Article structure

Manuscripts should be in English with total length not exceeding 10 standard pages, line-spacing 1.5, justified with 2.5 cm margins. The authors are advised to use Microsoft Word 97-2003, Times New Roman, 12 pt throughout the text. Pages should be numbered at the bottom right corner of the page.

The article should be arranged under the following headings: Introduction, Material and Methods, Results, Discussion, Conclusion, Acknowledgements and References.

Title page – includes:

- **Title** - concise and informative;
- **Author(s)' names and affiliations** – indicate the given name(s) and family name(s) of all authors. Present the authors' affiliation addresses below the names. Indicate all affiliations with a lower-case superscript after the author's name and in front of the appropriate address. Provide the full postal address information for each affiliation, including the country name.
- **Corresponding author** – clearly indicate who will handle the correspondence for refereeing, publication and post-publication. An e-mail should be provided.
- **Abstract** – state briefly the aim of the work, the principal results and major conclusions and should not exceed 150 words. References and uncommon, or non-standard abbreviations should be avoided.
- **Key words** – provide up to 5 key words. Avoid general, plural and multiple concepts. The key words will be used for indexing purposes.

Introduction – state the objectives of the work and provide an adequate background, avoiding a detailed literature survey or summary of the results.

Material and Methods – provide sufficient detail to allow the work to be reproduced. Methods already published should be indicated as a reference: only relevant modifications should be described.

Results – results should be clear and concise.

Discussion – should explore the significance of the results in the work, not repeat them. A combined *Results and Discussion* section is often appropriate. Avoid extensive citation and discussion of published literature.

Conclusions – the main conclusions of the study should be presented in a short section.

Acknowledgements – list here those individuals who provided help during the research and the funding sources.

Units – please use the International System of Units (SI).

Math formulae – please submit math equations as editable text, not as images.

Electronic artwork – number the tables and illustrations according to their sequence in the text. Provide captions for them on a separate page at the end of the manuscript. The proper place of each figure in the text should be indicated in the left margin of the corresponding page. **All illustrations (photos, graphs and diagrams)** should be referred to as "figures" and given in abbreviation "Fig.", and numbered in Arabic numerals in order of its mentioning in the manuscript. They should be provided in grayscale as JPEG or TIFF format, minimum 300 dpi. The illustrations should be submitted as separate files.

References – they should be listed in alphabetical order, indicated in the text by giving the corresponding numbers in parentheses. The "References" should be typed on a separate sheet. The names of authors should be arranged alphabetically according to family names. In the reference list titles of works, published in languages other than English, should be translated, original language must be indicated at the end of reference (e.g., [in Bulgarian]). Articles should include the name(s) of author(s), followed by the full title of the article or book cited,

the standard abbreviation of the journal (according to British Union Catalogue), the volume number, the year of publication and the pages cited, for books - the city of publication and publisher. In case of more than one author, the initials of the second, third, etc. authors precede their family names. Ideally, the names of all authors should be provided, but the usage of "et al" after the fifth author in long author lists will also be accepted.

For articles: **Davidoff, M. S., R. Middendorff, G. Enikolopov, D. Riethmacher, A. F. Holstein, D. Muller**. Progenitor cells of the testosterone-producing Leydig cells revealed. – *J. Cell Biol.,* **167**, 2004, 935-944.

Book article or chapter: **Rodriguez, C. M., J. L. Kirby, B. T. Hinton. The development of the epididymis.** - In: *The Epididymis - from molecules to clinical practice* (Eds. B. Robaire, B. T. Hinton), New York, Kluwer Academic Plenum Publisher, 2002, 251-269.

Electronic books: **Gray, H.** *Anatomy of the human body* (Ed. W.H.Lewis), 20th edition, NY, 2000. Available at http://www.Bartleby.com.

PhD thesis: **Padberg, G**. Facioscapulohumeral diseases. *PhD thesis*, Leiden University, 1982, 130 p.

Website: National survey schoolchildren report. National Centre of Public Health and Analyses, 2014. Available at http://ncphp.government.bg/files

Page charges

Manuscript publication is free of charges.

Ethics in publishing

Before sending the manuscript the authors must make sure that it meets the Ethical guidelines for journal publication of Acta Morphologica et Anthropologica.

Human and animal rights

If the work involves the use of human subjects, the authors should ensure that work has been carried out in accordance with *The Code of Ethics of the World Medical Association* (Declaration of Helsinski). The authors should include a statement in the manuscript that informed consent was obtained for experimentation with human subjects. The privacy rights of human subjects must always be observed.

All animal experiments should comply with the *ARRIVE guidelines* and should be carried out in accordance with the U.K. Animals (Scientific procedures) Act, 1986 and the associated guidelines *EU Directive 2010/63/EU* for animal experiments, or the National Institutes of Health guide for the care and use of Laboratory animals (NIH Publications No. 8023, revised 1978) and the authors should clearly indicate in the manuscript that such guidelines have been followed.

Submission Details

Acta Morphologica et Anthropologica is published twice a year as one volume with 4 issues. For
the first two issues (1-2) the deadline for manuscript submission is March 15th and for the next two issues (3-4), the deadline is September 15th. Electronic version for issues 1-2 is uploaded on the website till June 30th and for issues 3-4 – till December 30th.

Manuscript submission is electronical only.

The manuscripts should be sent to the Managing Editor email address ama.journal@iempam.bas.bg, ygluhcheva@hotmail.com with copy to iempam@bas.bg

All correspondence, including notification for Editor's decision, requests for revision, is sent by e-mail.

Submission declaration

Submission of the manuscript implies that the work described has not been published previously, is not considered under publication elsewhere, that its publication is approved by all authors, and that if accepted, it will not be published elsewhere in the same form, in English or in any other language, including electronically, without the informed consent of the copyright-holder.

Contributors

The statement that all authors approve the final article should be included in the disclosure.

Copyright

http://www.iempam.bas.bg/journals/acta/Author%20Copyright%20Agreement_last.pdf

Upon acceptance of an article, the authors will be asked to complete a "**Copyright Transfer Agreement**".

http://www.iempam.bas.bg/journals/acta/Copyright_Transfer_Agreement_Form_AMA.doc

Peer review

Once a manuscript is submitted, the Managing Editor (or the Editor-in-Chief) briefly checks the manuscript for conformance with the journal's Focus, Scope, Policies and style requirements and decide whether it is potentially suitable for publication and can be processed for review, or rejected immediately, or returned to the author for improvement and re-submission.

Manuscripts are peer-reviewed by the Editors, Editorial Board members, and/or external experts before final decisions regarding publication are made. The entire editorial workflow is performed in the following steps:

1. The submitted manuscript is checked in the editorial office whether it is suitable to go through the normal peer review process.
2. If deemed suitable, the manuscript is sent to 2 reviewers for peer-review. The choice of reviewers depends on the subject of the manuscript, the areas of expertise of the reviewers, and their availability.
3. Each reviewer will have 2 weeks to provide evaluation of the manuscript. The Editor may recommend publication, request minor, moderate or major revision, or provide a written critique of why the manuscript should not be published (rejected).

4. In case only one reviewer suggests rejection of the manuscript, the latter is subjected to additional evaluation by a third reviewer.
5. The manuscript will be published in a revised form provided that the authors successfully answer the critics received. The Editor-in-Chief is the final authority on all editorial decisions.

Open Access

This journal provides immediate open access to its content on the principle that making research freely available to the public supports a greater global exchange of knowledge.

After acceptance

Proof correction

The corresponding author will receive proofs by e-mail in PDF format and will be requested to return it with any corrections within two weeks.

ISSN 1311-8773 (print)
ISSN 2535-0811 (online)